Atmospheric Blocking in the Australasian Region in the Southern Hemisphere Winter

by

Michael J Pook, BSc, Grad Dip ASOS (Hons.)

Submitted in fulfilment of the requirements

for the degree of

Doctor of Philosophy

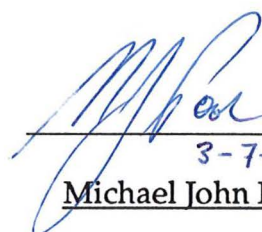Institute of Antarctic and Southern Ocean Studies

University of Tasmania

Hobart

Australia

December 1994

DECLARATION

This is to certify that the material comprising this thesis has never been accepted for any other degree or award in any tertiary institution and, to the best of my knowledge and belief, is solely the work of the author and contains no material previously published or written by another person, except where due reference is made in the text.

3-7-95

Michael John Pook

Authority of Access

This thesis may be made available for loan and limited copying in accordance with the Copyright Act 1968.

Michael John Pook

ABSTRACT

Previous studies of blocking in the Australasian region have sought to establish a link between the occurrence of blocking and the observed gradient of sea surface temperature (SST) from the cold waters of the Indian Ocean sector of the Southern Ocean to the relatively warm surface waters to the southeast of Australia.

This study investigates the distribution, gradients and seasonal cycles of SST over the Southern Ocean and concludes that the contribution of the west-east gradient in forcing the atmosphere is about an order of magnitude less than the effect of SST gradients in the meridional plane. Furthermore the meridional gradient is magnified during winter because of the interaction of several major influences in the Australian region. These include the significant cooling of the continents of Australia and Antarctica and the configuration of the Antarctic Circumpolar Current (ACC).

Where the ACC travels closer to the coast of East Antarctica surface temperature gradients are reinforced aloft by strong meridional temperature gradients induced by the elevated continent. The enhanced westerly thermal wind at high latitudes (south of 50°S) leads to a westerly wind maximum aloft and the steady cooling of inland Australia acts to weaken the meridional temperature gradient between 30°S and 45°S leading to a minimum in the westerly winds in this region. Strong meridional gradients in the north produce an intense westerly thermal wind north of 30°S. The configuration of mean winds in the middle troposphere is shown to generate positive values of relative vorticity [about 0.1 planetary vorticity] in the south and negative values of similar magnitude over eastern Australia.

A prolonged period of blocking in the Australasian region during the winter and early spring of 1989 is investigated in the context of interannual variabilty of blocking frequency. It is postulated that the active monsoon conditions over northern Australia associated with the La Niña of 1988-89 contributed to the lower than normal inland temperatures in the 1989 autumn and the following winter, thus amplifying the cyclonic vorticity generation process over eastern Australia. The enhanced Antarctic polar vortex reported in 1989 is also shown to have contributed to a strengthening of the westerly jet to the south of Australia. The configuration of SST anomalies in the autumn and early winter of 1989 is presented as a significant precursor to the subsequent blocking event. This hypothesis is investigated in a numerical general circulation model of the atmosphere driven by the observed SST anomaly.

ACKNOWLEDGEMENTS

Science is a very human form of knowledge. We are always at the brink of the known, we always feel forward for what is to be hoped. Every judgement in science stands on the edge of error, and is personal. Science is a tribute to what we can know although we are fallible.

J. Bronowski *The Ascent of Man* (1973)

Table of Contents

"It is difficult to understand how an anticyclone can, to all intents and purposes, stand still for several days when the whole surrounding atmosphere is moving forward; and we have not yet made out the explanation". H. C. Russell (1896)

Chapter 1

Introduction

1.1 Preamble

One hundred years after Russell (1896) made the discovery that anticyclones could occasionally become stationary in the vicinity of the Australian continent a full explanation for the process remains elusive. Whether or not these highs formed part of higher latitude ridges could not be determined from his limited data coverage but in the light of present knowledge of the synoptic climatology of the Australasian region, it seems likely. Nor has the problem of the intermittent development of quasi-stationary high presssure systems at higher than normal latitudes been resolved for other regions of the Southern Hemisphere or, in a general sense, for the Northern Hemisphere. The term blocking has been coined to describe such situations in which the westerly current normally found at these latitudes is diverted to the north and south around an extensive high pressure system which effectively blocks the approach of systems from the west.

1.2 Need for a Study of Blocking in the Australian Region

Baines (1990) suggests that atmospheric blocking on the synoptic scale is arguably the most significant problem for weather forecasting when viewed globally. He asserts that this results from "its general unpredictability, and the large length scales and lifetimes of the phenomenon" (Baines, 1990; p.124). This is despite the steady improvement in numerical weather forecasting models demonstrated by e.g. Simmons (1986) and generally acknowledged by professional weather forecasters.

Apart from the intrinsic interest in blocking as a topic of research in fluid dynamics and the demands of day to day weather forecasting, there are compelling reasons to pursue a greater understanding of the atmospheric version of the phenomenon. In the first instance, the effect of such a significant change in circulation can result in major anomalies of temperature and precipitation, which can have serious economic and social impacts. Rex (1950b) has discussed major anomalies of temperature and rainfall which have occurred over Europe in times of major blocking events. An event of this kind produced the extremely cold winter of 1963 in Europe in which the mean January temperature in Warsaw was 10°C below the long-term average (Gill, 1982). Summer blocking patterns can have equally serious impacts. Green (1977) reports that water resources, vegetable

production and juvenile tree plantations were seriously affected in western Europe by the drought of July 1976 which occurred when a blocking anticyclone formed over the region.

In addition to rainfall and temperature anomalies Schwerdtfeger (1984) has referred to the dramatic change in wind conditions from stormy westerlies to moderate northeasterlies which occurred during a ten day period in June 1952, when an intense block persisted between the Falkland and South Shetland Islands. He comments that these synoptic situations are unique in offering the opportunity for "a few days of weak, or not more than moderate, surface winds, welcome for oceanographic work, disembarking on islands, and other outdoor activities" (Schwerdtfeger, 1984; p. 156).

In this thesis it will be shown how a period of blocking during the Southern Hemisphere winter and early spring of 1989 resulted in anomalous precipitation patterns over south-eastern Australia. As a consequence, serious rainfall deficiencies developed over western and central Tasmania (see Chapter 4). This region is the catchment for the vast reservoirs which supply hydro-electric power to the state of Tasmania. Depletion of the hydro-electric water reserves in winter and spring required the managers of the system to switch to an expensive oil-fired generator to maintain supply of electricity during the following summer (Tasmanian Hydro-Electric Commission Archives).

Clearly, an improvement in the ability of forecasting systems to reliably predict the onset, longevity and breakdown of blocking patterns in a region could have significant economic and social impacts, as well as contributing to the safety of personnel engaged in hazardous activities which are dependent on weather.

1.3 Approaches to a study of Blocking

Previous studies of blocking action have followed approaches which can be resolved into three main categories:

- climatological and diagnostic

- numerical

- dynamical

Typical of the climatological type of study have been the investigations by Rex (1950b), Treidl et al. (1981) and Knox and Hay (1985) for the Northern Hemisphere and van Loon (1956), Wright (1974) and Trenberth and Mo (1985) in the Southern Hemisphere. These investigations have identified the main characteristics of blocking action in each hemisphere, including the principal locations of blocking highs at the surface and aloft, seasonal cycles of blocking activity and replacement processes. Coughlan (1983) has provided a comparative climatology of blocking behaviour in the two

hemispheres which has identified important contrasts between the characteristics of blocking action in the two hemispheres.

Numerical studies of blocking have been pursued by many investigators (see for example, Simpson and Downey, 1975; Noar, 1983; Mo *et al.*, 1987; Kung *et al.*, 1990). These investigations have made use of Atmospheric General Circulation Models (AGCMs) to follow the development of circulation anomalies when the models are forced by alterations to the topography or initial fields such as temperature or humidity at a given level. Lau (1992) has reviewed the success of climate models in the simulation of blocking in the longer term while Bengtsson (1992) has discussed limitations in the ability of present AGCMs to simulate blocking events of one to two weeks duration.

Dynamical studies of the blocking phenomenon are well represented in the literature. Among the more recent of these are the contributions of Green (1977), Egger (1978), Charney and DeVore (1979), Austin (1980), Charney *et al.* (1981), Frederickson (1983 and 1989) and Baines (1983). These studies have been characterised by attempts to solve the equations of motion for the atmosphere in simplified models (e.g. one or two levels) with prescribed orographic or thermal forcing. In most of these investigations the atmoshere has been assumed to be barotropic to simplify the problem. However, Frederickson (1983,1989) and Baines (1983) have attempted to treat the atmosphere as a baroclinic system.

In the first instance, this study employs the conventional climatological and diagnostic techniques of analysing observational data to investigate the location, intensity and duration of blocking activity in the Australasian region of the Southern Hemisphere during 1989, and making comparisons with the historical record. The knowledge gained from the first phase of the investigation is then applied to the general problem of the seasonal cycle of blocking activity and interannual variability.

Additionally, the identification of significant thermal contrasts between oceans and continents in this phase of the investigation and persistent anomalies in the SST fields will provide realistic temperature fields to force an AGCM in the second phase of the study.

Clearly, the integrity and applicability of the data sets employed are major considerations when drawing meaningful conclusions from the study and planning further investigations. Data sources will be discussed in the next chapter.

1.4 Aims of the Research

The fundamental questions concerning the initial development and subsequent persistence of blocking anticyclones in the Australasian region have been posed by Baines (1983). He concluded that baroclinic instability represents the most likely mechanism for the initiation of blocking while the maintenance of the blocked flow is best explained by a localised multiple equilibrium state associated with thermal forcing, probably by the sea surface temperature (SST) pattern. But Baines (1983) cautioned that it now

becomes necessary to take the problem back a further step and identify the factors which initiate the instability which causes blocking in a region.

In an attempt to gain insight into the mechanisms responsible for blocking, this study attempts to identify the physical factors which are unique to the Australasian region and which, when combined with the seasonal characteristics of the atmosphere, SST patterns and continental temperature, may account for the seasonal cycle of blocking frequency in the region. In particular, the contributions of the Australian and Antarctic continents to winter blocking and the influence of the major ocean currents in the region are investigated. The mechanisms discussed in the seasonal cycle are extended to link enhancements of seasonal blocking activity on an interannual scale to broader influences operating in the Pacific region.

1.5 Structure of the Thesis

The structure of this study of atmospheric blocking in the Southern Hemisphere winter can be resolved into four distinct phases. Sources of atmospheric, oceanic and bathymetric data are discussed in Chapter 2 with an analysis of some significant discrepancies between data sets. A review of the literature tracing the development of the current understanding of the phenomenon of blocking is presented in Chapter 3 and is followed in Chapter 4 by an analysis of a prolonged period of blocking in the Australian region in the winter and early spring of 1989. Possible associations of this event with oceanic and continental influences are explored in Chapter 5 and a conceptual model is presented which attempts to draw together the contributions to the development and maintenance of the phenomenon in the Australasian region. The fourth stage of the study is completed in Chapter 6 which records the results of a series of numerical experiments using an Atmospheric General Circulation Model to simulate the observed situation. A summary of the major conclusions of this investigation is given in Chapter 7.

Chapter 2

Data and Methodology

2.1 Introduction

The availability and quality of data sets for the vast regions of the Southern Ocean are major factors in this investigation of the broad aspects of winter blocking and possible associations with oceanic and continental influences in the Australian region. Previous investigations, particularly in the upper air (see for example, Trenberth, 1979; van Loon and Shea, 1988; Karoly, 1989; Pook, 1992), have shown that the data are satisfactory for the analysis of large scale features but the paucity of observations from conventional observing systems has been an impediment to more detailed study.

Venter (1957) has discussed the sources of meteorological data for the Southern Ocean and Antarctica prior to the International Geophysical Year (IGY) of 1957-58. He pointed out that the universal introduction of observations conforming to international standards for that region has been achieved as recently as 1939. However, the period following the IGY has been one of steady improvement in the availability of observations and the quality of analyses for the Southern Hemisphere. In support of this claim, Trenberth (1979) found significant differences between monthly and long-term means of zonal geopotential height and wind at 500 hPa derived from operational analyses produced by the Australian Bureau of Meteorology for the period 1972-78 and earlier analyses of Taljaard *et al.* (1969) and van Loon *et al.* (1971). He concluded that these differences could be only partly explained by the different data periods involved and argued that the strength of the daily Australian analyses lay in their historical continuity and the incorporation of observations from ships, aircraft and satellites.

The methodology used to prepare the daily analyses at the Australian National Meteorological Analysis Centre (ANMC) has been described by Le Marshall *et al.* (1985). As part of a major contribution to the Global Atmospheric Research Program (GARP) drifting buoy data from the Southern Ocean were incorporated into the ANMC analyses from December 1978, prior to the first Special Observing Period of the First GARP Global Experiment (FGGE) in January 1979 (Guymer and Le Marshall, 1981).

As well, Karoly (1989) has discussed some of the limitations of the ANMC analyses and drawn attention to the absence of satellite vertical temperature profile data prior to 1976. He has also cautioned that there is no reliable way to test the analyses in regions such as the majority of the South Pacific Ocean where there are no conventional upper air stations. This has special importance in the context of this study suggesting that anomalies calculated for the region must be treated with caution. Nowhere is this warning more important than in the vicinity of the Marie Byrd Land region of Antarctica, east of the Ross Sea (see Section 6.3).

2.2 Data Sources

The main data sets employed in this study and the sources of the data are as follows:

• Surface pressure and temperature data from the European Centre for Medium Range Weather Forecasts (ECMWF) global model for the period from June 1986 to the end of August 1989 Domain Limits: 36°N to 56°S, 34°E to 70°W. These data were supplied from the ECMWF/WCRP Level III-A Global Atmospheric Archive.

• Twice-daily 10 metre winds at 1200 and 0000 UTC, derived from the Bureau of Meteorology FINEST model (Leslie *et al.*, 1985; Mills and Leslie, 1985) and displayed on the Bureau of Meteorology RASP model 65 by 40 grid (ANMC, 1989) for the months of June, July and August 1989.

• Australian Bureau of Meteorology National Meteorological Centre (ANMC) 500 hPa gridpoint data issued at 1200 UTC each day including daily geopotential heights and 5-day running means at latitudes 45°S and 55°S (Pook, 1992).

• Daily infra-red satellite imagery (mainly at 0300 UTC) for the Australian region during 1989 from the Japanese geostationary satellite, GMS 3, located at 140°E in equatorial orbit. Images were obtained from the Bureau of Meteorology, Hobart.

• Reynolds blended sea surface temperature (SST) monthly means for each of the years 1982 to 1991 (Reynolds, 1988). These data were obtained in Network Common Data Form (netCDF) from the CSIRO Division of Oceanography, Hobart at a resolution of two degrees.

• SST from the Comprehensive Ocean-Atmosphere Data Set (Slutz *et al..*,1985) obtained in Network Common Data Form (netCDF) from CSIRO Division of Oceanography, Hobart. The monthly SST climatology fields were computed using the two degree resolution COADS data for the period (1950-1979). Coverage was extended to areas with insufficient in situ observations by using SSTs obtained from monthly climatological ice limits and monthly satellite SST fields. Complete details were presented by Reynolds and Roberts (1987) and a summary of these results has been included in Reynolds (1988).

• Multi-channel sea surface temperature (MCSST) from NOAA satellite series. A set of monthly means of SST for the period 1986-89 were obtained from the Remote Sensing Unit at CSIRO Division of Oceanography, Hobart.

• SST monthly means and anomalies from Bureau of Meteorology analyses for the period January 1985 to December 1990 were supplied on microfilm by the National Climate Centre, Melbourne.

- ANMC Southern Hemisphere analyses (SHANAL) for the period 1972-91. A set of grid-point data for the Southern Hemisphere on a 5 degree latitude by 5 degree longitude grid for standard levels form mean sea level (MSL) to the upper troposphere. Fields include pressure (p), temperature (T), geopotential height (z), specific humidity (q) and u (westerly) and v (southerly) components of the geostrophic wind.

- Wind maxima at 500 hPa. A set of daily 500 hPa hemispheric analyses and weekly means of main wind maxima in the Southern Hemisphere prepared by Dr T. Gibson (see Gibson (1989, 1992) for the period April 1976 to the present.

- Upper air analyses of the Australasian region at 850 hPa, 700 hPa, 500 hPa and 300 hPa for the standard times of 0000 UTC, 0600 UTC, 1200 UTC and 1800 UTC from the Tasmanian Regional Forecasting Centre of the Bureau of Meteorology, Hobart.

- Monthly means of wind stress (x and y components) at the surface of the ocean from Trenberth *et al* (1990). These data were obtained in Network Common Data Form (netCDF) on a 2.5° by 2.5° grid from CSIRO Division of Oceanography, Hobart. The climatology was derived from ECMWF wind fields at 1000 hPa for the period 1980-86.

- Stream flow in selected uncontrolled rivers of western Tasmania (data supplied by the Hydro Electric Commision of Tasmania). The rivers and the points at which stream flow was monitored are:
  > King River at Crotty,
  > Henty River at the Zeehan Road Bridge,
  > Franklin River at the Mount Fincham Track,
  > Collingwood River below Alma River, and
  > Huon River upstream of Sandfly Creek.

- Climate Diagnostics Bulletins, issued monthly by the Climate Analysis Centre (CAC), National Oceanic and Atmospheric Administration (NOAA), Washington, D. C.

- Climate Monitoring Bulletins, National Climate Centre (NCC), Bureau of Meteorology, Melbourne, Australia.

- Monthly Weather Reviews-Tasmania.Bureau of Meteorology, Hobart.

- Seasonal Climate Summaries (*Australian Meteorological Magazine*, published quarterly)

- Monthly Climatic Data for the World. National Oceanic and Atmospheric Administration (NOAA) U. S. National Climatic Data Centre.

- Bathymetry obtained via netCDF. ETOPO-5 The original depth and elevation data set was compiled by Dr Peter Sloss, NOAA-NGDC, Boulder, Colorado.

2.3 Data Processing (Analysis)

- **Atmospheric Data**

The initial interest in this study was triggered by a synoptician's response to what appeared to be a greater than normal incidence of blocking events in the region south of the Tasman Sea during the winter and early spring period of 1989. The identification in the first instance as a time of above average blocking activity was largely intuitive. In order to justify this assessment, criteria defining blocking were identified in the literature and applied to the 1989 events. Specifically, this called for the calculation of monthly and seasonal averages of mean sea level pressure, geopotential height at 500 hPa, u and v components of the geostrophic wind at 500 hPa and the Zonal Index (ZI). These fields were compared with the long-term means and anomaly fields constructed. Additionally, some subjective interpretation was required of synoptic charts at the surface and in the upper air.

There were two aspects to be considered. One was to determine whether individual blocking events satisfying prescribed criteria had occurred during the period and secondly, whether the extended period studied was one of significant anomalies against the background climatology.

One criterion common to most definitions is the requirement that 'the westerly current splits into two branches'. Qualitative and semi-objective analysis techniques were invoked to investigate some aspects of jet-stream behaviour during the study period. In particular, the technique of Guymer (1978) was invoked to infer aspects of the 1000-500 hPa thickness field and the location of the jet streams from satellite imagery. Analyses of wind maxima at 500 hPa carried out by Gibson (1989, 1992) were used as proxies for the jet stream locations near the tropopause.

- **Sea Surface Temperature Data**

Sea surface temperature data (SST) were available on a 2 degree by 2 degree grid for the globe (Reynolds, 1988) and for the Indian and Pacific Ocean sectors (ECMWF data set), while the ANMC Southern Hemisphere atmospheric data set is available on a 5 degree by 5 degree grid. In circumstances where correlations between the atmosphere and SST were sought the SST were interpolated onto the 5 degree by 5 degree grid by averaging the closest four data points. Linear correlation between atmospheric thickness and SST was investigated along selected latitudes over the Southern Ocean.

- **Data Inconsistencies and Incompatibilities.**

Inconsistencies in surface pressure data

A major aim of this study was to investigate whether a relationship could be established between atmospheric thickness and SST over the Southern Ocean. Initial attempts to calculate 1000-500 hPa thickness fields employed the ANMC 500 hPa grid-point geopotential heights at 1200 UTC (Pook,1992) adjusted by surface pressures from the ECMWF according to a simple algorithm of the form,

$$\Delta Z = Z_{500} - 0.784(p - 1000) \qquad (2.1)$$

where Z_{500} is the height of the 500 hPa surface in dam and p is surface pressure in hPa. In the development of this algorithm, atmospheric density (ρ) was assumed to be 1.3 kg m^{-2} and the acceleration due to gravity (g), 9.81 m s^{-2}.

The algorithm was tested for the Hobart daily radiosonde flights during June 1989 using the surface pressure at Hobart Airport and the result is displayed in Fig. 2.1. Estimated values exceed the reported values by a mean bias value of +1.1 dam . The Hobart Airport observing site was at an elevation of 3 m in 1989 (now 27 m) and when this correction is applied the bias reduces to approximately 8 geopotential metres (0.8 dam).
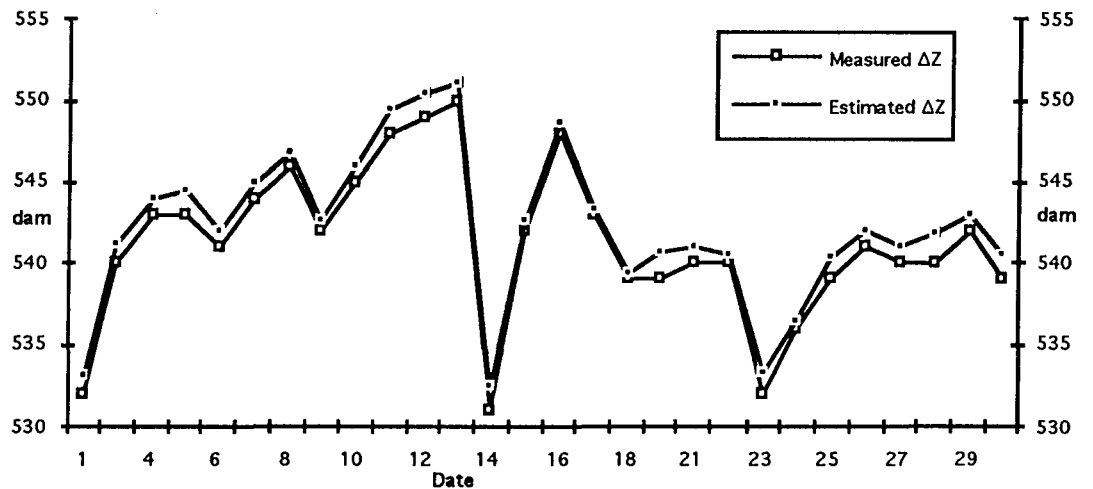

Fig. 2.1. Plot of 1000-500 hPa thickness from daily radiosonde trace versus the estimated value from 500 hPa height and surface pressure using a simple algorithm.

Difficulties arise when the algorithm is applied to grid points which are over the sea but close to land. The resolution of the ECMWF model results in a situation where surface pressure values for a grid point such as 44°S, 146°E (in the ocean) are seriously influenced by the elevation of nearby land. The model's treatment of the topography of Tasmania results in surface pressures at 44°S, 146°E which are approximately 10 hPa below surface pressures at 44°S, 144°E. Leaving aside contributions from the grid point identified as 44°S, 146°E, interpolated values of 1000-500 hPa thickness were calculated for a grid point at 45°S, 145°E from the remaining three closest grid points. Correlation between daily values of 1000-500 hPa thickness calculated from equation 2.1 for a grid point at 45°S. 145°E and daily thickness at Hobart Airport from radiosonde data are given in Fig, 2.2.
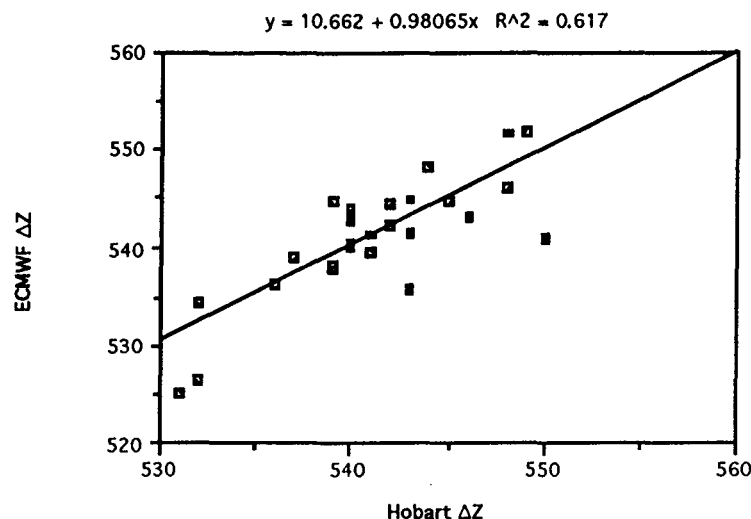
Fig. 2.2. 1000-500 hPa thickness (dam) from algorithm at 45°S, 145°E versus thickness at Hobart Airport.

The difficulties experienced in the application of surface pressures from the ECMWF to oceanic locations close to land suggested that an alternative method of calculating thickness should be employed. With the subsequent availability of ANMC atmospheric grid point data, thickness values could be obtained by the direct subtraction of geopotential heights at 1000 hPa from values at 500 hPa. This simple method has been used to calculate the thickness values referred to in the analysis sections of this study.

Inconsistencies in SST data sets

Investigation of time series of sea surface temperatures (SST) from ECMWF indicated a region of particularly warm surface water in the Indian Ocean sector of the Southern Ocean during the winters of 1986 and 1987. A comparison with SST from the Reynolds (1988) blended data set revealed significant differences in the region in 1986 and 1987 whereas there was close agreement between the data sets in 1989. Because the Reynolds SST includes data from drifting buoys and ships (Reynolds, 1988), and drifting buoys were flagged in the data record as having contributed to the final analysis in June 1986 and June 1987, the Reynolds analysis was regarded as the more reliable. In order to test this hypothesis, SST data were obtained from the NOAA Multi-Channel Sea Surface Temperature (MCSST) programme. Fig. 2.3 shows a comparison of ECMWF, Reynolds and MCSST temperature data along 55°S in June 1986. Between 75°E and 150°E, SST from the ECMWF are in the range of 2 to 4°C higher than the Reynolds and MCSST. Hart (personal communication) discussed this serious discrepancy with meteorologists at ECMWF in November 1992 and was advised to regard the SST values in the model output as unreliable prior to 1988, after which Reynolds SST were incorporated on a systematic basis. Further analysis of SST in this study have employed Reynolds and COADS SST exclusively.
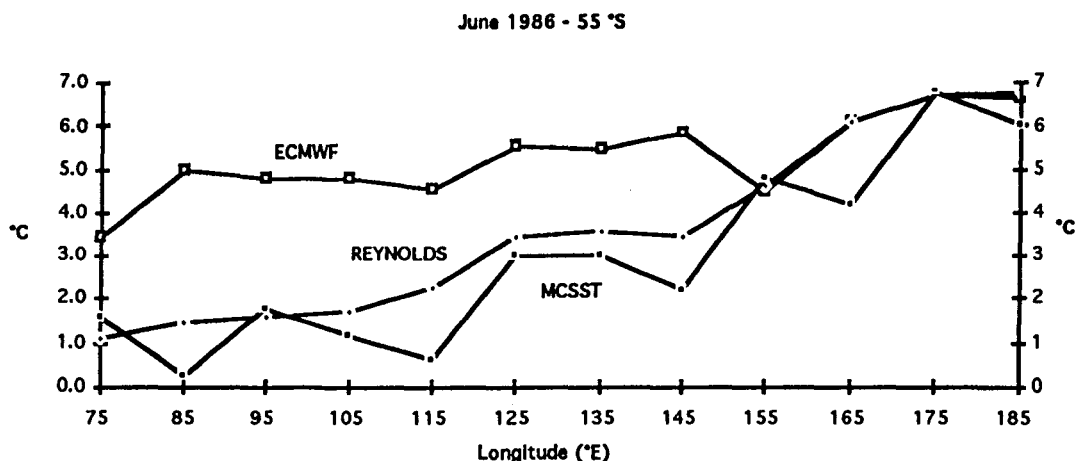
Fig. 2.3. Surface temperature along 55°S in June 1986 according to the ECMWF model, Reynolds blended SSTdata and data from the MCSST.

2.4 Summary

A search of the literature and careful examination of the existing data sets have revealed some inconsistencies for the Southern Hemisphere which could lead to serious errors of interpretation. From the available evidence, the conclusion was reached that the most reliable atmospheric data set for the Southern Hemisphere was that of the Australian Bureau of Meteorology dating from 1972. The most consistent monthly sea surface temperature data for recent years were considered to be those available from the Reynolds blended data set (Reynolds, 1988) while the longer term monthly means of SST were selected from the COADS (Reynolds and Roberts, 1987). As far as possible and except where otherwise indicated, data from these sources have been used exclusively throughout this study.

Data Set	Period of record	Spatial coverage	Parameter measured	Data manager
SHANAL	1972-1991	S H	p,T, z, q, u, v	Australian NMC
ECMWF	1 Jun '86 to 31 Aug '89	36°N-56°S 34°E-70°W	surface T, p	ECMWF
RASP	1 Jun '89 to 31 Aug '89	65 by 40 grid (150 km resolution) Aust.region 70°E - 170°W	u and v at 10 m level	Australian NMC
500hPa gridpoint data	1972 - 1990	SH at 45°S, 55°S at 10° Longitude intervals	z (daily values and 5 day running means)	Pook (1992)
Japanese GMS 3		0 to 60°S 70°E-175°E (at 40°S)	I-R imagery	Bureau of Meteorology
Bathymetry (etopo5)		global ( )	elevation (m)	Dr Peter Sloss, NOAA- NGDC
Wind Maxima at 500 hPa	1976 - present	Southern Hemisphere	geopotential contours (dam) and isotachs (knots)	Dr T Gibson Antarctic Co- Operative Research Centre

Table 2.1. Data description, areal coverage and period of record of data sets employed in this study.

Chapter 3

The Phenomenon of Atmospheric Blocking

3.1 Introduction

There have been many attempts to fashion a comprehensive theory of atmospheric blocking which can explain the initiation stage, maintenance and dissipation of blocked flow. Although considerable progress has been made in studying the separate phases of the life cycle for particular geographical regions the development of a universal model remains elusive.

Part of the difficulty in developing a global theory lies in the differences which have been identified between the characteristics of blocking in the two hemispheres. For a general theory to withstand scrutiny it must explain the apparent contradictions in the patterns of blocking in the Northern and Southern Hemisphere. In particular, the formation of blocks in the Northern Hemisphere commonly occurs upstream of the continents while in the Southern Hemisphere it is observed predominantly downstream of, or very close to, the three continents. Hence dominant forcing mechanisms may be substantially different in the two hemispheres.

Certainly, the absence of topographic influences in the Southern Hemisphere compared to the Northern Hemisphere has been remarked by many authors (see for example, van Loon, 1956 and Coughlan, 1983). Whereas the Himalayas and the Rocky Mountains of the United States, have a dominant influence on the mid-tropospheric flow in the Northern Hemisphere the Andes form the only comparable mountain chain in the Southern Hemisphere. It is noteworthy that the highest elevations in the Andes (>4000 m) lie equatorwards of 35°S. The only other mountain chain of significant dimensions in the mid-latitude westerlies is the Southern Alps of New Zealand which rise to over 3000 m. However, the entire South Island is confined to a north-south extent of approximately 5 degrees of latitude.

3.2 Historical Developments

Although the study of weather in the nineteenth century was preoccupied with depressions or cyclones, Austin (1980) argues that a shift in emphasis occured after Teisserenc de Bort concluded that seasonal weather conditions in Europe were strongly affected by the location and intensity of the major anticyclonic systems of the Northern Hemisphere. Similarly, the dominant influence of anticyclones on Australia's weather was first recognised prior to the turn of the century. Moreover, Russell (1896) concluded that the sub-tropical ridge of high pressure which encircles the Southern Hemisphere is made up of a series of relatively fast-moving individual high pressure cells which migrate from west to east at regular intervals. Russell (1896) also determined that the latitude of the tracks of these anticyclones displayed a seasonal cycle, ranging from between 37°S and 38°S in summer to much lower latitudes of about 29°S to 32°S in winter. However, his study of 1400

meteorological analyses revealed the surprising result that high pressure systems occasionally became stationary over Australia and statistics from 1891 indicated that 6% of anticyclones that crossed Australia in that year 'hesitated or actually stopped in their forward motion' (Russell, 1896, p 5). Despite this difficulty and buoyed by the results of his calculations of average speeds of anticyclones in their travels from South Africa (Natal) to Sydney, he confidently predicted that long range weather forecasting [0(1month)] could become a reality.

> If from Buenos Ayres we could get by cablegram the state of the weather from day to day, we should be in a position to forecast the coming weather for about a month in advance; and it may be that when our investigations, which are now in progress, are completed we shall be able to forecast far longer periods. Russell (1896, p. 9)

Gentilli (1971) comments that Russell's conclusions, first published in 1893, were criticised by others who argued correctly, as later information would confirm, that the anticyclonic cells did not move across the entire extent of the Indian Ocean but tended to form over the central Indian Ocean. A summary of some of the theories of the behaviour of anticyclones over the Southern Hemisphere from the early part of this century can be found in Taljaard (1972).

Karelsky (1954) carried out a major investigation of the frequency of occurrence and locations of low and high pressure centres in the region extending from the eastern Indian Ocean to the south-west Pacific. He developed maps of anticyclonicity and cyclonicity, defined as the time (in hours) during which anticyclonic (cyclonic) centres occupied a given 5° latitude by 5° longitude square during a stated period. This study was based on a data set of Australian Bureau of Meteorology MSLP analyses at 2300 UTC and 1100 UTC. Averages were calculated for the seven year period from 1946-1952 and the statistics were later extended to a fifteen year average (1946-1960) by Karelsky (1961). In a continuation of the earlier study, Karelsky (1956) conducted an investigation of surface circulation types from which he developed a classification scheme which included a category for blocking in the Tasman Sea and New Zealand region. This work has been a valuable resource for climatologists and meteorologists during the past four decades, providing a ready source of information on the preferred locations of cyclonic and anticyclonic centres for each month and each season. The publication also included maps of the average time of passage of anticyclonic and cyclonic centres through 5 degree latitude-longitude squares. Recently, Leighton and Deslandes (1991) have completed a similar study for the period 1965-87, noting that satellite imagery has been generally available during this period as well as additional sources of meteorological data including drifting buoys in the Southern Ocean.

The maps of Karelsky (1954, 1961) and Leighton and Deslandes (1991) clearly show the annual cycle of the sub-tropical ridge as it oscillates between its summer position just to the south of continental Australia and about 30°S in winter. In Fig. 3.1 the secondary maximum of anticyclonicity near and southeast of New Zealand in July is located well south of the mean ridge axis over Australia. This southwards displacement of the anticyclonicity

maximum at New Zealand longitudes contrasts with the low latitude location (between 35°S and 40°S) of the cyclonicity maximum in the North Tasman Sea in winter. It will be shown later that a dipole structure with a high pressure cell polewards of a cyclonic centre at lower latitudes is typical of blocking patterns.

While Karelsky established a climatology of anticyclones in the Australasian region, including a qualitative assessment of the occurrence of blocking, van Loon (1956) conducted an extensive investigation into the occurrence of blocking throughout the Southern Hemisphere. Based on a five year set of surface synoptic charts for the period July 1950 to June 1955, he identified three localities in the hemisphere where significant blocking events tend to occur. In each case the preferred region was found to the east or south-east of the major continents; in the Tasman Sea and south-west Pacific Ocean, in the Scotia Sea region and between Marion and Crozet Islands in the Indian Ocean. van Loon (1956) contrasted the positions of the blocking regions in the Southern Hemisphere with those in the Northern Hemisphere and tentatively concluded that the blocking highs in the south are stabilised by the supply of warm air from the continents to the north-west.

Restricted to surface synoptic data because of the limited upper air network in the Southern Hemisphere, van Loon developed a set of criteria to define a blocking situation. These criteria are discussed in Section 3.4 where comparisons are made with a blocking definiton for the Northern Hemisphere (Rex, 1950a) and a later scheme for the Southern Hemisphere by Wright (1974). Of particular importance was the conclusion that the qualifying period for blocking in the Southern Hemisphere should be six days compared to the ten days required for the Northern Hemisphere (Rex, 1950a). van Loon (1956) argued that this reduction in persistence time was necessary because of the higher mean zonal index in the south and the limitations of the data set.

Gentilli (1971) summarised the historical investigations into the characteristics of anticyclones in the Australasian region without adding significantly to an understanding of the phenomenon. On the other hand, Radok (1971) established the importance of the jet streams in the upper atmosphere to the relative locations of the blocking anticyclones in the Australasian region and the associated cyclonic portions to the north. He drew attention to the zonal velocity minimum of the upper tropospheric winds to the south of the Australian continent in winter and contrasted this region with the Indian Ocean sector where the strongest westerly jet stream is observed. Radok (1971) cited the work of Grant (1952) to extend the understanding of the velocity minimum downstream from the strong zonal flow upstream. Grant (1952) had argued that the seminal contribution of Rossby (1947) to the development theory of jet streams required modification to explain the observed latitudinal profiles of velocity at the level of wind maximum. She altered the equations derived by Rossby (1947) to obtain an expression which gave a more convincing fit to the observations. Radok (1971) concluded that the vorticity generated in the Indian Ocean sector in the intense shear zones of that region becomes more uniformly distributed near Australia leading to barotropic systems of large amplitude and slow

movement. 'In this way the Australian region in winter takes the character of a backwater region, with features unlike those prevailing over the rest of the Southern hemisphere' (Radok, 1971, p. 31).
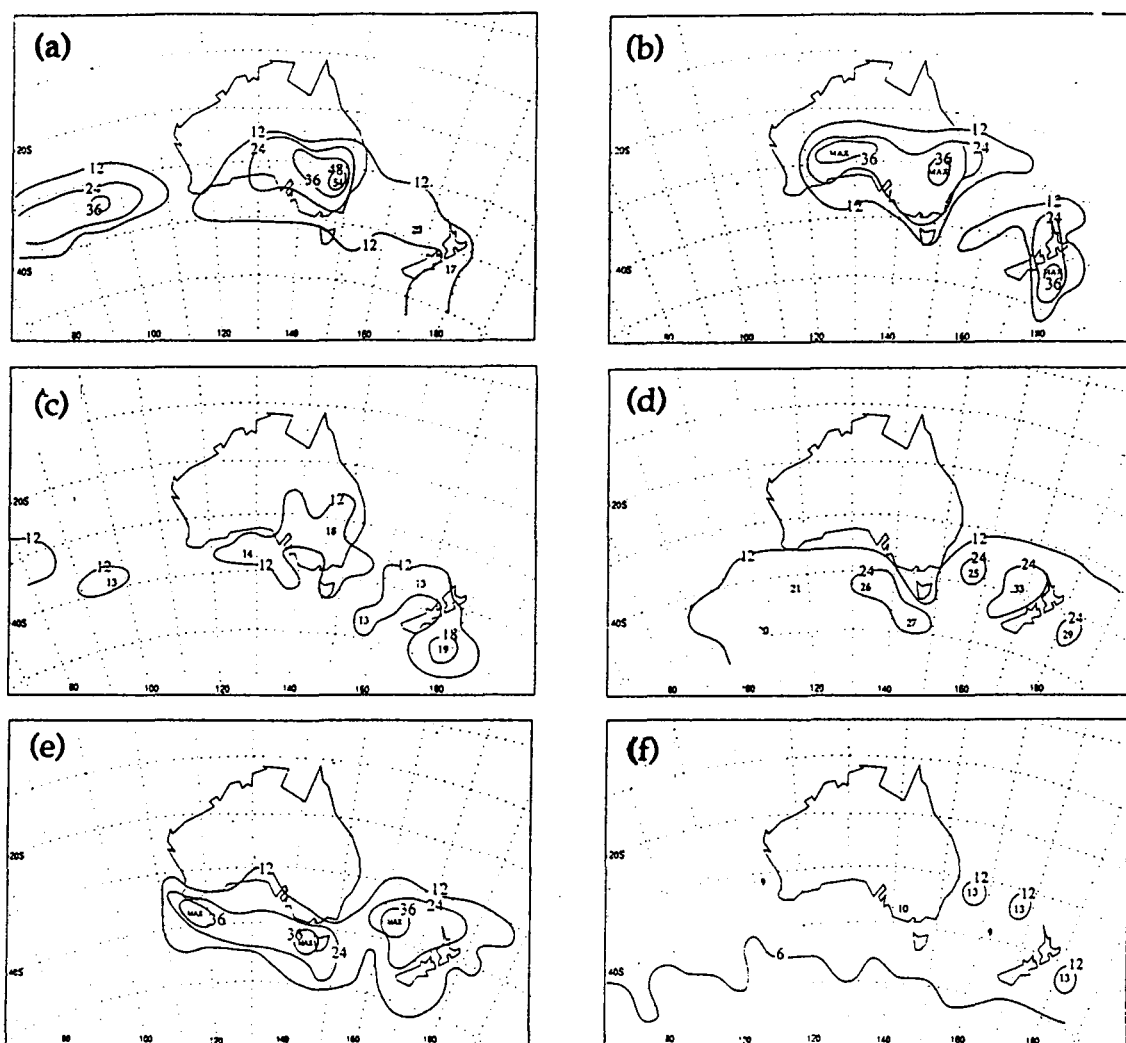

Fig. 3.1 July mean of (a) anticyclonicity; (b) Karelsky (1946-60) anticyclonicity (reproduced in the same form as Leighton-Deslandes charts); (c) anticyclone immobility index (1965-87); (d) cyclonicity (1965-87); (e) Karelsky (1946-60) cyclonicity (reproduced in the same form as Leighton-Deslandes charts); (f) cyclone immobility index. (after Leighton and Deslandes, 1991)

The extensive review of the synoptic meteorology of the Southern Hemisphere by Taljaard (1972) discussed in detail the movement and development of anticyclonic systems. In particular, he emphasised the thermal structure of the anticyclones which form poleward of 40°S, separating the highs into shallow cold-cored systems which form in the cold surges on the western flank of cyclone families and warm-cored blocking systems which intensify as they extend to higher latitudes. Taljaard (1972) reiterated that the movement of highs in the eastern sections of the oceans in the Southern Hemisphere is characterised by a process whereby cells 'bud off' from the parent high pressure cell and form new closed circulation highs to the east. He also pointed to the bifurcated tracks of anticyclones east of Australia and suggested that a primary cause of the asymmetric tropospheric circulation pattern over Australia and the western Pacific Ocean in winter was the SST distribution in the region enhanced by the low temperature of the southern half of continental Australia during this time of year. This surface temperature distribution with southern Australia forming a cold sink within warmer ocean waters to the west, east and south, is partially preserved in the temperature structure which is observed in the upper troposphere and has been associated with a double wind maximum in the middle and upper atmosphere by van Loon (1972b).

Taljaard (1972) also drew attention to the role of the monsoon circulation of southern Asia in enhancing the subtropical jet stream over the central and eastern Indian Ocean during the southern winter. Marked northerly component winds in the upper troposphere in this region form the returning branch of the Hadley cell which transfers the ascended air from the convergence zone over southern Asia to the region of steady descent and warming north of the subtropical jet stream.

Following the expansion of the upper air network, an investigation of blocking activity in the Southern Hemisphere by Wright (1974) made use of MSLP and 500 hPa analyses prepared by the Australian Bureau of Meteorology Southern Hemisphere Analysis Centre (SHAC) and the International Antarctic Analysis Centre (IAAC) for varying periods between 1950 and 1971. Wright (1974) established that, beyond the occurrences satisfying the blocking definition of van Loon (1956), there was a more common phenomenon in which the surface anticyclone did not remain stationary for an extended period but underwent a process of weakening and eastwards movement only to be replaced by a new high pressure cell in the previous location. This behaviour of the surface anticyclones was accompanied by a clearly identifiable ridge in the middle troposphere (500 hPa) which moved only slowly eastwards. Wright (1974) developed a new definition of blocking for the Southern Hemisphere to take account of this occurrence and this has been included in Section 3.4. He also raised the possibility of the longitudinal gradient of SST playing a role in the incidence of blocking and remarked on the apparent persistence of positive SST anomalies in the Tasman Sea region during a period of enhanced blocking activity in the early 1970's.

Hirst and Linacre (1981) re-examined the statistical analysis of Wright (1974) and identified an apparent semi-annual wave of blocking frequency which appeared to propagate through the Australasian region. In Fig. 3.2 the maxima and minima of blocking frequency can be seen migrating from west to east. Hirst and Linacre (1981) conjectured that three waves of this type may be established around the hemisphere at any one time. As well, they postulated that the mean long wave structure in the atmosphere in the Australian region which is characterised by a pronounced trough near 110°E and a ridge at approximately 170°E is most likely to be a consequence of the SST pattern of cold water to the west and warmer water to the east of Australia.

Sector	A	B	C	D
	60°E	110°E	150°E	180°	150°W

	A	B	C	D	Mean*
January	1	7	24	12	9.2
February	5	9	28	13	12.2
March	7	6	11	23	10.6
April	11	5	9	12	9.0
May	9	9	17	8	10.2
June	1	10	31	5	9.8
July	2	3	22	8	7.6
August	2	2	20	12	7.4
September	13	4	13	22	12.4
October	2	8	12	12	7.6
November	5	10	13	3	8.6
December	2	10	21	17	10.8*
Annual mean	5%	7%	18%	13%	10%
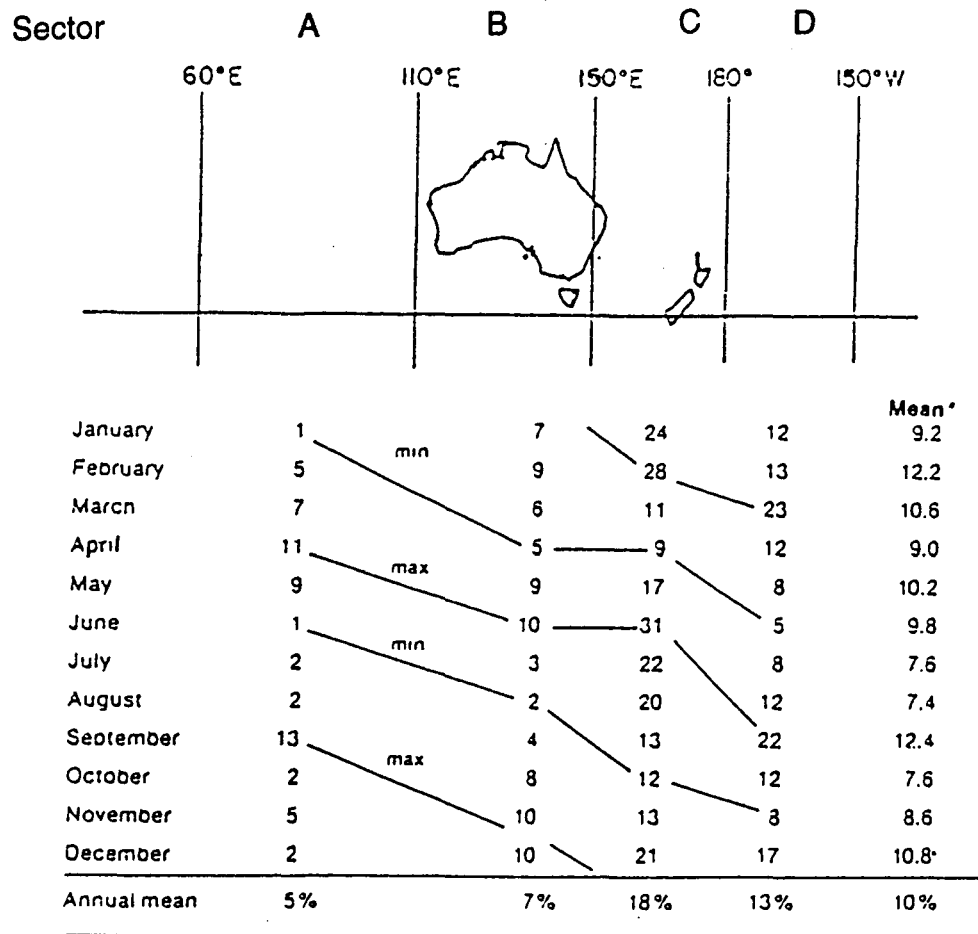
Fig. 3.2 Mean percentage of days on which blocking occurred per 30 degrees of longitude in each month and longitude sector. Lines join months with maximum and minimum frequencies respectively (Hirst and Linacre, 1981).

3.3 Statistics of blocking

The first detailed climatology of blocking activity in the Northern Hemisphere was carrried out by Rex (1950b). He identified two regions where blocking most commonly occurred, in the high latitudes of the eastern Atlantic and the eastern Pacific Oceans. Treidl (1981) conducted an investigation of over 30 years of synoptic analyses and confirmed that the highest frequency of development of blocking highs was to be found in the

eastern Atlantic and over western Europe with a secondary maximum in the eastern Pacific.

In the Southern Hemisphere, van Loon (1956) developed the first systematic climatology of blocking action which identified the three main geographical locations for the incidence of the phenomenon as discussed in Section 3.2. His geographical distribution of blocking was reproduced by Coughlan (1983) as his Fig. 4. Wright (1974) confined his statistical analysis to the region of the Southern Hemisphere from 60°E to 150°W and was able to obtain the relative frequency of blocking action within 10° longitude sectors according to his modified definition (see Section 3.4). Owing to a limited data set of analyses for the Indian Ocean sector (1958-71) the statistics for this region were adjusted to be equivalent to the 22 year period (1950-71) for which data were available in the other sectors (see Fig. 3.2).

Lejanäs (1984) employed a zonal index defined in terms of the geopotential height difference at the 500 hPa level between 35°S and 50°S to investigate the incidence of blocking in the Southern Hemisphere. Negative values of the index for a specific meridian together with negative mean values of the index over the 30° of longitude centred on that meridian are taken as specifying blocking on a given day. His analysis concluded that blocking does not occur as frequently in the Southern Hemisphere and there is one preferred region for blocking in this hemisphere; the Pacific east of Australia. In the other two regions where blocking occurs, viz. the Atlantic and the Indian Ocean Lejanäs (1984) found significantly less blocking than previously reported by van Loon (1956).

A comprehensive comparison of blocking statistics for the Northern and Southern Hemispheres has been given by Coughlan (1983). While acknowledging characteristics common to blocking activity in each hemisphere he drew attention to significant contrasts between the patterns of blocking in the two hemispheres and these are summarised in Table 3.1.

	Northern Hemisphere	Southern Hemisphere
No. of dominant blocking regions	2	3
Meridians of maximum blocking activity	40°E-40°W, 120-170°W	40-70°E, 160°E-160°W, 40-70°W
Position of blocking maxima relative to continents	upstream	downstream
Mean Latitude of blocking action	56°N	45°S

Table 3.1 Characteristics of blocking action in the Northern and Southern Hemisphere (based on Coughlan, 1983).

3.4 Definitions of Blocking Action

A systematic effort to set down criteria by which the phenomenon of blocking could be identified was accomplished by Rex (1950a). Taking advantage of the upper air network which had been established over the Northern Hemisphere by the middle of the century, he identified five necessary conditions for an atmospheric block to occur. These are:

* the basic westerly current (at 500 hPa) must split into two branches,

* each branch current must transport an appreciable mass,

* the split-jet system must extend over at least 45 degrees of longitude,

* a sharp transition from zonal flow upstream to meridional flow downstream must be observed across the current split, and

* the pattern must persist with recognisable continuity for at least ten days.

Owing to the unavailability of comprehensive upper air data for the Southern Hemisphere, van Loon (1956) developed a set of three basic requirements for satisfactorily defining a blocking situation from mean sea level pressure data. He emphasised that the dependence on observations from seasonal whaling operations to complete mean sea level pressure analyses and the unreliability of the existing mean pressure charts made it unsatisfactory to employ pressure anomalies as indicators of blocking activity for the Southern Ocean.

The three criteria of van Loon (1956) are:

* the displacement of the blocking system, as given by the movement of the centre of the high, must be less than 25 degrees of longitude at 45°S during the total period of the blocking.

* the centre of the blocking high must be at least 10 degrees south of the normal position of the sub-tropical high pressure belt as given by Vowinckel (1955).

* the blocking must last for at least 6 days

As discussed in Section 3.2, Wright (1974) identified a more common form of blocking in the Australasian region than the narrow definition of van Loon (1956) could permit. He developed an alternative definition of blocking to take account of the occurrence of a 'process which may be called one of displacement and replacement' (.Wright, 1974; p. 3).

The four criteria of his definition are:

* the basic westerly current splits into two branches.

- the 5-day mean 500 hPa ridge at 45°S (defining the longitude of the block) has a rate of progression of less than 20 degrees of longitude per week and progresses no more than 30 degrees of longitude during the entire blocking occurrence.

- The ridge of high pressure at the longitude of blocking is at least 7 degrees south of the normal position of the sub-tropical high pressure belt (as derived by Taljaard *et al.* , 1969) and is maintained with recognisable continuity.

- The occurrence lasts for at least six days.

It is noteworthy that none of the definitions which have been discussed in this chapter include consideration of the cyclonic portion of the blocking dipole structure although Wright (1974) asserts that the cyclonic systems involved cannot be regarded as less important than others.

Charney *et al.* (1981) commented on the diversity in the criteria applied to the identification of blocking events from climatological data. They reduced the criteria to two basic principles, the kinematic structure of the flow pattern and its longevity. Because of the restrictions imposed by their dynamical model they chose a semi-objective definition based on the persistence of geopotential height anomalies in daily 500 hPa analyses. Departing from some previous schemes which had arbitrarily selected one standard deviation as the threshold for a significant anomaly Charney *et al.* (1981) sought a more soundly based criterion. From an analysis of data from 15 Northern Hemisphere winters from 1963-77 they concluded that a positive anomaly of 20 dam persisting for at least 10 days was a useful definition of a blocking event, provided the physical presence of a ridge could be established. Trenberth and Mo (1985) developed an objective method to determine the temporal frequency and spatial distribution of blocking in the Southern Hemisphere. Essentially, their objective definition of blocking requires a large positive anomaly (e.g. ≥ 10 dam) of 500 hPa geopotential height to persist for at least 5 days. The anomalies calculated in their analysis were obtained by subtracting the grand mean plus the first 4 harmonics of the time series for each grid point in order to remove the annual cycle in a similar manner to Trenberth and Swanson (1983).

3.5 Indices of Blocking Action

Wright (1974) has described a blocking index (BI) which was developed by the Extended Forecast Section of the Bureau of Meteorology in Melbourne. The BI has been in continual use since the 1970's and is defined as:

$$BI = U_{27.5} + U_{57.5} - (U_{42.5} + U_{47.5}) \quad \ldots\ldots\ldots\ldots 3.1$$

where U represents the zonal component of the mean geostrophic wind at the latitude (°S) specified by the suffix. Hence the index measures the relative influences of the zonal components of the geostrophic wind at middle, high and low latitudes. High values of BI indicate situations in which the high and low latitude westerly winds are strong or the mid-latitude westerly flow

is weak, or a combination of both. Configurations of this type correspond to blocking activity but the index is unable to convey information on the degree of meridionality of the flow or the latitudinal separation of the zonal wind maxima.

An alternative index of blocking has been developed by Gibson (1994, personal communication) which attempts to provide an objective measure of the degree to which the polar wind maximum (PWM) and the subtropical wind maximum (STWM) are separated at a given longitude. This index is defined as:

$$\beta_i = 3[\sin \phi_{pi} - \sin \phi_{si}] - [\sin \phi_{p(i-1)} + \sin \phi_{p(i+1)}] + [\sin \phi_{s(i-1)} + \sin \phi_{s(i+1)}] - [\sin \phi_p - \sin \phi_s]$$

$$.................... 3.2$$

where ϕ_{pi} and ϕ_{si} are the weekly mean latitudes in longitude sector i, of the PWM and STWM respectively, and ϕ_p and ϕ_s represent the area-averaged means (at ten degrees of longitude) of ϕ_{pi} and ϕ_{si} around the hemisphere. The index registers high values when there is a persistent 'split' in the westerlies so that the PWM and STWM are well separated during the period under consideration. During these situations the first two terms in Equation 3.2 exhibit large positive values.

Gibson (1993) has employed his blocking index to investigate trends in the occurrence of winter blocking events in the Southern Hemisphere during the decade 1982-91. He concluded that there is an apparently decreasing trend for blocking activity in the hemisphere and in the region from 75°E to 175°W over the decade, but the trend is not statistically significant. On the other hand, poleward trends in the mean latitudes in winter of the STWM of 1.8 degrees of latitude per decade and the PWM of 1.1 degrees of latitude per decade were found to be statistically significant.

3.6 Proposed Mechanisms for Blocking Development

At the heart of the question of predictability of the atmosphere are the spatial and temporal scales of the influential waves. Gill (1982) has discussed the problem of adjustment of a rotating fluid in a gravitational field and summarised the characteristic scales of the equilibrium states of the atmosphere and ocean. Considerations of divergence and the conservation of quantities such as potential vorticity rule out the possibility of large anticyclonic cells preserving their individual identity as they encircle the earth in the manner envisaged by Russell (1896). Rather the climate system has to be regarded as dynamic with the regular development, evolution and decay of eddies of synoptic scale dimensions within the broad pattern of planetary Rossby waves.

Within this framework, it is possible for anomalous flow patterns, such as blocking and other quasi-stationary phenomena, to emerge in the atmosphere. Gill (1982, p543) has discussed how "studies of the forcing of barotropic flow by topography indicate that it is possible to have two stable response patterns to the same forcing. In one, the forcing produces a strong zonal flow which is so fast that standing waves are not produced by the

topography. .... The alternative pattern has the flow slightly subcritical". This pattern is similar to blocking.

Rex (1950a) examined blocking as a possible analogue of the 'hydraulic jump' phenomenon in an open channel. Later, Egger (1978) cautioned that the analogy was flawed because the intensity of the turbulence generated in a hydraulic jump contrasts markedly with the observed flow patterns in blocking highs. Egger (1978) employed a simple model of the atmosphere to demonstrate that blocking can be caused by the nonlinear interaction of forced waves with slowly moving free waves.

Austin (1980) investigated the role of planetary waves in the development of blocking anticyclones. She concluded that stationary planetary waves forced by thermal gradients and topography can amplify and, while retaining their normal phase, interfere with one another to split the mid-tropospheric flow. The result is that the synoptic-scale cyclonic vortices are steered to the south and north producing vorticity anomalies near the tropopause and contributing to the maintenance of the block in the manner described by Green (1977). Schutts (1983) proposed an 'eddy straining hypothesis' in which anticyclonic forcing occurs on the poleward side and cyclonic forcing is found on the equatorwards side of the blocking region. Questioning the hypothesis of Green (1977) which proposed that 'eddy transfer of vorticity could maintain a blocking anticyclone against surface dissipation without implying that it might cause a block', Schutts concluded that vorticity transport by eddies can maintain blocking patterns against "being blown away by the mean flow rather than against friction" (Shutts, 1983. p 741).

Coughlan (1983) has extended Austin's approach to the Southern Hemisphere, identifying enhanced wave numbers one to four as being favourable to blocking activity in the Australasian and west Pacific Ocean. He placed considerable emphasis on the positions and orientations of the troughs of these planetary waves, particularly over the Australian region where there is a pronounced bowing of wave number one in winter contrasting with a westward tilt of wave number two. The combination of the two in winter demonstrates that momentum transfer occurs into the sub-tropical jetstream from both the equatorward and poleward sides.

Baines (1983) has reviewed the literature of blocking and identified various mechanisms postulated as capable of initiating blocking action and two mechanisms which he regarded as potentially contributing to the maintenance of blocking. His review of the mechanisms regarded as possible initiators of blocking action considered four main candidates; hemispheric resonance of forced Rossby waves, local enhancement or 'resonance' due to superposed effects forcing Rossby lee waves, non-linear interaction of forced lee waves and, baroclinic instability of three-dimensional flows. For the Southern Hemisphere and particularly, the Australasian region, his conclusion was that blocking was not generally hemispheric in character but essentially a local atmospheric response. Baines (1983) suggested that the most likely mechanism leading to the onset of blocking in the region was baroclinic instability induced by thermal forcing or possibly orographic influences in the manner suggested by Frederickson (1983, 1989). He further

argued that this identification of a mechanism did not deal with the problem of isolating the processes which create the initial instability in the flow. Such processes are associated with heat, momentum and vorticity advection which is presumably triggered by the local forcing due to thermal and topographic influences. The important distinction (from other models) in this theory is that 'the blocking situation arises spontaneously from some other possibly quite different state, and need not be forced directly (Baines, 1983; p 30-31).

Karoly (1983) has suggested the possibility that blocking may be a manifestation of planetary scale horizontal teleconnections in the troposphere. His review of observational and modelling studies of teleconnection patterns was confined to the Northern Hemisphere as most upper air time series for the Southern Hemisphere are limited in spatial coverage and period of observation. As a possible explanation of the observed and modelled patterns Karoly (1983) discusses properties of planetary wave propagation on the sphere and concludes that the propagation of forced,stationary, barotropic Rossby waves is one of the basic processes operating. The wave train path closely resembles a great circle path.

3.7 Suggested Maintenance Mechanisms

Charney and De Vore (1979) have investigated a periodic barotropic channel flow with forcing and concluded that the system could have three equilibrium states, provided the system is close to resonance and the forcing is sufficiently large. One of the resulting states is unstable and, of the two stable states, one has a high zonal index and the other, meridional or low index structure corresponding to a blocking situation. This approach has been challenged by Lindzen (1986) who argues that the resonance condition which is required to be met is unlikely to be achieved in realistic situations. Similarly, Baines (1983) discounts the model of Charney and De Vore (1979) for the Australian region suggesting that substantial modification would have to be made to take account of the local rather than hemispheric nature of blocking action in the region. He postulates that the maintenance of blocking is most likely related to the dipole-like 'modon' solutions of the equations of motion for solitary Rossby waves. Baines (1983) derived a solution requiring a quadrupole configuration of heating and cooling and argued that the thermal forcing in this situation could be provided by a realistic SST pattern.

General Circulation Models (GCM) offer the possibility of realistic simulations of blocking activity in the atmosphere and the prospect of testing hypotheses in sensitivity experiments. Lau (1992).suggests that recent applications of numerical models to blocking have revealed that the structural characteristics of blocking highs in a model atmosphere are in good agreement with the observations. Bengtsson (1992) has reported that improvements to the specifications in the European Centre for Medium Range Forecasts (ECMWF) model have resulted in advances in prediction and simulation of blocking. By changing various forcing factors in the GLA fourth-order GCM Mo *et al.* (1987) examined the conditions contributing to

the maintenance of a blocking episode in the Australasian region throughout a period of two weeks in June 1982. They concluded that the block was maintained by asymmetric heating resulting from land-sea thermal contrast in the Australia-New Zealand region. As will be discussed in Chapter 6, Kung *et al.* (1990) demonstrated for the Northern Hemisphere that predictability of winter blocking can be enhanced when a realistic SST pattern is prescribed.

3.8 Dissipation of Blocking Action.

There has been very little discussion in the literature on the breakdown and dissipation of blocking systems. Presumably, it is implicitly assumed that the decay process is essentially the reverse of the initiation and maintenance processes. Baines (1983) speculates that a block may result in particular patterns of air-sea interaction which could eventually alter the meridional gradients of SST which favoured the maintenance of blocking in the first instance. He suggests that studies of the fluxes of heat, water vapour and momentum between ocean and atmosphere are required during blocking situations to determine the extent to which the atmosphere and ocean interact.

3.9 Conclusion

Blocking in the Southern Hemisphere has been found to have the characteristics of an essentially local phenomenon. It occurs most frequently in three preferred locations to the east or southeast of the continents. Of these three regions the sector which includes the Tasman Sea and the southwest Pacific is the dominant zone for blocking activity throughout the hemisphere. Blocks appear as local enhancements of the climatological low index circulation in this region with frequency maxima in winter and early spring and to a lesser extent, in summer.

Of the many hypotheses put forward to explain the onset of blocking in a particular location, baroclinic instability has gradually gained favour as the most likely mechanism. Once established, the blocking behaviour needs to be maintained. The main candidate for this function in the Southern Hemisphere, at least, is the so-called 'modon' mechanism discussed by Baines (1983). In this process thermal forcing can be provided by SST patterns.

Processes which lead to the dissipation of blocking action have not been widely studied and progress in this area is dependent upon advances in the understanding of the mechanisms of development and maintenance.

Chapter 4

An extended period of blocking action in the Australasian region in 1989

4.1 Introduction

During the winter and early spring of 1989, a persistent pattern of quasi-stationary anticyclones occurred in the Australasian region. In winter, this behaviour was regularly identified in the Tasman Sea and New Zealand region, and in September, significant positive mean sea level pressure (MSLP) anomalies were observed in the southwest Pacific Ocean region (see e.g. NOAA Climate Diagnostics Bulletins, 1989; Bureau of Meteorology Climate Monitoring Bulletins, 1989). The pronounced atmospheric circulation changes accompanying the slow-moving highs resulted in a major redistribution of winter rainfall patterns in southern Australia with parts of western and central Tasmania experiencing serious deficiencies, while the Bass Strait islands and southeastern Victoria recorded significantly above average rainfall (Gaffney, 1990b).

As well, there were marked differences between the distribution of temperature anomalies over continental Australia and Tasmania during the winter months. Gaffney (1990a) reported that the autumn of 1989 was a period of below-normal maximum temperatures and above-average minimum temperatures over the mainland and he attributed these anomalies to extensive cloud coverage and record rainfall throughout most of northern and eastern Australia. In the winter of 1989 negative anomalies of maximum temperature (-1 to -2°C) persisted throughout most of mainland Australia while minimum temperatures were close to average over the majority and a little below average in a belt extending eastwards from Western Australia across the interior of the continent (Gaffney, 1990b). By way of contrast, maximum temperatures were close to average in Tasmania during the winter but there were negative anomalies of minimum temperature for western and central Tasmania for the same period, suggesting a decrease of cloudiness and, or windspeed from the climatological means (see e.g. Bureau of Meteorology, Monthly Weather Reviews, Tasmania).

In this chapter anomalies of climatological elements will be estimated for the winter and early spring of 1989. Monthly and seasonal anomalies will be developed to investigate the intensity and longevity of the anomalous circulation patterns observed during the period. Additionally, individual blocking episodes occurring during this period will be identified from a variety of analyses and from published climatological summaries. Since the slow movement of anticyclones in the Tasman Sea and New Zealand region is not unusual (van Loon, 1956; Wright, 1974; Hirst and Linacre, 1981; Trenberth and Mo, 1985) further analysis is required to determine whether the situations involving high latitude ridging qualify as 'blocking' events. Various criteria have been applied to define a 'block' in the Southern Hemisphere. The schemes of van Loon (1956), Wright (1974) and Trenberth and Mo (1985) have been discussed in Chapter 3. The technique of van Loon

is confined to analysis of the MSLP fields and has not been used here. On the other hand, Wright developed a set of criteria from surface pressure and 500 hPa geopotential data and Trenberth and Mo (1985) concentrated on the 1000 hPa and 500 hPa pressure levels, making exclusive use of analyses for the Southern Hemisphere from the Australian National Meteorological Centre. These sets of criteria have been applied to the data and the results are presented in Section 4.11.

The first step in the analysis will be to investigate the structure and evolution of the major jet streams during the period and the persistence of anomalies. This will be followed by analyses of the mid-tropospheric geopotential fields, 1000-500 hPa thickness and surface pressure, wind and precipitation. Circulation indices relating to the strength of the zonal westerlies, blocking intensity and the Southern Oscillation will be applied to the situation and time-series of the indices developed to indicate interannual variability.

4.2 Jet Stream Structure

The definition of blocking attributed to Wright (1974) requires that the upper westerly flow splits into two branches which transport mass to the north and south of the block. This behaviour of the westerlies is commonly referred to as a 'split jet' structure. Numerous authors have pointed out that a cyclonic portion of the blocking system is frequently present north (S. H.) of the high pressure centre (Wright, 1974; Coughlan, 1983; Baines, 1990). It is proposed here that the diffluent flow pattern associated with a split can be separated into two main types, which are recognisable on upper air analyses and geopotential thickness charts. In each case a cold-cored low pressure centre is found equatorward of a warm-cored high presure cell. A schematic depiction of one possible flow model is shown in Fig. 4.1(a) and this will be defined as a cyclonic involution in this study. This configuration is frequently referred to as a tilting trough which has the effect of transferring westerly momentum equatorwards. Fig. 4.1(b) depicts the alternative case of the anticyclonic involution which is similar to Fig. 1 of Coughlan (1983).
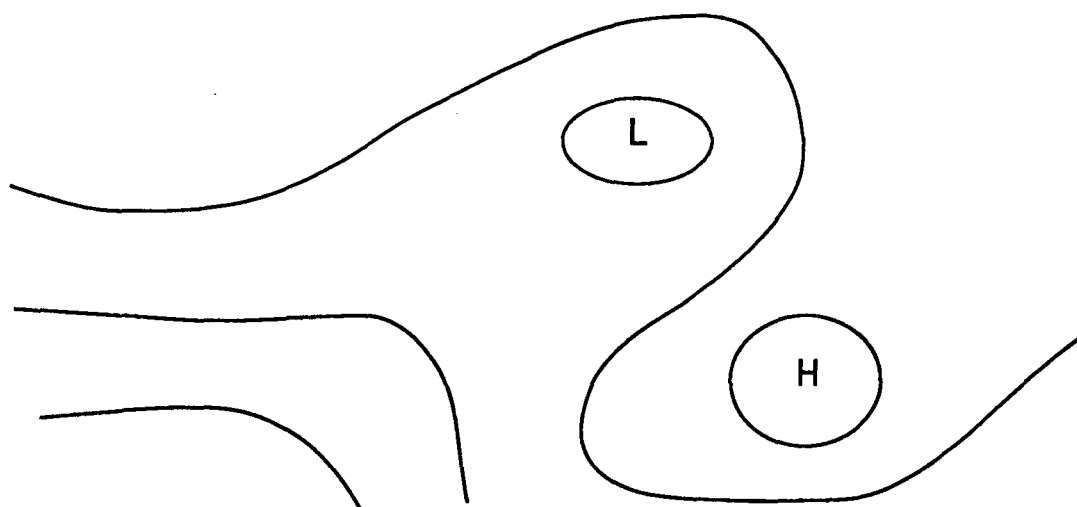
Fig. 4.1 (a). The configuration of geopotential thickness contours known as a cyclonic thermal involution.
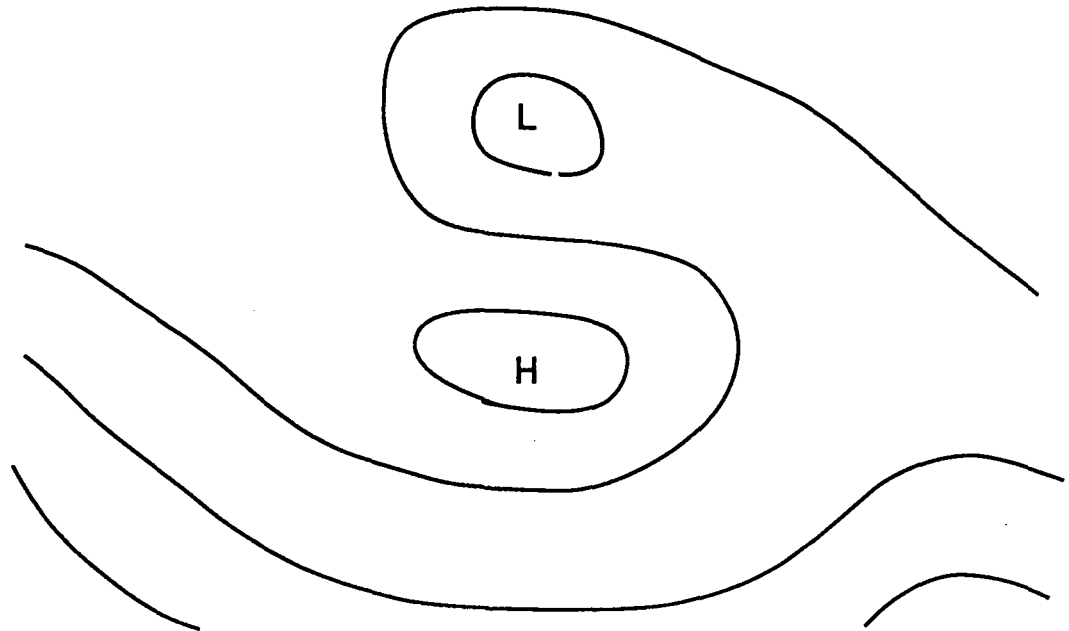
Fig. 4.1(b). An anticyclonic thermal involution.

In this section mean wind maxima or jet streams have been identified from monthly and seasonal climate reviews of the Southern Hemisphere circulation. In some cases of apparent blocking individual wind maxima on daily analyses have been located and tracked over time. In identifying significant blocking episodes satellite imagery, including movie loops, has been employed as a first indicator of blocking action. An example of this powerful tool is given in Fig. 4.2 which shows a cloud scene over the Australian region from the infra-red radiometer on the Japanese geostationary satellite, GMS 3, during an episode of high-latitude ridging on 24 July 1989. The 0000 UTC (1000 EST) image reveals the absence of cloud in western Tasmania and the surrounding ocean, a cut-off low pressure system in the North Tasman Sea and an extensive area of closed cellular cloud (stratocumulus) in the South Tasman Sea and south of New Zealand. consistent with high pressure ridging in the area (Guymer, 1978). To the west, cold fronts can be seen in the cyclogenetic region south and southwest of Western Australia.

Although the synoptic chart has been the traditional vehicle for depicting the development, movement and decay of major weather systems, experience extending over 15 years of geostationary satellite imagery for the Australian region has emphasised the value of the 'view from space'. The characteristic signature of blocking observed from the satellite is most striking on time-lapse film loops. Cold fronts approaching a stationary high, as in the situation of 24 July 1989 shown in Fig. 4.2, are observed to lose intensity rapidly as their associated depressions are steered southeastwards over the Southern Ocean. Fig. 4.3 demonstrates this process occurring on 25 July 1989 with clear indications that the cloud band to the south of Tasmania has become disorganised. By 26 July 1989 (not shown), the cold front had dissipated to such an extent that it could not be discerned on GMS satellite imagery.

Fig. 4.2 (opposite) A cloud scene over the Australian region from the infra-red radiometer on the Japanese geostationary satellite, GMS 3, at 0000 UTC (1000 EST) on 24 July 1989 during an episode of high-latitude ridging . The image reveals the absence of cloud in western Tasmania and the surrounding ocean, a cut-off low pressure system in the North Tasman Sea, a cold front south of Western Australia and an extensive area of closed cellular cloud in the South Tasman Sea and south of New Zealand.
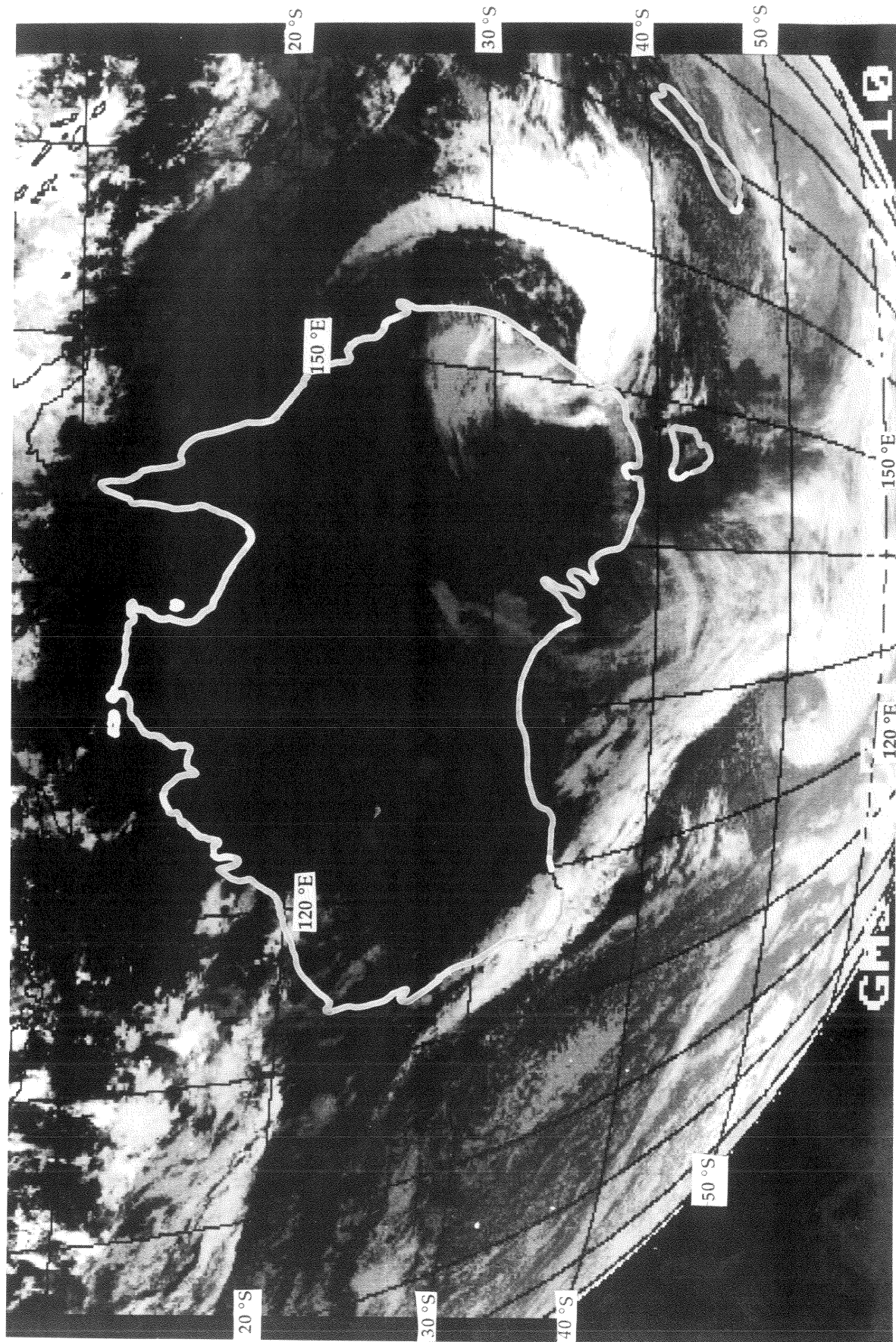
Fig. 4.3 (opposite) An infra-red image at 0000 UTC (1000 EST) on 25 July 1989 from GMS 3 indicating that the cloud band associated with the cold front to the south of Tasmania has become disorganised.
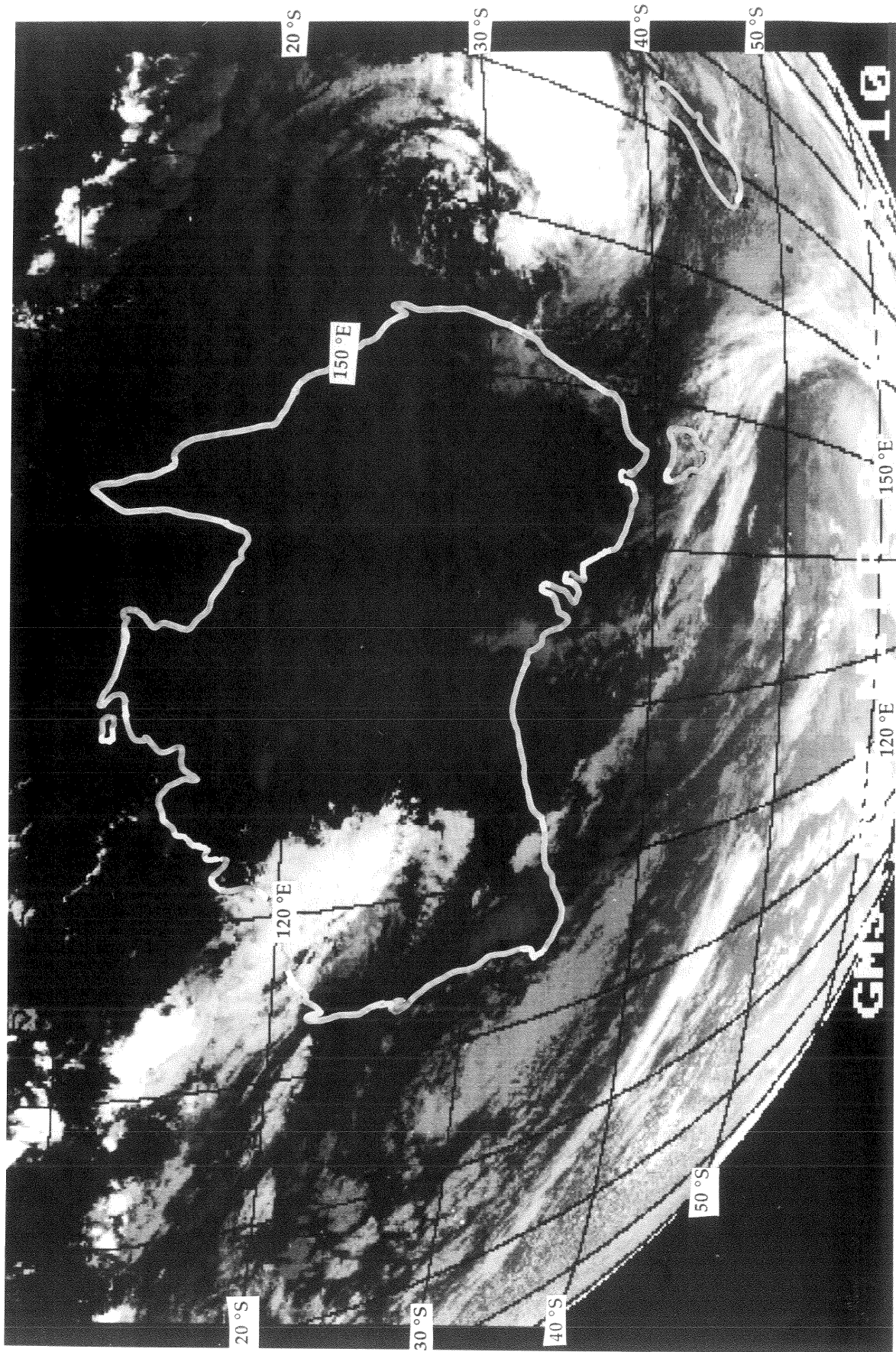
In a set of Training Notes on the interpretation of satellite cloud imagery, Bell *et al.* (1988) contend that the position of the upper tropospheric wind maximum or jetstream can be inferrred from the characteristic cloud pattern which occurs on the warm (equatorial) side of a baroclinic zone. Drawing heavily on the pioneering work of Weldon (1975) they have adapted his extratropical cloud model to the Southern Hemisphere by a simple process of creating an inverse mirror image of the original Northern Hemisphere model. The three principal components of this model are:

a) the jet associated cloud,
b) the vorticity comma cloud, and
c) the vortex deformation cloud.

Although playing an important role in the identification of frontal systems and depressions the 'comma' cloud and vortex deformation cloud will not be discussed further. The jet associated cloud (the so-called 'baroclinic leaf') results from upward motion of moist air in the warm conveyor belt, the main properties of which have been described by Mason (1985). On the poleward side, descending motion produces adiabatic warming and drying in the air moving through the upper trough, resulting in a sharp cloud border. The wind maximum is considered to occur in the clear air close to, and poleward of, the cloud band (Bell *et al.*, 1988). Fig 4.4 illustrates a typical configuration of baroclinic leaf, relative wind maximum and upper tropospheric trough in the middle latitudes of the southern hemisphere.
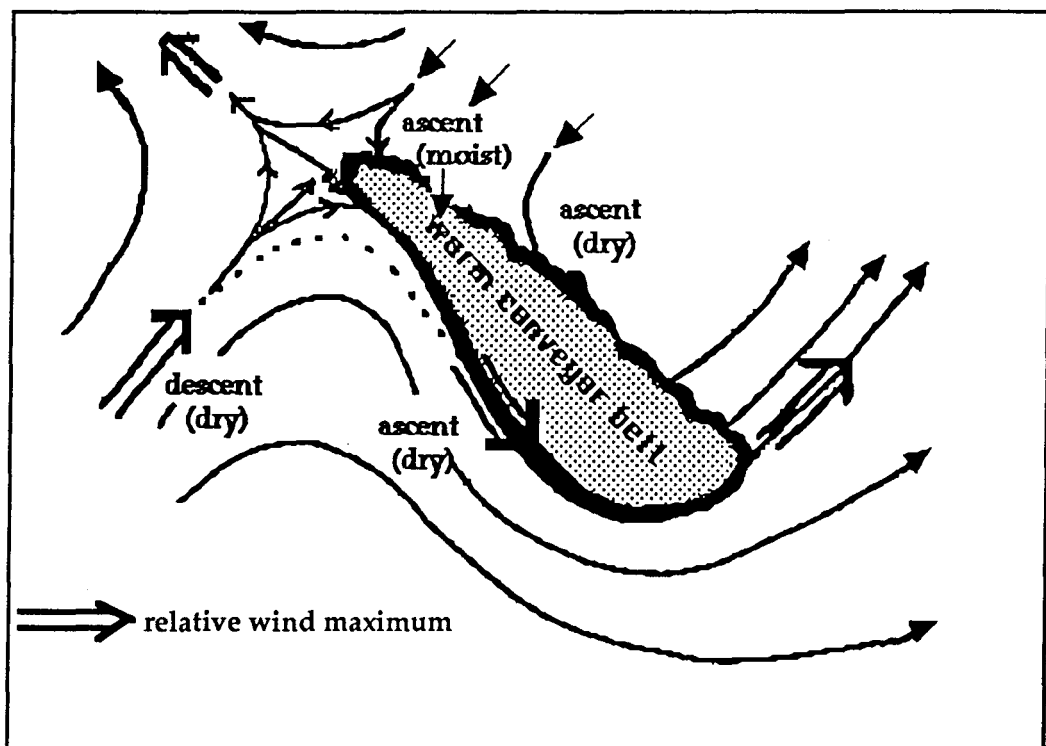
Fig. 4.4 Schematic diagram of the relative airflow in a warm conveyor belt originating at low altitudes and ascending ahead of the trough (after Bell *et al.*, 1988).

Using this model, the location of the speed maxima of the upper level westerly winds can frequently be inferred from satellite imagery. Fig. 4.5 demonstrates the jetstream configuration over Western Australia and the Great Australian Bight at 00 UTC on 21 July 1989, during a blocking event. In this example, sharp cloud edges on the poleward sides of the major cirriform cloud masses over northwestern and southwestern Australia have been interpreted as indicating the positions of the sub-tropical wind maximum (STJ) and an arm of the Polar Front Jet (PFJ). The proximity of the wind maxima suggests that interaction has occurred between the two jet streams eastwards of a cold trough which is located over the southwest corner of Western Australia. Immediately downstream, the PFJ filament has deviated southeastwards while the STJ limb has continued eastwards, providing a source of cyclonic vorticity via horizontal shear, to the cut-off cyclone in the Tasman Sea. The cloud band to the west of Tasmania near 140°E appears to be undergoing deformation along an axis running northeastwards into western Victoria. The appearance of this cloud band combined with the subsidence and inferred outflow in the South Tasman Sea indicates the presence of a neutral point in the flow to the southwest of Tasmania.

Gibson (1989, 1992) has conducted systematic daily analysis of the principal wind maxima at 500 hPa throughout the Southern Hemisphere since 1976. In his analysis scheme, four major wind maxima are isolated on the ANMC Southern Hemisphere Analysis at 1200 UTC each day. The wind maxima are treated as proxies for the jetstreams which occur at higher levels near the tropopause. The 'jets' are named according to their latitudinal range as Sub-Tropical, Mid-Latitude, Polar and Antarctic, respectively. Daily locations of these wind maxima are consolidated regularly into a weekly average position.

For the situation shown above (viz. 21 july, 1989), the analysis of Gibson (personal communication, 1993) in Fig. 4.6 (a) clearly shows the splitting of the westerlies into two main branches at 1200 UTC on 20 July 1989, 12 hours prior to the cloud imagery in Fig. 4.5. The availability of the upper wind observations has enabled the analyst to identify a mid-latitude wind maximum (MLJ) between the STJ and PFJ and the analysis indicates that interaction has occurred between the PFJ and MLJ rather than the STJ as inferred from the interpretation in Fig. 4.5. Obviously, such fine detail is not readily available from the cloud imagery alone. The change in wind direction from northerlies south of Western Australia to southerlies over Tasmania requires the presence of a neutral point west of Tasmania as suggested in Fig. 4.5.

Subsequent behaviour of the wind maxima is indicated in Figs. 4.6 (b), 4.6 (c) and 4.6 (d) at 24 hour intervals. This sequence of analyses reveals as well the dynamic nature of the cyclonic portion of the blocking system. The cut-off depression over the North Tasman Sea on the 20 July appears to have been revitalised by the development, cutting off and eastwards migration of another low over the Great Australian Bight on 21, 22 and 23 July 1989.

Fig. 4.5 (opposite) The jet stream configuration over Western Australia and the Great Australian Bight at 00 UTC on 21 July 1989, during a blocking event. STJ represents the sub-tropical wind maximum and PFJ, the northern filament of the polar wind maximum. The cold trough over the southwest corner of Western Australia has been located by the open cellular cloud off the west coast.

150 °E

cut-off low

STJ

PFJ

120 °E

cold pool

trough

20 °S

30 °S

40 °S

50 °S

20 °S

30 °S

40 °S

50 °S

120 °E

150 °E
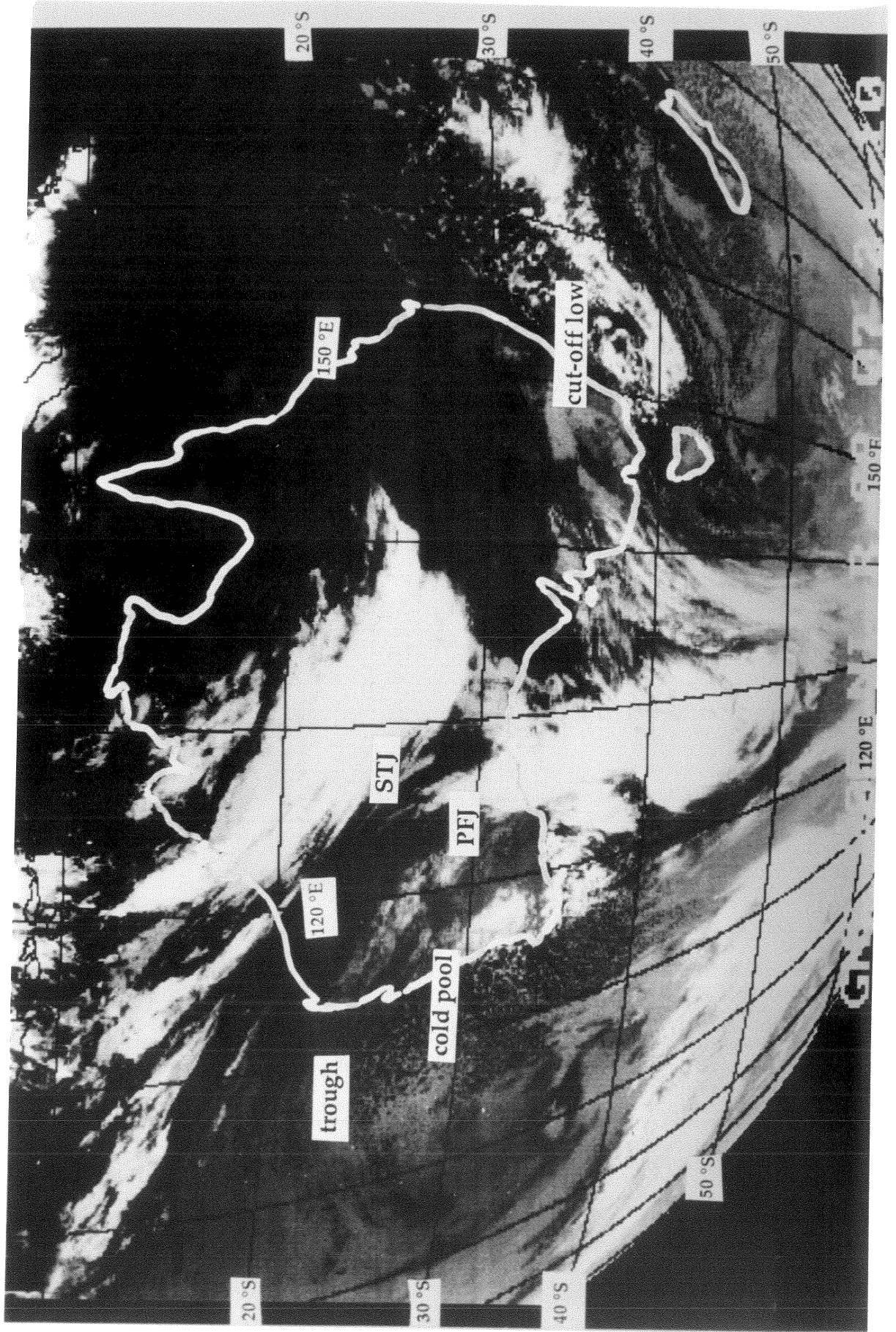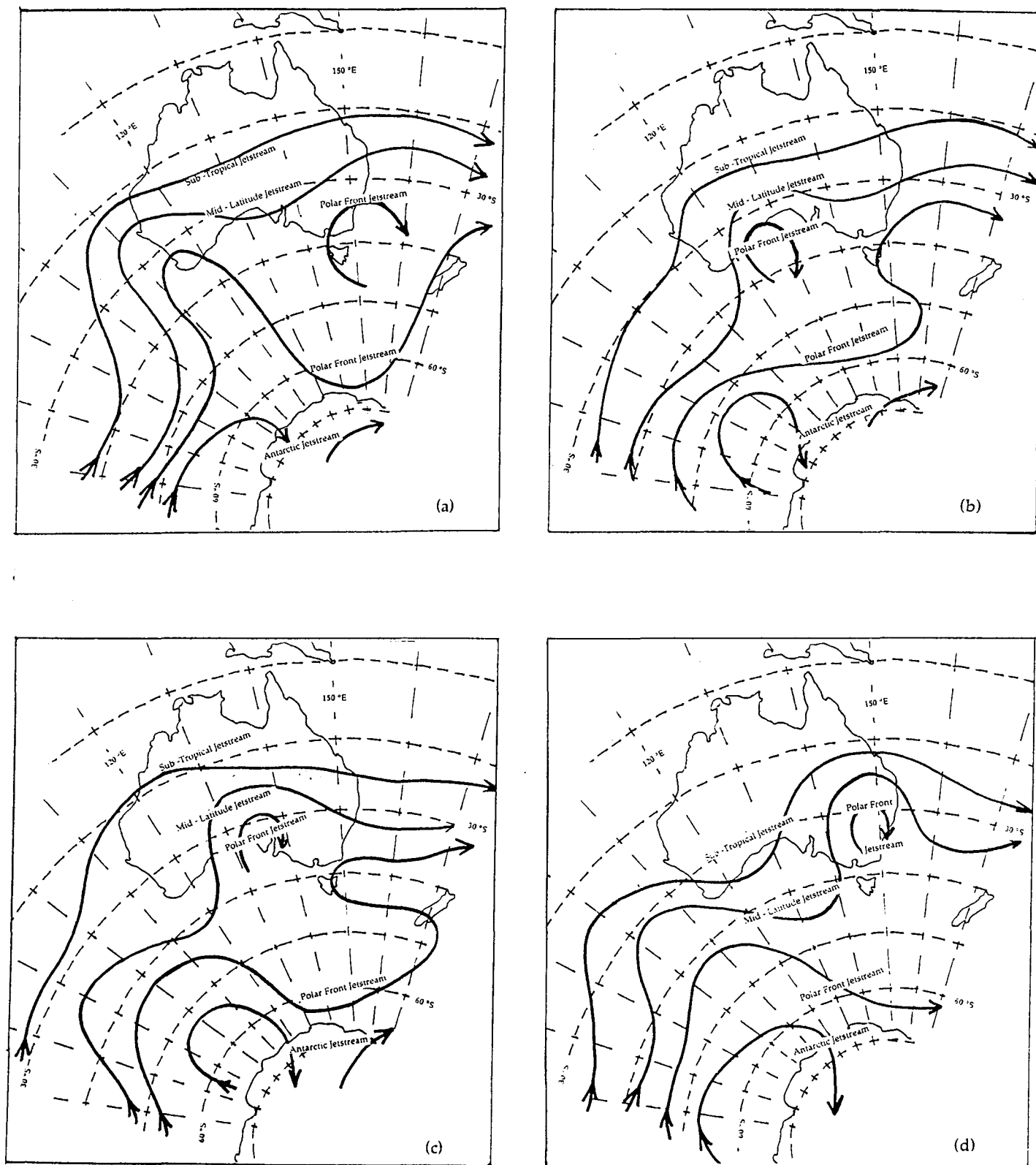
Fig. 4.6 The configuration of the jet streams during a blocking event showing the splitting of the westerlies into two main branches at 1200 UTC on (a) 20 July 1989, (b) 21 July 1989, (c) 22 July 1989 and (d) 23 July 1989 (after Gibson,1993).

A set of upper air analyses has been obtained from the Bureau of Meteorology's Tasmanian Regional Forecasting Centre in Hobart, for the period under consideration (see Chapter 2). These analyses are the forecasters' working versions and have not undergone post-analysis, nor have the observations been subjected to a systematic verification procedure. On some charts the method of analysis is by way of a streamline-isotach technique, while, on others, contours of geopotential height have been interpolated. However, in a significant number of cases winds estimated from satellite imagery have been plotted at lags of approximately 6 hours. For the situation on the 21 July 1989, I have incorporated the satellite derived winds for the 400 hPa level at 00 UTC into the 300 hPa chart and reanalysed the chart. The reworked analysis (Fig. 4.7) shows peak wind speeds exceeding 160 knots (86 m s^{-1}) over central and eastern Australia, a sharp split in the flow pattern south of the Great Australian Bight and a region of very light winds (less than 20 knots) over and to the south of the South Tasman Sea.

Obviously, the satellite wind observations have particular value over the Southern Ocean, which is universally recognised as a data-sparse region (Venter, 1957; Trenberth, 1979; van Loon and Shea, 1988; Karoly, 1989). The only observations available from land platforms in this region are surface and upper air reports from Macquarie Island and surface observations from Campbell Island, south of New Zealand. In the situation shown in Fig. 4.7 there remains a region to the southwest of Western Australia which is particularly important in determining the structure of the jetstream but for which there were no direct observations of geopotential height or wind.

In situations where there are no upper air observations an alternative analysis technique can be employed to determine atmospheric thickness and, hence, by thermal wind argument, the jetstream structure. Guymer (1978) developed a system of analysis whereby an experienced analyst could combine interpretation of satellite imagery with mean thickness and MSLP fields to construct a 1000-500 hPa thickness chart. Using ESSA visible light imagery and extending the pioneering work of Martin (1968), Zillman (1969), Zillman and Price (1970, 1972), Troup and Streten (1972), Streten and Troup (1973) and Streten and Kellas (1973), he produced thickness anomalies which could be tied to recognisable features of the cloud field. With the increased availability of TIROS Operational Vertical Sounder (TOVS) data, this method has fallen out of favour but, in the situation under consideration, the technique provides a semi-objective means of employing GMS imagery to complete the analysis.

Guymer (1978) has argued that the maximum thickness gradient, indicating the approximate position of the polar front jetstream, will be found between 536 and 544 dam when the curvature of the contours is cyclonic, and between 536 and 528 dam when the curvature is anticyclonic, the latter case resulting in a super geostrophic wind. In Fig. 4.7 the ridge over the Southern Ocean to the southwest of WA has been determined by first locating the 1000 to 500 hPa thickness ridge according to the technique described above and
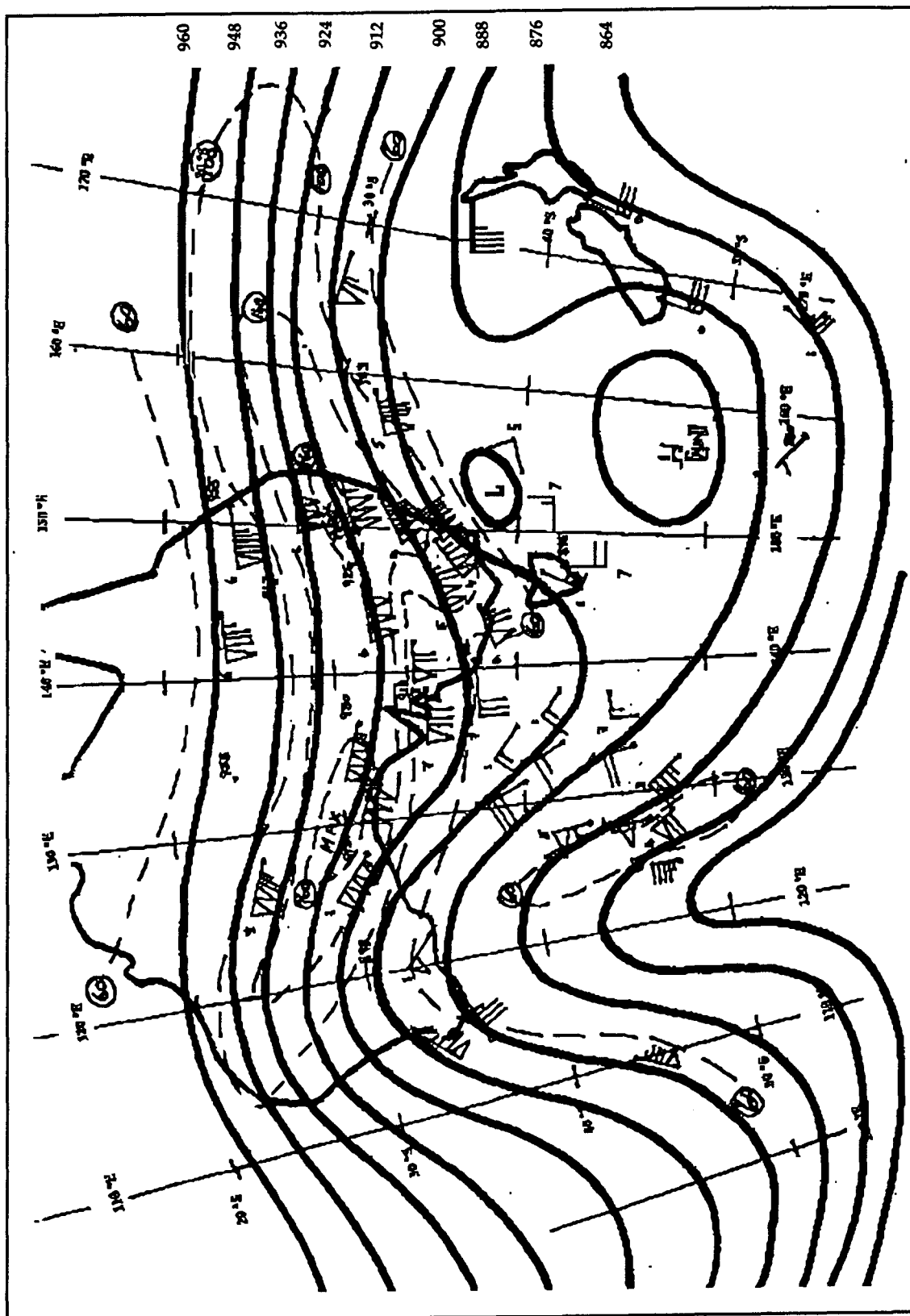
assuming that the 300 hPa ridge lies close to and has the same orientation as the thickness ridge. The position of the jetstream over the Indian Ocean has been inferred from the pattern of the cirrus cloud in the region after the method previously discussed (Bell *et al.* ,1988).

Monthly means of the westerly wind component (u component) at 500 hPa from the ANMC data set clearly reveal the bifurcated structure of the mid-tropospheric wind field in the Australian region, over extended periods in the winter and early spring of 1989. Mean fields of u for the months of May, June, July, August and September 1989 are presented in Fig. 4.8. In April 1989 (not shown) a broad band of westerly flow covered the middle latitudes with maxima of approximately 30 m s^{-1} located to the southwest of Western Australia and south of Africa. The pattern for May [Fig. 4.8 (a)] shows the development of a split in the westerlies east of New Zealand. This abrupt change in mean zonal flow from April to May was accompanied by the appearance of blocking episodes in the south western Pacific Ocean (Gaffney, 1990a). The National Climate Centre of the Bureau of Meteorology reported in its monthly bulletin that the cold phase of the Southern Oscillation was coming to an end (NCC, 1989). There was a further change in the mean u field between May and June [Fig. 4.8 (b)] as the westerly wind minimum migrated westwards from New Zealand to southeastern Australia and the sub-tropical wind maximum strengthened over central Australia.

According to Gaffney (1990b), mean blocking activity in June 1989, as measured by a Blocking Index (BI) discussed in Section 4.6, was only slightly above average in the Southwestern Pacific Ocean and Tasman Sea region. The comparison between June and July is an interesting one. Despite the pronounced involution and split jet structure of the mid-tropospheric flow in the Australian region for an extended period late in July 1989 (see Fig. 4.6), the monthly mean u component [Fig. 4.8 (c)] closely resembles the long-term mean. Long-term mean values for the zonal component of the geostrophic wind at 500 hPa in the month of July have been presented by van Loon (1972). His Fig. 5.3 (1972, p89) indicates that the Tasman Sea and New Zealand region is, on average, in a zone of weak westerly flow during winter with lowest values below 10 m s^{-1}. This is the 'climatological split in the westerlies' referred to by, *inter alia* , Trenberth and Mo (1985, p3).

Fig. 4.8 (d) depicts a broad band of strong westerly flow over the middle latitudes of the Indian Ocean during August of 1989 splitting into an intense westerly jet (>30 m s^{-1}) north of New Zealand and a strong jet (>25 m s^{-1}) near 60 °S to the southeast of New Zealand. These two wind maxima are separated by a region of weak westerly flow surrounding an area of mean easterly wind to the east of New Zealand. A similar pattern is evident for the month of September 1989 [Fig 4.8 (e)]. In this case, the mean westerly wind maxima to the north and south of New Zealand are somewhat weaker than in the preceeding month but the single jetstream in the Indian Ocean sector is slightly stronger and has migrated eastwards. August and September 1989 were periods of well above average blocking activity in the western and central Pacific (Gaffney, 1990b; Bureau of Meteorology, 1989c,d).
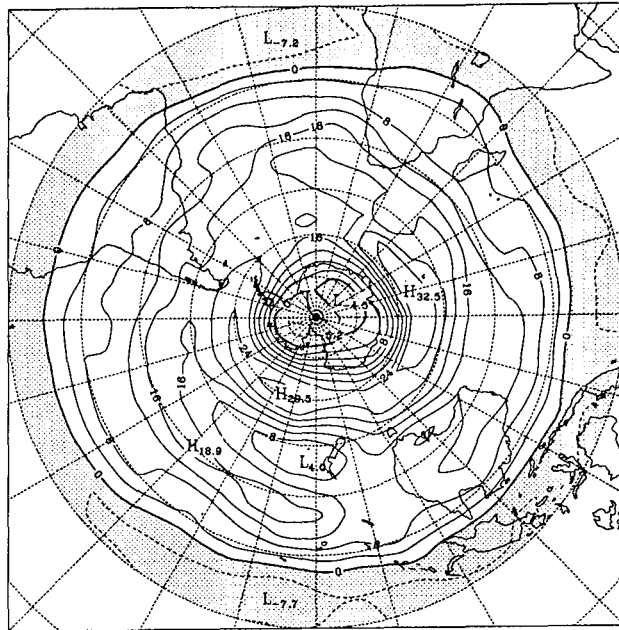
Figure 4.8a
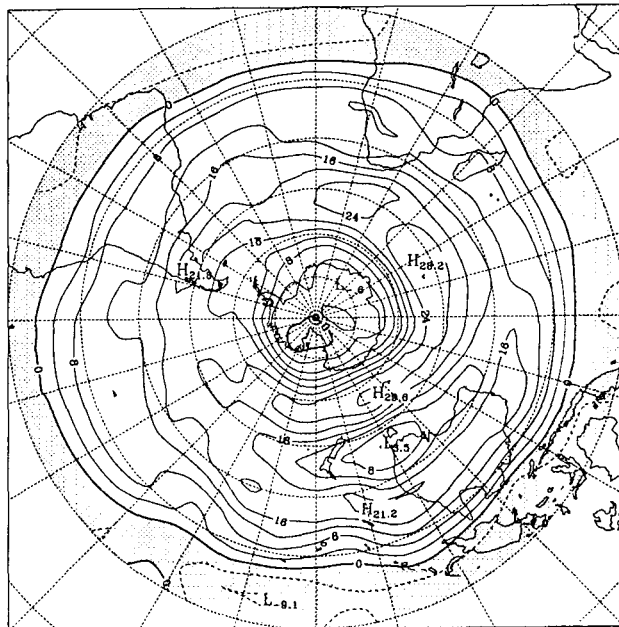
Figure 4.8b
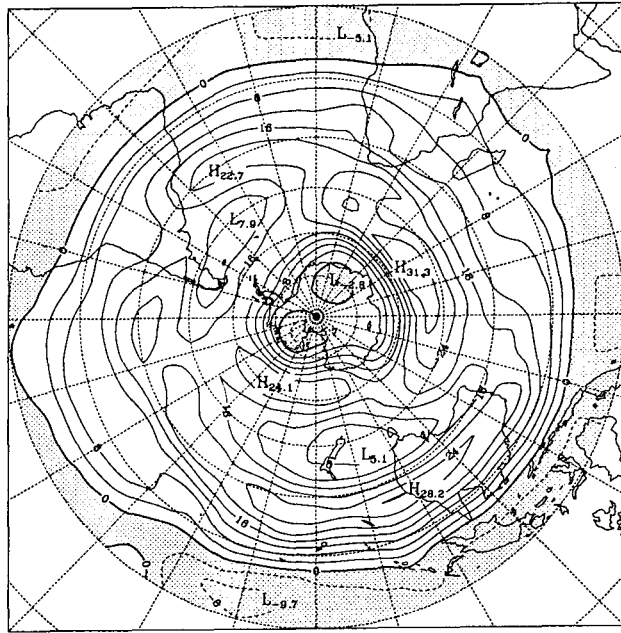
Figure 4.8c
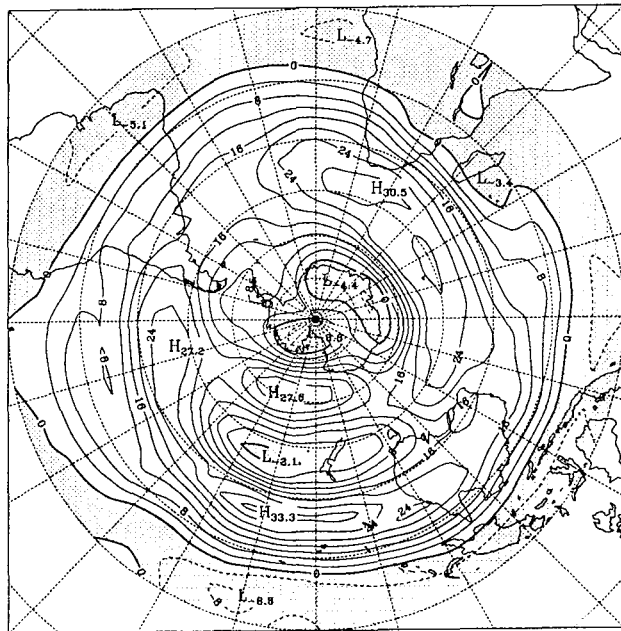
Figure 4.8d
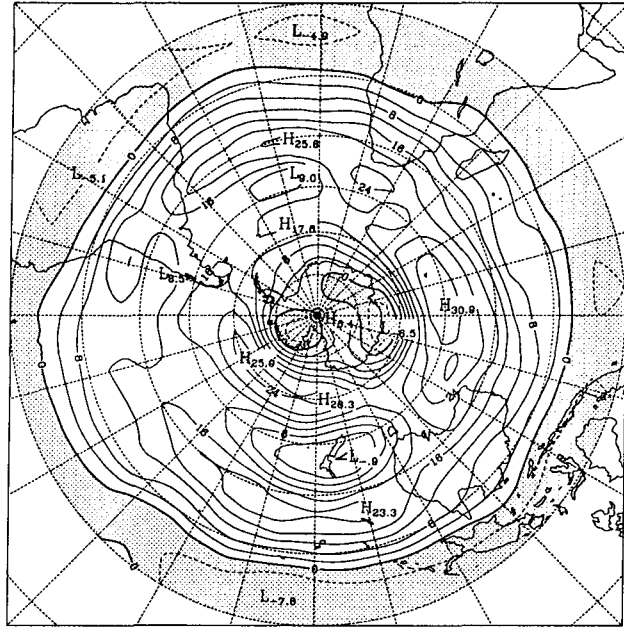
Figure 4.8e

Figure 4.8. Zonal component of the geostrophic wind at the 500hPa level for the months of (a) May (b) June (c) July (d) August and (e) September 1989. (Stippling indicates regions of mean easterly wind)

The persistence of involuted mid-tropospheric flow in the Tasman Sea-New Zealand region and the western and central Pacific Ocean was particularly striking during the months of August and September. Reference to the analyses of Gibson (1993, personal communication) again draws attention to the longevity of these patterns at 500 hPa. Fig. 4. 9 (a) illustrates the extent of the split in the westerlies on 16 August 1989 and Fig. 4.9(b) shows a similar pattern in the Pacific region on 28 August. The intervening period was characterised by weak and only brief interruptions to the split pattern.

It appears that split westerly flow first developed in May 1989, weakened slightly in June but returned in July and persisted until late in September. It was reported by the Bureau of Meteorology in its Climate Monitoring Bulletin of June 1989 that "The stronger winter hemisphere Hadley circulation (in the Pacific) resulting from the enhanced convective activity appears to have been responsible for the forcing of the mid-latitude subsidence further south than usual." (Bureau of Meteorology, National Climate Centre, 1989a, p1). The maximum wind analyses of Gibson (1993, personal communication) support the contention that amplification of the high latitude westerlies occurred between the anticyclones and the Antarctic region where negative geopotential height anomalies were observed throughout the period.

Also, these analyses raise the question of whether or not the split jet structure exists independently and precedes manifestations of blocking at lower levels or develops with it. The observational evidence reported in this section suggests that the split jet structure was well established, at least in the middle troposphere, throughout the period. It will be shown that manifestations of blocking at lower levels occurred in a desultory manner in the Tasman Sea and New Zealand region during the period with peaks in May, late July, August and September.

(a)

(b)
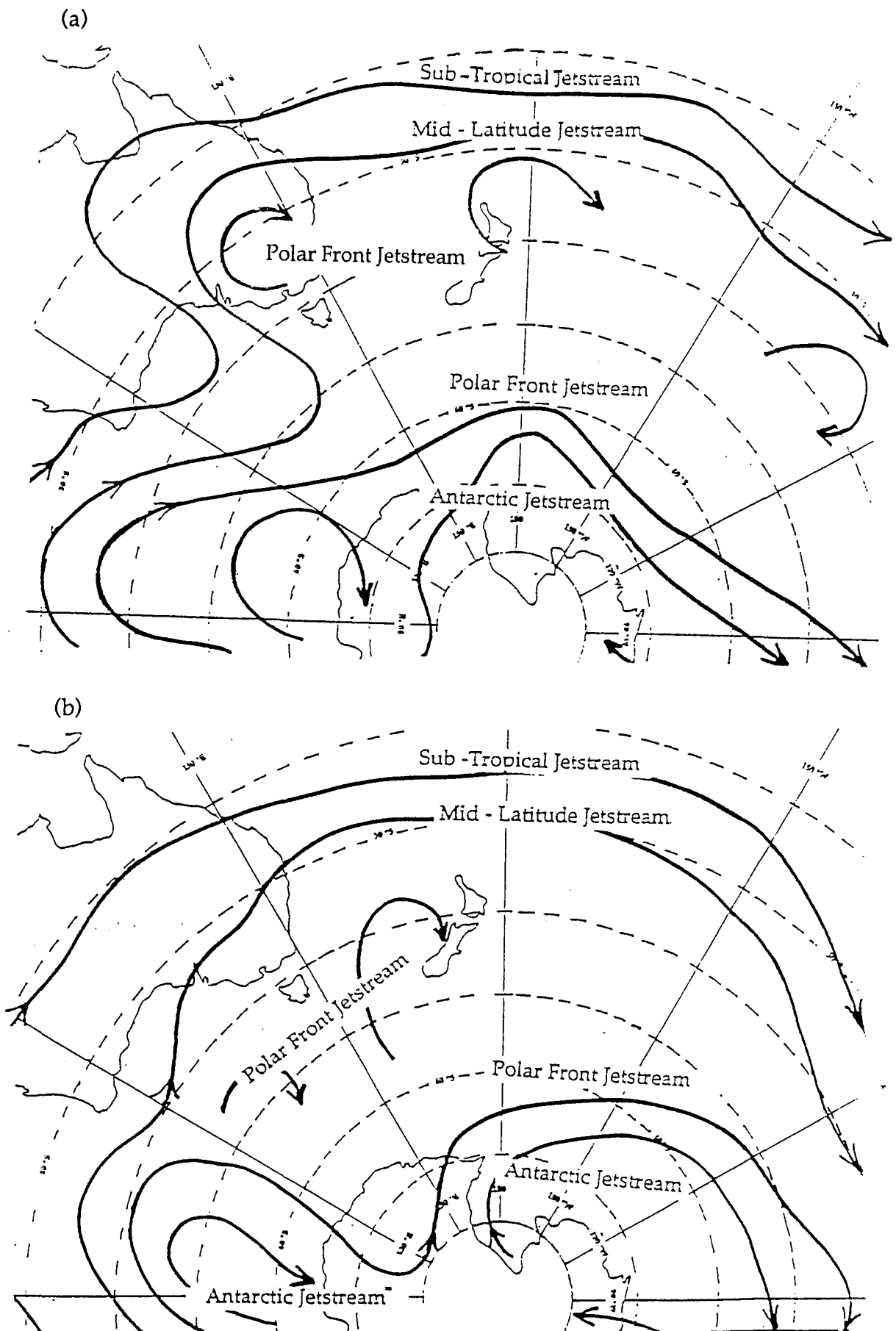
Fig. 4.9 The configuration of the major jet streams in the western Pacific Ocean on (a) 16 August 1989, and (b), 28 August 1989 [from Gibson, 1993 (personal communication)]

4.3 500 hPa Geopotential Fields

4.3.1 Monthly and Seasonal means of 500 hPa Geopotential Height

Monthly and seasonal means of 500 hPa geopotential height in 1989 have been extracted from ANMC gridpoint data based on daily analyses at 1200 UTC for the southern hemisphere. Fig. 4.10 (a) gives the means at 45 °S for the individual months of June, July, August and September, 1989 and Fig. 4.10 (b) shows the values at 55 °S for the same months. The essentially 3 wave pattern is apparent at 45 °S, particularly in the latter half of the period. At 55 °S, wave number 1 is evident. The dominant ridge at each of these latitudes is to be found between 155 °E and 185 °E in seven out of the eight examples. The exception occurred at 45 °S in the month of July, when amplification of the upstream and downstream ridges swamped the New Zealand ridge.
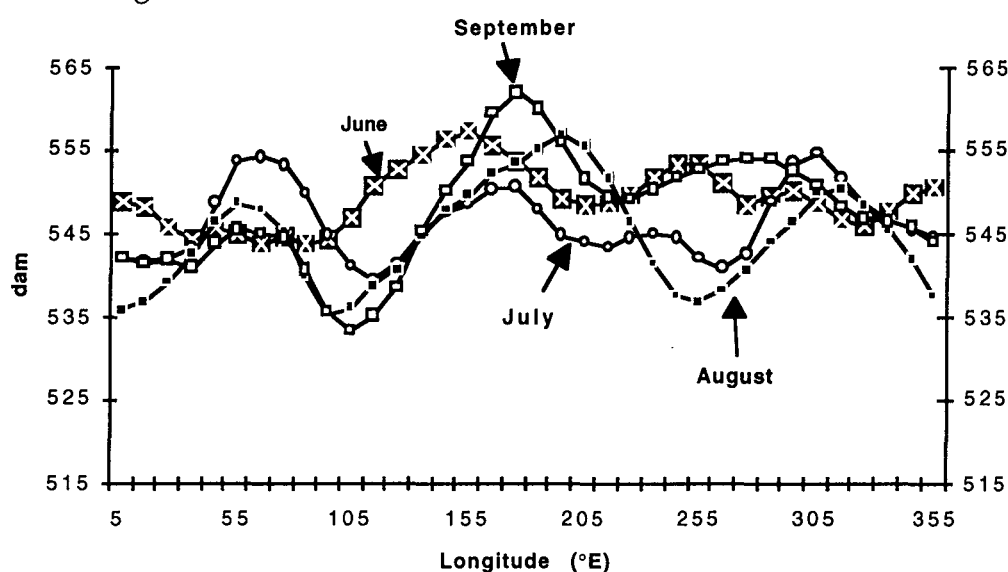
Fig. 4.10(a). Monthly means of geopotential height (1200 UTC) at 45 °S for the months of June, July, August and September 1989.
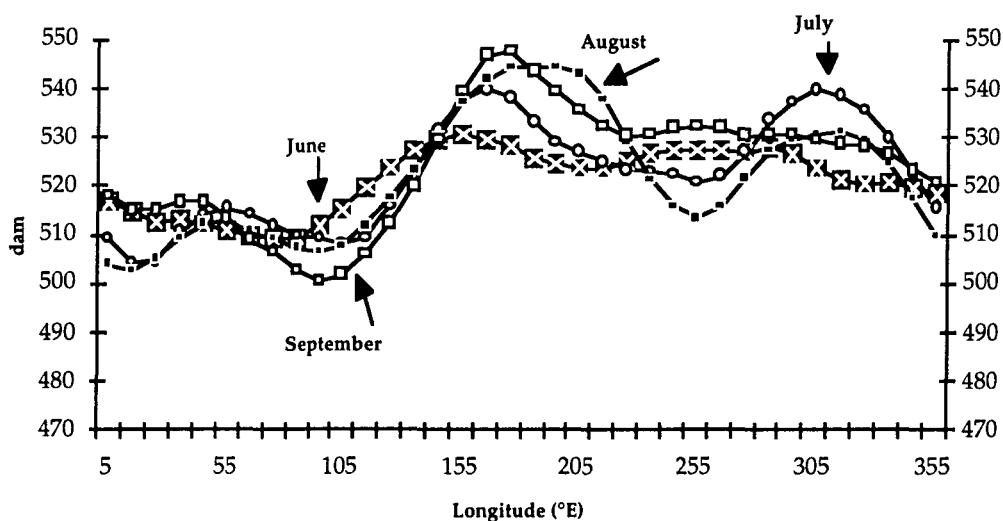
Fig. 4.10(b). Monthly means of geopotential height (1200 UTC) at 55 °S for the months of June, July, August and September 1989.

Mean geopotential heights for the 4 month period, June to September, 1989 are illustrated in Fig. 4.11 and reveal the dominant wave number of 3 at 45 °S and the less well defined pattern at 55 °S. In each case, the most significant ridge is clearly located at New Zealand longitudes.
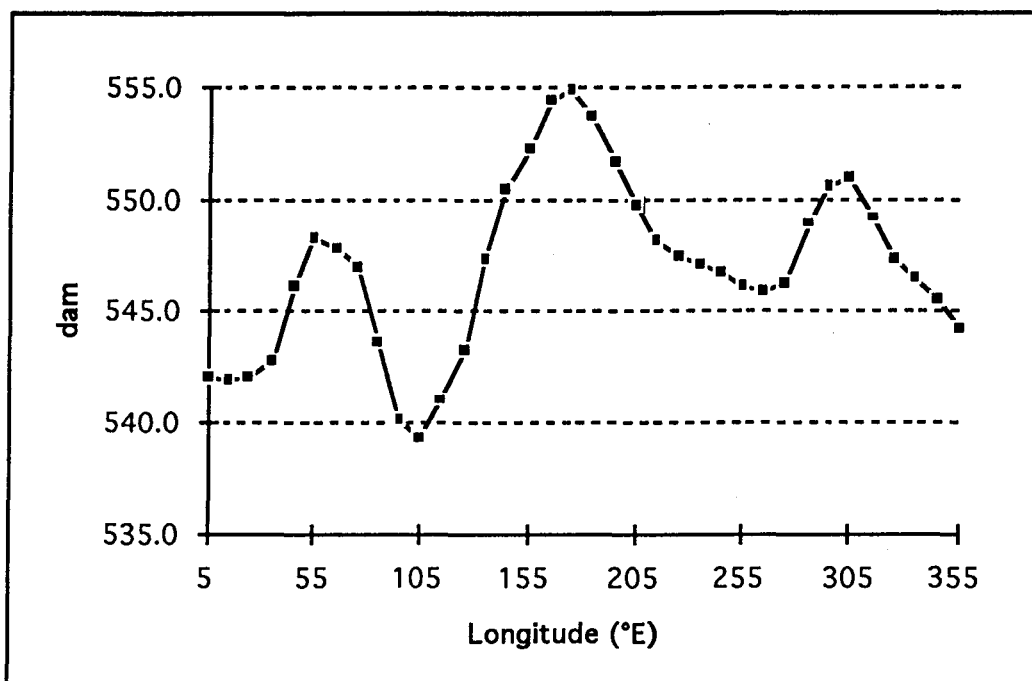
Fig. 4.11 (a). Mean 500 hPa geopotential height (1200 UTC) at 45 °S for the period, June, July, August and September, 1989.
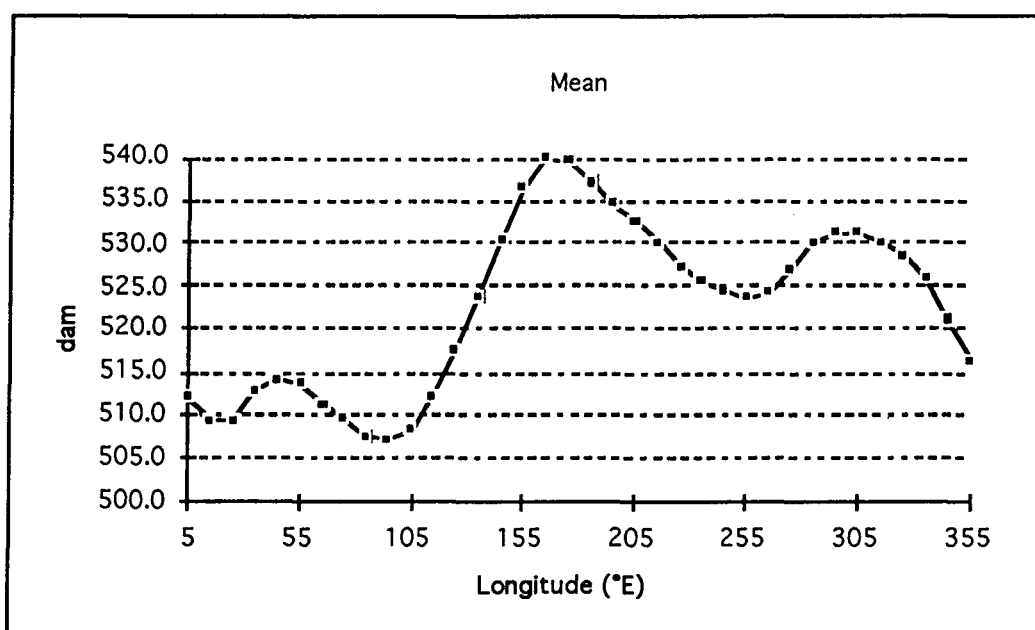
Fig. 4.11 (b). Mean 500 hPa geopotential height (1200 UTC) at 55 °S for the period, June, July, August and September, 1989.

The amplitude of the ridge at 55 °S in the Tasman Sea-New Zealand sector for the four month period June to September 1989 can be compared with a 20 year mean for these months calculated for the years 1972 to 1991 from the ANMC data set. In contrast to geopotential heights presented previously in this section,which were derived from analyses at 1200 UTC, these data have been drawn from observations at 00 UTC. Fig. 4.12 (a) illustrates the contrast

between the mean 500 hPa geopotential heights over this four-month period in 1989 and the long-term means at 55 °S for gridpoints at longitude intervals of 5°. For the gridpoints from 150 °E to 180 °E the 1989 means were the highest recorded over the 20 year period. Whereas heights were well above average in the New Zealand sector mean heights were significantly below average in the Indian Ocean sector reflecting the intensity and duration of troughs in the region to the southwest of Western Australia. This area was identified by Gaffney (1990b) as one of three regions around the hemisphere displaying negative anomalies of 500 hPa geopotential height in the 1989 winter. The other (significantly more intense) negative anomalies were located southwest of South America and south of Africa.
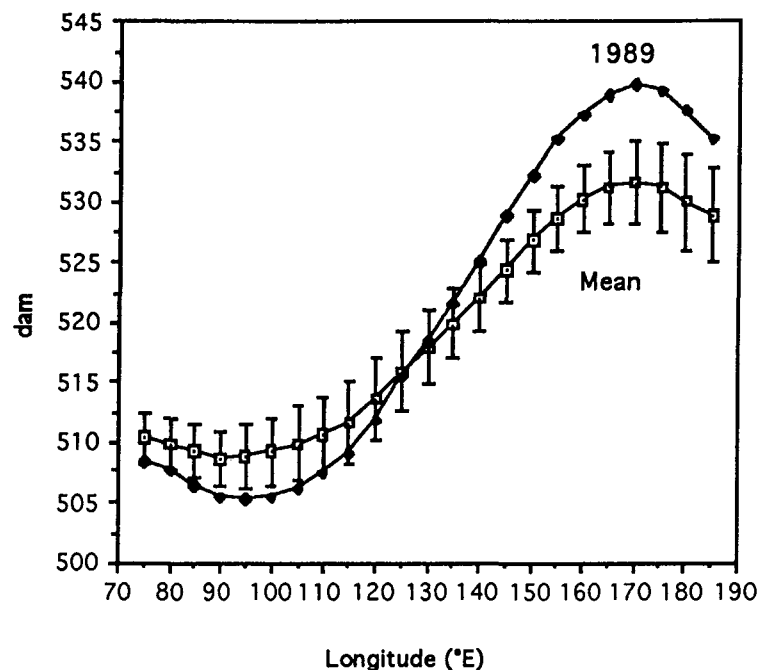
Fig. 4.12 (a) Mean geopotential height (dam) at 00 UTC of the 500 hpa surface at 55 °S for the period June, July, August and September 1989 compared to a 20 year mean (1972-91) for these months. Error bars on the mean represent the standard deviation at each gridpoint. (ANMC data)

The significance of the positive anomaly can be gauged by normalising the departures from the long-term mean. In Fig. 4.12 (b) departures from the mean exceeding 2 standard deviations occur between 150 °E and 180 °E.and more than 1 standard deviation east of 140 °E. The negative anomalies of near or slightly more than 1 standard deviation are restricted to the zone between 80 °E and 110 °E.
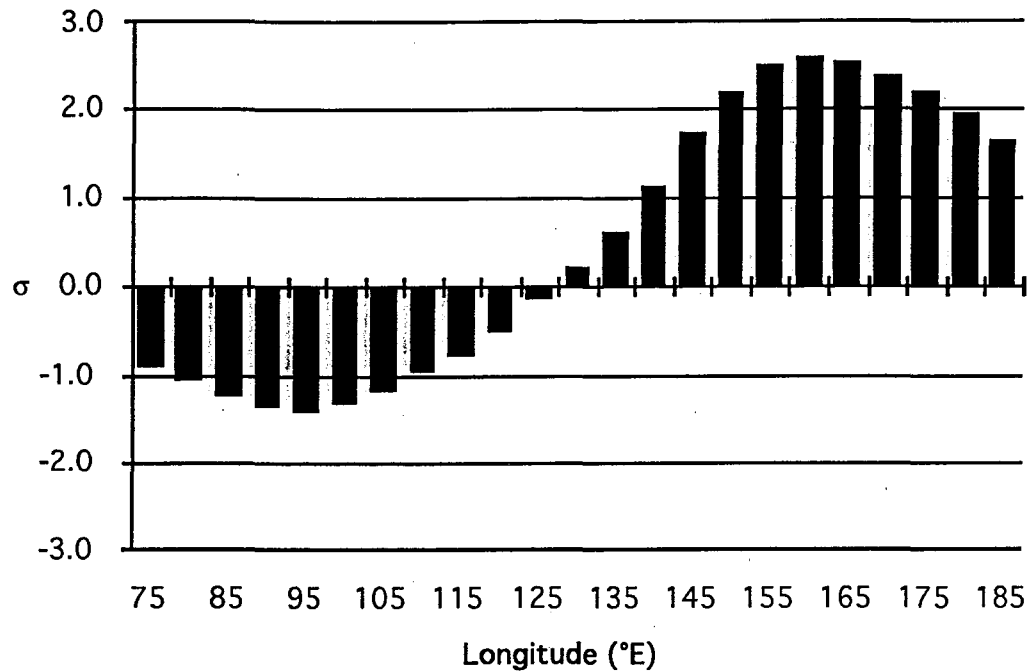
Fig. 4.12 (b) Normalised departure from the long-term mean of geopotential height at 55 °S for the months of June, July, August and September 1989. (ANMC data at 00 UTC)

4.3.2 Hovmöller Analysis of Geopotential Heights

Application of the Wright (1974) definition to the event in the winter and early spring of 1989 requires a method of determining the behaviour of the 5-day running means of geopotential height of the 500 hPa surface at 45 °S. A useful method for looking at 500 hPa fields is to employ a longitude-time section for each latitude under consideration. These so-called Hovmöller charts enable the analyst to separate atmospheric long waves from the short wave features. In this manner, planetary or Rossby waves can be dissociated from the background noise, thus giving an indication of the persistence and location of long-lived features of the atmospheric circulation.

Reference to Fig. 4. 13(a) reveals that there was a persistence of ridging at 45 °S in the longitude band between, approximately, 145 °E and 165 °W, during the four month period, June to September, 1989. However, the ridges at this latitude were relatively short-lived and mobile during much of June, 1989. On 26 June an amplification of the ridge occurred which approximately met the second criterion of the Wright (1974) definition (i.e. the 5 day mean ridge at 45°S moves no more than 20° of longitude per week and no more than 30° during the blocking episode), until dissipation became evident on the 4 July. Other significant events occurred from 23 July to 10 August, 16 August to 27 August, 2 to 16 September and 23 September until ,at least, the end of the month.
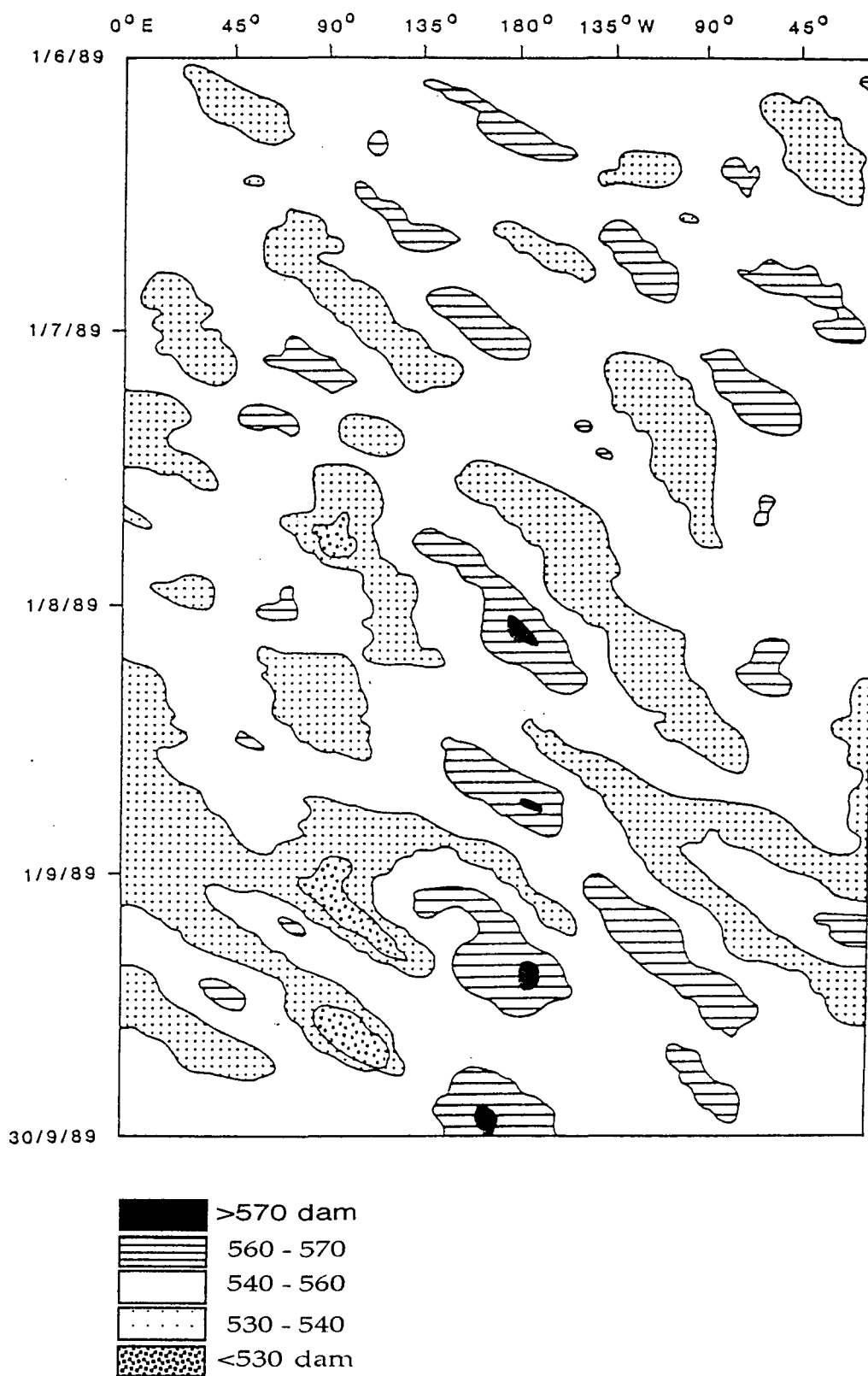
Fig. 4.13 (a) Hovmöller analysis at 45°S of 5-day mean 500 hPa geopotential heights around the Southern Hemisphere for the months June, July, August and September 1989.
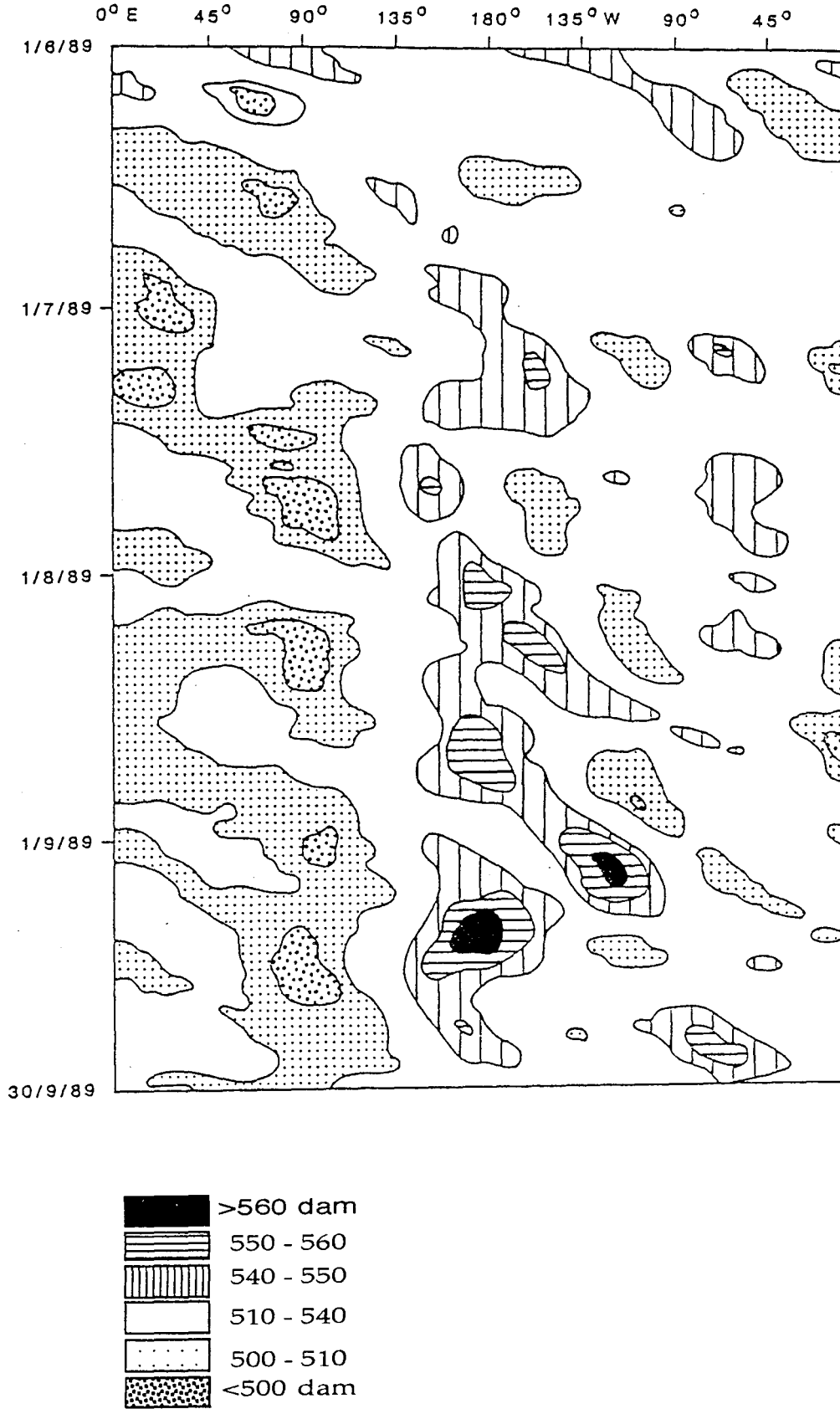
Fig. 4.13 (b) Hovmöller analysis at 55°S of 5-day mean 500 hPa geopotential heights around the Southern Hemisphere for the months June, July, August and September 1989.

If the analysis of the Hovmöller charts is extended to 55 °S, the pattern of ridge intensification and persistence is more readily apparent. In Fig. 4.13(b), the ridges are clearly defined and moving only slowly eastwards. Retrogression is apparent in the mean ridges and the Indian Ocean trough. However, there is also evidence at this latitude of the frequent appearance of significant ridges in the central and eastern Pacific, which is consistent with the jetstream structure previously discussed in Section 4.2. It is also noticeable that Indian Ocean troughs, despite their intensity at 55 °S , did not migrate eastwards of about 120 °E during the four month period. This is in contrast to the behaviour at 45 °S where recognisable geopotential minima can be traced as they migrate from the Indian Ocean to the Central Pacific until late in August when the pattern became almost stationary.

4.4 Geopotential Thickness Fields

The 1000 - 500 hPa geopotential thickness is a useful indicator of the mean temperature of the lower troposphere. As discussed in Pook (1992), there is a marked warming and cooling of the atmosphere over southern Australia with the seasons. This can be inferred from the amplitude of the annual cycle of 500 hPa geopotential height at a station such as Adelaide (34° 50' S) and a long-term zonal mean at 35 °S (Trenberth, 1979). To some extent, the annual cycle in 500 hPa height is influenced by the seasonal cycle of mean sea level pressure (MSLP) as the sub-tropical ridge migrates from north of 30 °S in winter to near 40 °S in summer. Atmospheric thickness analysis removes the contribution of the surface pressure and can be employed as a measure of temperature variability in the atmospheric column.

In Fig. 4.14, the monthly means of 1000 - 500 hPa thickness over the Southern Hemisphere trace the development of a thickness trough over southeastern Australia during the late autumn and winter of 1989. This cooling trend is accompanied or followed by the slackening of thickness gradients in the vicinity of the Tasman Sea over subsequent months and the tightening of the gradient south of the Tasman Sea and New Zealand, particularly around the coast of Victoria Land in Antarctica. The thickness minimum was centred over East Antarctica for most of the period but shifted towards the Pole in September. As the elevation of East Antarctica exceeds 4000 m in places and a large proportion of the Plateau is above 3000 m (Schwerdtfeger, 1984) resulting in surface pressures at Vostok (3488 m) of rarely more than 650 hPa, the significance of 1000 - 500 hPa thickness in this region is questionable.
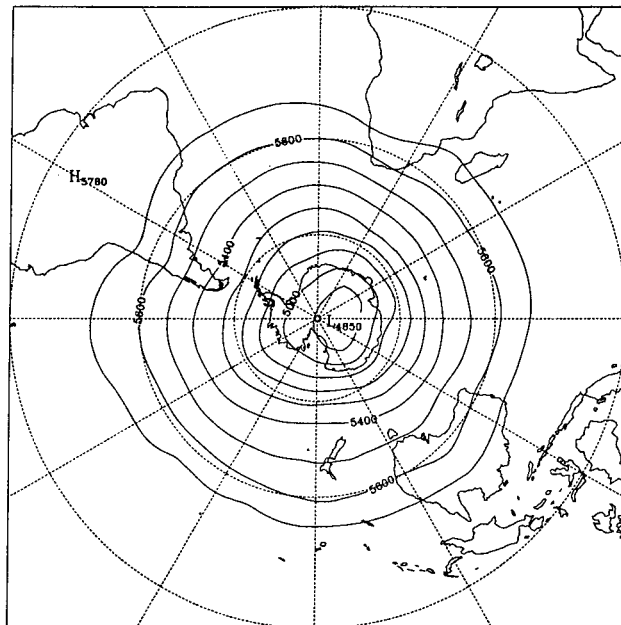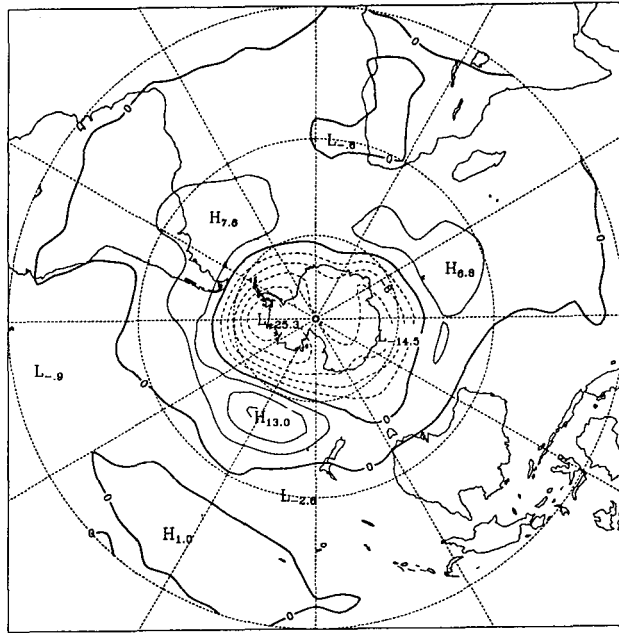
Figure 4.14a
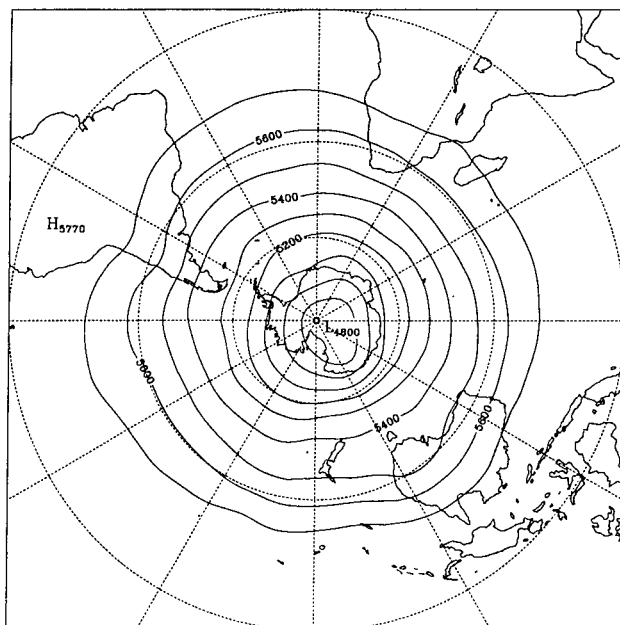
Figure 4.14b
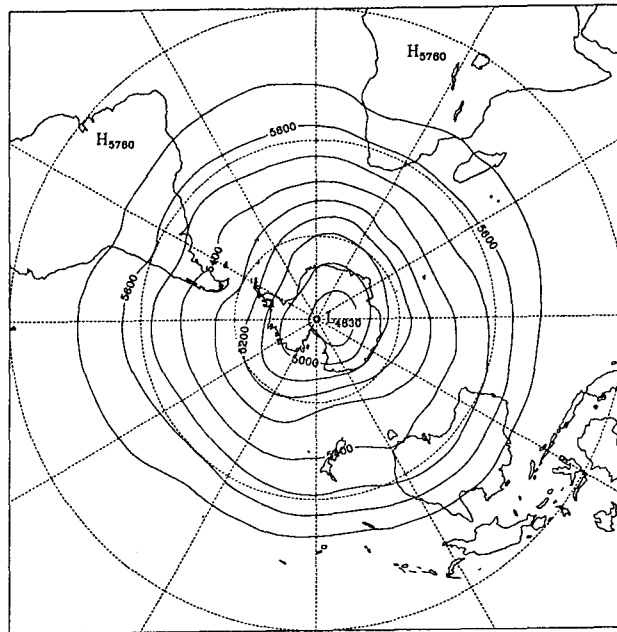
Figure 4.14c
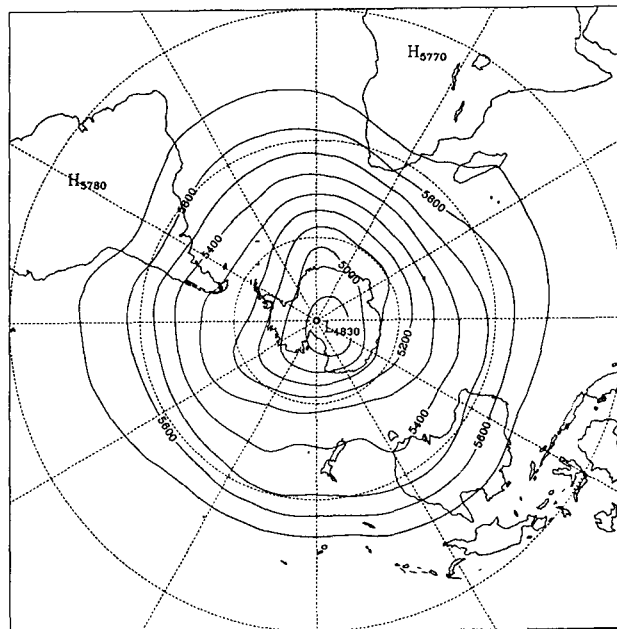
Figure 4.14d
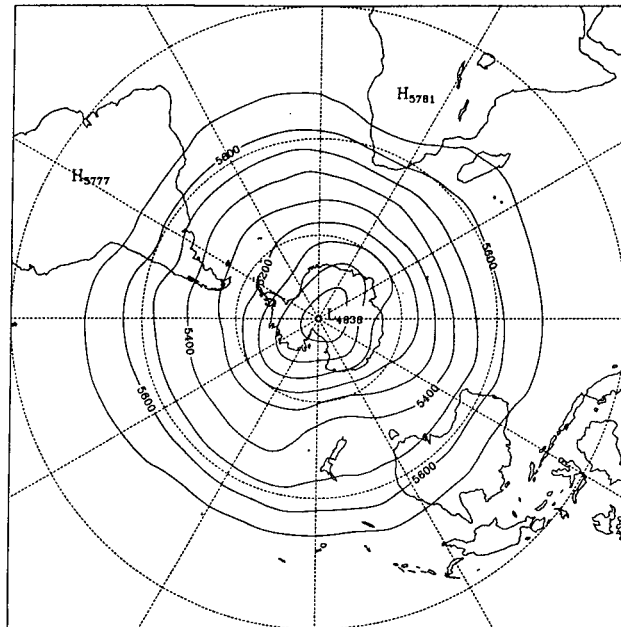
Figure 4.14e

Figure 4.14. Mean geopotential thickness of the 1000 to 500 hPa layer for the months of (a) May (b) June (c) July (d) August and (e) September 1989.

4.5 Surface Pressure and Pressure Anomalies

Application of the blocking criteria discussed in Chapter 3 requires knowledge of the mean position of the belt of anticyclones commonly referred to as the subtropical ridge, which encircles the Southern Hemisphere . Monthly mean positions of the sub-tropical high pressure ridge and, or the prominent high pressure cells which contribute to the ridge have been estimated for the Southern Hemisphere by numerous researchers. Towards the end of the nineteenth century Russell (1896) concluded that the latitude of anticyclone tracks in the Australian region varied from a northern limit near 29°S in winter to as far south as 38°S in summer. Karelsky (1956, 1961) carried out an extensive investigation into the numbers of anticyclones crossing 5° by 5° latitude - longitude squares and expressed his results as 'anticyclonicity', the number of hours an anticyclone centre remained within a given square. Vowinckel (1955) developed a climatology of Southern Hemisphere MSLP over a 5 year period and this was subsequently employed by van Loon (1956) in framing his definition of blocking. A detailed climatology of Southern Hemisphere MSLP developed by Taljaard *et al.* (1969) is still widely used and a ten year climatology was developed from analyses of the Australian National Meteorological Analysis Centre by LeMarshall *et al.* (1985). These data sets provide benchmarks with which to compare the positions of quasi - stationary highs during the 1989 blocking event. For the purposes of this study long-term means have been calculated from a 20 year archive of ANMC analyses at 00 UTC for the period from 1972 to 1991 and anomalies are relative to this data set.

In Fig. 4.15, the monthly anomalies of MSLP at 00 UTC are shown for the months of May to September 1989. The monthly charts confirm the existence of positive anomalies southeast of Australia and in the southwest Pacific Ocean throughout the period supporting the finding of Gaffney (1990b) who reported that MSLP was significantly above average to the southeast of Australia during the winter of 1989. Positive MSLP anomalies are also apparent to the southeast of South America and reach a maximum in August [Fig. 4.15 (d)]. Negative anomalies are obvious to the south and southwest of Western Australia, particularly in the period from July to September. Over the entire period an area of intense negative anomalies persists to the southwest of South America, close to the coast of Marie Byrd Land in Antarctica. Similar results have been reported in the NOAA monthly Climate Diagnostics Bulletins.

Of particular significance to the understanding of the blocking process in the Australasian region is the apparent progression from zonal flow in May 1989 (Fig. 4.15a) to a marked meridional structure around the hemisphere later in the period. Notably, the intensification of the positive MSLP anomalies to the southeast of Australia and South America appear to occur simultaneously (see Figs. 4.15c and 4.15d) suggesting a process which is hemispheric in nature, presumably operating in response to the amplification of the atmospheric long waves.

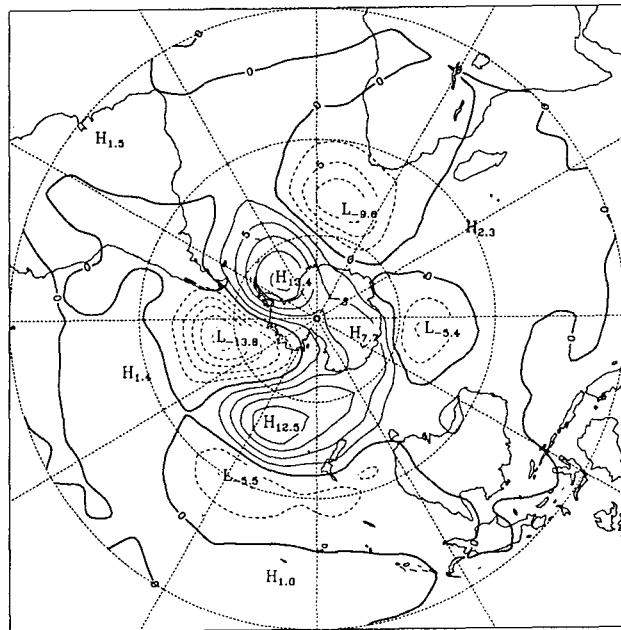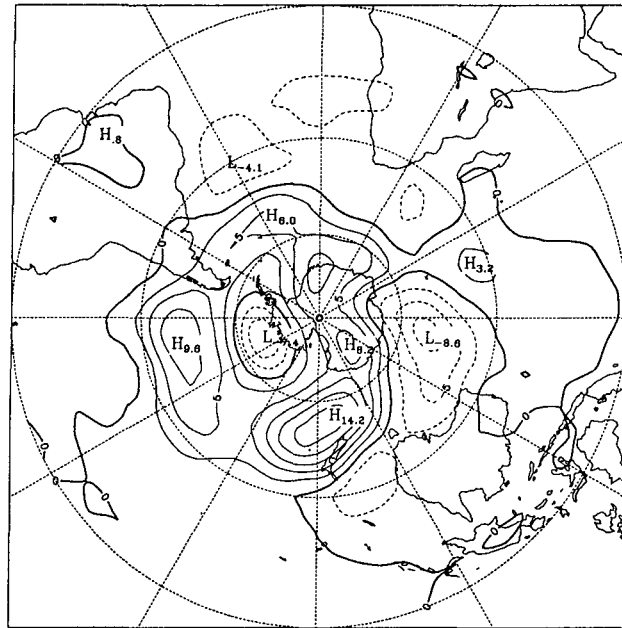Figure 4.15a
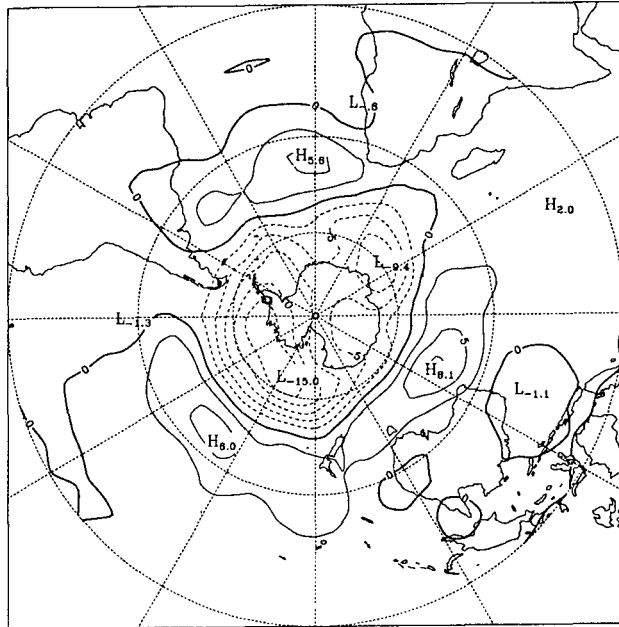
Figure 4.15b
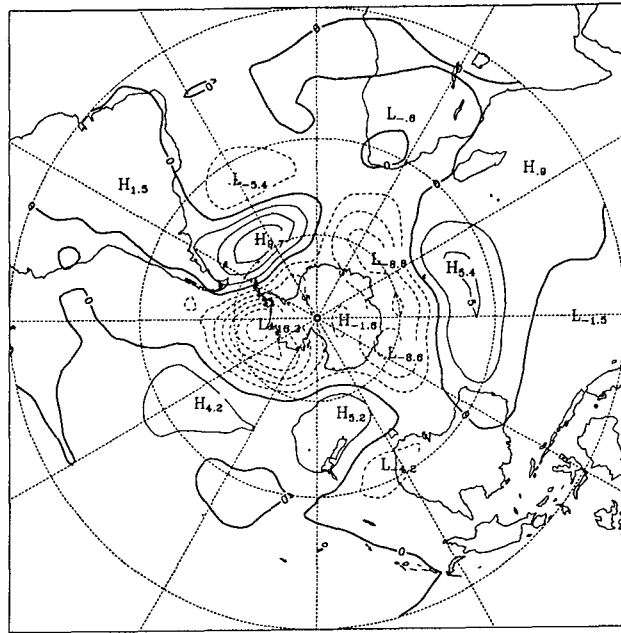
Figure 4.15c

Figure 4.15d

Figure 4.15e

Figure 4.15. Mean sea level pressure anomaly in hPa for the months of (a) May (b) June (c) July (d) August and (e) September 1989. (20 year mean from NMAC analyses at 2300 UTC)

Additionally, by way of comparison, a four year climatology has been compiled from ECMWF analyses for the period May 1986 to September 1989. In Fig. 4.16 anomalies of surface pressure (not MSLP) in August of 1989 are shown relative to the four year mean for August. The significant positive anomaly to the south and southeast of New Zealand closely mirrors the ANMC and NOAA patterns discussed previously.
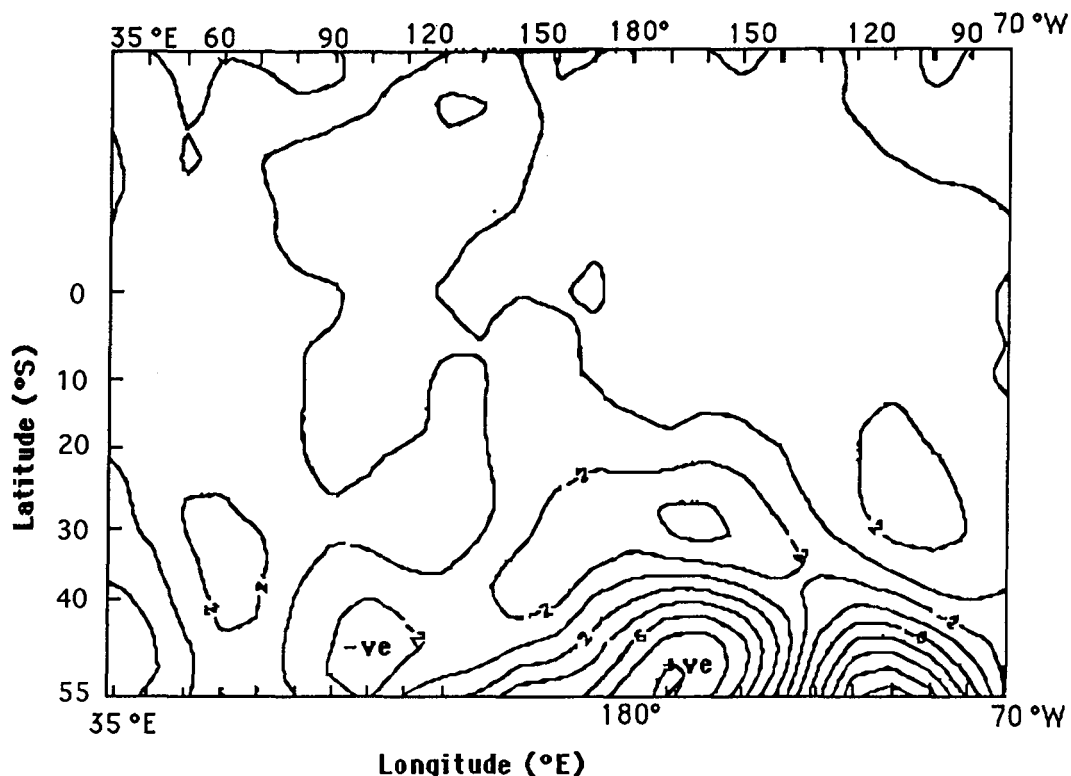
Fig. 4.16. Surface pressure anomaly for August 1989 calculated from daily ECMWF analyses for the years 1986 to 1989.

The monthly means of MSLP at Macquarie Island (54° 30′ S, 158° 56′ E) for the winter months of 1989 point to the intensity and the high latitude of the surface high pressure centres during this period. Table 4.1 has been constructed from mean 0900 EST MSLP observations held on the Bureau of Meteorology archive and compares the monthly means in mid-1989 with the long-term averages and the highest monthly means on record. Monthly mean MSLP was near average in May and June but moved significantly above the long-term average in July. Monthly means at Macquarie Island approached the highest on record in August and September 1989.

	May	June	July	August	September
1989	1001.7	1002.8	1009.2	1009.9	1008.9
Mean (≥32y)	1001.3	1003.0	1004.1	1002.4	997.1
Anomaly	+ 0.4	- 0.2	+ 5.1	+ 7.5	+ 11.8
Highest on record	1010.0 (1985)	1013.7 (1982)	1016.3 (1973)	1010.8 (1965)	1009.4 (1976)

Table 4.1 Monthly means of mean sea level pressure (hPa) at Macquarie Island in 1989 compared to the long-term means and the highest recorded monthly mean pressure.

The complete sequence of MSLP charts for the Australian region for the months of June, July, August and September, 1989 is shown in Appendix A. Several episodes of blocking are evident throughout the period. Fig. 4.17 illustrates a period during July 1989 when blocking was clearly reflected in the surface pressure pattern and coincided with the split jet structure illustrated previously in Fig. 4.6. As many authors have indicated (e.g. Wright, 1974; Coughlan, 1983; Trenberth and Mo, 1984) surface anticyclones do not normally maintain their identity for extended periods during blocking episodes in the Southern Hemisphere. Instead, individual cells are regularly replaced by new highs which migrate from the west and intensify as they move into the vicinity of the long-wave ridge in the upper atmosphere. This process of replacement is evident in the synoptic charts for the period under investigation and can be observed in Fig. 4.17 on the 25, 26 and 27 July. In this sequence, a weak ridge of high pressure south of Western Australia on 25 July is rapidly absorbed into the blocking anticyclone centred to the southeast of Australia resulting in an apparent retrogression of the region of high pressure south of Australia.

It is also evident from this sequence of synoptic charts that the cyclonic portion of the block can undergo significant change at the surface. In Fig. 4.17, the surface low which is located to the east of Tasmania on 20 July weakens and moves eastwards before being absorbed into the trough in the Tasman Sea on 22 July. At this time a cut-off low forms to the south of the Great Australian Bight and 24 hours later (23 July) becomes part of an extensive region of low pressure over southeastern Australia. Subsequently, this depression intensifies over the western Tasman Sea and migrates slowly towards New Zealand. In this case, the process of cutting off and development of the surface low closely parallels the situation in the middle troposphere which was depicted in Fig. 4.6.
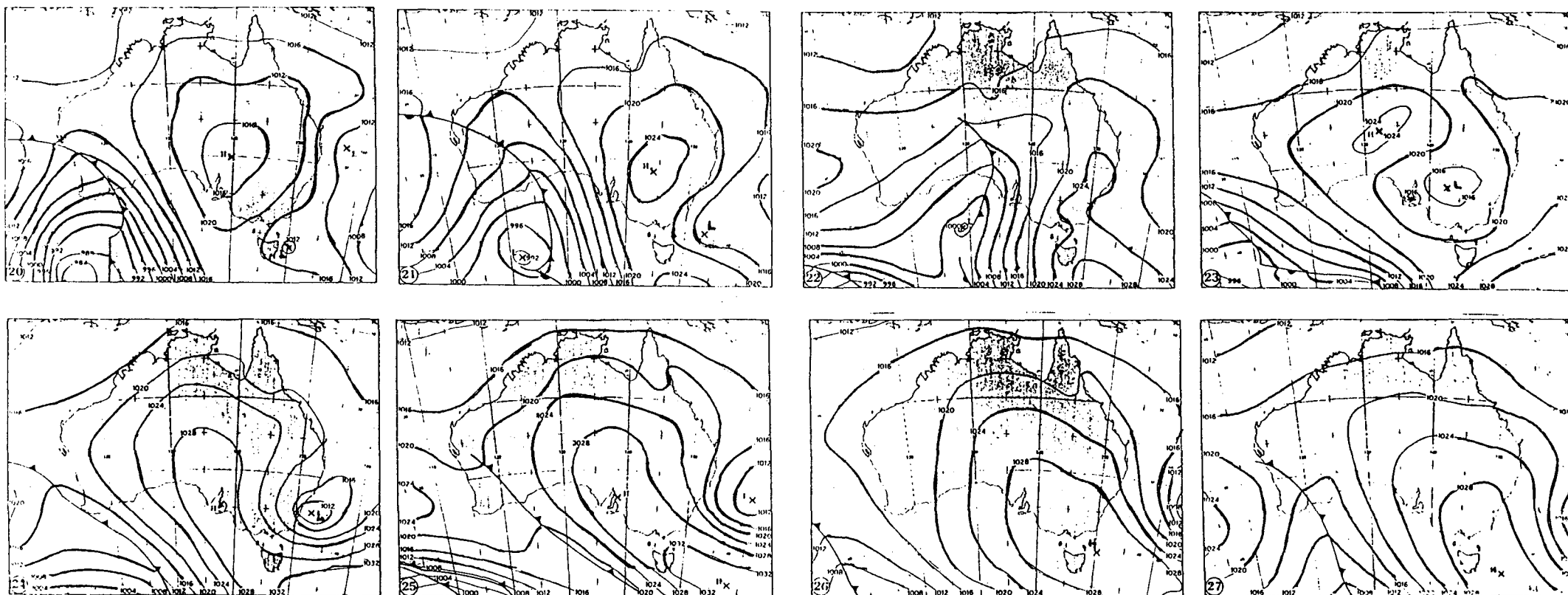
Fig. 4.17 A sequence of synoptic analyses at mean sea level over
eight successive days from 20 July to 27 July 1989 tracing the
development of an intense anticyclone to the southeast of
Australia and its subsequent vey slow movement.

4.6 Zonal Index

The strength of the mid-latitude westerly current undergoes a significant reduction wherever blocking occurs. Pook (1992) has described a zonal index (ZI) employed by the Tasmanian Regional Forecasting Centre of the Bureau of Meteorology, Hobart, which can be calculated readily from the difference between geopotential heights of the 500hPa surface at 35 °S and 55 °S. The differences are calculated for twelve standard meridians from 75 °E to 175 °W and the values summed to produce an index for each analysis. Typical values of the index range from 350 to 750 dam. Although the ZI is an indication of the strength of the mid-tropospheric westerlies across 110 degrees of longitude, the greatest variability is detectable in the eastern sector (125 °E to 175 °W).

Long-term (1971-1989) monthly means of the ZI reveal the strong seasonal signal from a minimum in July to maxima in January and October. Fig. 4.18 (from Pook, 1992) demonstrates the seasonal cycle and draws attention to the low values of ZI in winter.
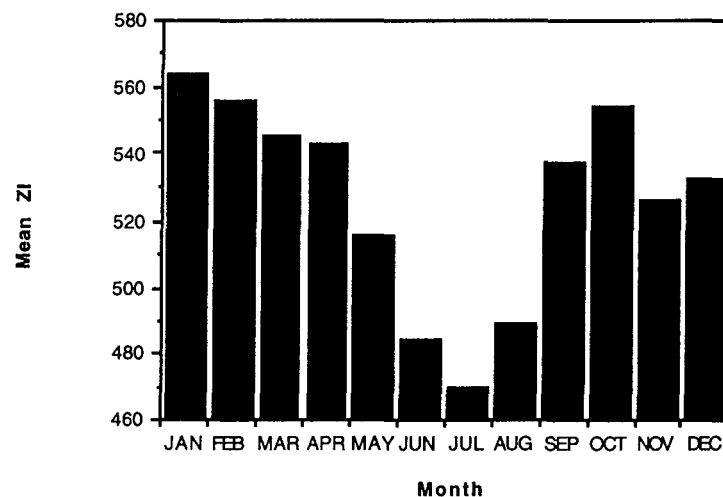
Fig. 4.18 Monthly mean zonal index (ZI) over the region from 75 °E to 175 °W (from Pook, 1992).

A time-series of monthly means of the ZI for the region from 75 E to 175 W, during the period January, 1986 to December, 1989 is shown in Fig. 4.19. Splitting the ZI into western and eastern sectors draws attention to the high degree of variability in the east. The ZI from 75 °E to 125 °E is labelled ZI (W) and ZI (E) refers to the sector from 135 °E to 175 °W. The mean ZI (E) for the 4 year period is 218.9 dam with a standard deviation of 40.4 dam and the mean ZI (W) is 316.6 with standard deviation of 30.9.

The period from June 1989 to September 1989 is particularly interesting as the decline in the ZI can be attributed to the extremely low values of ZI (E) while ZI (W) remained relatively high. Historically the ZI has been employed by forecasters in Hobart as a means of predicting surges in the zonal westerlies migrating from the Indian Ocean into the Australian region. The

negative correlation (r = -0.62, n =12) between the two components of the ZI during 1989 must raise serious doubts about its applicability for the predictive role.
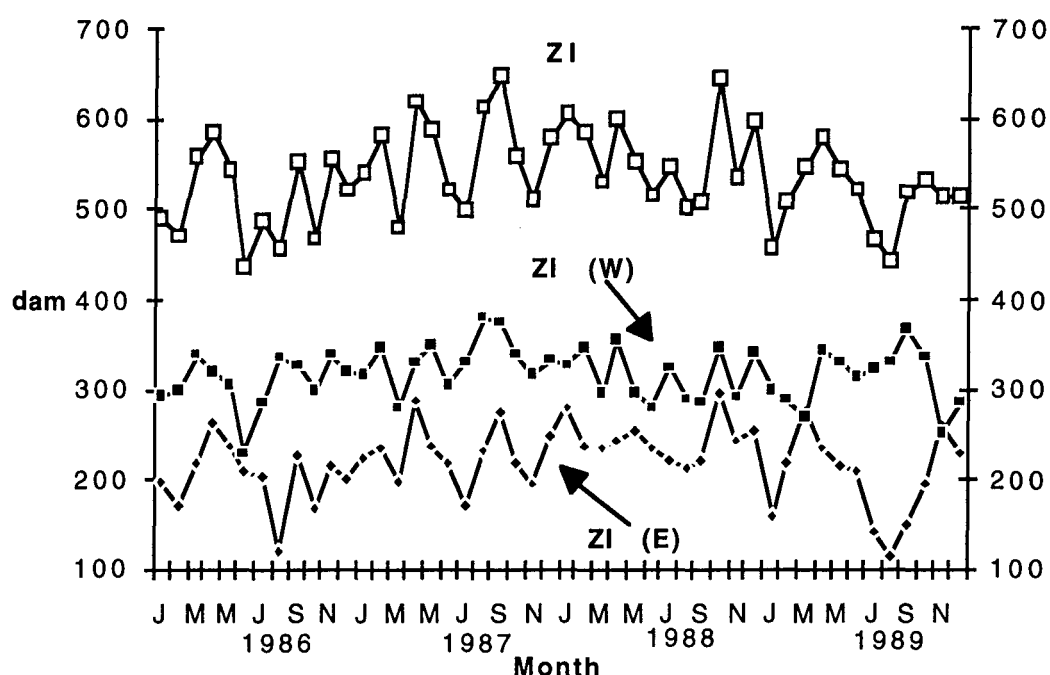
Fig. 4.19 Time series of the monthly mean of the ZI and its east and west components for the period 1986 to 1989.

The ZI can be converted to a geostrophic wind, u, at a specified latitude from the relationship

$$u = -\frac{g}{f}\left(\frac{\partial z}{\partial y}\right) \qquad 4.1$$

where g is the acceleration due to gravity, f is the Coriolis parameter for the specified latitude and the term in brackets represents the change in geopotential height with latitude on a particular constant pressure surface.

Fig. 4.20 shows the time series of daily geostrophic wind at 500 hPa, calculated at 45 °S from the ZI, for the months of June, July, August and September, 1989. During June, westerly winds in excess of 20 m s⁻¹ migrated into the region east of 155 °E on two occasions. In July, only one isolated case of a geostrophic wind in excess of 20 m s⁻¹ was evident in this belt of 30 degrees of longitude, comprising the Tasman Sea and New Zealand sector. From 1st August to 27th September, 1989, no westerly geostrophic winds exceeding 20 m s⁻¹ were found east of 155 °E and in only one instance (21 m s⁻¹ on 19th August), east of 145 °E.
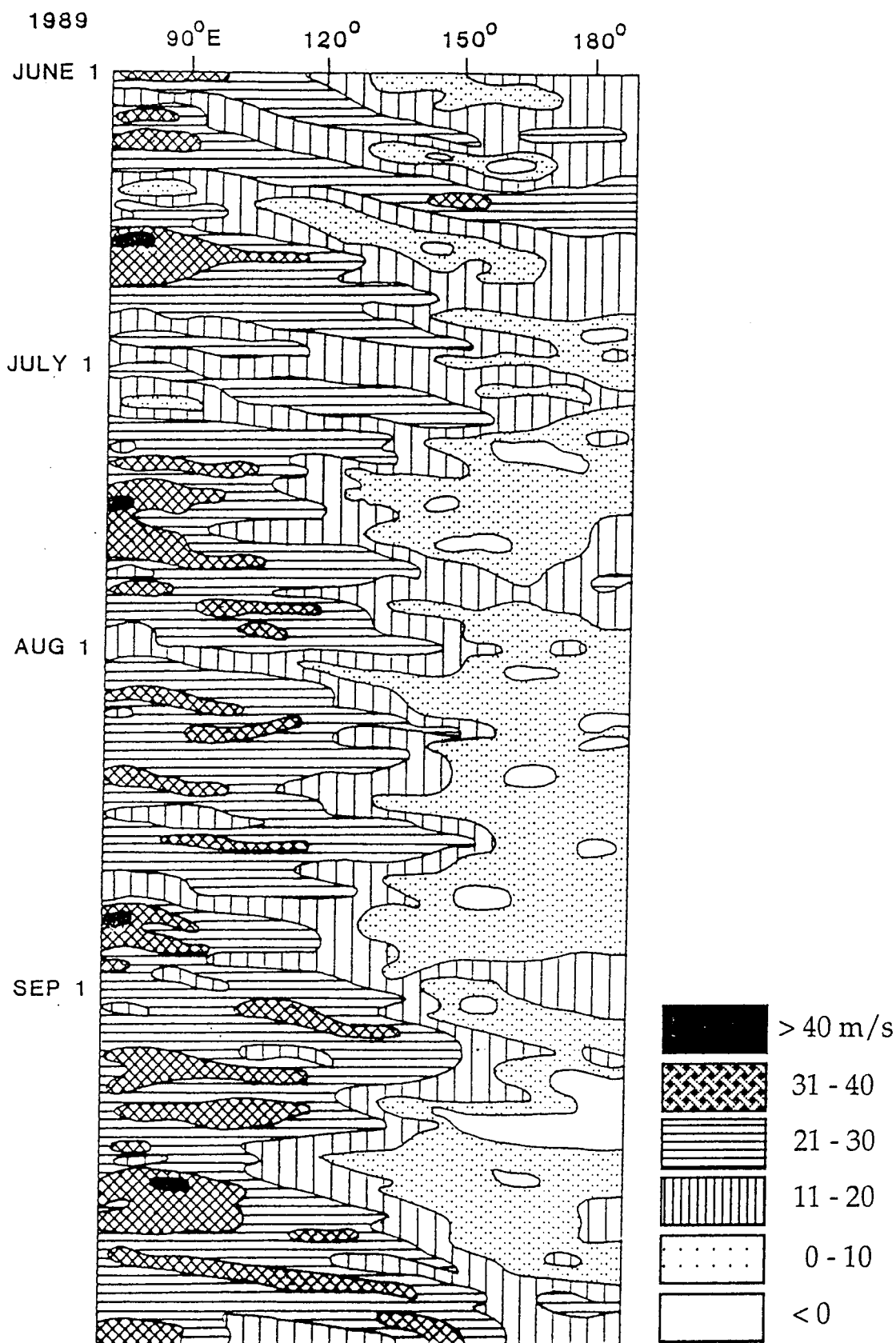
Fig. 4.20 Time series of westerly (u component) geostrophic wind at 500 hPa calculated at 45 °S from the ZI for the months of June, July, August and September 1989.

The contrast between the strength of the westerly winds in the region to the west of 145 °E and those in the east is particularly striking. Despite high values of ZI(W) in this predominantly Indian Ocean sector the overall ZI was significantly below average. Continuity would require that this westerly momentum entering the blocked region should be balanced by appropriate horizontal transfer to higher and, or lower latitudes. In order to satisfy this requirement it would appear that the flow to the south and north of the block was anomalously strong during the period. This is certainly evident in Figs. 4.8 (d) and 4.8 (e) for the months of August and September 1989.

4.7 Blocking Indices

Attempts to estimate the degree to which blocking is occurring around the hemisphere, or in a particular region, have historically depended upon the application of indices. Wright (1974) has described a blocking index (BI) which was developed by the Extended Forecast Section, Bureau of Meteorology in Melbourne. The BI has been in continual use since the 1970's and is defined in Chapter 3.

Gaffney (1990 b) has presented a Hovmöller analysis of the BI for the winter of 1989. In his Fig. 9, values of BI exceeding 50 m s^{-1} first made an appearance in mid June near 130 °E. A major peak in the index occurred during the early part of July and although weakening during the month the maximum remained anchored in the Tasman Sea and New Zealand region. Early in August, a steep increase in the BI occurred. It was accompanied by an eastwards migration of the maximum into the western Pacific Ocean sector. Fig. 4.21 (a) shows the August mean BI compared to a ten year mean (1973-1982).

An alternative blocking index (β) developed by Gibson (1994, personal communication) has been discussed in Chapter 3. Fig. 4.21 (b) shows the behaviour of this index during the winter and early spring of 1989.

The time series of weekly values of the index reveals episodes of relatively short-lived blocking events in the Australian region in June and blocking activity east of the Dateline from late June to mid July. During July high values of the index develop at Tasman Sea longitudes and persist until mid September with only a brief relaxation early in August. During August, as well, a second maximum of blocking activity makes its appearance in the western and central Pacific Ocean and this 'double block' structure persists into the early part of September. The persistent splitting of the jet stream structure during this period was discussed in Section 4.2 and examples of the mid tropospheric flow patterns observed were given in Fig. 4.9. The double structure is recognisable again towards the end of September following a slight retrogression of the centre of activity near Australia.

During the four month period the only evidence of blocking in the Indian Ocean sector is a maximum value of the index near Africa in the first week of June 1989, the only time when geopotential heights at 500 hPa exceeded 540 dam at 55°S in that period [see Fig. 4.13 (b)].
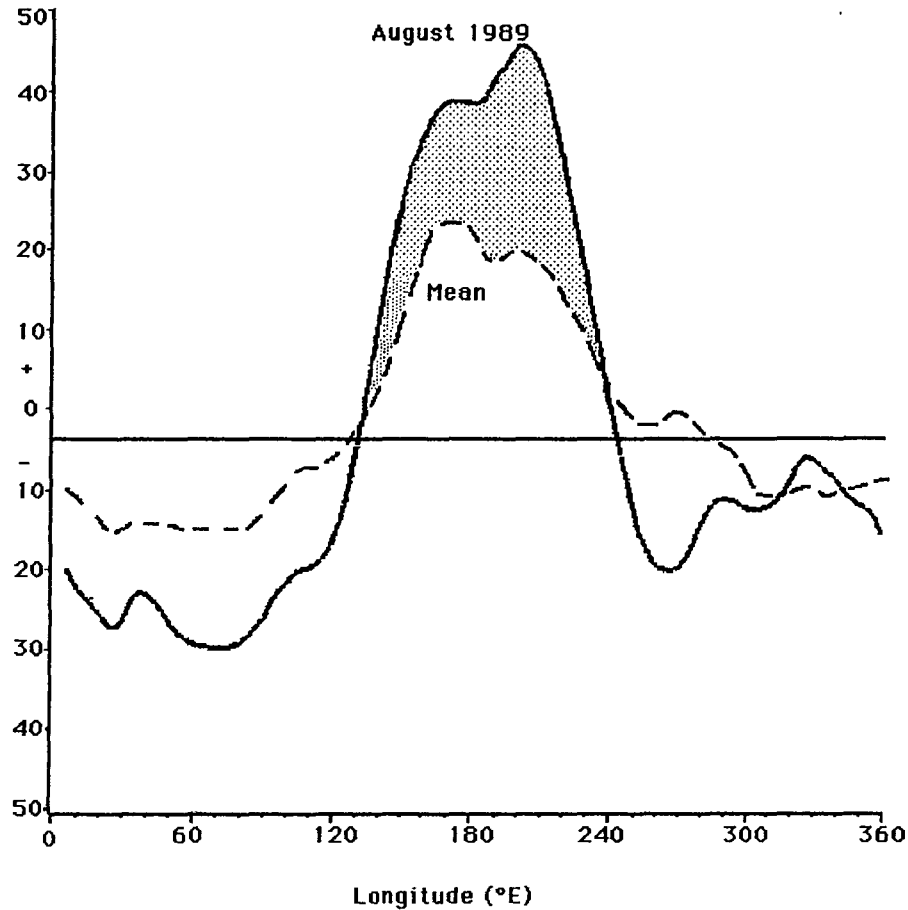
Fig. 4.21 (a) August 1989 mean blocking index (bold line) compared to a ten year mean (dashed line). (Bureau of Meteorology, National Climate Centre).
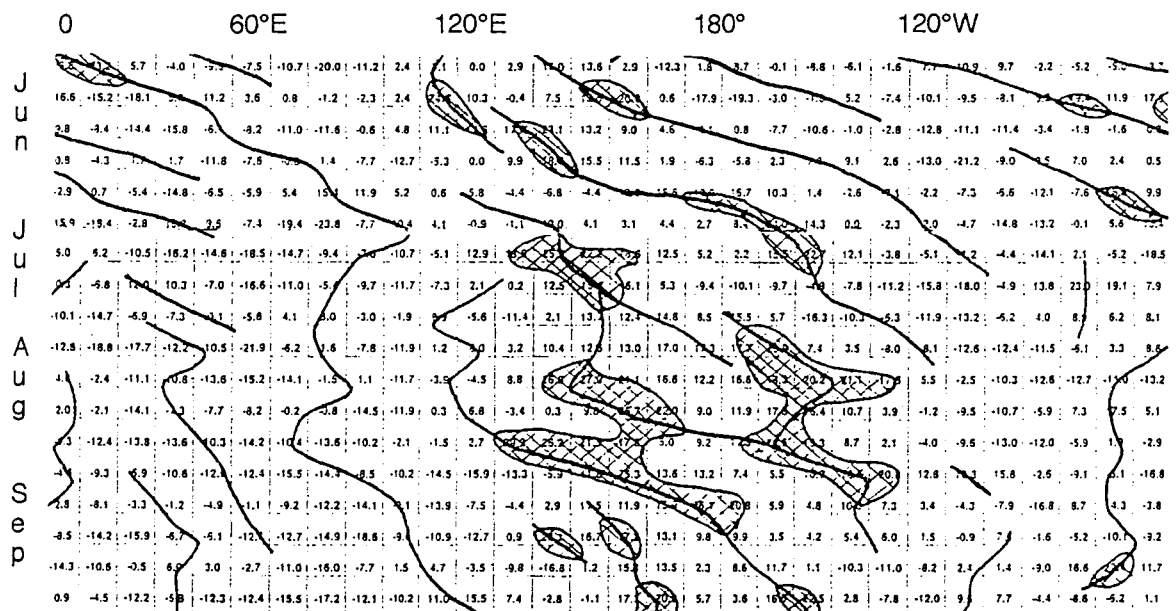

Fig. 4.21 (b). Time series of the mean weekly value of the Gibson Blocking Index during the winter and early spring of 1989. Hatched areas represent high values of the index (>17.5) and are associated with blocking. Solid lines join relative maxima for each week (Gibson, 1994).

4.8 Surface Wind Field

Fig. 4.22 (a) depicts the mean u component of the wind estimated for the 10 metre level from the Bureau of Meteorology FINEST model for the winter (June, July and August) of 1989, presented on the RASP grid. A broad area of strong westerly components (≥ 10 m s^{-1}) is evident in the mid-latitudes of the Indian Ocean sector but mean westerly components of approximately 6 m s^{-1} were a feature of the circulation in the region to the south of the Tasman Sea and New Zealand. Fig. 4.22 (b) shows the mean v component for the same period. Combining the two components indicates the persistence of strong northwesterly winds south of the Tasman Sea during the period. However, investigation of the 1000 hPa wind data set from ANMC reveals that there was a sharp transition from westerly winds (positive u components) to easterlies (negative u components) over the South Tasman Sea and New Zealand region from June to July.

In a similar manner to the situation at 500 hPa (see Fig. 4.8), the area of easterly component winds migrated into the western Pacific in August and westwards again in September. This behaviour further confirms the equivalent barotropic nature of the atmosphere during the event.
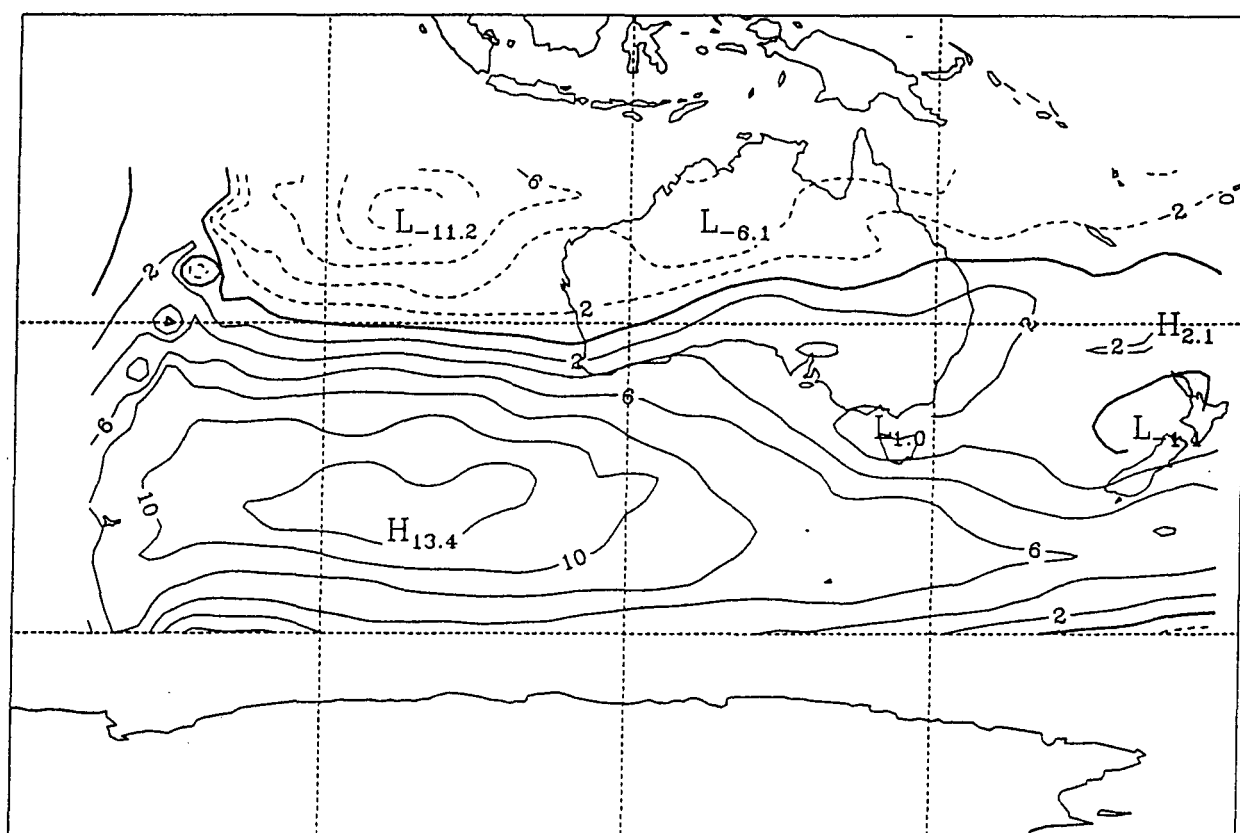
Fig. 4.22 (a) Mean u - component (westerly) of the estimated wind at the 10 metre level (m s^{-1}) from the Bureau of Meteorology FINEST model for the period 1 June to 31 August 1989.
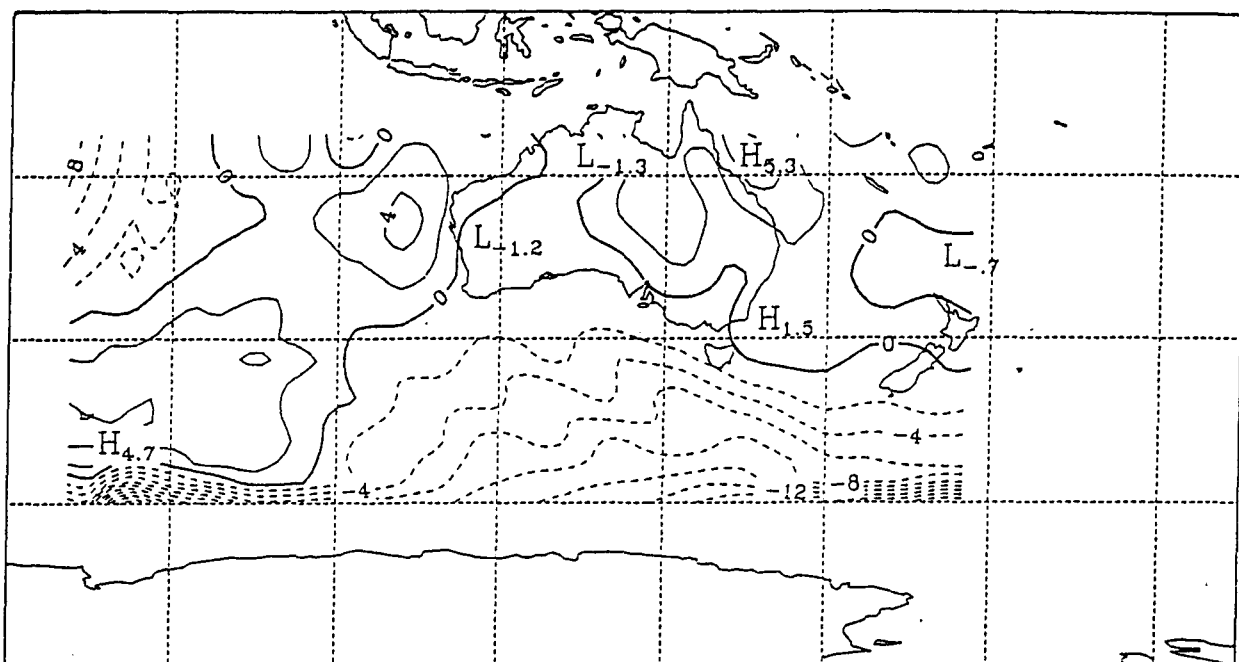
Fig. 4.22(b) Mean v - component (southerly) of the estimated wind at the 10 metre level (m s^{-1}) from the Bureau of Meteorology FINEST model for the period 1 June to 31 August 1989.

4.9 Rainfall

Following well above average autumn rains over most of Australia (decile ranges 8 to 10) which, according to Gaffney (1990a), were associated with a combination of the strong positive SOI signal, positive SST anomalies in the Australian region, southward displacement of the subtropical ridge and active phases of the 30 to 60 day cycle, rainfall patterns changed markedly during the winter months. Whereas rainfall totals for autumn were the highest on record for parts of central and southern Australia (WMO, 1992), Gaffney (1990b) reports that most of the continent received average rainfall (decile ranges 4 to 7) in the winter of 1989. His Fig. 12 shows that the notable exceptions to the general pattern were parts of South Australia and Victoria which experienced very much above average rainfall (decile ranges 8 to 10) and the southwest corner of Western Australia and most of Tasmania which suffered from serious rainfal deficiencies (decile ranges 1 to 3).

Winter rainfall for Tasmania in 1989 has been compiled for the rainfall districts defined in Bureau of Meteorology Monthly Weather Reviews. District averages for the 1989 winter are shown in Figs. 4.23(a) and 4.23(b), with comparative figures for winter rainfall in 1986, 1987 and 1988. A map depicting Tasmanian rainfall districts is given in Fig. 4.23(c). For the districts of Northern Tasmania, the East Coast and the Midlands [Fig. 4.23 (a)], the winter rainfall was not significantly reduced in 1989. Certainly, rainfall totals were well above the extremely low values which were recorded in 1987, during an ENSO event.
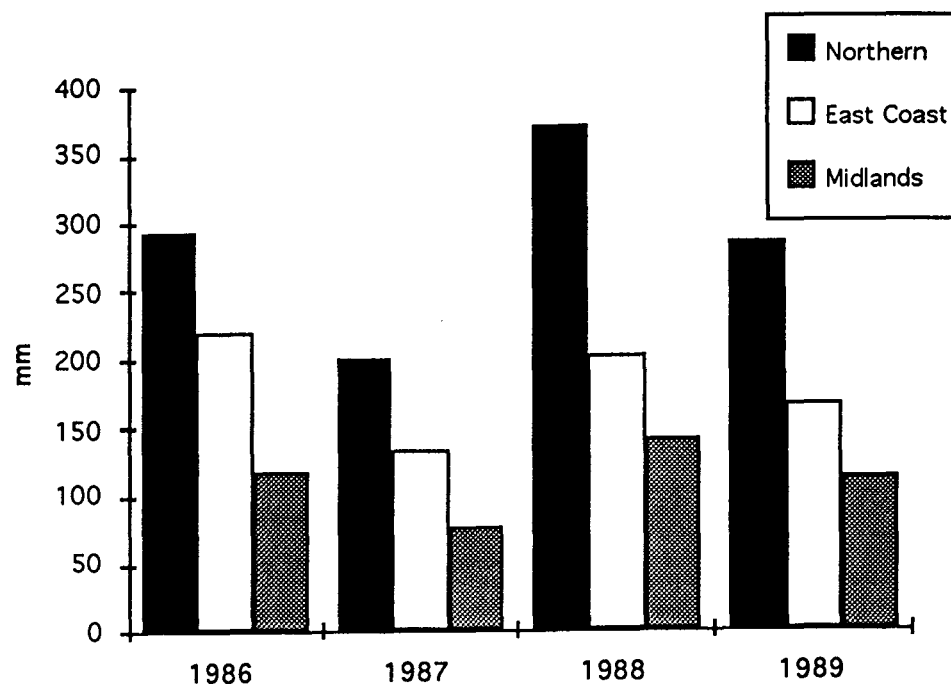
Fig. 4.23(a). Comparison of district average rainfall in the Northern, East Coast and Midlands districts of Tasmania for the winters of 1986,1987,1988 and 1989
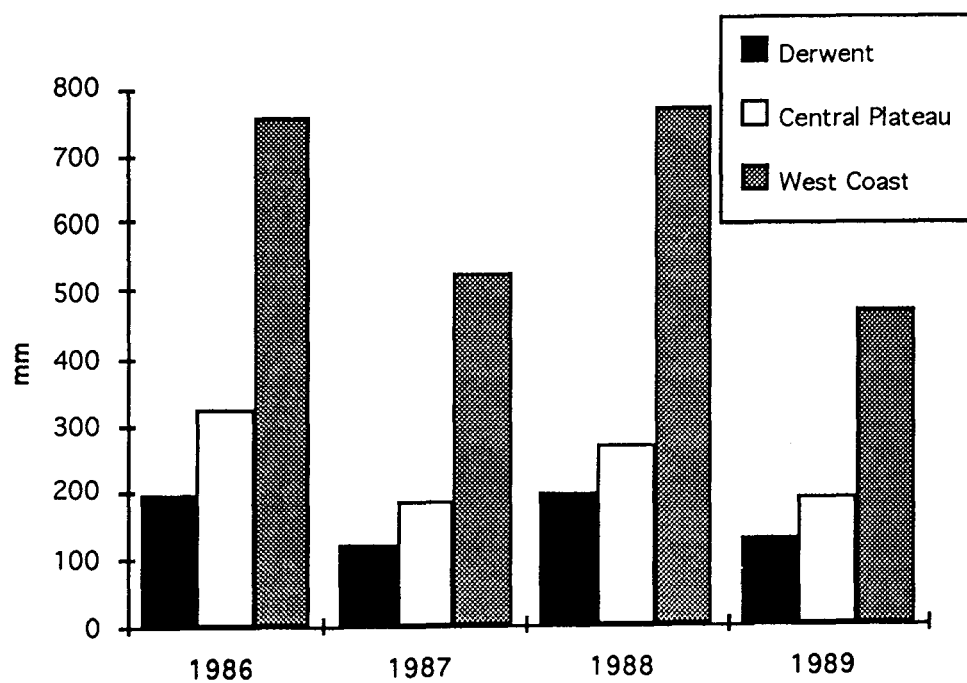
Fig. 4.23(b) Comparison of district average rainfall in the Derwent Valley West Coast and Central Plateau districts of Tasmania for the winters of 1986,1987,1988 and 1989.

Rainfall Districts

91 Northern
92 East Coast
93 Midlands
94 Southeast
95 Derwent Valley
96 Central Plateau
97 West Coast
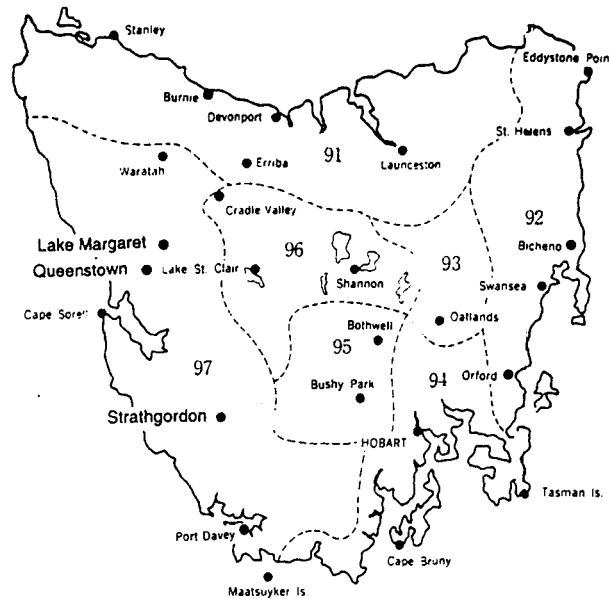
Fig. 4.23(c) Tasmanian rainfall districts and a selection of reporting stations.

It was a decidedly different pattern for the Derwent, Central Plateau and West Coast districts [Fig. 4.23 (b)]. The Central Plateau and Derwent recorded similar rainfall in 1989 to the 1987 values, but the West Coast district experienced lower winter rainfall in 1989 than in 1987. Furthermore, breaking up the West Coast district into individual stations reveals that the northern stations, Lake Margaret and Queenstown, received totals slightly below the 1987 winter rainfall, while Strathgordon, in southwestern Tasmania, was significantly drier than in 1987. Fig. 4.24 illustrates the negative gradient of winter rainfall from north to south in the West Coast district in 1989 and interannual variability over a four year period from 1986 to 1989. Rainfall at Strathgordon in August 1989 was 121 mm, the lowest August rainfall in 20 years of record (Bureau of Meteorology, Tasmania, 1989c). The distribution of winter rainfall over Tasmania and the southern Australian mainland is consistent with a persistence of blocking in the southern Tasman Sea and New Zealand sector with cut-off lows steering across Bass Strait and Victoria towards the northern Tasman Sea to reinforce the cyclonic portion of the block.

The rainfall deficiency over western Tasmania during the winter of 1989 was accompanied by a marked reduction in stream flow in the uncontrolled rivers of the region. Tasmania has an extensive hydro-electric power scheme and the flow in many of the state's rivers is manipulated by the Hydro-Electric Commission (HEC) of Tasmania. Hence, the effects of reduced rainfall over the catchments may be masked by the release of water from storages into these streams. In Fig. 4.25 the monthly mean flow in the upper reaches of the Huon River in southern Tasmania during 1989 is contrasted with a 17 year mean and demonstrates the uncharacteristic decline in the stream flow in the late winter and early spring of 1989. Reduced stream flow in this uncontrolled river is particularly evident in September of 1989, the month in which peak flows are normally attained.
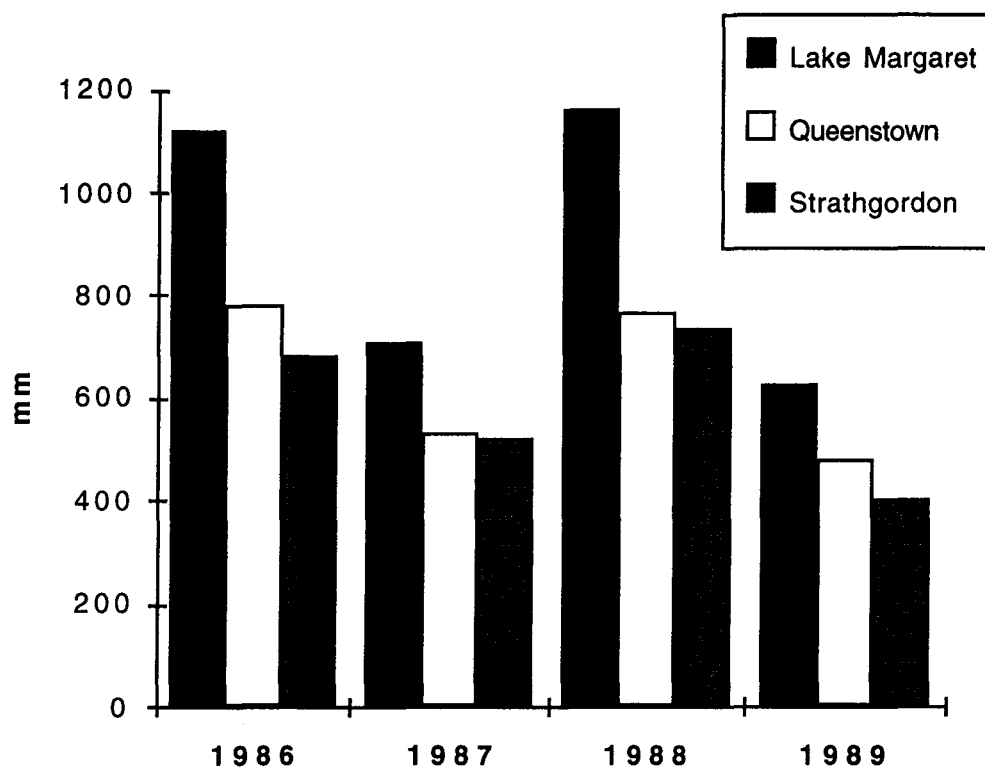
Fig. 4.24 Comparison of winter rainfall (mm) in the West Coast district of Tasmania for the period 1986-1989 at Lake Margaret, Queenstown and Strathgordon.

Huon River Streamflow
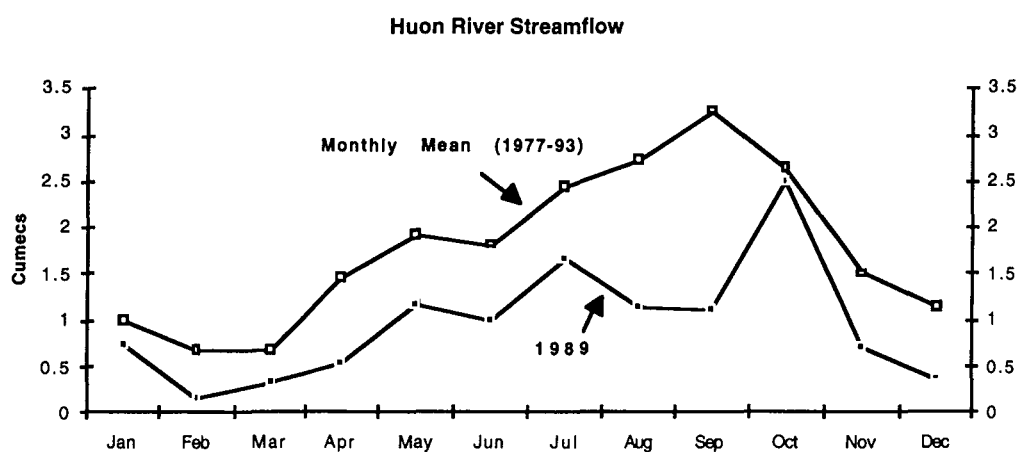
Fig. 4.25 Monthly means of stream flow in cubic metres per second (Cumecs) of the Huon River measured upstream of Sandfly Creek for 1989 and for all years of record.

4.10 The Southern Oscillation Index

As components of the major cycle within the atmosphere-ocean system in the Australasian region the Southern Oscillation and El Niño phenomena must be considered in any discussion of the interannual variability of major synoptic disturbances such as blocking. The dominant cycle of atmospheric pressure variations occurs between two main regions, the tropical Australian and Indonesian area, and the south-eastern tropical Pacific (Philander, 1990). There is a strong negative correlation between pressure variations in these two regions and its cyclical behaviour was given the name Southern Oscillation by Sir Gilbert Walker [see Walker and Bliss (1932) and reviews by Allan (1988) and Enfield (1989)]. The term, El Niño, has been expanded to encompass the phase of the Southern Oscillation when SST in the central and eastern tropical Pacific Ocean are anomalously high, and La Niña has been used to describe the other extreme of the cycle (Philander, 1990). The more general expression, El Niño-Southern Oscillation (ENSO), will be used here for the warm phase, when positive SST anomalies migrate into the eastern equatorial Pacific.

Although the Southern Oscillation is a consequence of the interannual variability of the tropical Pacific SST, the variations in SST across the Pacific basin are now believed to be linked to the surface wind anomalies which are induced by the strength of the zonal equatorial atmospheric circulation, the Walker Circulation (Cane, 1992). Graham and White (1988) have argued that the SST, zonal wind stress and the depth of the warm upper layer of the ocean interact through a complex feedback process, and produce a natural oscillation of the ocean-atmosphere system in the tropical Pacific, with links to higher latitudes. Cane (1992) has presented a conceptual model of this 'delayed oscillator mechanism' in terms of equatorial ocean dynamics. In this model Kelvin wave packets induced by westerly wind anomalies in the central equatorial Pacific propagate eastwards and depress the thermocline in the eastern Pacific. This excess of warm water is balanced by equatorial Rossby waves propagating westwards from the area of wind forcing and reflecting from the western boundary in the form of relatively cold Kelvin waves which propagate eastwards to once again reduce the SST in the east.

A quantitative measure of the Southern Oscillation is usually expressed in terms of the intensity and phase of the pressure difference between the Central Pacific and the Northern Australia-Indonesia region (Allan, 1988). This so-called Southern Oscillation Index (SOI) has been defined by Gaffney (1990a, p73) as "10 times the Tahiti minus Darwin MSL pressure anomaly divided by the standard deviation for the month , based on the period 1882 to 1985". When an ENSO occurs the index becomes strongly negative and may maintain negative sign for several months or more.

Several studies have concentrated on monthly and seasonal relationships between the SOI and atmospheric variables (e.g. van Loon and Shea 1987; Williams 1987; Drosdowsky 1988; Karoly 1989). Drosdowsky (1988) has demonstrated, for the Australian continent, that negative values of the SOI are well correlated, during the winter and spring months, with higher geopotential heights in southern Australia. Pook (1992) has investigated

seasonal correlations between the ZI and SOI over the period from 1971 to 1989. The correlation between the mean SOI for the winter months (JJA) and a winter mean of the ZI, here used as an indicator of blocking, yields a correlation coefficient (r = -0.48, n = 19), which is significant at the 0.05 significance level. The scatter diagram is shown in Fig. 4.26.
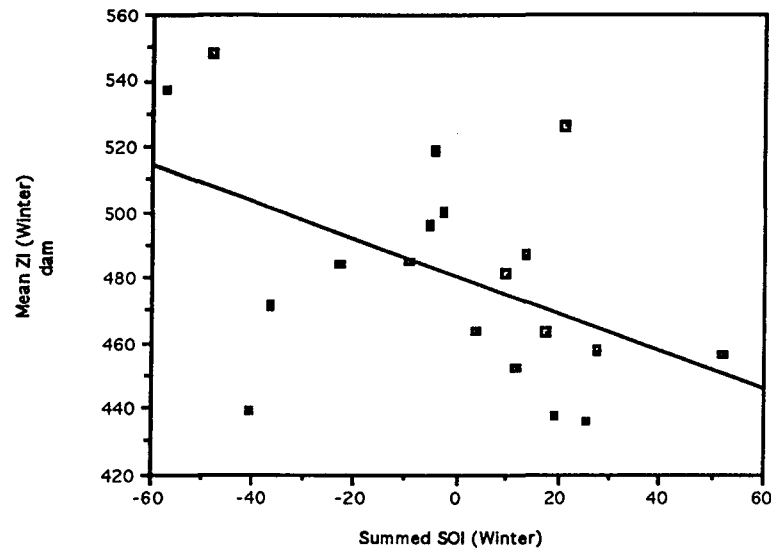

Fig. 4.26 Plot of mean zonal index (ZI) against a summed SOI for the winter months (JJA) over the period 1971-89.

Similar analyses for the other seasons reveal that the weakest correlation is obtained for the spring months while the strongest correlations occur in summer and autumn. Table 4.2 gives the correlation coefficients for each of the seasons and the annual relationship.

Season	r	n
Summer (DJF)	- 0.54	18
Autumn (MAM)	-0.60	19
Winter (JJA)	- 0.48	19
Spring (SON)	- 0.32	19
Annual	- 0.46	18

Table 4.2. Correlation coefficients (r) for the regression analyses between the SOI and mean ZI for each season and the annual value. (from Pook, 1992)

Investigation of the zonal index in terms of geopotential height variability at the northern boundary (i.e. 35°S) and at the southern boundary (i.e. 55°S) suggests that the influence of the Australian continent is a critical factor in the relationship between the ZI and ENSO. van Loon and Shea (1987) have drawn attention to the occurrence of positive mean sea level pressure (MSLP) anomalies over southern Australia during the late autumn and winter months (MJJ) of ENSO years. Composite geopotential fields for three ENSO events have been presented by Karoly (1989) and reveal similar characteristics to the van Loon and Shea (1987) results, for the winter months (JJA). Gaffney (1988) has demonstrated that positive anomalies of MSLP and

500 hPa geopotential height occurred over southern Australia and the
Tasman Sea during the winter (JJA) of the 1987 ENSO.

In the winter of 1989 the SOI remained in a positive phase following the
extreme positive excursion during the La Niña which reached its peak in the
latter half of 1988 and again early in 1989. Gaffney (1990b) reports that the
SOI remained positive from July 1988 to July 1989. Although falling to -5.6 in
August the index returned to positive again during September and October
1989 (Gaffney, 1992).

The negative correlation between SOI and ZI considered here suggests the
possibility of a post ENSO phase which is conducive to blocking in the
Australian region.

4.11 Application of Blocking Definitions to the 1989 Event

4.11.1 Wright's Criteria

Application of Wright's definition to the blocking event in 1989 requires
analysis of mean sea level pressure maps, 500 hPa fields and the positions
and intensity of the jetstreams. The latter involves, to some extent, subjective
assessments of upper air charts and satellite imagery. The full definition has
been discussed in Chapter 3.

It was demonstrated in Section 4.2 that splitting of the mid and upper
tropospheric flow was a persistent feature of the synoptic analyses during
the winter and early spring of 1989 and was first apparent in May 1989. In
the cases of the specific blocking episodes discussed in the text split jet
structures are clearly evident. The question of whether the split structure
developed before the appearance of blocking at lower atmospheric levels or
was coincidental with it, is difficult to determine defintively. On the balance
of the evidence presented here the former is favoured.

Application of the second criterion of Wright's definition excludes all
occurrences of slow moving highs as blocks until 28 June when an
amplification occurred in the 5-day mean geopotential heights at 45 °S to a
value of 562 dam at 145 °E [see Fig. 4.13(a)]. This pulse propagated
eastwards over a period of approximately 8 days and lost intensity after
reaching the Dateline. The mean ridge progressed approximately 30° of
longitude in a week but no more than 35° in the episode. Strictly speaking,
this would disqualify the event as blocking according to criterion no. 2. The
events in late July and during August and September more closely accord
with the restrictions of the second criterion. When the 5 day running means
at 55 °S are considered, they display a more consistent and slow moving
pattern. In cases of blocking, such as the 1989 episode, the ridging was
centred at high latitudes and the definition appears to be deficient to the
extent that it only takes account of the mid-tropospheric ridge at the 45th
parallel.
The third criterion is the easiest to apply in the 1989 situation. As the axis of
the sub-tropical ridge over eastern Australia and the Tasman Sea is located

near or sligtly north of 30 °S in winter (Taljaard, 1971), it is only necesary for the surface highs to be situated south of 37 °S to satisfy the criterion. Commonly the anticyclones in the 1989 episode were multi-centred but in all cases the southern cell was located well south of 40 °S and in several instances, south of 50 °S. The effect of these high latitude anticyclonic centres was evident at Macquarie Island as was previously discussed in Section 4.5 and illustrated in Table 4.1.

4.11.2 Trenberth and Mo (1985) Criteria

The technique employed by Trenberth and Mo (1985) to determine the temporal frequency and spatial distribution of blocking in the Southern Hemisphere was discussed in some detail in Chapter 3. Essentially, their objective definition of blocking requires a large positive anomaly (e.g. ≥ 10 dam) of 500 hPa geopotential height to persist for at least 5 days. The anomalies in their analysis were obtained by substracting the grand mean plus the first 4 harmonics of the time series for each gridpoint in order to remove the annual cycle.

As this analysis has been confined to the winter months, means of 500 hPa geopotential height for the 4 month period from June to September have been calculated for each gridpoint for the period from 1972 to 1991. It should be noted (see Chapter 2) that the long-term means in this case have been constructed from NMAC analyses at 00 UTC whereas the daily geopotential heights in 1989 were extracted exclusively from the 1200 UTC analyses. Anomalies are therefore defined as departures of daily geopotential heights at 1200 UTC from this winter mean. Fig. 4.27(a) shows the positive anomalies (≥15 dam) at 12 gridpoints at 55 °S relative to this long-term mean during the winter and early spring of 1989. Throughout June and early in July anomalies migrated through the region from the west but few satisfying the threshold criterion were observed east of 150 °E. A marked change in the pattern occurred during July after which significant anomalies were mostly confined to the eastern sector.

In order to approximate the technique of Trenberth and Mo (1985), transient anomalies were then filtered out by applying the condition that the anomaly should persist at a gridpoint for at least 5 days. Only anomalies which met this condition would then define a blocking event. In Fig. 4.27(b) these persistent anomalies are identified. It is immediately apparent that long-lived anomalies of this magnitude only made an appearance in the Tasman Sea-New Zealand sector towards the end of July. Thereafter, persistent anomalies occupied this sector at regular intervals until the end of September. Strict application of the criterion would confine the incidences of blocking to six episodes. Of these, two occurred west of 130 °E and the other four east of this meridian and predominantly east of 150 °E. In the three later events, anomalies exceeding +15 dam at gridpoints near the Dateline had lifetimes of the order of 10 days. Trenberth and Mo (1985) have demonstrated in their Figs. 6 and 7 that this region has the highest incidence
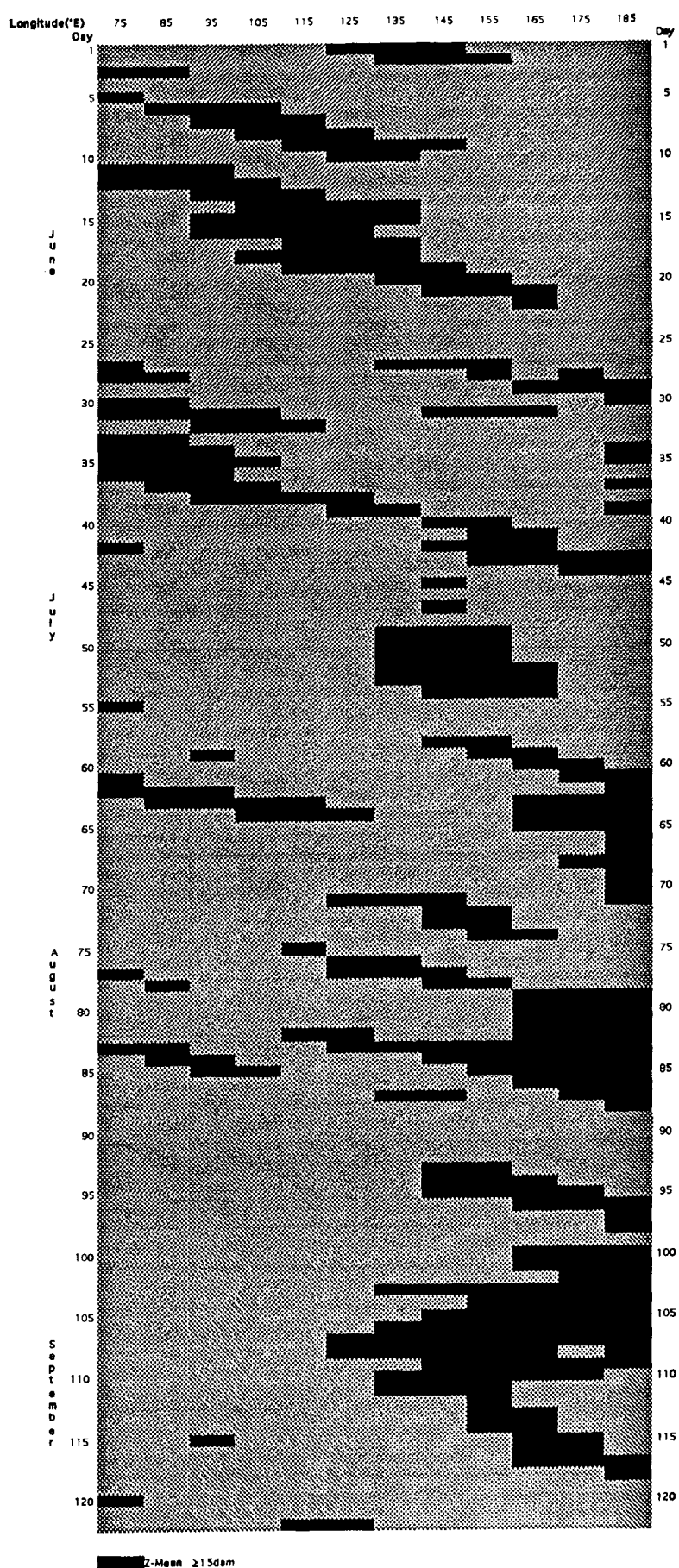
Fig. 4.27(a). Anomalies of daily 500 hpa geopotential height at 55 °S (1200 UTC)of at least 15 dam for the months of June, July, August and September 1989 relative to a long-term mean.
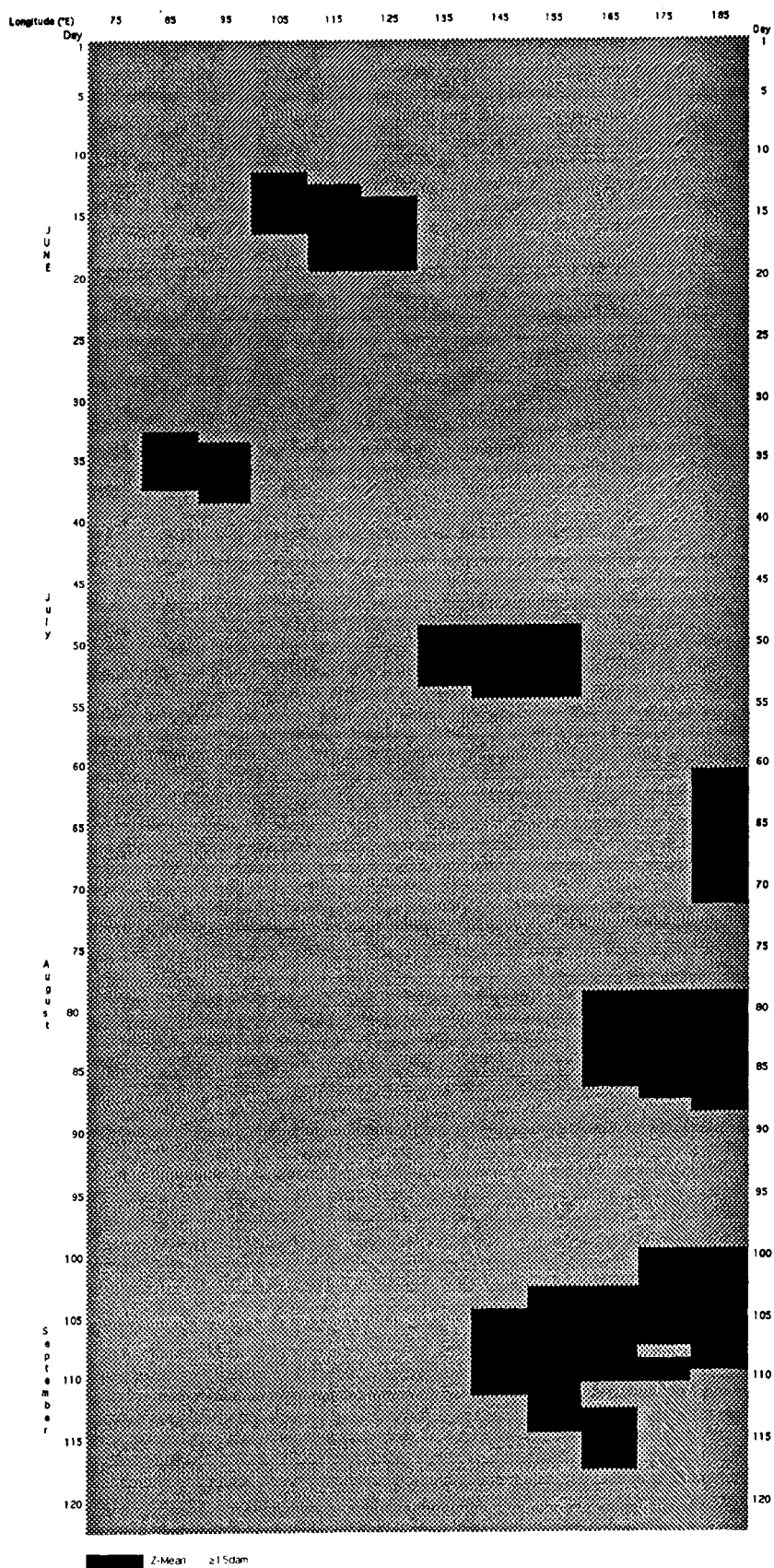
Fig. 4.27 (b) Anomalies of geopotential height at 55 °S exceeding 15 dam and persisting for at least 5 days.

of positive and negative anomalies persisting for at least 5 days in winter (~4 per annum). When the residence period is extended to a minimum of 10 days the maximum frequency of occurrence shifts to East Antarctica and the Antarctic Peninsula, with a secondary maximum (~1.2 per annum) at 180°.

4.12 Conclusion

The 1989 event

The blocking events which occurred during the winter and early spring of 1989 qualify as excellent examples of the phenomenon in the Southern Hemisphere. Numerous indicators have been employed in this chapter to test the intensity, longevity and spatial extent of the blocks during this period and the events have been examined relative to blocking criteria for the Southern Hemisphere developed by Wright (1974) and Trenberth and Mo (1985).

This analysis adds to the already considerable weight of evidence which points to the dominance of wave number 3 in winter blocking situations in the Tasman Sea-New Zealand region (e.g. Trenberth and Mo, 1985: Mo, 1983; Trenberth and Swanson, 1983, Noar, 1983). But in this case, although mean geopotential heights in the peak ridge at 55 °S were 20 year maxima (see Section 4. 3), the secondary ridge near South America was not greatly diminished by comparison. As indicated by Gaffney (1990b), positive MSLP anomalies southeast of South America and especially over the Weddell Sea region in the 1989 winter, were only slightly below those in the Southwest Pacific. The South American region is an area where major blocking episodes have been been observed previously (Schwerdtfeger, 1984). Furthermore, winter anomalies of geopotential height at 500 hPa and 300 hPa over the Antarctic Peninsula and Weddell Sea were larger than for the region studied. The purely localised nature of the Tasman Sea blocking which has been discussed by numerous authors (e.g. Baines, 1983) is brought into question by the findings of this study and may require further evaluation.

The implication of a broader mechanism at work in this situation, possibly extending over the Pacific Basin and environs, the Southern Hemisphere or even the globe, is further indicated by the persistence of the split jetstream structure in the South Pacific and Australia throughout the period May to September 1989 (see Section 4. 2). Trenberth (1980) drew attention to a quasi-biennial oscillation in the meridional circulation in the New Zealand region which van Loon (1984) demonstrated was consequent upon variations in the position of the long-wave trough in the region. Trenberth and Mo (1985) argue that this variability forms an integral part of the Southern Oscillation. It is noteworhty that the blocking episode discussed in this chapter occurred as the major La Niña of 1988-89 was drawing to an end. It was shown in section 4.10 that correlations between the ZI and SOI presented by Pook (1992) are able to explain a portion (approximately 25%) of the variance in the winter relationship. In this case, it is argued that an enhanced Hadley circulation between Indonesia, Southeast Asia, the Maritime Continent and the South Pacific may have been the major contributing factor to the onset, intensity and persistence of the split jetstream structure during the winter of

1989. In turn the Hadley circulation was amplified by the stronger than normal Walker cell in the tropical Pacific accompanying La Niña. Other factors such as the strength of the Asian and Indian monsoons have not been considered. Intensification of the Polar Front Jetstream was ensured by the persistence of negative geopotential height anomalies over Marie Byrd Land in Antarctica and the eastern Pacific sector (Gaffney, 1990b).

If the phase and intensity of the Southern Oscillation were contributing factors in the event in 1989 it remains to be explained how the major blocking activity remained anchored near New Zealand longitudes. This region near the 'climatological split in the westerlies' (Trenberth and Mo, 1985) is the most favoured location for blocking in the Southern Hemisphere (e.g. Wright, 1974; Hirst and Linacre, 1981). Apart from the limited topographical influence of the South Island of New Zealand, the most obvious local forcing factor in this region is the pronounced west to east SST gradient from the Indian Ocean to the South Tasman Sea and Southwest Pacific Ocean and meridional gradients of SST. These factors will be discussed in detail in Chapter 5.

Chapter 5

Atmosphere, Ocean and Continental Interactions in a Prolonged Blocking Event

5.1 Introduction

The collected works of Jerome Namias abound with papers discussing the symbiotic relationship between the atmosphere and surface layers of the ocean, particularly the eastern North Pacific Ocean (e.g. Namias, 1959; Namias, 1963; Namias, 1965; Namias, 1969; Namias, 1970 and Namias, 1976). Woods (1984) has given a detailed analysis of the interaction between the upper ocean and the atmosphere. More recently, Shukla (1986) and Newell and Wu (1992) have discussed aspects of the physical mechanisms involved in associating changes in atmospheric parameters with identifiable changes in the ocean , including temperature anomalies.

Shukla (1986) has emphasised that the relationship between the atmosphere and ocean surface is dependent on the actual temperature of the sea surface and therefore the amount of heat energy available, as well as the temperature gradient between the sea surface and the constantly changing atmospheric boundary layer. Hence the influence of tropical oceans is greater than those of the high latitudes where energy inputs are significantly lower. In the Australian region, numerous studies have investigated the relationships between SST in the tropical Pacific Ocean and rainfall in Australasia (e.g. Nicholls, 1989; Lough, 1992). Other studies have followed a less direct path by concentrating on links between the Southern Oscillation and rainfall and circulation anomalies in the Australasian region (e.g.. McBride and Nicholls, 1983; Williams, 1987; Drosdowsky, 1988). An extensive review of research conducted into the influences of the El Niño Southern Oscillation (ENSO) phenomenon on the Australasian region has been carried out by Allan (1988), while Tyson (1986) has examined correlations between the SOI and rainfall and circulation indices for southern Africa. Other investigators have looked beyond the Pacific Ocean to the waters surrounding Australia, including the Indian Ocean, and demonstrated correlations between SST (and SST configurations) and annual rainfall over Australia (Streten, 1981; Streten, 1983) or winter rainfall over Australia (Nicholls, 1989; Simmonds and Rocha, 1991; Drosdowsky, 1993). Simmonds and Rocha (1991) have employed numerical model simulations to investigate the physical processes involved in the interaction between the tropical Indian Ocean and winter climatic patterns over Australia.

Apart from considerations of high latitude source regions of atmospheric airmasses in the Southern Hemisphere (e.g. Gentilli, 1971; Taljaard, 1972), studies which examine the importance of the middle and high latitude oceans in influencing atmospheric circulation anomalies in the Australasian region are scarce when compared to similar studies carried out in the tropics. Nevertheless, investigations of the possible association between Antarctic sea ice extent with its seasonal and interannual variability, and synoptic and

mesoscale atmospheric systems have been widely reported (Streten and Pike, 1980; Budd, 1982; Carleton, 1989; Carleton,1992). Allison (1989) and Worby and Allison (1991) have discussed the processes whereby interactions occur among the atmosphere, ocean and Antarctic sea ice and the critical dependence on the thickness of the ice and the open water fraction in the energy exchange. Budd (1986) reports that atmospheric circulation can be significantly altered in general circulation models (GCM's) by manipulation of the extent of the Antarctic sea ice and the configuration of the SST. A numerical experiment employing a prescribed SST anomaly as input to the Melbourne University GCM (Simmonds *et al.*, 1988) has been conducted as part of this study (see Chapter 6).

Hirst & Linacre (1981) drew attention to the semi-annual cycle of blocking frequency in the Australian region which was evident in the earlier data analysis of Wright (1974). Their tentative conclusions suggested that the west to east SST gradient along middle latitudes from the Indian Ocean to the Tasman Sea may be a factor in the high frequency of occurrence of blocking in the Tasman Sea-New Zealand region but they did not relate the pronounced seasonal cycle of blocking activity to any seasonal cycle of SST or SST gradient. This study attempts to identify aspects of the observed SST distribution and its seasonal variability which could be associated with the observed atmospheric behaviour. The possibility of examining relationships of this type has become reality with the availability of high quality data sets of SST such as COADS (Slutz *et al.* , 1985), Reynolds Blended SST (Reynolds, 1988) and GOSTA (Bottomley *et al.* , 1990). In this chapter, zonal and meridional SST gradients in the Indian Ocean and Australian region are examined for evidence of seasonality and interannual variability. No attempt has been made in this study to examine the fluxes of heat, water vapour and momentum as this would have expanded the thesis to include boundary layer considerations and modelling. Rather, the observed temperature anomalies are treated as the broad response to these atmosphere-ocean interactions.

5.2 Outline of Chapter

This chapter will focus on the spatial structure of the SST field in the Australian region, its observed variations with the seasons and its interannual variability. In particular, the physical factors which contribute to the long-term mean SST distribution will be identified and the significance of these factors to the Southern Ocean circulation discussed. The examination of the SST patterns will be quantified by calculating gradients of temperature along meridians between Antarctica and 25°S across the Southern Ocean from the Indian Ocean sector to the Southwest Pacific sector.

Having established the broad parameters of the distribution of SST over the region it will be demonstrated that the lower troposphere responds to the oceanic influence in a clearly defined manner when examined on time-scales of approximately one month. It will be shown that when atmospheric thickness is used as a proxy for atmospheric temperature, statistically significant correlations can be derived between SST and 1000 to 500 hPa atmospheric thickness.

Although strong atmospheric links will be established with the SST pattern in the region, terrestrial effects play a significant role in the warming and cooling of the atmosphere. This aspect will be examined with particular reference to the effects of the Australian and Antarctic continents on atmospheric temperature structure and its seasonal and interannual variability. The linking of the atmosphere, ocean and continental influences in establishing suitable conditions for the onset and maintenance of atmospheric blocking in this geographical region will be summarised in a conceptual model.

Finally, the interannual variability of the SST gradients, continental temperatures and atmospheric circulation patterns will be discussed within the framework of the conditions prevailing prior to and during the intense blocking event which occurred during the winter and early spring of 1989. The detailed climatology of this event was discussed in Chapter 4, where the broader influences of the Southern Hemisphere circulation were examined as well.

5.3 SST gradients in the Indian Ocean and Australian Region

Seasonal and annual cycles

The annual and seasonal cycles of SST over the Southern Hemisphere have been described in detail by several authors (e.g. Gordon and Molinelli, 1982 ; Levitus, 1982; Olbers *et al.*, 1992) and more recently, modelling studies have reproduced the essential details in the FRAM Atlas (Webb *et al.*, 1991). Although the seasonal analyses of van Loon (1972) presented meridional cross-sections of air temperature gradient at selected meridians (per 5° latitude) in the Southern Hemisphere, variability of the SST gradients which are contained within these data sets have not been widely reported. In this study, seasonal cycles of meridional and zonal SST gradients are calculated and presented.

South to North Gradients of SST

Following the approach employed in the study of the Zonal Index (ZI) as a measure of mid-tropospheric winds (see Chapter 4), the monthly meridional SST gradients over the Southern Ocean were assessed initially from the COADS (Slutz *et al.* , 1985) by calculating the difference between the SST at 35 °S and 55 °S. The SST gradients over this 20° latitude interval have been calculated along meridians at intervals of 2° longitude. In Fig. 5.1, the mean meridional difference between 35 °S and 55 °S for longitudes from 74 °E to 174°W is compared with the mean difference over the longitude bands from 74 °E to 130 °E and from 130 °E to 174°W Throughout most of the year the curves are closely in phase with clear minima evident in August. The north to south gradient in the eastern sector is considerably smaller than in the west during all seasons (by approximately 3°C) but the amplitude of the seasonal signal is similar in each case. There is a discernible divergence in early autumn when the mean SST gradient in the west continues towards a maximum in April while the eastern gradient declines gradually from its peak in February. Further dissection of the western component of the mean

gradient reveals that a phase change can be traced from west to east across the domain. Fig. 5.2 shows that the peak at 74 °E occurs in February and at 114 °E in April. At 124 °E, the month of maximum gradient is less well defined but the maximum clearly occurs in autumn. As well it can be shown that the average meridional gradient for the nigher latitude band of 45 °S to 55 °S reaches a maximum in April.
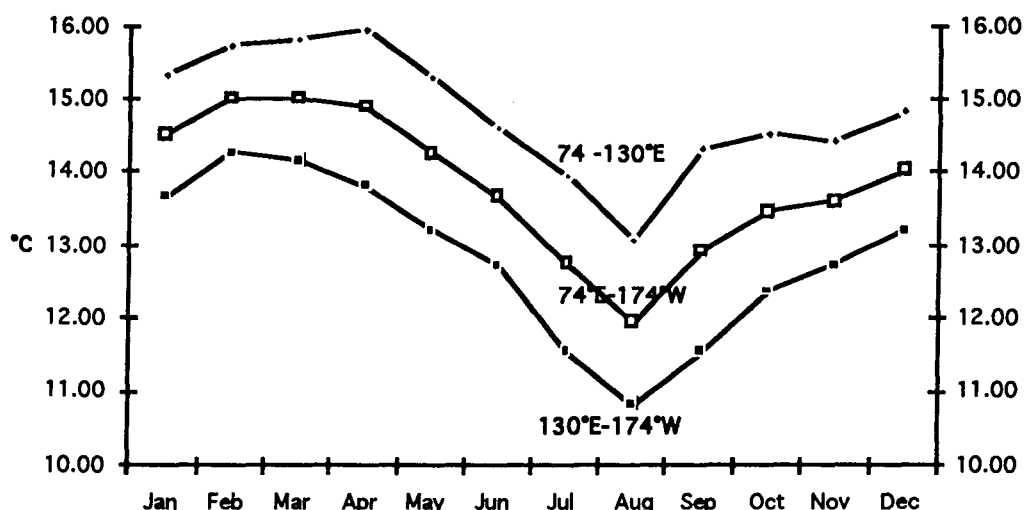
Fig. 5.1. Monthly meridional SST difference between 35 °S and 55 °S averaged over longitudes from 74 °E to 130 °E (top), 74°E to 174°W (middle) and 130°E to 174°W (lower) (from the COADS).
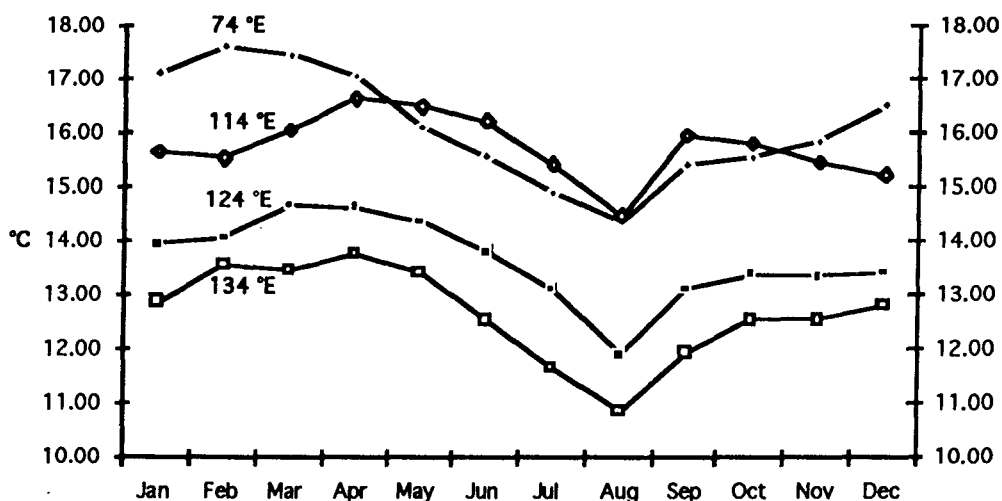
Fig. 5.2 Monthly meridional SST difference between 35 °S and 55 °S at 74 °E, 114 °E, 124 °E and 134 °E (COADS data).

From a comparison of the annual cycles of SST at various latitudes over the Southern Ocean it is apparent that the major contribution to the peak meridional gradient occurs at the southern boundary. Fig. 5.3 contrasts the annual SST cycle over the Southern Ocean at middle and high latitudes for two longitude intervals in the Australian region. Gloersen *et al.* (1992) have demonstrated that mean monthly sea ice concentration around Antarctica reaches a minimum in February but increases rapidly in April and May during the period of rapid cooling of the Southern Ocean following the autumnal equinox. From Fig. 5.3 it is evident that SST at 60°S fall rapidly during autumn. Thereafter, SST in the high latitudes continue to fall only gradually during the winter and early spring apparently constrained in the western sector [Fig. 5.3(a)] by the ice point of sea water (approximately -1.8°C) and the insulating effect of the sea ice itself (Allison *et al.*, 1993). In the eastern sector, van Loon (1967) has drawn attention to the marked circulation change observed south of New Zealand at Campbell Island between March and June which suggests that atmospheric processes may play a part in arresting the decline in SST here. By comparison, steady cooling continues in the mid-latitudes (e.g. 40°S) during winter, resulting in a diminution of the gradient between middle and high latitudes by late winter.
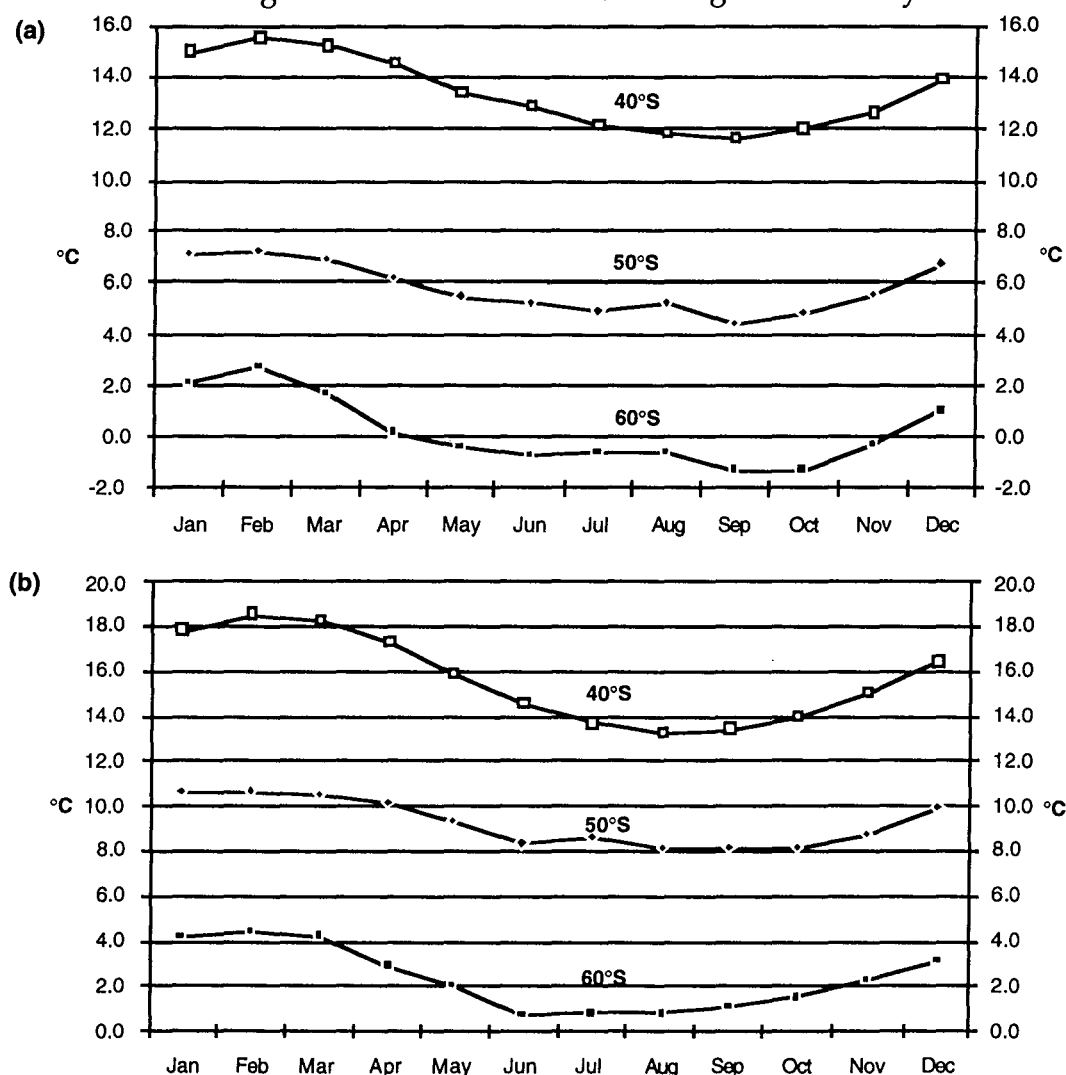
Fig. 5.3 Monthly means of SST at latitudes 40°S, 50°S and 60°S, averaged over longitude intervals, (a) from 104°E to 134°E and (b), from 154°E to 176°W (from the COADS).

It is important to note that, although the seasonal changes in meridional SST gradients are significant when viewed in the broad-scale there is considerable fine structure within these data. This is evident particularly when the north-south SST changes are broken up into smaller latitude intervals (e.g. 5° of latitude). Over the longitude interval from 154 °E to 176 °W the annual cycles of meridional SST gradient between 40 and 45 °S and 55 and 60 °S are shown in Fig. 5.4(a). The high latitude peak gradient in July contrasts with the minimum in the lower latitude band while the situation is reversed in February and March.
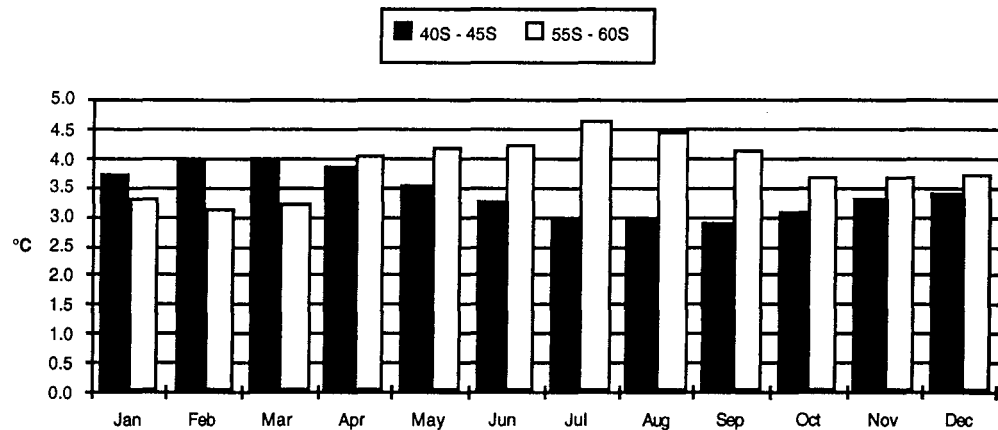
Fig. 5.4 a. Monthly mean meridional SST gradient (per 5° Latitude) averaged over the longitude interval from 154 °E to 176 °W for latitude bands 40-45°S and 55-60°S.

Fig. 5.4(b) provides a contrasting pattern for the Indian ocean sector. In this region (74 to 104 °E) the gradients between 40 and 45 °S and also 45 and 50 °S (not shown) are higher than those at more southern latitudes throughout the year. The gradient between 55 and 60°S in these longitudes reaches a maximum in the winter months but the peak value is only 2.3°C/5°Latitude compared to a maximum value of 4.6°C/5°Latitude for the same latitude band in the Tasman Sea sector. In each case, however, it is significant that the gradients are steeper at the lower latitudes in summer compared to winter and steeper in winter than in summer at the higher latitudes.
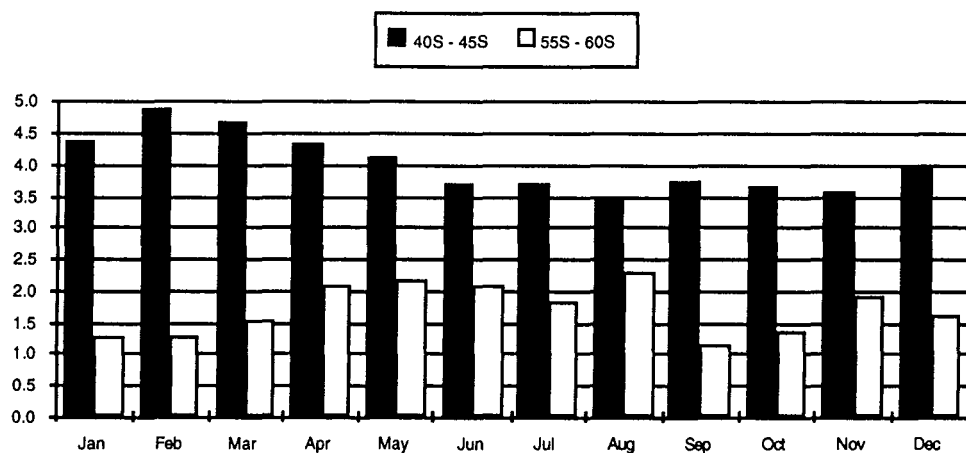
Fig. 5.4 b. Monthly mean SST gradient (per 5° Latitude) averaged over the longitude interval from 74 °E to 104 °E for latitude bands 40-45°S and 55-60°S (COADS data).

West to East SST Gradients

The possible association of atmospheric blocking with the marked west to east SST gradient over the waters south of Australia between the cold Indian Ocean sector and the relatively warm Tasman Sea and Southwest Pacific Ocean was first noted by Taljaard (1972). The concept was pursued by Wright (1974) in his detailed study of blocking frequency in the Australian region. Hirst and Linacre (1981) made reference to this possible association and argued for a detailed analysis of the role of the ocean in the phenomenon. Coughlan (1983) summarised this previous work and illustrated the magnitude of the SST gradient along 50 °S in the Southern Ocean for the month of October in his Fig. 13, which was derived from data published in the US Navy Marine Climatic Atlas of the World.

Pook (1993) has demonstrated that the west to east gradient of SST at high latitudes (e.g. south of 50°S) displays a seasonal cycle with the maximum gradient occurring in the Australian region in October and a secondary maximum in April. Fig. 5.5 depicts SST as a function of longitude in the Southern Hemisphere at 50 °S and 56 °S in summer (January), autumn (April), winter (June) and spring (October). At 50°S the maximum gradient in October occurs between 110°E and about 125°E. Over this longitude interval the SST climbs from 3°C to 6°C, which is at least 1°C greater than the increase observed for the other months shown. Between 110°E and 165°E the SST increases by approximately 6°C in October, 5.5°C in April, 5°C in June and 4.5°C in January.

Along 56°S the variation of SST in October is greatest between 145°E and 170°E where an increase of about 5°C is observed. This region will be identified in Section 5.4 as an area in which southward displacement of the Antarctic Circumpolar Current occurs. Overall, SST increases along 56°S between 110°E and 165°E for the 4 months considered here, are at least 1°C less than the corresponding changes at 50°S (Fig. 5.5 (a).

The SST at lower latitudes do not display the strong west to east warming from the central Indian Ocean sector to the Tasman Sea, which is evident south of 45 °S. Fig. 5.6 (a) shows seasonal plots of SST against longitude along 40°S between 34°E and 150°W contrasted with Fig. 5.6 (b) which depicts plots of SST over the same longitude range at 46°S.

At 40°S the temperature decreases by approximately 3°C between 60°E and 100°E and then climbs by a similar amount across the interval from 100°E to 155°E, in the central Tasman Sea, where the East Australian Current (EAC) carries relatively warm water eastwards towards New Zealand. South of Western Australia there is a temperature maximum which is most pronounced in winter. In contrast to the situation at 40°S, the temperature curves along 46°S [Fig. 5.6 (b)], display broadly similar features to the seasonal plots at 50°S in Fig. 5.5 (a) throughout the longitude sector east of 74°E.
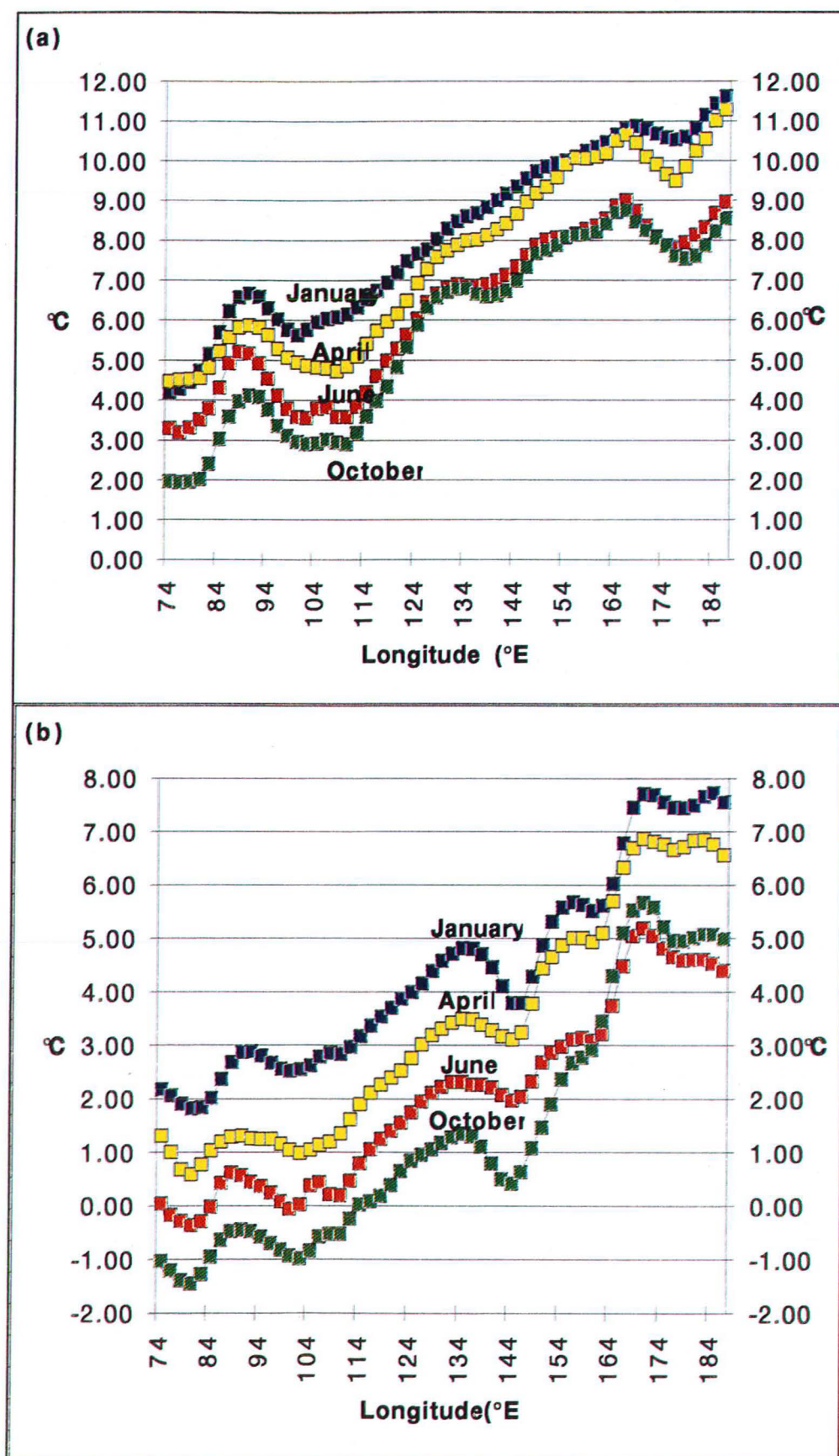
Fig. 5.5. SST as a function of longitude for the months of January, April, June and October, (a) along 50°S and (b) along 56°S (from the COADS).
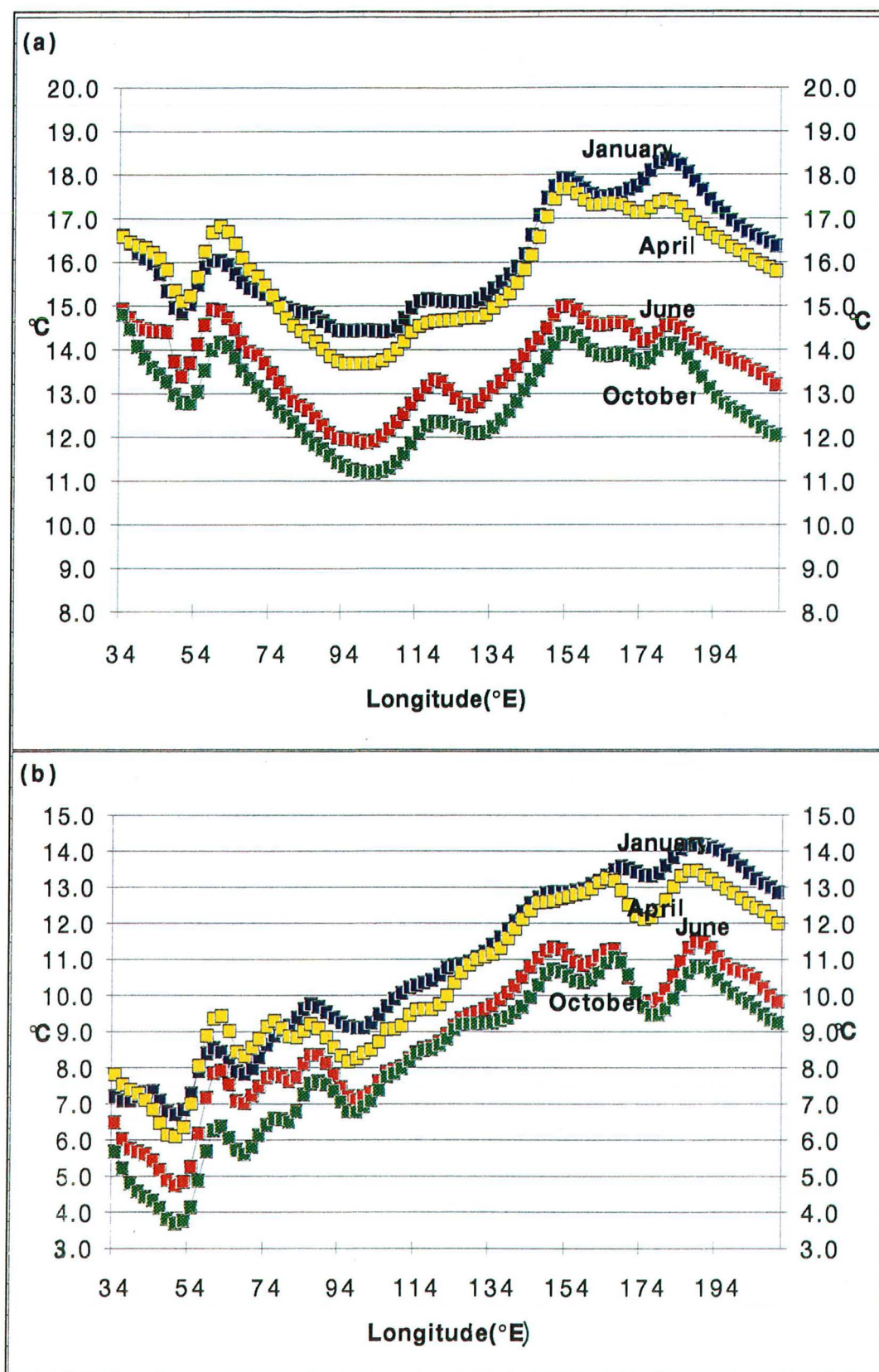
Fig. 5.6. SST as a function of longitude for the months of January, April, June and October, (a) along 40°S and (b) along 46°S (from the COADS)

Hirst and Linacre (1981) have shown that the month of October represents a significant minimum of mean blocking activity. However, this corresponds to the time of maximum west to east SST gradient south of Australia. By way of contrast, the months of maximum blocking frequency (viz. January and June) represent periods when the west to east SST gradient is at a minimum. Hence, the west to east SST gradient must be regarded as an inadequate explanation for seasonal blocking frequency in the region. This does not mean that it is not involved in some way with the mechanism of blocking but the evidence suggests that it has a secondary rather than primary role in the process.

5.4 The Antarctic Circumpolar Current

Nowlin and Klinck (1986) have discussed in detail the distinguishing characteristics of the Antarctic Circumpolar Current (ACC). In particular, they have identified the ACC as a major eastward flowing surface current associated with a zone of transition between surface waters with Antarctic characteristics and those with sub-Antarctic properties. Gordon et al. (1978) showed that the geostrophic surface current relative to 1000 dbar displays varying widths and strengths around the hemisphere while the latitude of the core of the current varies considerably around the hemisphere. Nowlin and Klinck (1986) argue that the latitudinal variation is closely related to 'geomorphological influences', a conclusion previously reached by Gordon (1967) and emphasised by Streten and Zillman (1984), Budd (1986) and Gloersen et al. (1992).

Fig. 5.7 shows the bathymetry of the World's oceans. In the Southern Ocean prominent features include the Kerguelen Plateau to the south of the central Indian Ocean, the Indian-Antarctic Ridge south of Australia, the Pacific-Antarctic Ridge which extends east-northeastwards into the South Pacific Ocean and the Campbell Plateau and Macquarie Rise extending south of New Zealand. Fig. 5.8 traces the main arms of the ACC in relation to the bottom topography. The axis of the current reaches its northernmost extent in the Indian Ocean where the main current is steered north of the Kerguelen Plateau. South of Australia the axis of the current is at an approximate latitude of 50 °S. It diverts southeastwards around the Macquarie Rise and the Campbell Plateau to approximately 65 °S.

The ACC is associated with well defined oceanic fronts in the temperature and salinity fields. The broad features of the surface fronts are shown in Fig. 5.9. In the vicinity of the Tasman Sea and New Zealand the southernmost front, the Polar Front, moves closer to Antarctica. Hence, in the region south of New Zealand it has been shown by Heath (1981) to have north-west to south-east orientation from about 56 °S at 160 °E to near 65 °S at 180°. The waters around and to the south of the South Island of New Zealand are characterised by strong fronts which are evident on satellite imagery (Butler et al., 1992; Vincent et al., 1991). In particular, the Subtropical Convergence has been shown by Vincent et al., (1991) to extend south of the South Island with the Tasman Current advecting warm water down the west coast. However, on the eastern side, the Southland Front is oriented parallel to the

coast and joins the Subtropical Convergence north of 45°S near the southern edge of the Chatham Rise. This results in a sharp contrast between the warm subtropical waters in the Tasman Sea and the cold subantarctic waters to the east .

The steering effect of the bottom topography on the ACC and the resulting displacements of the major fronts explain many of the features of the observed behaviour of the SST gradients discussed in Section 5.2. In particular, the marked increase in temperature near 150°E in Fig. 5.5 (b) demonstrates the effect of crossing the Polar Frontal Zone at 56°S.
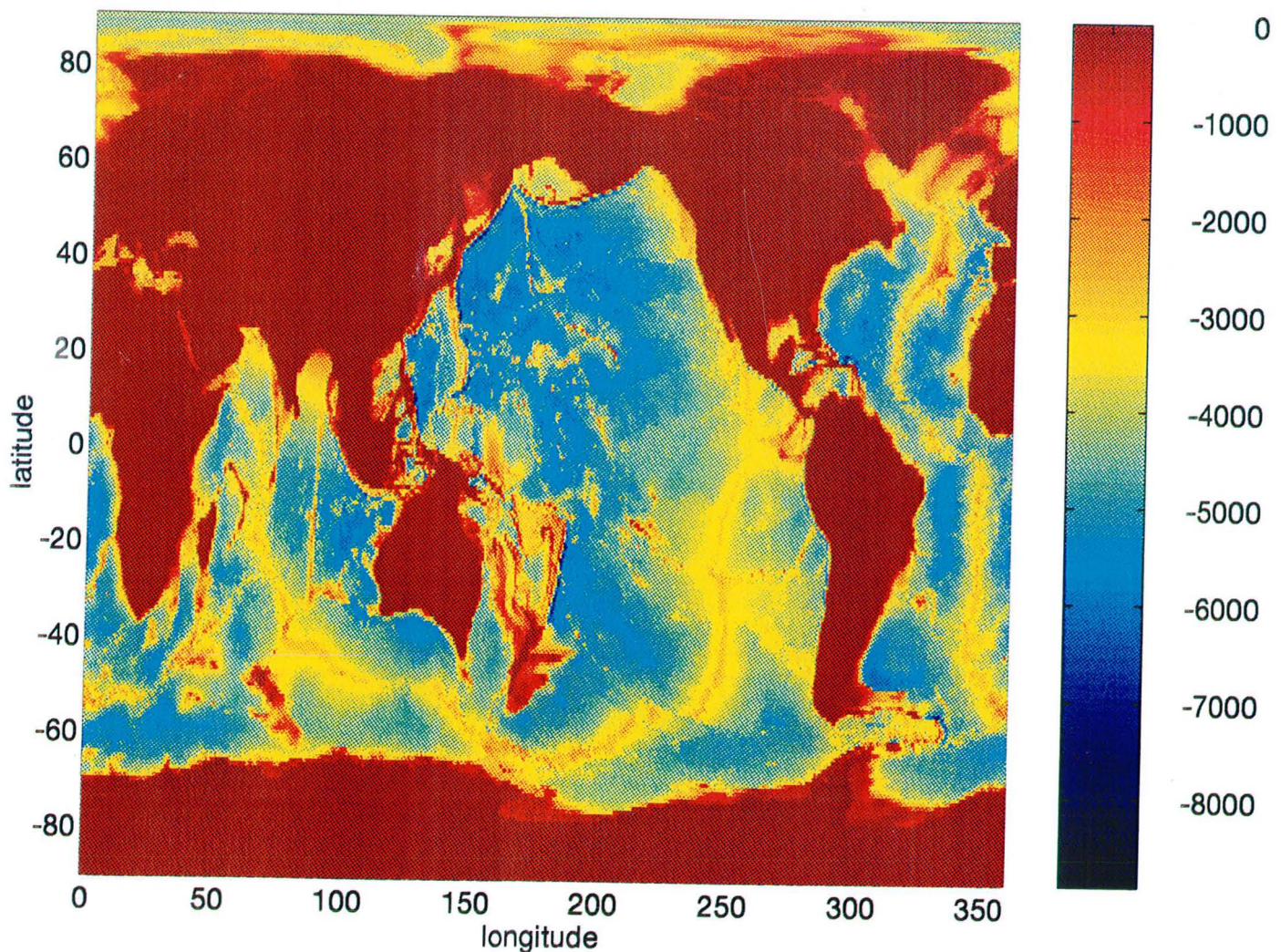
Fig. 5.7. The bathymetry of the world's oceans (m). For simplicity, all topography of less than 1000 m depth (including the continents) is shaded red.
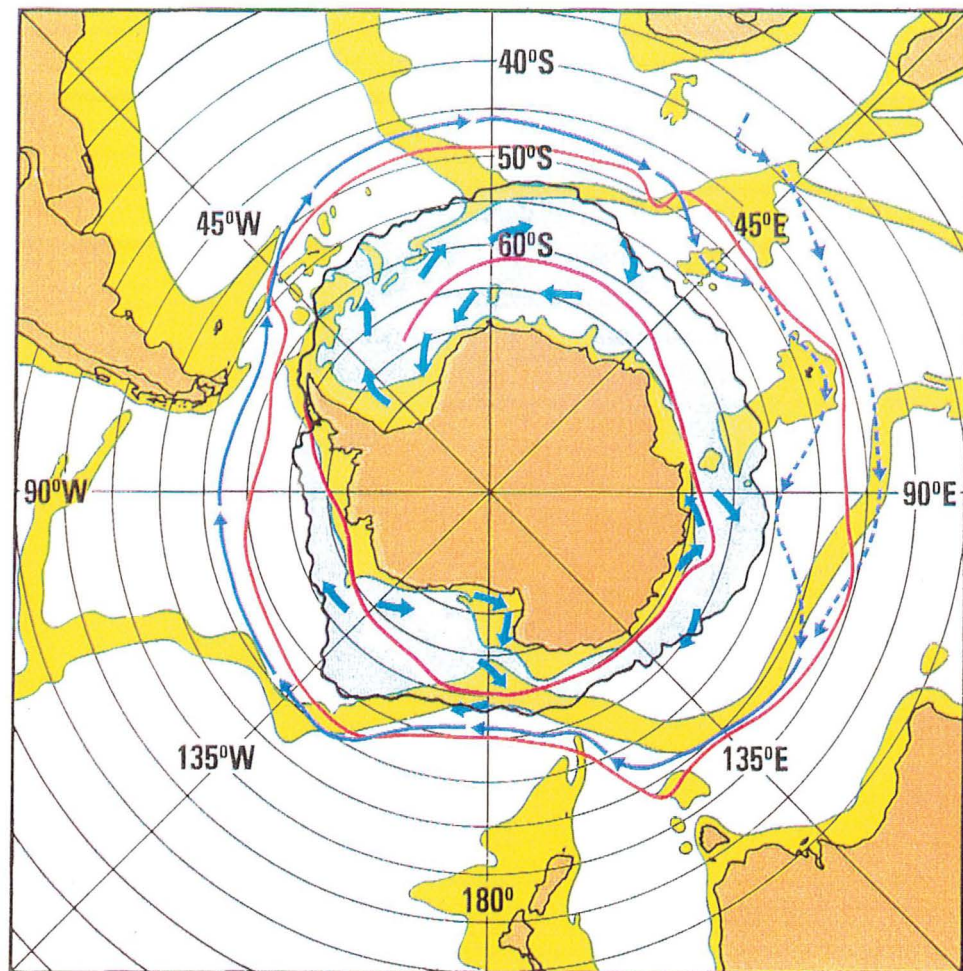
Fig. 5.8. Large-scale oceanographic features in the Southern Ocean. The yellow areas in the oceans represent bottom topography more shallow than 3000 meters. The axis of the Antarctic Circumpolar Current is shown by the long blue arrows with uncertainties in the Indian Ocean sector represented by the dashed blue lines. The orange line near 50 °S indicates the nominal location of the oceanic polar front, called the Antarctic convergence. The red line near the Antarctic Continent indicates the nominal location of the Antarctic divergence. The short blue arrows indicate selected major features of nearshore currents, such as the cyclonic Weddell gyre and the current at the edge of the Ross Ice Shelf. Light-blue shading depicts the region typically covered by sea ice in midwinter." (reproduced from Gloersen *et al*, 1992 and Zwally *et al*, 1983, by permission of P. Gloersen)
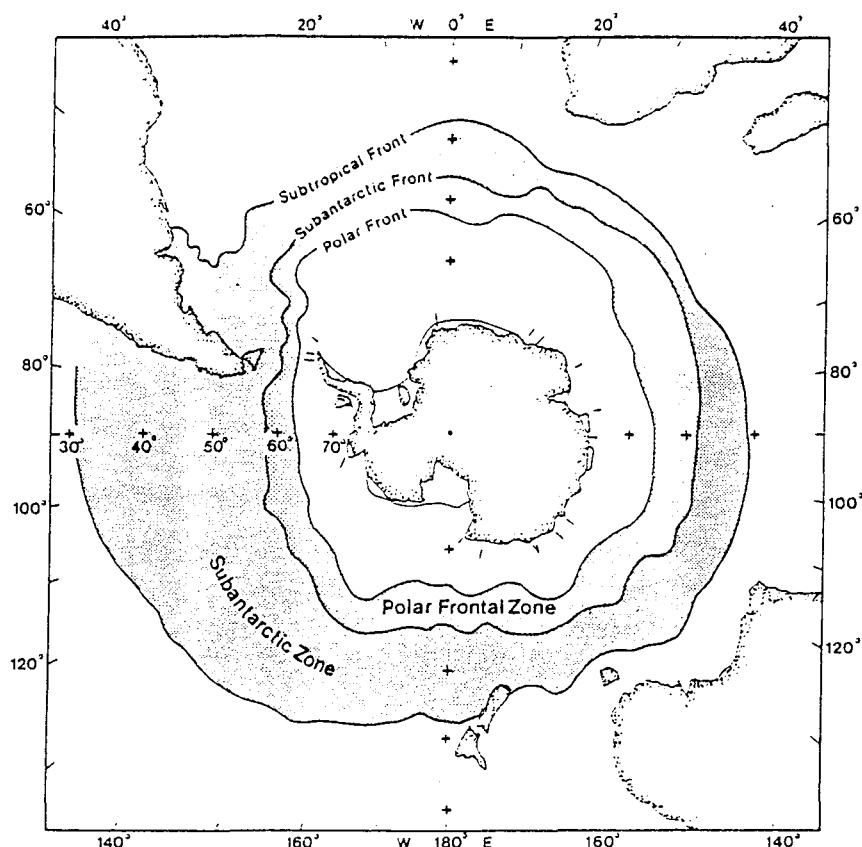
Fig. 5.9. Estimated positions of the major surface fronts of the Southern Ocean. The thin line near the coast of Antarctica indicates the mean extent of the sea ice in summer (from Nowlin and Klinck, 1986).

5.5 Atmospheric Temperature Gradients.

The vertical and horizontal structure of the temperature of the free air in the Southern Hemisphere atmosphere has been described in detail for the seasons by Taljaard et al. (1969). Further analysis and discussion of the fields has been presented by van Loon (1972a). Descriptions of the distribution of air temperature over latitudes south of 40°S have been given by Schwerdtfeger (1970) and van Loon and Shea (1988).

Van Loon (1972) drew attention to the marked contrast between the tropospheric gradients per 5° latitude for meridional sections at 40 °E and 160 °E. Drawing on the detailed analyses of Taljaard et al. (1969) which became possible following the expansion of the upper air network after the International Geophysical Year (IGY) of 1957-58, he demonstrated in his figures 3.35 and 3.36 the strong winter gradients between 30°S and 50°S at 40 °E and the relatively weak gradients between those latitudes along 160 °E. Moreover, there is a marked contrast between gradients throughout the troposphere at these meridians. Whereas the meridional gradient weakens with altitude over the western Indian Ocean the gradient at 160 °E increases with height south of 55 °S, particularly in the winter months.

Meridional cross-sections have been developed in this study from recently assembled data sets (see Chapter 2). They display the main features indicated by van Loon (1972). In Fig. 5.10, mean north to south cross-sections of temperature gradient per 5 degrees of latitude are illustrated for the month of June at 40°E, 70°E, 100°E, 140°E and 160°E. As in the cross-sections of van Loon (1972), surface temperature gradients have been included with those of the overlying air. Gradients at the sea surface have been calculated from the COADS (Slutz *et al.*, 1985) and atmospheric gradients have been calculated from mean monthly ANMC analyses for the period 1972 to 1991. At the Antarctic coast (approximately 65°S) where the SST converge to -1.8°C, the approximate freezing point of sea water, mean air temperatures for representative Antarctic bases have been inserted. The stations selected were Syowa (39.6°E), Davis (78°E), Casey (110.5°E) and Dumont d'Urville (140°E). Along 140°E, the cross-section intersects the Australian continent. As will be demonstrated in Section 5.6 large seasonal temperature changes are observed over inland Australia. Clearly, values substituted for land areas in the COADS data must be treated with caution. In these cross-sections, surface temperatures have been substituted at grid points, 25°S, 30°S and 35°S, from mean air temperature records at 0900 hours (Local Time) for selected climate stations (Climatic Averages Australia, 1988). These stations are listed in Table 5.1 with their co-ordinates and length of record. The synoptic hour of 0900 was chosen because it coincides with the ANMC upper air data which were obtained from analyses at 2300 UTC and also, because the temperature at 0900 closely approximates the mean daily temperature [defined as 1/2(maximum + minimum temperature)] at these locations.

Station	Position	Year record began
Birdsville Police Station	25° 55'S, 139° 21' E	1892
Broken Hill (Patton St.)	31° 59'S, 141° 28'E	1889
Adelaide Airport	34° 57'S, 138° 32'E	1955

Table 5.1 Climate stations near 140°E from which surface air temperatures were obtained for the cross-sections in Figures 5.10, 5.11, 5.12 and 5.13.
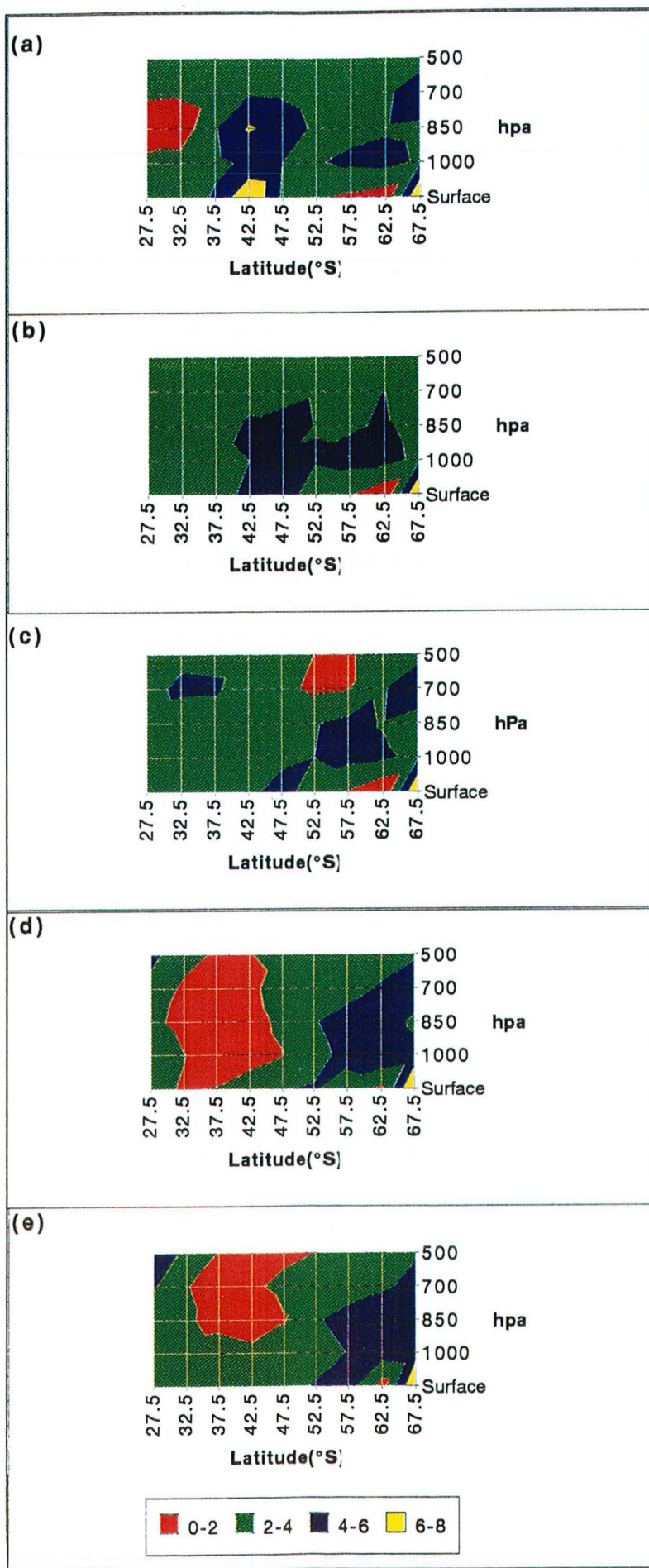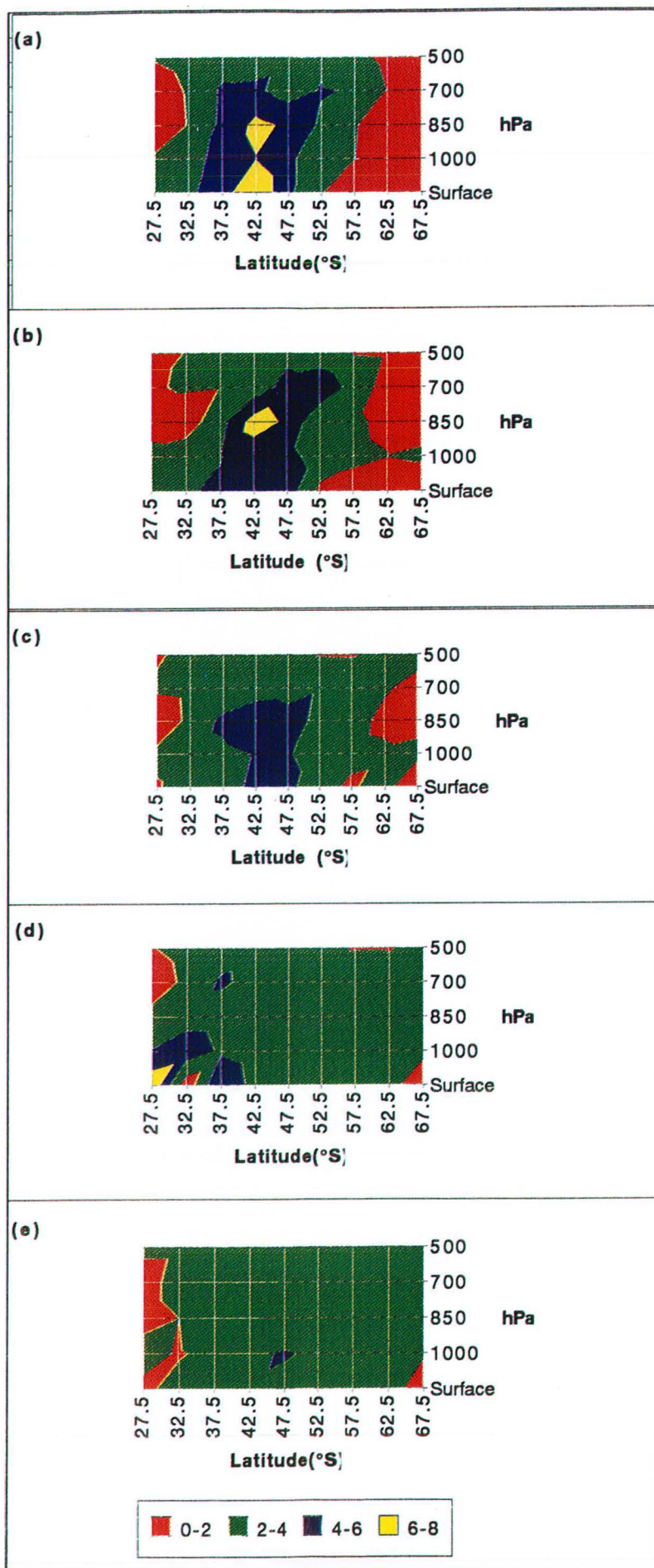
Fig. 5.10 Mean meridional cross-sections of temperature gradient (per 5° latitude) in June along (a) 40°E (b) 70°E (c) 100°E (d) 140°E and (e)160°E.

As can be seen from the cross-sections, the configuration of temperature gradients changes markedly from west to east. Near African longitudes, the maximum gradients occur at the surface between 40° and 45°S, where interaction takes place between the Aghulas Retroflection and the Antarctic Circumpolar Current (see Fig. 5.8), but this zone of maximum temperature gradient migrates southwards and weakens on the eastern cross-sections. At 140°E the zone of maximum surface and low level temperature gradient is found south of 50°S and at 160°E the zone of maximum gradient shifts south of 60°S.

Zones with temperature gradients per 5° of latitude of less than 2°C are almost exclusively confined to the eastern cross sections and only at 140°E does the weak gradient intersect the surface. It is notable that the region of slack gradient above 850 hPa at 160°E closely resembles in shape and extent the pattern at 140°E but is displaced towards the south at the higher altitudes. Examination of mean winds at and above 850 hPa in winter suggests that this is a result of advection of air from the Australian continent. Air-sea interaction is presumably the dominant influence near the surface.

Of particular interest is the sloping frontal structure evident on the cross-sections at 70°E and 100°E. In Fig. 5.10 (b) there is a broad region of strong gradients (4-6 °C/5 °lat) at low levels in mid-latitudes. Above 1000 hPa it divides into two branches, one almost vertical as in Fig. 5.10 (a), and the other sloping gently upwards and southwards. Along 100°E [Fig. 5.10 (c)], the belt of maximum gradient is more sharply defined and ascends from the surface near 47°S to 700 hPa near the Antarctic coast; a slope of approximately 1 in 600. The region of the Southern Ocean between 70°E and the waters south of Western Australia is well known to meteorological analysts as a cyclogenetic area (Streten and Troup, 1973). Physick (1981) carried out an analysis of the enhanced data set from the First GARP Global Experiment (FGGE) and demonstrated that a maximum of cyclogenesis was centred at 55°S, 110°E during the winter of 1979. Previously, Astapenko (1964) had established that a zonal trajectory of cyclones exists along 50°S in the eastern Indian Ocean in winter and forms part of a three-pronged pathway for cyclones originating near, and to the northwest of Kerguelen Island.

The contrast between the meridional temperature gradients in winter and spring is evident from a comparison of Fig. 5.10 with the mean cross-sections for October which are shown in Fig. 5.11.

The most striking change in the cross-sections is evident in the east where the regions of slack temperature gradients over Australia and the Tasman Sea during winter have all but disappeared. At 140°E and 160°E, a strong front slopes from the surface near 50°S to 700 hPa at the coast of Antarctica. In the western cross-sections, it is apparent that the zones of maximum temperature gradient at 40°E and 70°E between latitudes 40°S and 45°S remain almost vertical but have intensified. Along 100°E there is a weakening of the frontal surface which was well defined in the June cross-sections in Fig. 5.10.
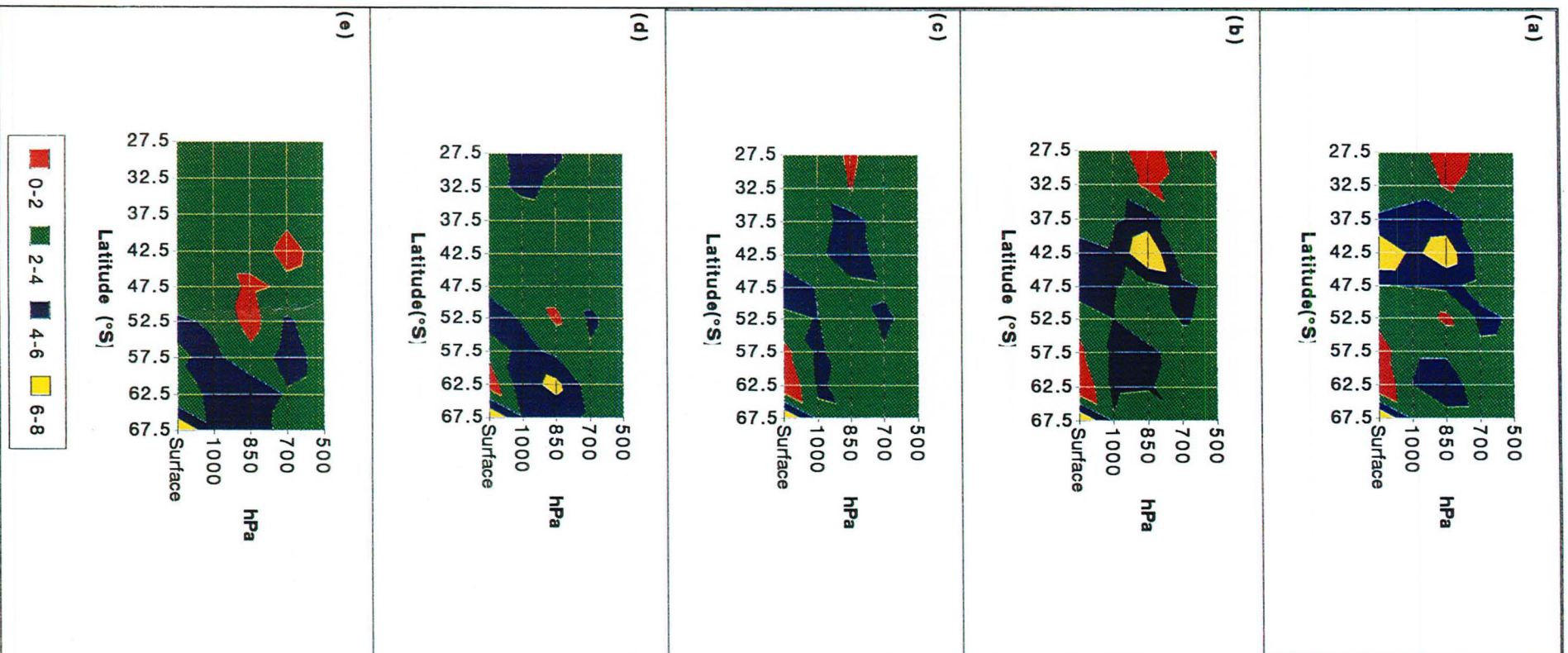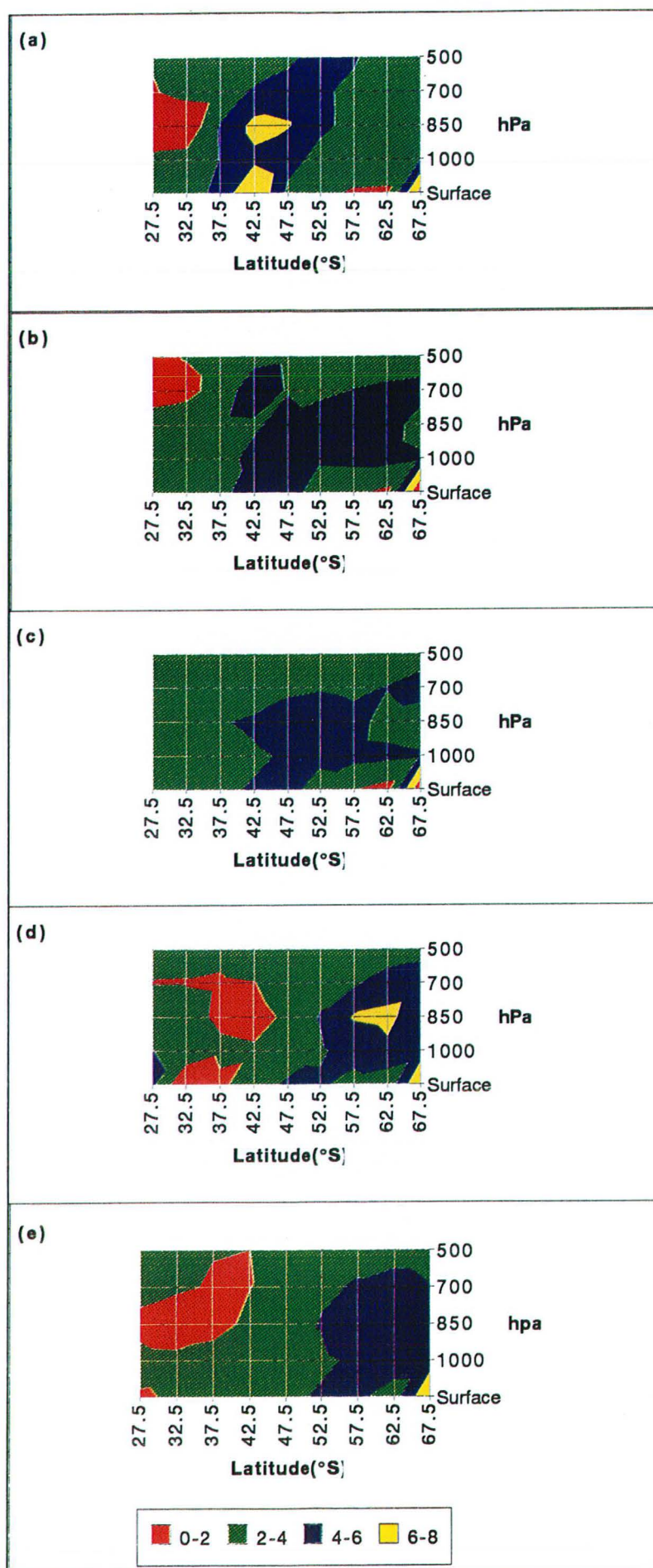
Fig. 5.11 Mean meridional cross-sections of temperature gradient (per 5° latitude) in October along (a) 40°E (b) 70°E (c) 100°E (d) 140°E and (e) 160°E.

The change from spring to summer is accompanied by an increase in the north-south temperature gradient over central and southern Australia but trends towards increasing gradients are not evident in other regions. The mean meridional cross-sections for January retain the core of strong temperature gradients at mid-latitudes at 40°E and 70°E. In Fig. 5.12 (a) and Fig. 5.12 (b) the pattern remains similar to October between latitudes 35°S and 50°S, but at higher latitudes towards Antarctica there is a marked reduction in the temperature gradient. This reduction is evident also in the eastern cross-sections as the atmosphere over Antarctica warms markedly during the summer (Schwerdtfeger, 1984).

The cross-section in the eastern Indian Ocean at 100°E in January [Fig. 5.12 (c)] does not exhibit the sloping zone of strong gradient which was evident in winter and, to a lesser extent, in spring. Instead, the almost vertical region of enhanced gradient extending to 700 hPa closely resembles the structure at similar latitudes at 40°E [Fig. 5.12 (a)] and 70°E [Fig.12 (b)]. Again, this marked change in the pattern during summer appears to be related to the seasonal cycle of temperature over East Antarctica and points to the significance of the reversal of sign in the north-south gradient of solar radiation at the top of the atmosphere in the high latitudes during summer (Wendler and Pook, 1992).

Fig. 5.12 (d) demonstrates the development of gradients between 1.2 and 1.6 °C per degree of latitude over central Australia in January. At this time of year the mean surface air temperature at 0900 (local time) at Birdsville (see Table 5.1) soars to 30°C (Climatic Averages Australia, 1988). Further south, the mean surface air temperature at 0900 at Broken Hill (near 32°S) is 22.7°C and at Adelaide (approximately 35°S), 21.9°C. As discussed earlier in Section 5.5 (p 91), temperature data from these stations were substituted for the surface temperatures in the COADS. Hence, the surface temperature gradient on the cross-section at 32.5°S appears weak. At 1000 hPa this slackening of the gradient is not detectable and suggests that the selection of the climatological stations along 140°E is not realistic in summer. A result more consistent with the 1000 hPa gradients would be obtained by taking the difference between the 0900 temperatures at Birdsville and Adelaide and calculating the gradient over this interval (approximately 9 degrees of latitude). This procedure would give a north-south temperature gradient over continental Australia of 4.5°C per 5° of latitude.

At high southern latitudes the gradients at 140°E [Fig. 5.12 (d)] become uniform and relatively weak (2-4 °C per 5 °latitude). However, near the coast of Antarctica, the temperature gradients in the Australian region do not fall to the low values evident on the cross-sections from the Indian Ocean sector.

The pattern at 160°E [Fig. 5.12 (e)] is similar to the cross-section at 140°E [Fig. 5.12 (d)] except in the low latitude region where the gradients over the ocean have declined from their relatively high values in October [Fig. 5.11 (e)].

Fig. 5.12 Mean meridional cross-sections of temperature gradient (per 5° latitude) in January along (a) 40°E (b) 70°E (c) 100°E (d) 140°E and (e) 160°E.

Nothwithstanding the marked increase in the temperature gradients over eastern Australia in summer and the slackening of the gradients near Antarctica which was apparent in the January cross-sections, the situation changes rapidly after the autumnal equinox in March. Fig. 5.13 presents cross-sections of mean north-south temperature gradients for the month of April.

In each case it is evident that the gradients near Antarctica have increased markedly as the input of solar radiation declines and the growth of sea ice around the Antarctic coast enters its most rapid phase (Gloersen *et al.* 1992). The sloping atmospheric fronts are once again apparent on the cross-sections in the Indian Ocean sector [Figs. 5.13 (b) and (c)] and similar structures also appear at higher latitudes in the Australian sector [Figs. 5.13 (d) and (e)]. In most respects the cross-sections in April resemble the winter (June) cross-sections (see Fig. 5.10).

At 140°E [Fig. 5.13 (d)], the effect of the cooling of the Australian continent is also evident with temperature gradients declining over the interior in step with the solar cycle. This weakening of the gradient is apparently advected eastwards to be apparent in the lower and mid-troposphere at 160°E between latitudes 30°S and 40°S. The contrast between Fig. 5.11 (d) for October and Fig. 5.13 (d) for April emphasises the significant changes which occur in the continental temperature gradients in the periods around the equinoxes.

The extent of the annual cycle of cooling and warming of the Australian and Antarctic continents is clearly evident in the sequence of cross-sections for the various seasons (Figs. 5.10 to 5.13). The configuration of the temperature gradients in the Australian sector at the various seasons will be invoked in the explanation of the winter maximum of atmospheric blocking in the region which will be presented in Section 5.8.

Thus far, the cross-sections studied have been bounded in the south by East Antarctica, the majority of which exceeds 3000 m in elevation (Schwerdtfeger, 1984). Extending the analysis of the temperature gradient structure further east, just beyond New Zealand's longitudes, moves to the region of the Ross Sea and away from the high profile of East Antarctica which ends abruptly at the Transantarctic Mountains. To the north of the Ross Sea the Polar Front (Antarctic Convergence) reaches its most southern latitude (see Fig. 5.9). Further to the north, a complex pattern of fronts and currents has been identified to the south and east of New Zealand (Heath, 1981, 1985; Butler *et al.* ,1992; Vincent *et al.*, 1991). According to Heath (1981) the complexity of the frontal structures in the ocean is compounded by the effects of the Campbell Plateau which extends approximately 1000 km to the south of New Zealand (see Fig. 5.7).

In Fig. 5.14 meridional cross-sections have been constructed along 180°E for the months of January, April, June and October to enable comparisons to be made with the sections in Figs. 5.10 to 5.13.

Fig. 5.13 Mean meridional cross-sections of temperature gradient (per 5° latitude) in April along (a) 40°E (b) 70°E (c) 100°E (d) 140°E and (e) 160°E.
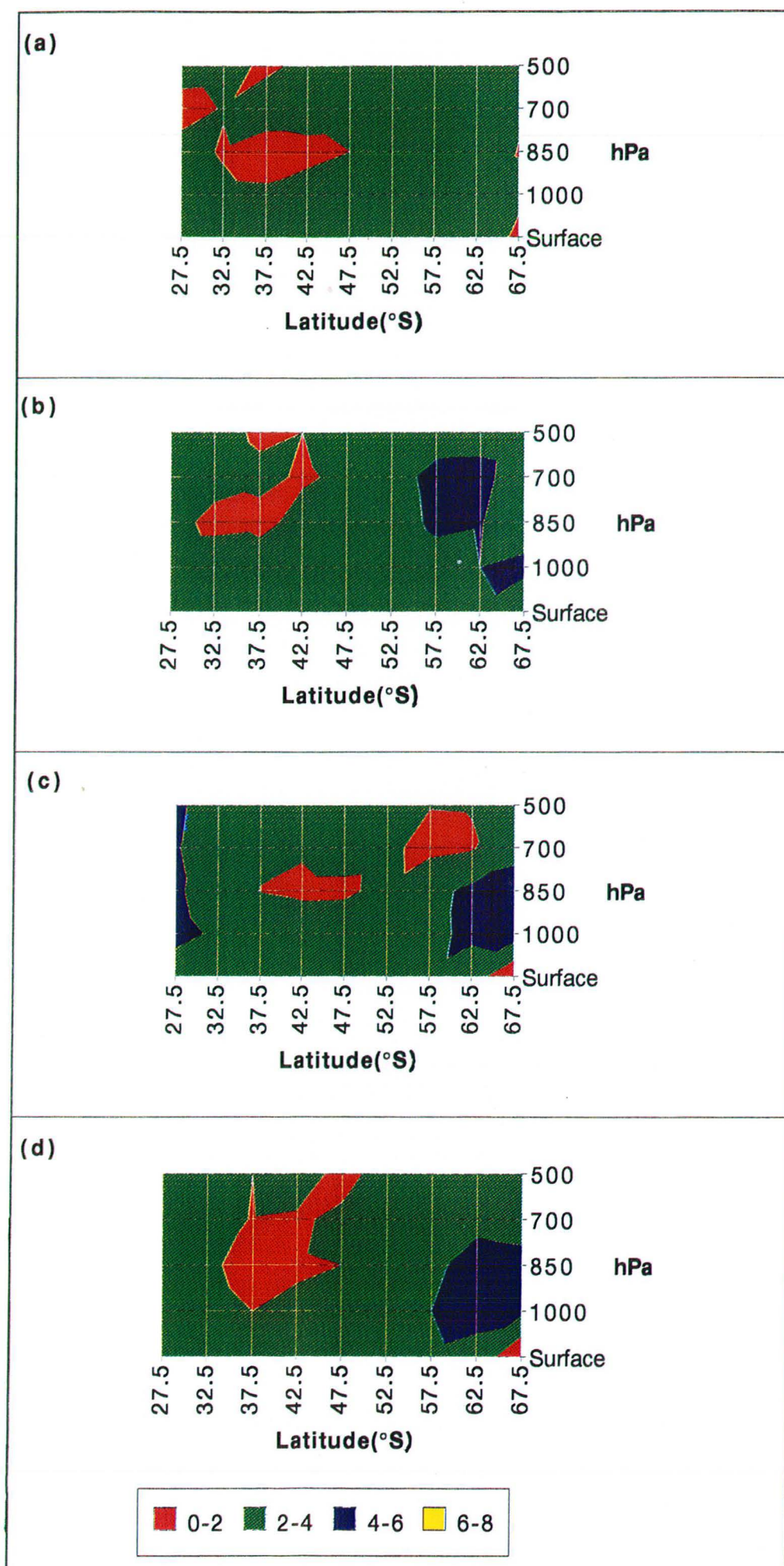
Fig. 5.14 Mean meridional cross-sections of temperature gradients (°C per 5° latitude) along 180°E for the months of (a) January (b) April (c) June and (d) October.

Inspection of the meridional temperature gradient cross-sections along the International Date Line (180°) reveals that the seasonal cycle is expressed at low latitudes by a strengthening of the gradient north of 30°S in June, and at high latitudes by a slackening of the gradient in summer.

In Fig. 5.14 a region of weak (<2°C/5° latitude) meridional temperature gradient is preserved in mid-latitudes above 1000 hPa throughout the annual cycle. Such a thermal structure is consistent with the 'pronounced split in the flow across New Zealand with a minimum in the strength of the zonal westerlies' which has been reported by Trenberth and Mo (1985, p14).

5.6 Atmospheric Thickness and Surface Temperature

Seasonal and annual cycles

Geopotential thickness of the atmosphere between two pressure surfaces provides a useful proxy for temperature in the layer. The mean 1000 to 500 hPa thickness in both winter and summer grades from maximum values in the tropical regions of the Southern Hemisphere to minimum values at the Pole. However, estimates of the 1000-500 hPa thickness over Antarctica can be misleading as the elevation of the continent ensures that the 1000 hPa contour is not found above the surface and on the high plateau of East Antarctica, the mean station level pressure at a station such as Vostok (3488 m) is approximately 624 hPa in July (Schwerdtfeger, 1984). Even in the high southern latitudes over the Southern Ocean the 1000 hPa surface would have to be sought below sea level because of low atmospheric mass (Schwerdtfeger, 1970).

The annual range of atmospheric thickness can be shown to be greatest where the surface temperature exhibits maximum variability. Unlike the Northern Hemisphere where the annual range of monthly mean surface temperature exceeds 50 °C in parts of Asia and 40 °C in central Canada, the maximum range in the Southern Hemisphere north of 65 °S nowhere exceeds 20 °C (Gill, 1982). The isopleths of annual range on his Fig 2.1 clearly indicate the positions of the major continents despite there being no continental boundaries drawn. However, the annual range of temperature on the high plateau of East Antarctica more closely approaches the range in the Northern Hemisphere. At Vostok, the variation between the monthly mean temperatures in January and August is 36 °C (Schwerdtfeger, 1984).

It is instructive to compare the measured range of geopotential thickness between summer and winter over the continents and oceans. In Fig. 5.15 (a) the change in 1000-500 hPa thickness from January to June is shown along 145 °E (crossing Eastern Australia) and 160 °E (through the Tasman Sea). Clearly, a significant discrepancy is evident between the meridians at latitudes where the Australian continent comes into play and those over the oceans. At 30 °S the 1000 to 500 hPa thickness range from January to June is 74.5 geopotential metres greater over the continent (i.e. 145 °E) than it is over the Tasman Sea (160 °E). Furthermore, the range in thickness observed over eastern Australia at 30 °S (233 m) closely approximates the range recorded over the Antarctic continent at 85 °S (236 m). Cross-sections selected along

meridians over the Indian Ocean display similar features to the Tasman Sea cross-section (160 °E). Fig. 5.15 (b) gives the mean January to June variation in thickness at 40 °E and 100 °E.
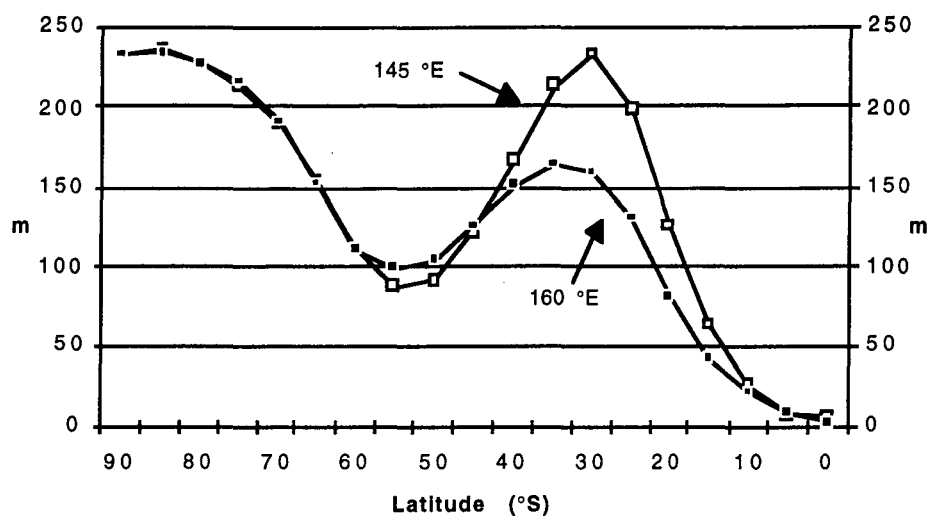
Fig. 5.15 (a). Difference (geopotential metres) between mean 1000-500 hPa thickness in January and June along 145 °E and 160 °E. (based on ANMC analyses at 2300 UTC, 1972-91)
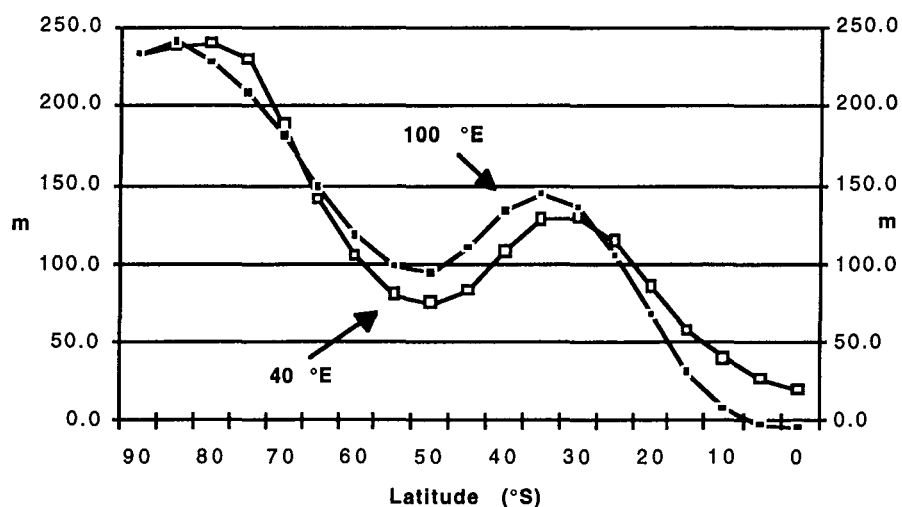
Fig. 5.15 (b). Difference (metres) between mean 1000-500 hPa thickness in January and June at selected latitudes along 40°E and 100 °E. (based on ANMC analyses at 2300 UTC, 1972-91)

Despite passing between the coasts of Africa and Madagascar and intersecting the coast of East Africa near 15 °S, the 40° meridian has a similar thickness range profile to that of the purely maritime meridian at 100 °E. In each case the dominant signal of seasonal change in thickness is detectable over Antarctica with a maximum over the high plateau of East Antarctica. The secondary maximum occurs in the subtropics as in Fig. 5.15 (a) but is approximately 100 metres less than the range at 145 °E. As well, the secondary peak for the maritime cross-sections occurs between 30 and 35 °S while the continental cross-section clearly peaks at 30 °S.

Correlations Between Atmospheric thickness and SST

Correlations between 1000 to 500 hPa atmospheric thickness and surface temperatures would appear to have greatest physical meaning where the measurements of temperature are taken close to sea level and hence, a maximum depth of atmosphere is considered. Here, mean 1000-500 hPa atmospheric thickness for June from the ANMC Southern Hemisphere data set has been compared with SST from the COADS.

Fig. 5.16 shows plots of 1000-500 hPa atmospheric thickness and SST along latitudes 50°S, 55°S and 60°S in the Southern Ocean over longitudes from 35°E to 165°W.
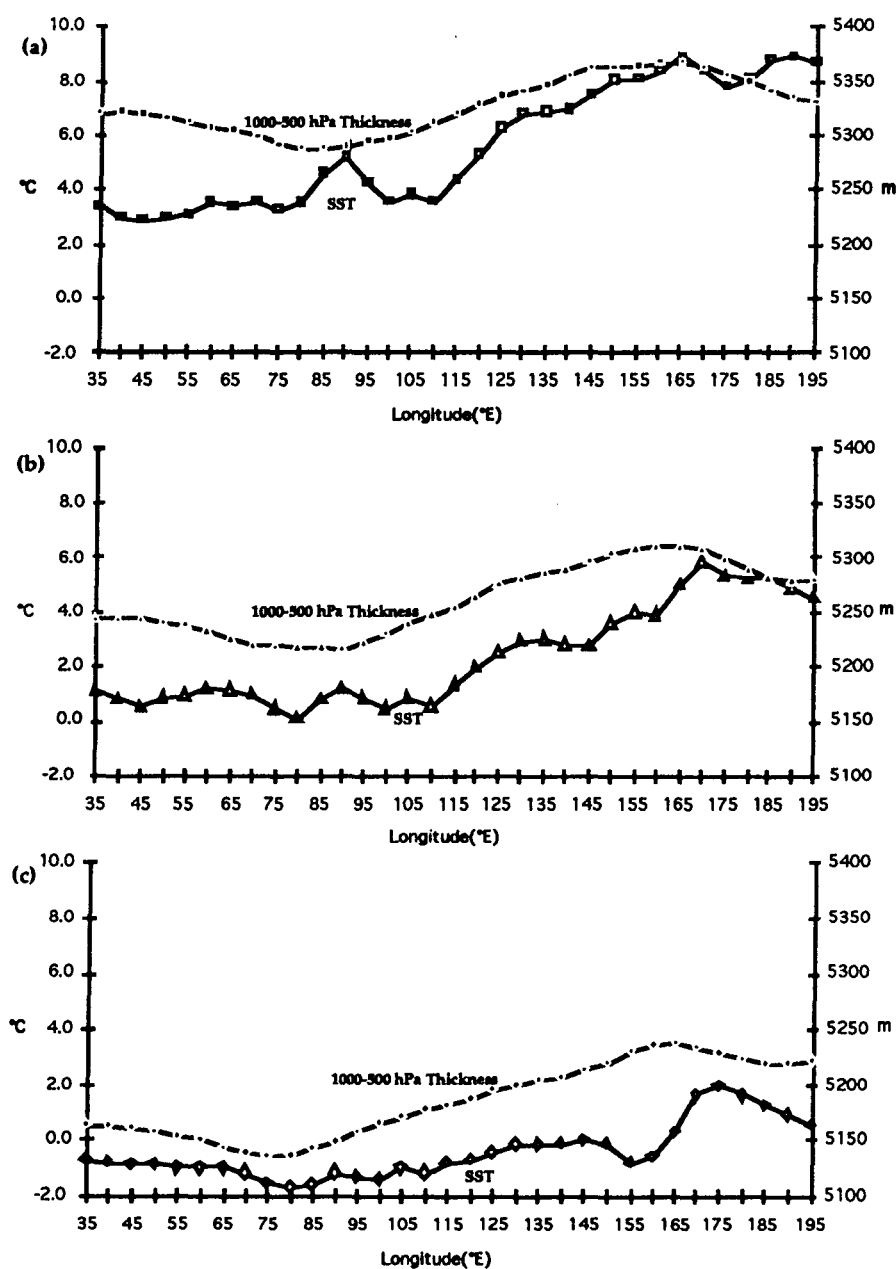
Fig. 5.16 Plots of mean 1000-500 hPa thickness and SST for the month of June at grid points over the Southern Ocean along (a), 50°S, (b), 55°S and (c), 60°S.

There is generally good agreement between SST and atmospheric thickness in the three diagrams but there is a significant discrepancy in the Indian Ocean sector at 50°S [Fig. 5.16(a)]. In this plot the narrow band of warmer water centred on 90°E is not accompanied by a corresponding maximum in mean atmospheric thickness. This is a region of marked disturbance to the Antarctic Circumpolar Current as it swings to the south-east after passing to the north of the Kerguelen Plateau (see Fig. 5.8). It is also evident that the warming of the sea surface east of 180° runs counter to the trend to lower values of atmospheric thickness along 50°S. This divergence is not apparent at higher latitudes.

The positive gradient of SST from the Indian Ocean south of Australia to the Tasman sea has been discussed in 5.3. From Fig. 5.16 it is apparent that there is a corresponding gradient of atmospheric thickness. Because of the predominance of wave numbers 1 to 3 in the mean atmospheric circulation (Coughlan, 1983) and as wave number 3 has been identified as being dominant in blocking in the region (Trenberth and Mo, 1985; Coughlan, 1983;) it is advisable to consider a broad longitudinal range (e.g. greater than 120 °) when making comparisons with non-atmospheric parameters. Here the longitude band has been selected between 35°E and 165°W and covers the sector of the Southern Ocean from Africa to east of New Zealand. Fig. 5.17 gives the lines of best fit from a linear regression of geopotential thickness on SST at grid points at 5° intervals along 50°S in summer (January) and winter (June).
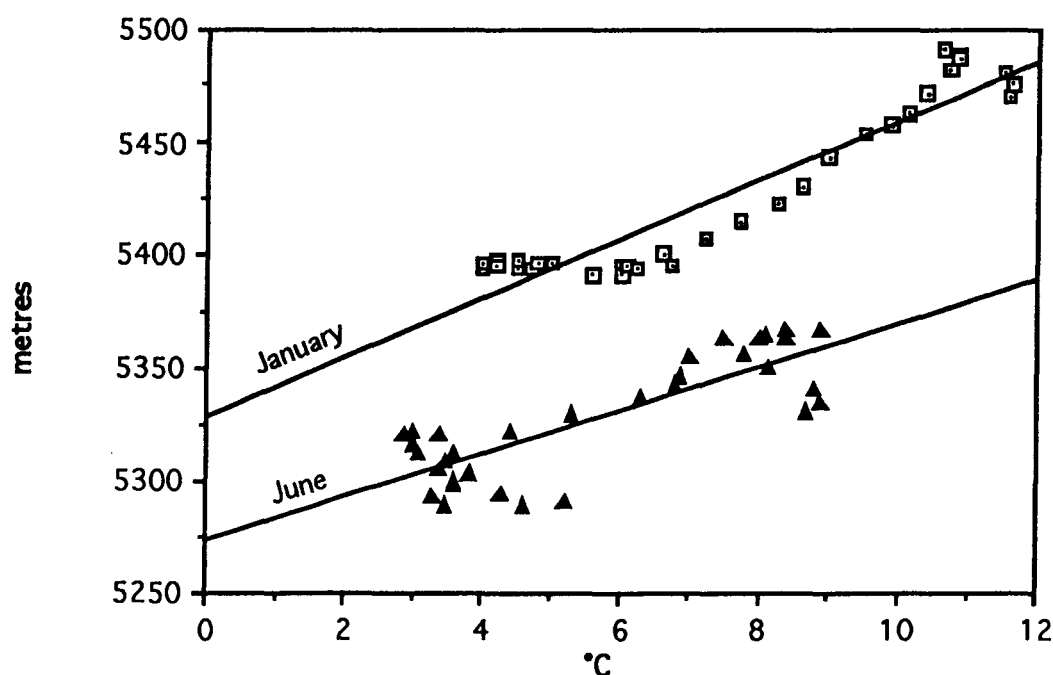
Fig. 5.17 Regressions of mean 1000-500 hPa thickness on mean SST (COADS) for the months of January (top) and June (lower) along latitude 50°S from 35°E to 175°W.

The correlation between mean 1000-500 hPa thickness and SST is significant at the 1% level in January, ($r = 0.94$, $n = 33$) and June, ($r = 0.82$, $n = 33$). Similar results were obtained for linear regressions carried out for the intermediate seasons.

Table 5.2 shows the results obtained from the linear regression of 1000-500 hPa thickness on SST at 33 grid points along 50°S for the months of January, April, June and October.

Month	r	r²	n
January	0.94	0.89	33
April	0.92	0.85	33
June	0.82	0.67	33
October	0.89	0.80	33

Table 5.2 Correlation coefficients and coefficients of variation for the regression relationships between monthly means of 1000-500hPa thickness and SST at grid points at intervals of 5°Longitude along 50°S between 35°E and 165°W.

The correlation between the mean difference in SST over the broad band of latitude between 35 °S and 55 °S along selected meridians and monthly means of atmospheric thickness difference between the same latitudes has also been found to be significant at the 1% level. In Fig. 5.18, the regression relationships between atmospheric thickness gradient and SST gradient over this latitude interval are given for (a), January (r = 0.8, n = 33) and (b), June (r = 0.75, n = 33).

(a)

(b)
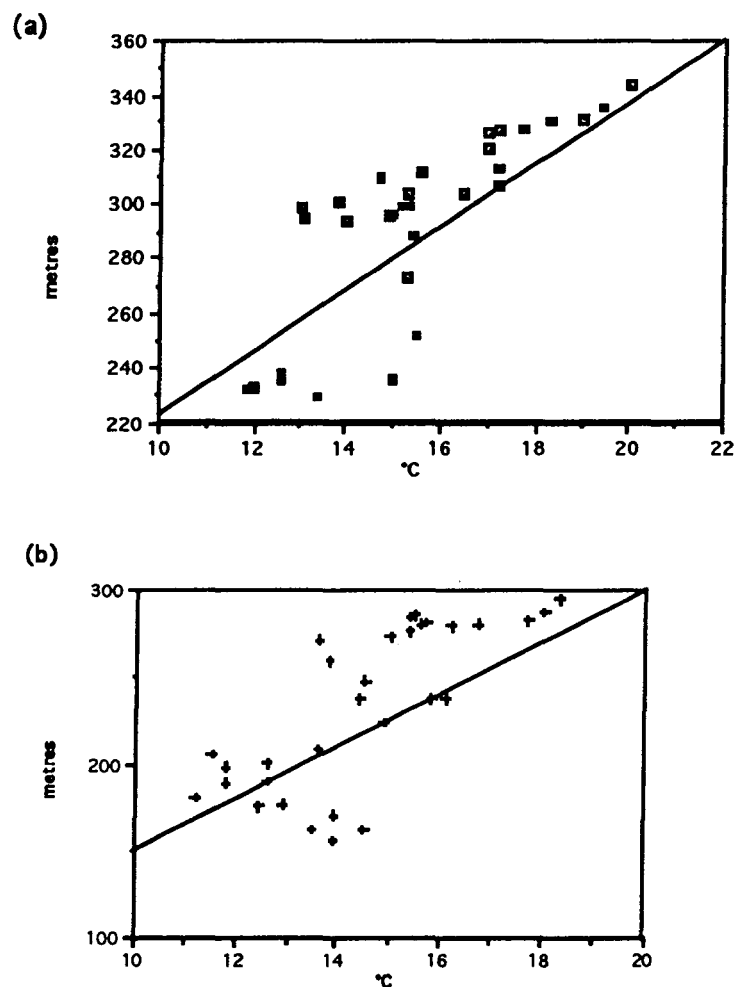
Fig.5.18. Regressions of the mean difference in 1000-500 hPa thickness (geopotential metres) along meridians at 5 ° intervals between 35 and 55°S on the mean gradient of SST (COADS) for the same meridians in (a) January and (b) June.

5.7 The Thermal Wind

However, meridional gradients of SST and atmospheric temperature over the broad latitude range examined in Fig. 5.18 do not explain the observed wind maxima in the atmosphere, where there is a concentration of momentum into jets. It is argued in this thesis that the upper wind structure in the region is more likely to be influenced by the effect of SST gradients in the meridional plane over much smaller latitude ranges (e.g. 5°) than the 20° range considered above. The difficulty here is that it is apparent that intense gradients of SST are not preserved in the atmosphere to great heights and can be seen to gradually weaken with altitude [van Loon, 1972; and see also Figs. 5.10 (a), 5.11 (a), 5.12 (a) and 5.13 (a)]. In the cross-sections presented previously the strong temperature gradients in the western Indian Ocean are apparent to about the 700 hPa level and then weaken.

In atmospheric layers for which the mean meridional temperature gradient is known, application of the thermal wind equation in the form ;

$$\frac{\partial T}{\partial y} = \frac{f(u_1 - u_2)}{R\ln(\frac{p_1}{p_2})} \qquad \dotfill 5.1$$

where the term on the left represents the mean meridional temperature gradient in the layer, f is the Coriolis parameter, u_1, u_2 are westerly wind components at lower and upper atmospheric levels respectively and p_1, p_2 are barometric pressures at those levels, would yield the vertical shear in the zonal wind structure in the atmosphere (Pedder, 1981). However, wind shears generated from surface temperature gradients alone display serious inconsistencies with observation.

Equation 5.1 can only be applied reliably where there is knowledge of the vertical structure of the temperature gradients throughout the atmospheric layer under consideration. Consequently, regions of strong surface temperature gradients require reinforcement at higher altitudes for their effects to produce significant wind shear over deep atmospheric layers. This is clearly the situation south of the Tasman Sea sector in winter [see Figs. 5.10 (d) and 5.10 (e)]. Here the SST gradient reaches a maximum in the vicinity of the Antarctic Convergence. Aloft, the temperature gradient created by the negative radiation balance over the elevated contours of East Antarctica supports the surface gradient with the result that a marked thermal wind is generated, giving rise to a mid-tropospheric wind maximum.

Mean temperature gradients estimated for the tropospheric layer from the surface up to 500 hPa have been calculated from the temperature data used to construct the cross-sections in Figs. 5.10 to 5.13. Fig. 5.19 shows the summer (January) and winter (June) u components of the thermal wind along 140°E. It is immediately apparent from the section along this meridian that the wind shear is significantly affected by the annual cycle of changes in meridional temperature gradients over the continents of Australia and Antarctica. In winter [Fig. 5.19 (b)] there is a clear double maximum with peaks over northern Australia and near the Antarctic coast. By way of

contrast the summer pattern is characterised by strong shears over southern
Australia and a gradual reduction in thermal wind with higher latitude.
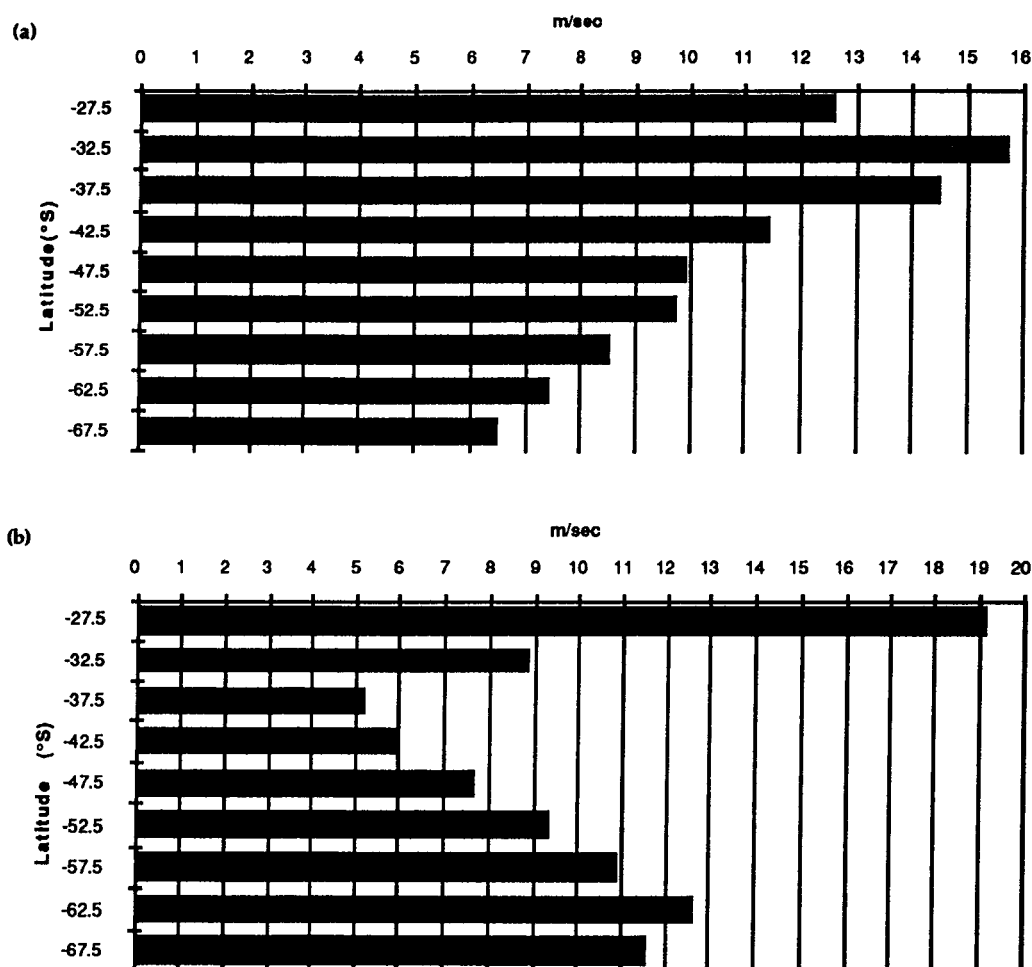
Fig. 5.19 U components of the 1000-500 hPa thermal wind at 140°E derived from mean
temperature gradients for the months of (a), January and (b), June..

An overall impression of the seasonal changes in thermal forcing over the
Southern Hemisphere can be obtained from mapping the 1000-500 hPa wind
shear. In Fig. 5.20, monthly means of the u component of the thermal wind
derived from the ANMC Southern Hemisphere data set have been mapped
on a polar stereographic projection for the months of January, March, June
and October.

In the Australian region striking features of the seasonal changes include the
maximum wind shear near the East Antarctic coast in winter and the
corresponding minimum over the Tasman Sea and New Zealand. The
intense elongated maximum over northern Australia and in the vicinity of
the Tropic of Capricorn in the Pacific Ocean persists throughout the year,
although it weakens over the Australian continent in summer. The thermal
wind in this region represents the strong vertical shear from the
southeasterly trade winds at the surface to the westerly subtropical jet
stream aloft.

(a)
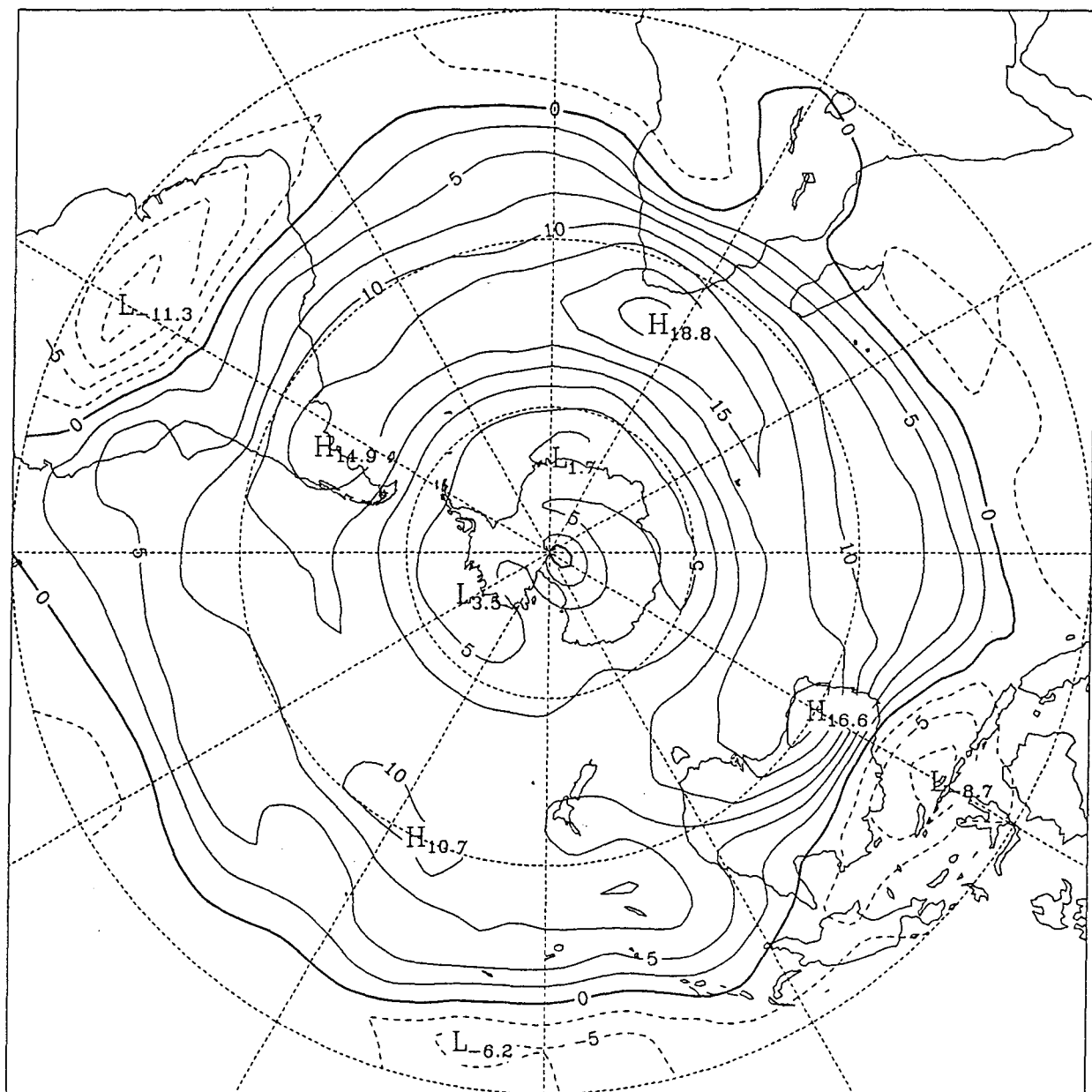
(b)
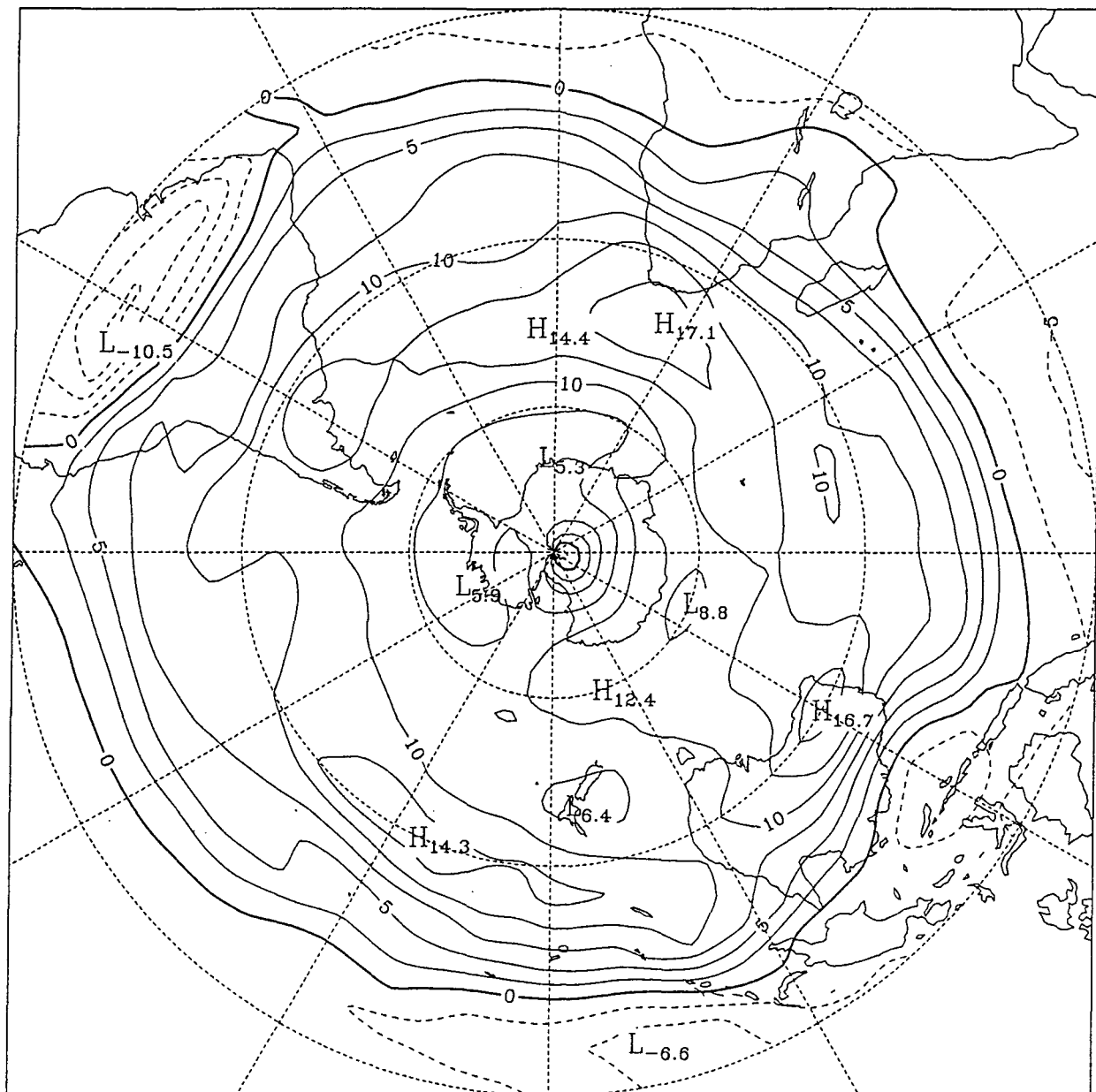
(c)
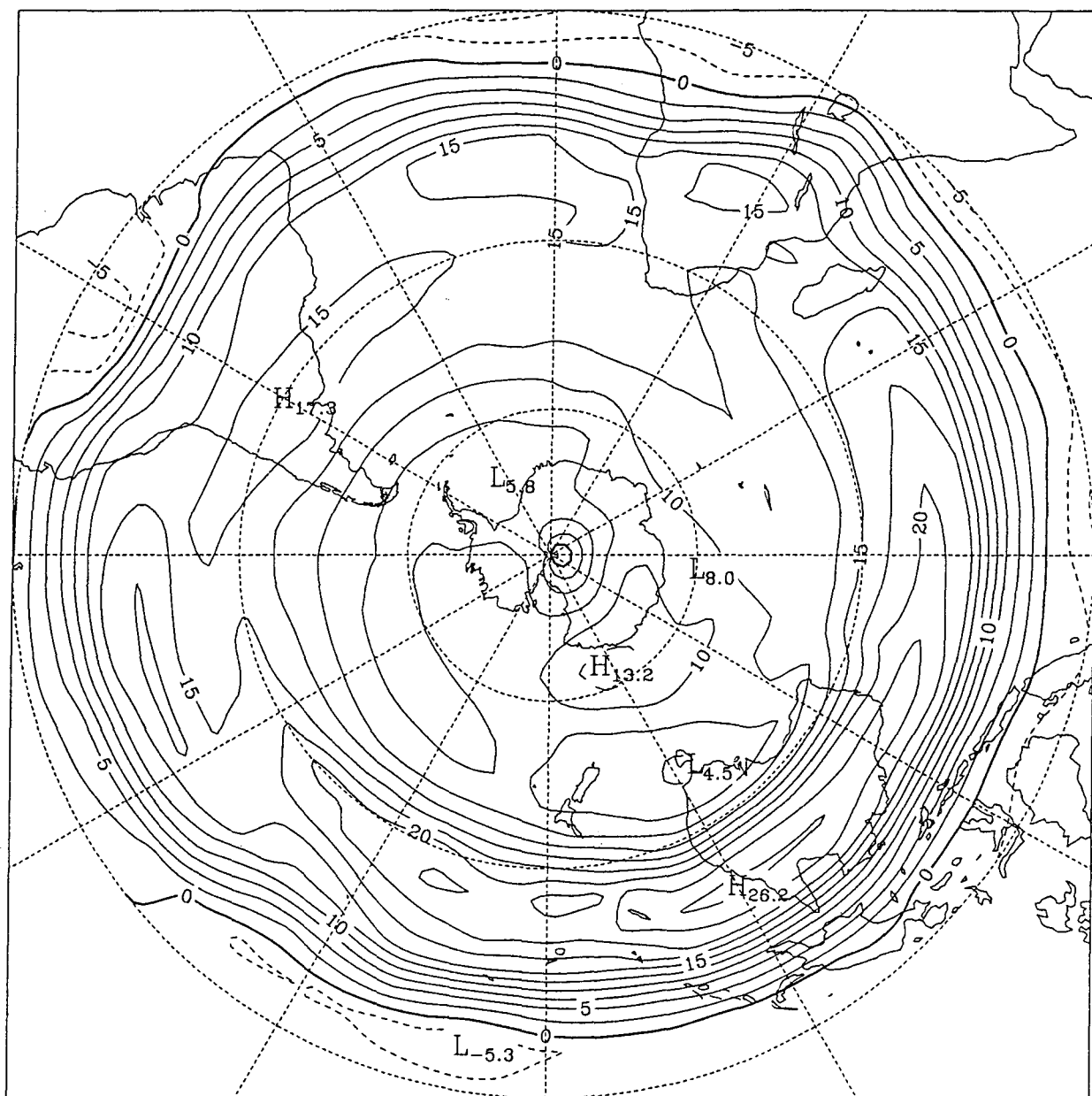
(d)
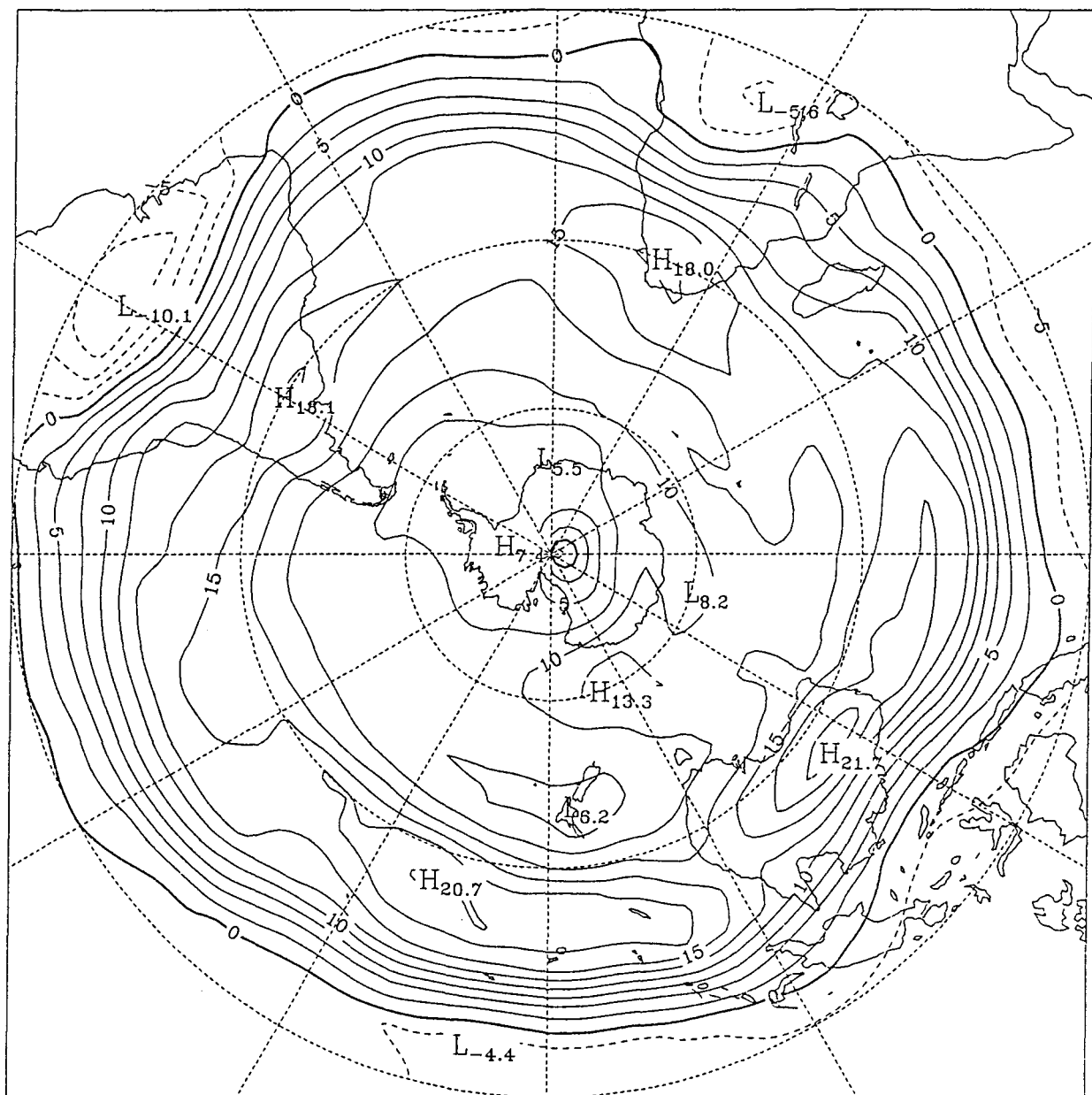
Fig. 5.20 Mean u component (westerly) of the thermal wind (m s⁻¹) between 1000 hPa and 500 hPa for the Southern Hemisphere in the months of (a) January, (b) March, (c) June and (d) October (ANMC data).

5.8 Vorticity Considerations in the Middle Troposphere

In the previous section, thermal wind considerations were invoked to demonstrate how changes in south to north temperature gradients across the Southern Ocean contribute to the observed jetstream structures. In particular, seasonal influences of the continents of Australia and Antarctica result in marked changes in the distribution of wind maxima in the Tasman Sea and New Zealand region. Inspection of charts of mean wind components in the upper atmosphere over the Southern Ocean suggests that the generation of anticyclonic vorticity by horizontal wind shear between high latitudes and lower latitudes may be a key climatological component in the process of blocking in the Australasian region.

The vertical component of relative vorticity is given by the expression,

$$\zeta = \frac{\partial v}{\partial x} - \frac{\partial u}{\partial y} \qquad \ldots\ldots\ldots \qquad 5.2$$

where u and v are components of velocity in the x and y directions, respectively.

The south to north gradients of temperature ensure via the thermal wind relationship that, for middle and upper tropospheric levels, the second term on the right hand side of Equation 5.2 has the more important effect of the two. At 140°E, the decrease in the mean u component of the wind at 500 hPa for the month of June is approximately 4.5 m s^{-1} from 50°S to 45°S. The positive (anticyclonic) relative vorticity acquired by air parcels via this horizontal wind shear is approximately 10^{-5} s^{-1} while the coriolis parameter (f) has a value of order 10^{-4} s^{-1}·at these latitudes. Mean v components for the month of June contribute an approximate relative vorticity value of 4.5*10^{-6} s^{-1} south of Tasmania. If we consider the 5° by 5° square centred on 47.5°S, 147.5°E, combination of the two terms on the right hand side of Equation 5.2 gives a value for the relative vorticity (ζ) of 1.5*10^{-5} s^{-1}. Fig. 5.21 (a) illustrates in schematic form the configuration of mean velocity components for the month of June between 45°S and 50°S and 145°E and 150°E.

Extending the analysis northwards to eastern Australia reveals that, in winter, the configuration of mean westerly components is such that the westerlies increase steadily northwards of 35°S. Fig. 5.21 (b) illustrates the configuration of mean velocity components for the month of June between 25 and 30°S and 145 and 150°E. In the mean, positive relative vorticity of magnitude 0.14f is generated in winter to the south of Tasmania and between 25°S and 35°S, negative (cyclonic) relative vorticity of magnitude 0.16f is generated over eastern Australia.
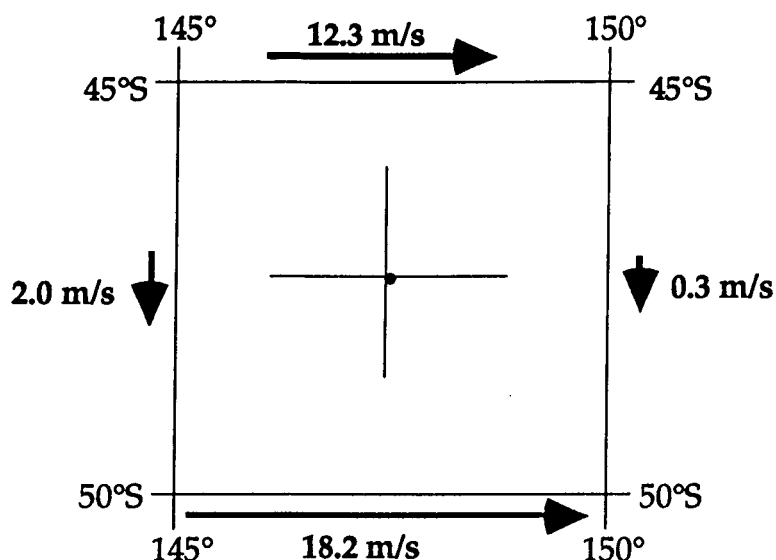
Fig. 5.21 (a). Schematic representation of the configuration of mean velocity components to the south of Tasmania at 500 hPa in June generating anticyclonic vorticity at 47.5°S, 147.5°E.
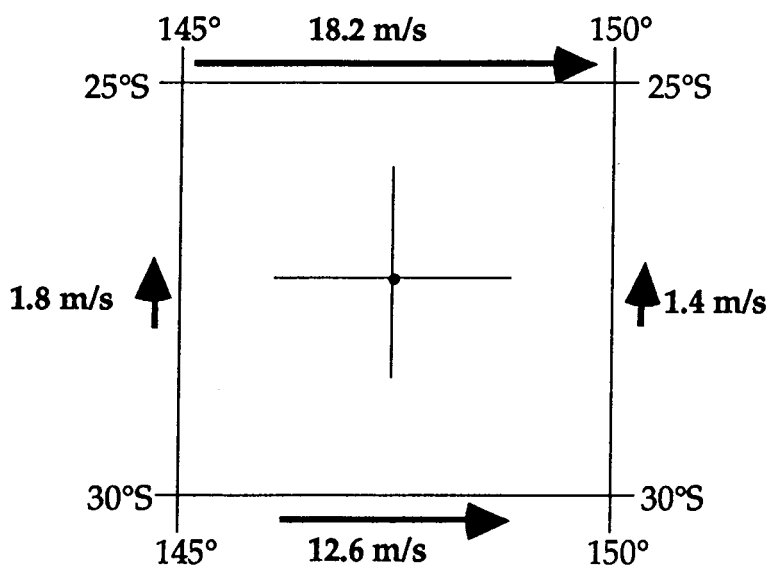
Fig. 5.21 (b). Schematic representation of the configuration of mean velocity components over southern Queensland at 500 hPa in June generating cyclonic relative vorticity at 27.5°S, 147.5°E.

Westwards of Tasmania's longitudes, the relative magnitude of u components in June at 45°S and 50°S gradually reverses so that to the west of 120°E the westerly component is stronger at the lower latitude. Although this relationship holds in general throughout the year, differences in u component between 45°S and 50°S are very much smaller in January and the reversal in sign occurs south of the Great Australian Bight in summer. In Fig 5.22 the westerly component of wind at 500 hPa has been mapped over the Southern Hemisphere and clearly shows the relative latitudes of the jetstreams over the Indian Ocean sector and in the Australian region in each season.

(a)
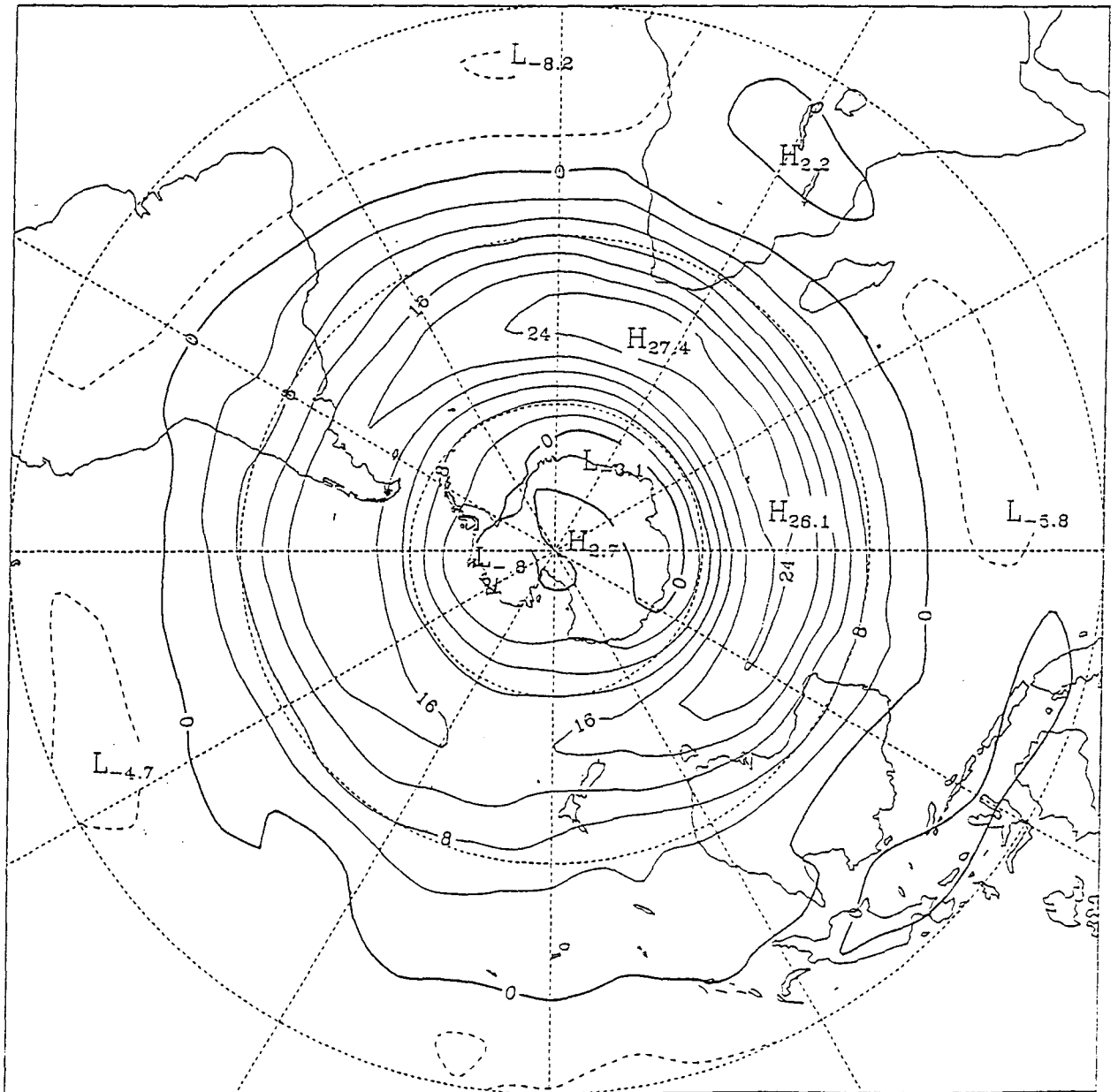
(b)
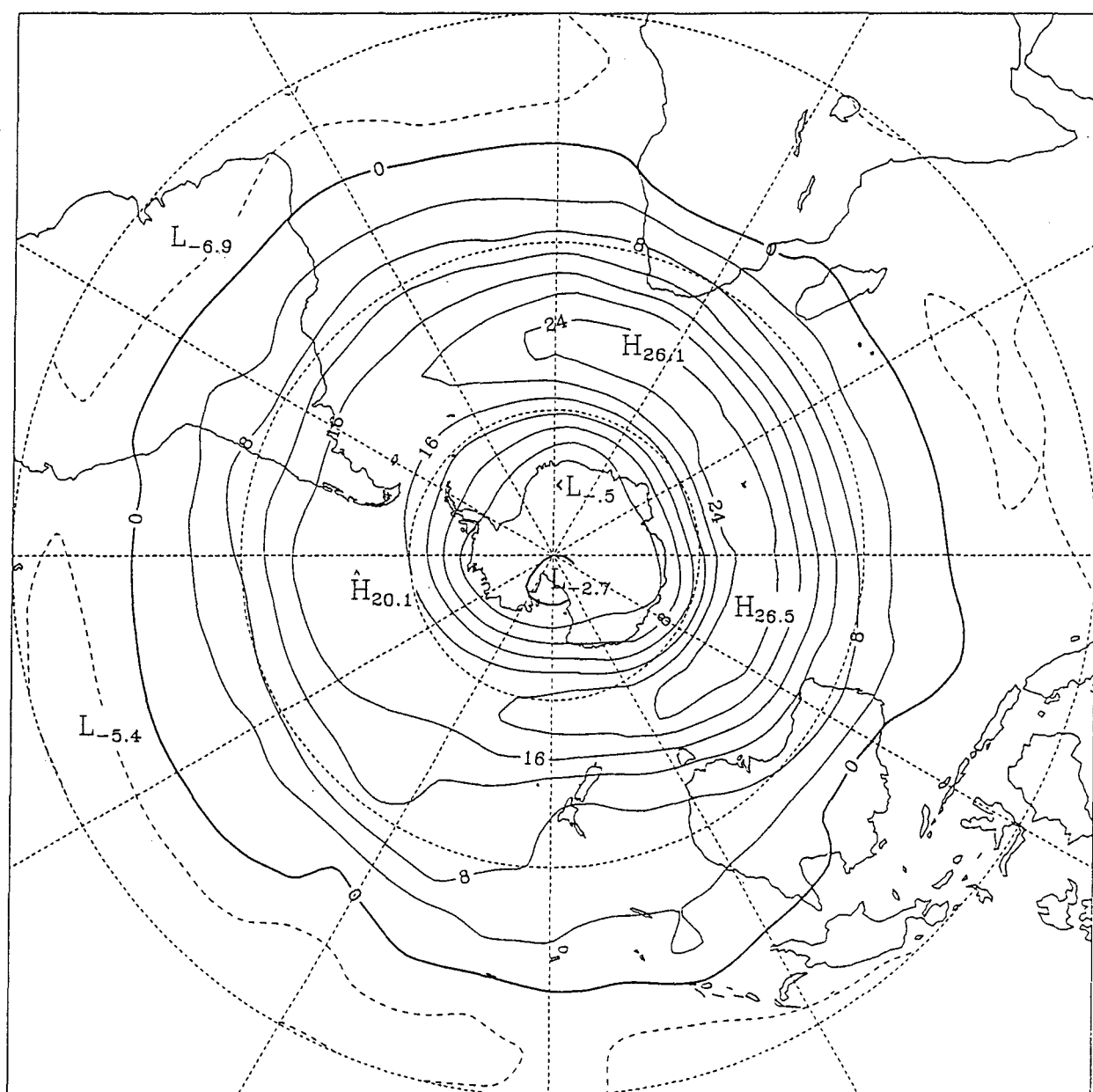
(c)
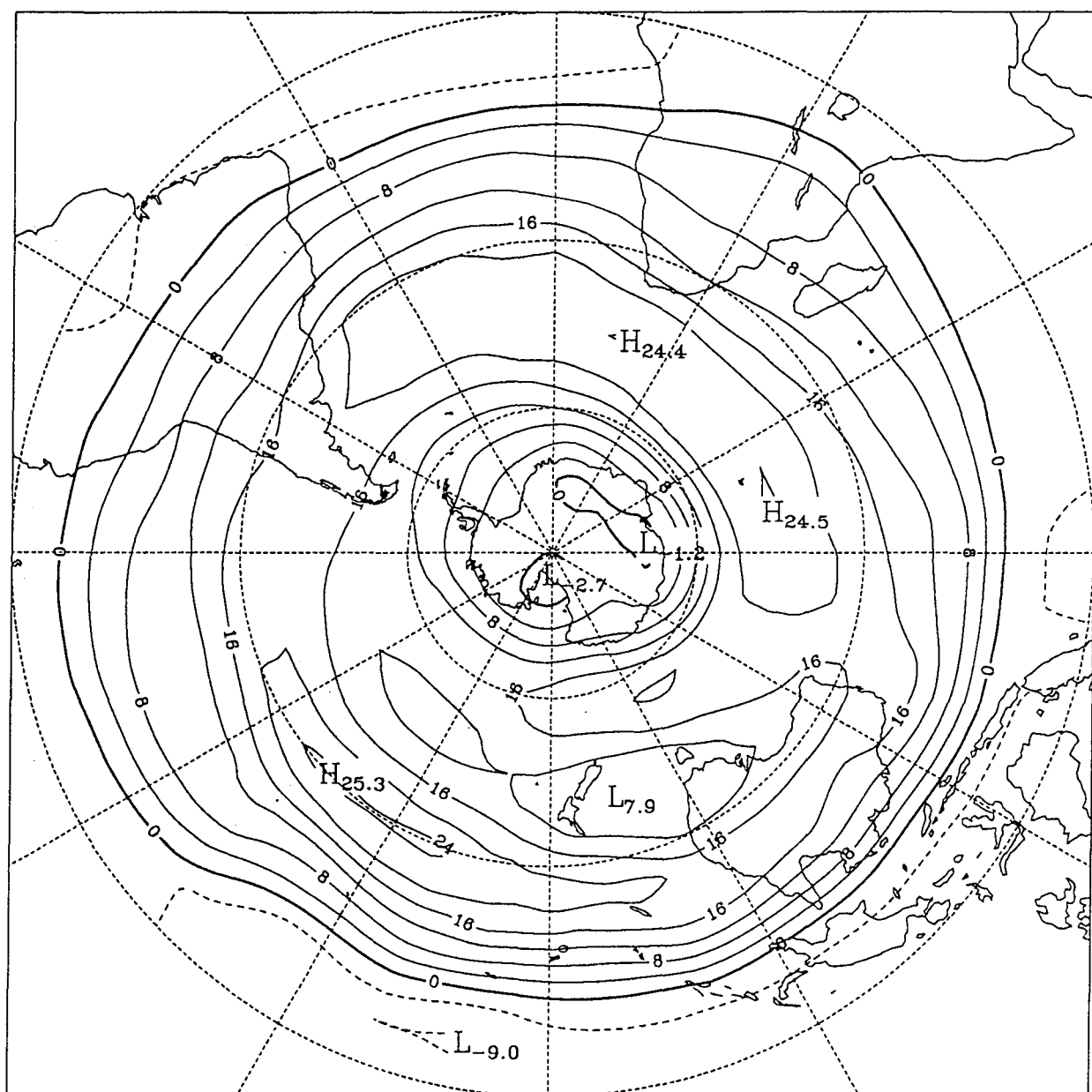
(d)
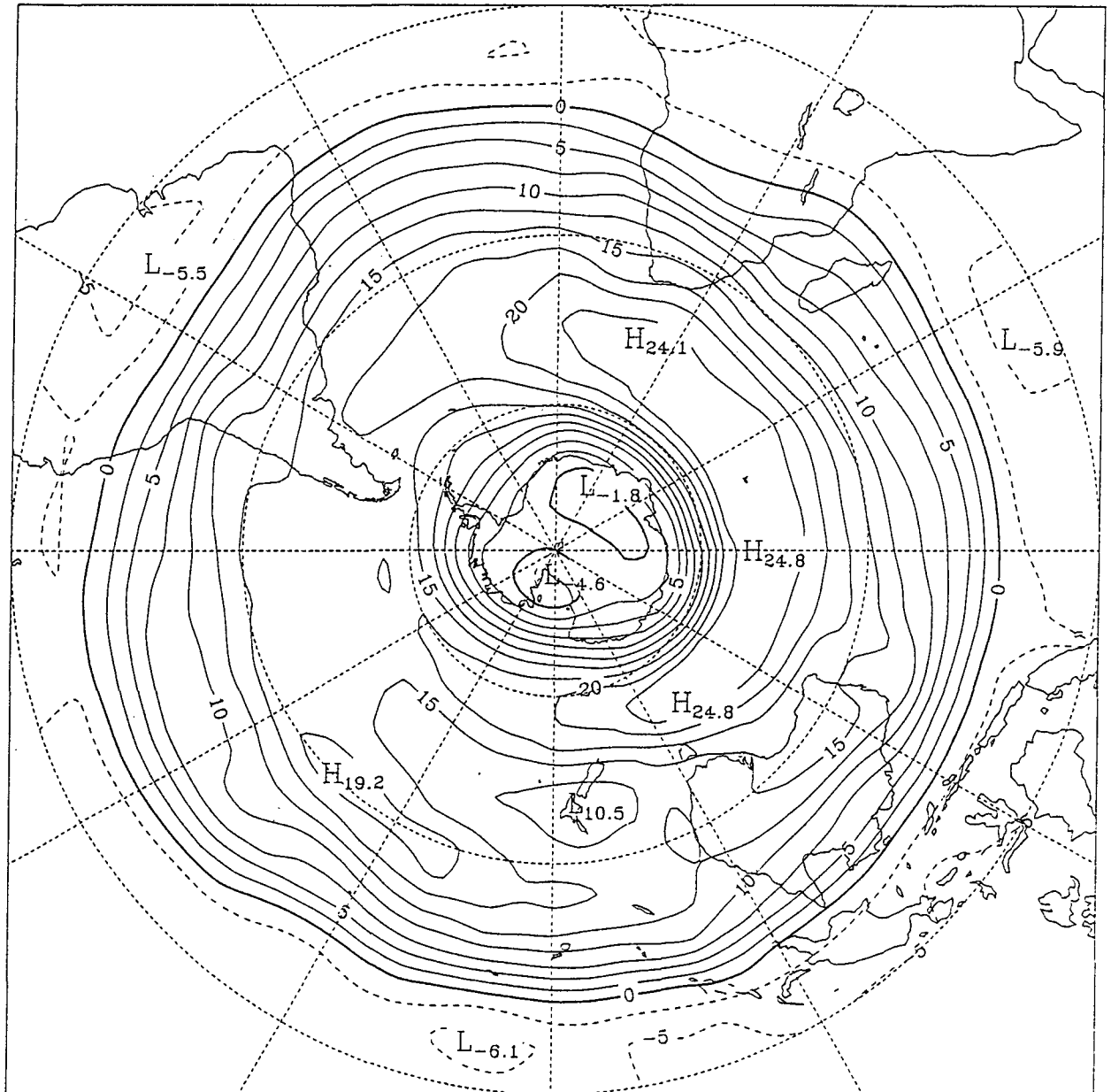
Fig. 5.22 Mean u component (westerly) of the geostrophic wind at the 500 hPa level (m s⁻¹) for the months of (a) January, (b) March (c) June and (d) October (ANMC data).

The double-jet structure in the Australian and New Zealand region which is evident in June (Fig. 5.22 (c)) has been discussed by Physick (1981) in his study of 1979 (FGGE year) winter storm tracks. Earlier, Astapenko (1964) had identified the major cyclone trajectories for the Southern Hemisphere. In his diagram for winter, reproduced by Physick (1981) as his Fig. 6, the 'West Australian' and, to a lesser extent, the 'Tasmanian' storm tracks follow the orientation of the isotach maximum as it shifts to higher latitudes south of eastern Australia and the Tasman Sea.

Green (1977) has argued that anticyclonic vorticity generated by the action of the eddies on the scale of synoptic weather systems in the middle and upper atmosphere could be expected to descend to lower levels in the subsiding air associated with a high pressure region. Such a process operating to the south and southeast of Australia would result in the regular advection of anticyclonic vorticity downstream in the predominantly westerly airstream and the formation of a warm-cored high pressure system through a process of subsidence. Further examination of the mean monthly velocity fields to the south and southeast of Australia confirms that the latitude of the zonal wind maximum does not vary substantially throughout the year. Maximum westerly wind speeds are observed in autumn and spring. On the other hand, the pattern over eastern Australia is apparently driven by the continental heating and cooling cycle and it is only in winter that the configuration shown in Fig. 5.22 (c) is observed. The resulting cold cored low pressure system in the middle troposphere near the east coast of Australia lies to the northwest of the warm cored anticyclone to the southeast of the continent. The dipole structure created in this manner closely resembles the classic blocking pattern depicted by Coughlan (1983) in his Fig. 1 and discussed in Chapter 4 of this thesis.

The mechanism described above supports the maximum blocking frequency which is observed in June. It does not account for the secondary maximum in summer (Wright, 1974; Hirst and Linacre, 1981). However, it should be noted that the analyses of persistent anomalies of geopotential height over the Southern Hemisphere presented by Trenberth and Mo (1985) show a significantly lower frequency of positive anomalies in the New Zealand sector in summer than in winter. Moreover, the analyses shown in their Fig. 6 demonstrate that there is a clear maximum frequency of occurrence of positive geopotential anomalies to the south of Tasmania in winter.

5.9 SST during the 1989 Blocking Event

The patterns of SST during June, July and August 1989, as obtained from the Reynolds Blended SST data set (Reynolds, 1988) are shown in Fig. 5.23 (a), (b) and (c). Over the Southern Ocean, the maps draw attention to the front in the western Indian Ocean sector where the Agulhas current interacts with the ACC. In the Australasian region the isotherms are oriented from northwest to southeast at high latitudes and the meridional SST gradient is enhanced in the ACC south of the Macquarie Rise and New Zealand.

Mean SST fields have been calculated from the Reynolds Blended data over the 12 year period from 1982 to 1993 and comparison with this long-term mean yields the anomaly field for the month of June 1989 given in Fig. 5.24(a). Outstanding features of this anomaly pattern include the strong (>2 °C) positve anomaly to the southeast of South America and positive signals in the Tasman Sea, just south of Western Australia and to the southeast of New Zealand. Negative anomalies of the order of 1 to 2 °C are evident over the Southern Ocean to the south of Africa, in high latitudes at mid-Indian Ocean and mid-Pacific longitudes and in the region just to the east of New Zealand. The contrast between SST of the warm Tasman Sea on the western side of the South Island and those of the cold subantarctic waters to the east has been shown by Vincent et al. (1991) for May 1989 and the persistence of this pattern was demonstrated by Butler et al. (1992). Consistent with reports of La Niña conditions prevailing at this time (e.g. Nydam, 1990) negative anomalies are apparent in the tropical waters of the central and eastern Pacific Ocean. According to Holbrook and Tomczak (1991) the positive SST anomaly in the western waters of the Tasman Sea was apparent prior to June. They reported that SST in the East Australian Current between 29°30'S and 32°30'S during May 1989 were approximately 2°C warmer than a ten year mean while surface salinities were about 0.5‰ lower than the mean.

By August 1989 the anomaly pattern had undergone some changes but the broad structure remained. In.Fig. 5.24 (b), the negative anomaly in the central tropical Pacific in August is weaker than it was in June but the positive anomaly in the south Tasman Sea is largely unchanged. The negative anomaly just to the east of New Zealand appears to have been absorbed into the broad cold pool in the high southern latitudes of the Pacific Ocean. It is readily apparent that the strong positive anomaly north of the Weddell Sea has retained its identity throughout the winter months.

In order to make a quantitative assessment of the strength of the meridional temperature gradients at the surface and in the lower troposphere in the winter of 1989 relative to the long-term means shown previously, changes in temperature over 5 degree latitude intervals have been calculated. These gradients are shown for June 1989 in Fig. 5.25. There are some differences in the sources of data for this diagram from those used in the construction of the cross-sections in Figs. 5.10 to 5.13. As in the previous analyses, upper air temperatures are from ANMC analyses at 2300 UTC but temperatures at the sea surface are from the Reynolds Blended Data Set and Antarctic station data have been extracted from the relevant *Monthly Climatic Data for the World*.

(a)
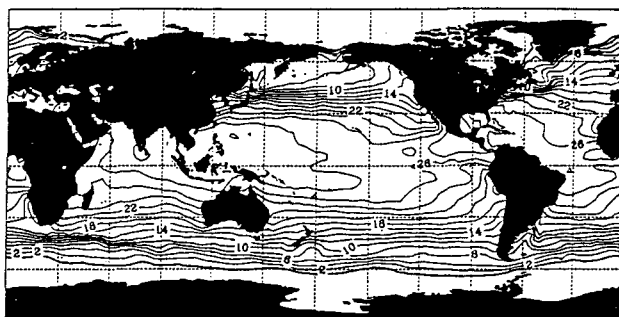
(b)
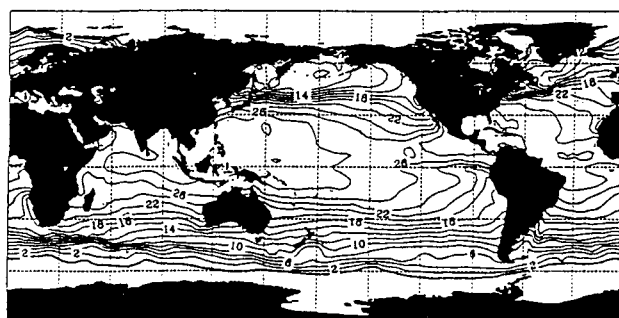
(c)
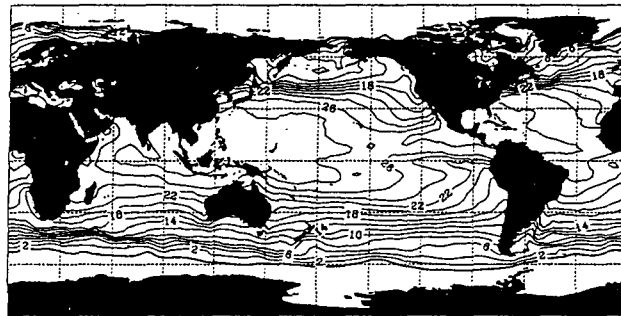
Fig. 5.23 Sea surface temperature (°C) over the Southern Hemisphere for the months of (a) June, (b) July and (c) August 1989 [from the Reynolds Blended Data Set (Reynolds, 1988)].

(a)
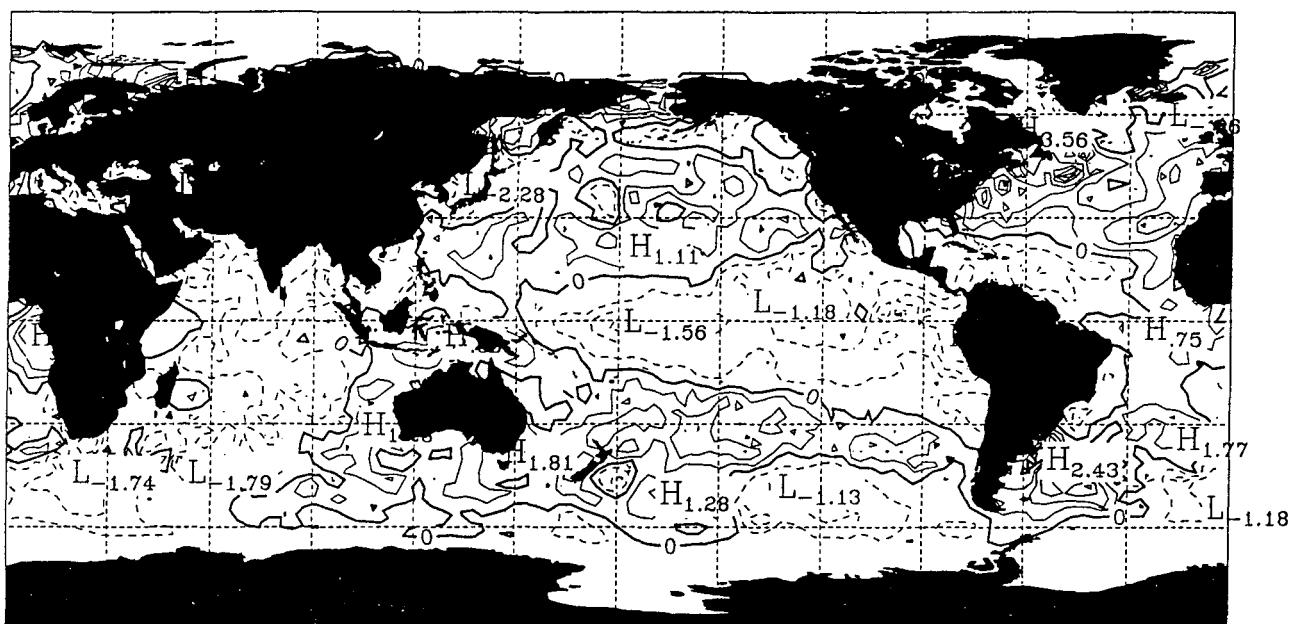
(b)
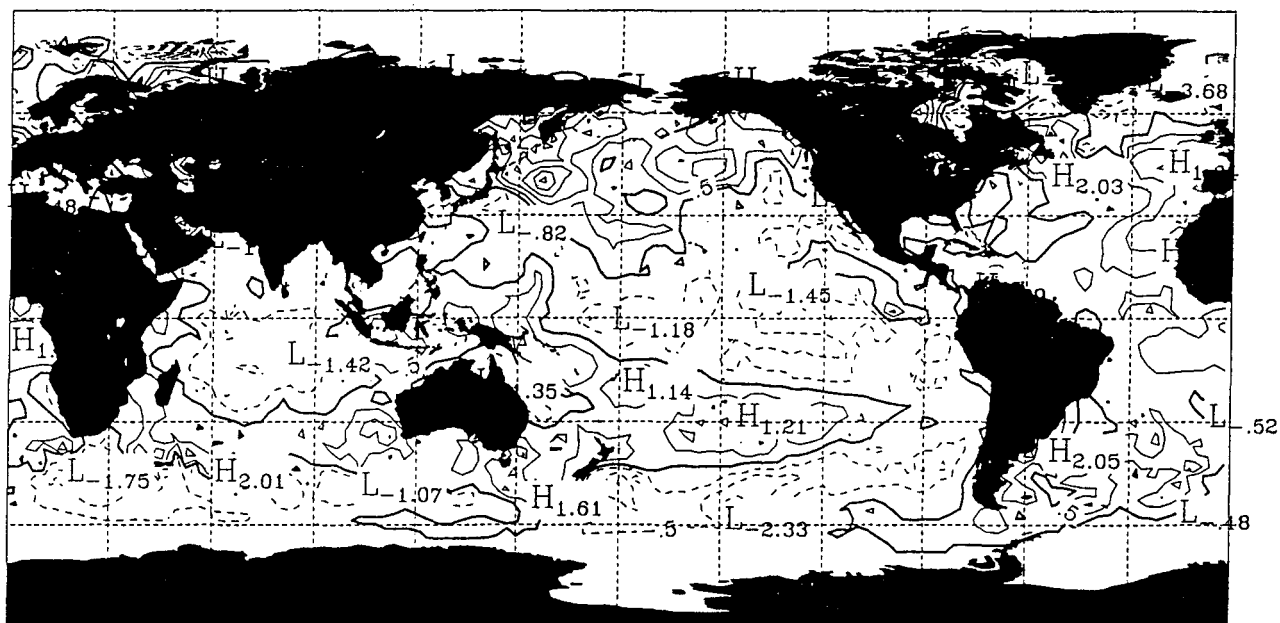
Fig. 5.24 SST anomalies over the global oceans in (a) June 1989 and (b) August 1989 relative to a 12 year mean (from the Reynolds Blended Data Set (Reynolds, 1988)].
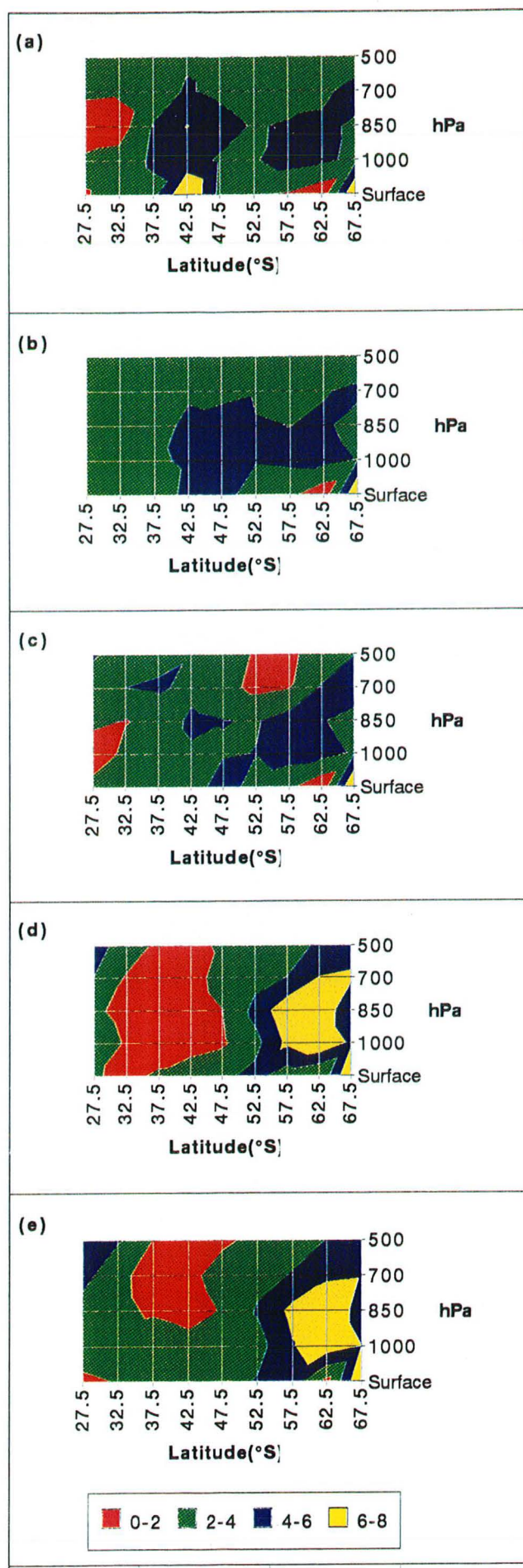
Fig. 5.25 Mean meridional cross-sections of temperature gradient (°C per 5° latitude) for June 1989 along (a) 40°E (b) 70°E (c) 100°E (d) 140°E and (e) 160°E.

Although broadly matching the characteristics of the mean June cross-sections depicted in Fig. 5.10, there are important differences. At 40°E the SST gradient centred on 42.5°E is slightly more intense than the mean but there are no significant departures from the mean pattern aloft. It is in the eastern cross-sections that the major differences are apparent. These largely relate to the intensity of the gradients at high latitudes near Antarctica where negative 1000-500 hPa thickness anomalies were observed throughout the winter of 1989 (NOAA Climate Diagnostics Bulletins, 1989). Also, the region of gradients of $\leq 2°C$ per 5 degrees of latitude is more extensive at 140°E than in the mean cross-section, particularly at the 850 hPa level. The intense gradient near Antarctica is also evident at 160°E but the area of slack gradient centred on 40°S is very similar to the mean pattern in Fig. 5.10 (e).

The thermal wind pattern resulting from the meridional temperature gradients has been calculated from the difference between the u components of the geostrophic wind at 500 hPa and 1000 hPa and is shown in Fig. 5.26. Although the projection exaggerates the area at high latitudes it is clear from the figure that the maximum westerly thermal wind to the south of Australia along 60°S (18 m s^{-1}) is similar in strength to the wind shear across central Australia (approximately 24 m s^{-1}) and is significantly stronger than the mean value in Fig. 5.20 (c). Between the two extremes the minimum value below 3 m s^{-1} near Tasmania stands out in stark contrast.

The mean geostrophic wind components at the 500 hPa level have been extracted from the ANMC analyses for the month of June 1989. Fig. 5.27 shows u and v components (averaged over two grid points in each case) over eastern Australia [Fig. 5.27 (a)] and south of Tasmania [Fig. 5.27 (b)]. Comparison with Fig. 5.21 indicates a marked increase in the wind maximum to the south of Australia in 1989, a weakening of the geostrophic wind at 45°S and a slight increase at 25°S. Anomalies in the v components are more subtle in the higher latitude case but nonetheless there is a change of sign along 150°E. However, Fig. 5.27 (b) shows a significant change along 150°E from a mean southerly to a 2 m s^{-1} northerly in June 1989.

The positive (anticyclonic) relative vorticity generated in this instance by the mean u components in the 5° by 5° square centred on 47.5°S, 147.5°E is approximately 2.35*10^{-5} s^{-1}. Mean v components for the month of June 1989 give a mean relative vorticity value of about 5.2*10^{-6} s^{-1}. Combining the two terms gives a value for the mean relative vorticity (ζ) for the month of June 1989 of 2.9*10^{-5} s^{-1} (of magnitude about 0.3f) and approximately twice the value computed in Section 5.8 from the long-term mean u and v components for June. For the 5° by 5° square centred on 27.5°S, 147.5°E the relative vorticity contributions combine to produce a negative (cyclonic) value of -1.9 * 10^{-5} s^{-1} (also about 0.3f). Fig. 5.27 (a) illustrates in schematic form the configuration of velocity components for the square centred on 47.5°E and Fig. 5.27 (b), the square centred on 27.5°S, 147.5°E.
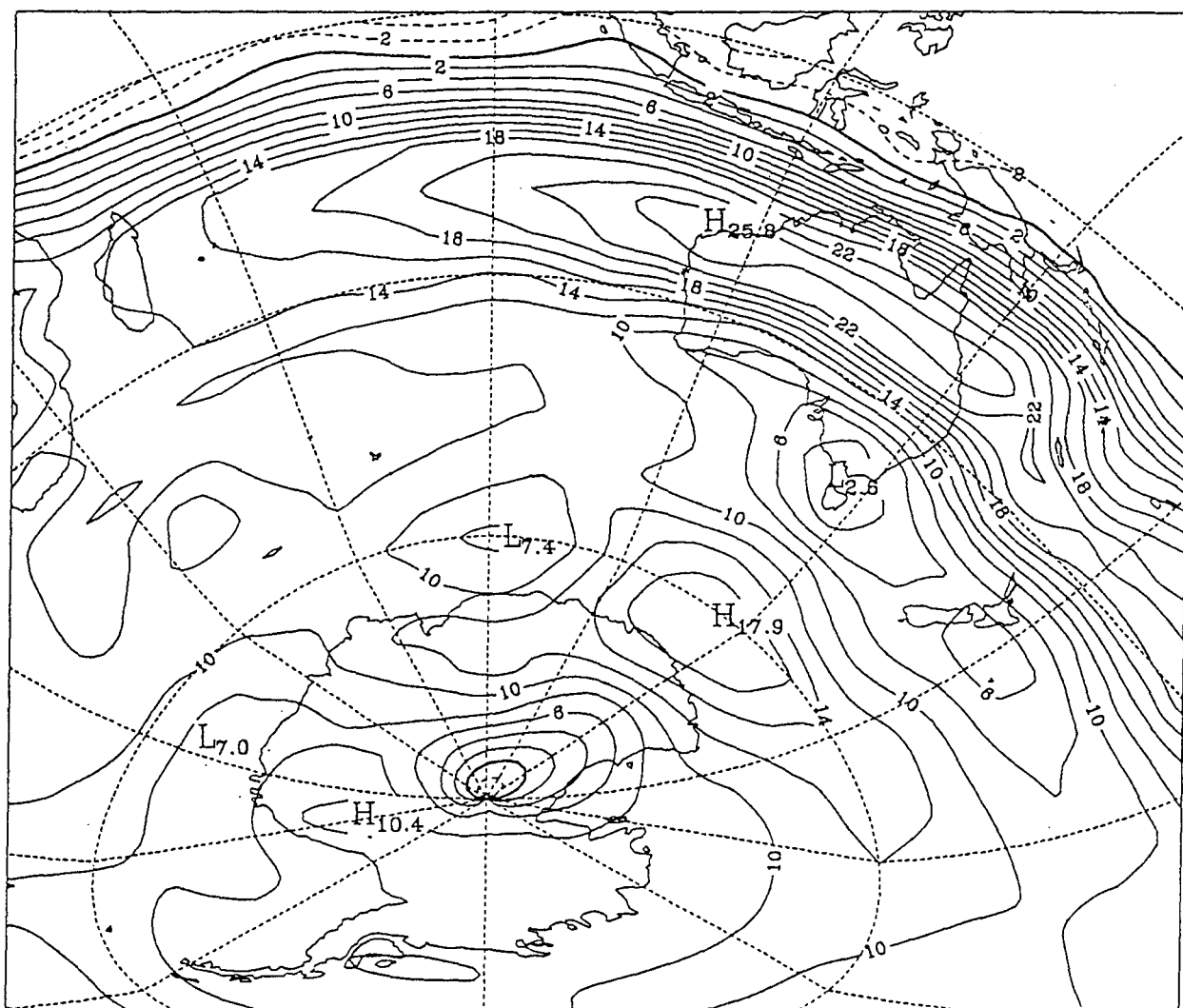
Fig. 5.26 Mean u component (westerly) of the wind shear between 1000 and 500 hPa for
the month of June 1989 (ANMC data).
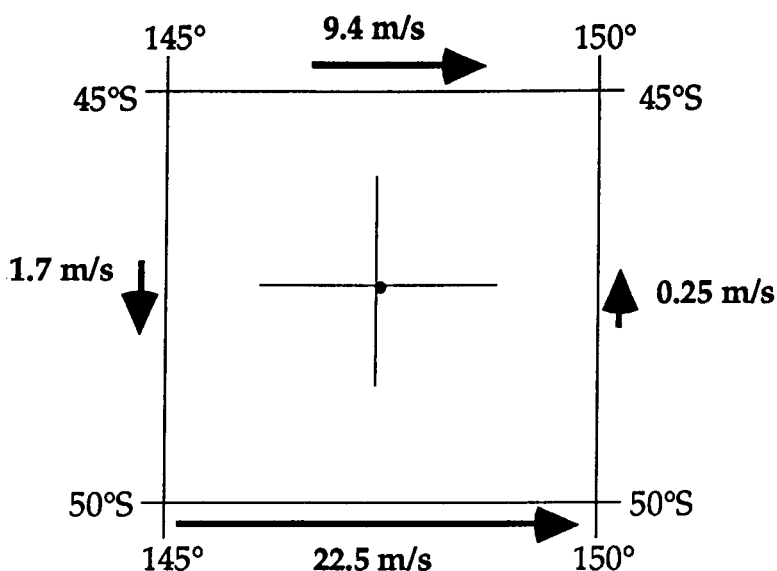
Fig. 5.27.(a). Schematic representation of the configuration of mean velocity components to the south of Tasmania at 500 hPa in June 1989 generating anticyclonic vorticity at 47.5°S, 147.5°E.
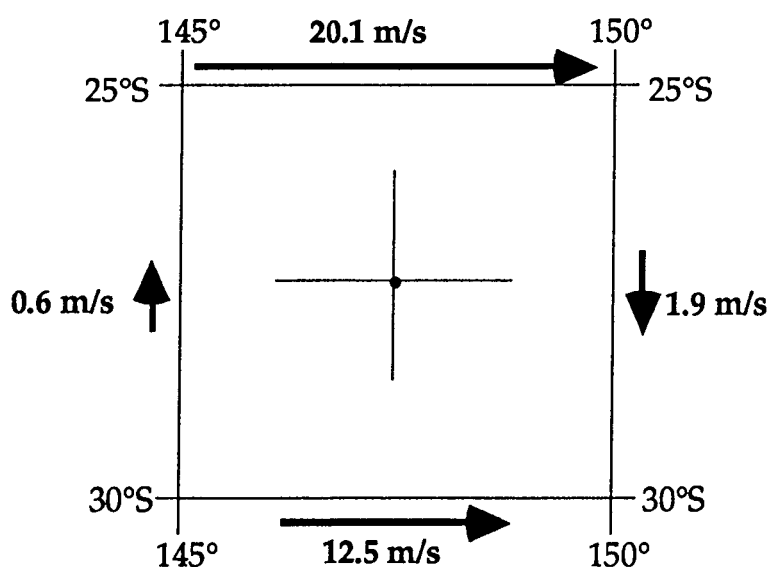
Fig. 5.27 (b). Schematic representation of the configuration of mean velocity components over southern Queensland at 500 hPa in June 1989 generating cyclonic relative vorticity at 27.5°S, 147.5°E.

The explanation for the enhanced cyclonic vorticity generation over eastern Australia is almost certainly related to the negative air temperature anomalies which developed during autumn when much of central and northern Australia experienced seasonal rainfall totals in the highest decile range (Gaffney, 1990a). Negative anomalies ranging from 1 to 2°C for daily maximum temperatures persisted across Australia in the winter months while minimum temperatures were near average (Gaffney, 1990b). Nunez (personal communication) has demonstrated in a boundary layer model that, when soil moisture values are set at 80% saturation, boundary layer temperature can be reduced by more than 5°C relative to the situation for dry soil conditions and the same cloud cover.

The negative anomalies over the Australian continent contrast with the positive SST anomalies in the waters about the east coast (see Fig. 5.21) and separately reported by Holbrook and Tomczak (1991). This configuration can explain the appearance of a mean northerly component of wind at 500 hPa near the east coast of Australia in June 1989 [Fig. 5.27 (b)].

Feedback Mechanisms

Baines (1983) has discussed some possible feedback processes that may occur during periods of blocking. He has referred to changes in insolation resulting from extended periods of anomalous cloud coverage leading to changes in SST and subsequently acting to alter the atmospheric forcing. Experiments which measure accurately the fluxes of heat and moisture in blocking situations have yet to be carried out for the South Tasman Sea or more generally for the Southern Ocean.

An extensive period of atmospheric blocking at high latitudes in the Tasman Sea and southwest Pacific Ocean region could be considered to provide a significant change to momentum transfer between the atmosphere and ocean from the climatological mean. This aspect of the 1989 winter blocking event was investigated by taking daily 10 metre winds (winter means of these winds are presented in Fig. 4.22) from the Australian region FINEST model for the months of June, July and August 1989 and calculating wind stress at the ocean surface for each observation using the Bulk Formula in the form of Hellerman and Rosenstein (1983):

$$\tau_x = \rho C_D u(u^2 + v^2)^{\frac{1}{2}} \qquad \ldots\ldots\ldots\ldots 5.3$$

$$\tau_y = \rho C_D v(u^2 + v^2)^{\frac{1}{2}} \qquad \ldots\ldots\ldots\ldots 5.4$$

where τ_x and τ_y are, respectively, the zonal and meridional exchanges of momentum between the atmosphere and ocean, ρ is the density of air (taken to be 1.3 kg m^{-3}) and C_D is the drag coefficient reduced to 10 m height and neutral conditions (Large and Pond, 1981). The assumption of neutral conditions has been discussed by Hellerman and Rosenstein (1983) who concluded that winter cold outbreaks in the vicinity of Asia and North America result in significantly higher τ_x than for the neutrally stable condition. The predominance of northerly wind components to the south and southwest of Australia during the winter and the scarcity of cold outbreaks were taken as suggesting the prevalence of stable rather than unstable conditions.

Fig. 5.28 gives the mean x and y components of wind stress in the Australian region for the winter of 1989 and reveals the intensity of the maximum of eastwards stress to the southwest of Australia and the peak in zonal and meridional components south of Tasmania and the Tasman Sea. Negative values of τ_x are evident near New Zealand.

(a)
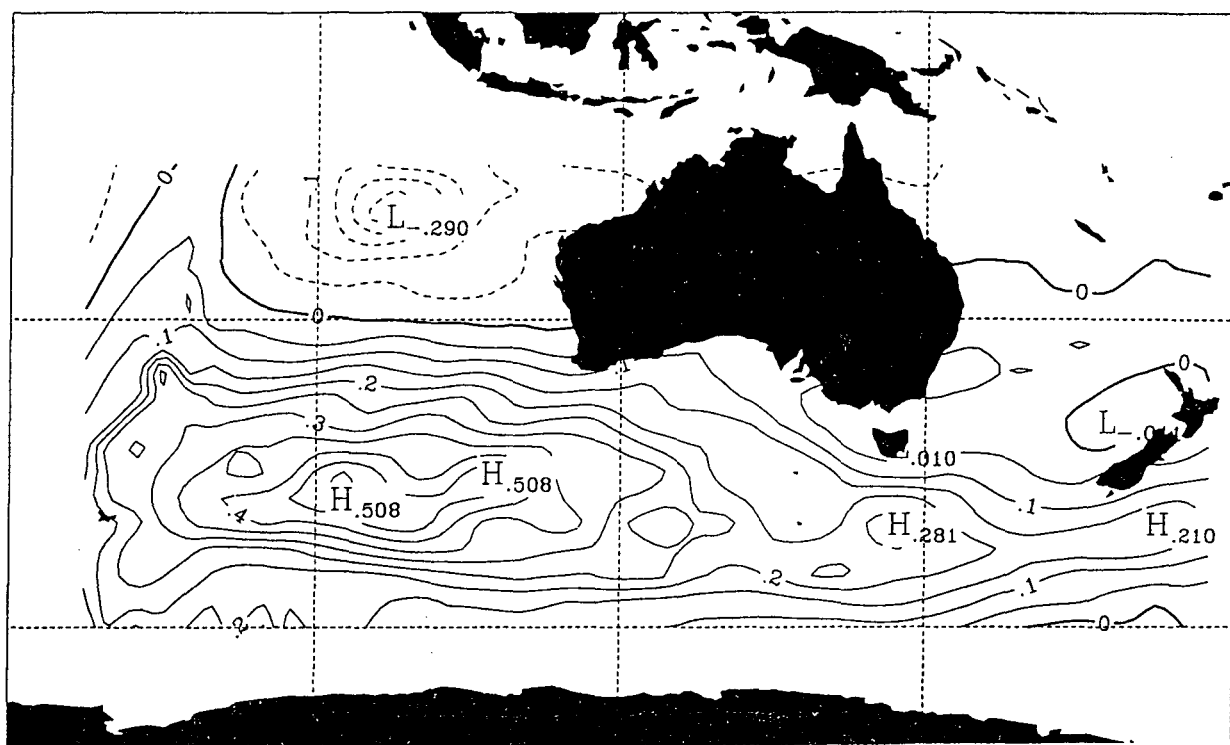
(b)
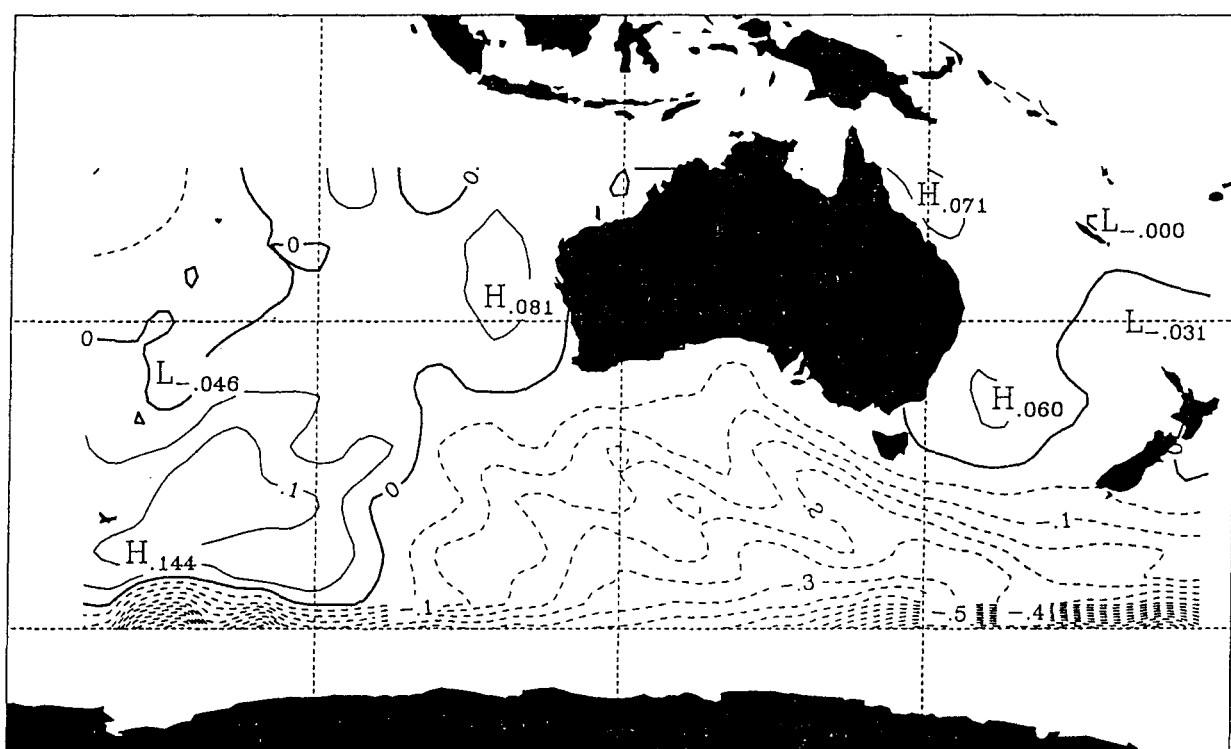
Fig. 5.28 Zonal (a) and meridional (b) wind stress (in units of N m⁻²) for the Australian region averaged for the months of June, July and August 1989.

Climatologies of wind stress have been presented for the Southern Ocean by, *inter alia*, Nowlin and Klinck (1986) in their Fig. 2, Hellerman and Rosenstein (1983), and more recently, by Trenberth *et al.* (1992). The results presented in Fig. 5.28 for the winter of 1989 indicate a significant increase in eastward stress over the Southern Ocean compared to these long-term means. Fig 5.29 shows the mean eastward stress for July according to Trenberth *et al.* (1992).
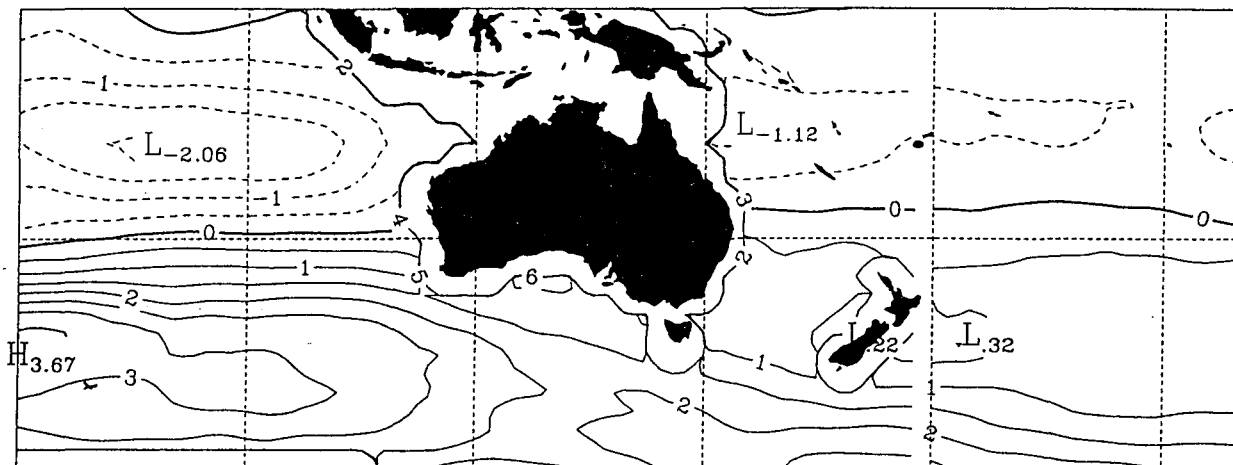
Fig. 5.29 Mean eastward wind stress for the month of July (units of 0.1 N m^{-2}) for the Australasian region (from Trenberth *et al.*)

5.10 A Conceptual Model of Winter Blocking

From the results presented in the earlier sections of this chapter it is reasonable to postulate that the frequency maximum of atmospheric blocking observed to occur to the southeast of Australia in winter results from a unique conjunction of physical influences. These include the configuration of the Australian and Antarctic continents, the role of bottom topography in directing the ACC to high latitudes south of the Tasman Sea, the longitudinal extent of Australia in the sub-tropics, and the solar cycle. Superimposed on these fixed inputs there are variable influences which give rise to an interannual variability in the intensity of temperature gradients in the ocean and atmosphere. A key factor in this variability is the ENSO cycle which affects cloudiness and precipitation over northern, central and eastern Australia, the position of the Sub-Tropical Ridge, the strength of the Trade Winds and dependent regional ocean currents, and the intensity of the zonal westerly winds to the south of Australia. Although oceanographic responses to wind forcing can be expected to be slow at middle and high latitudes the results presented here suggest that the mechanism of blocking may significantly change the wind stress patterns over periods of several months possibly affecting local surface currents and SST.

A conceptual model of the processes involved in the seasonal cycle of blocking and its interannual variability is presented in Fig. 5.30.
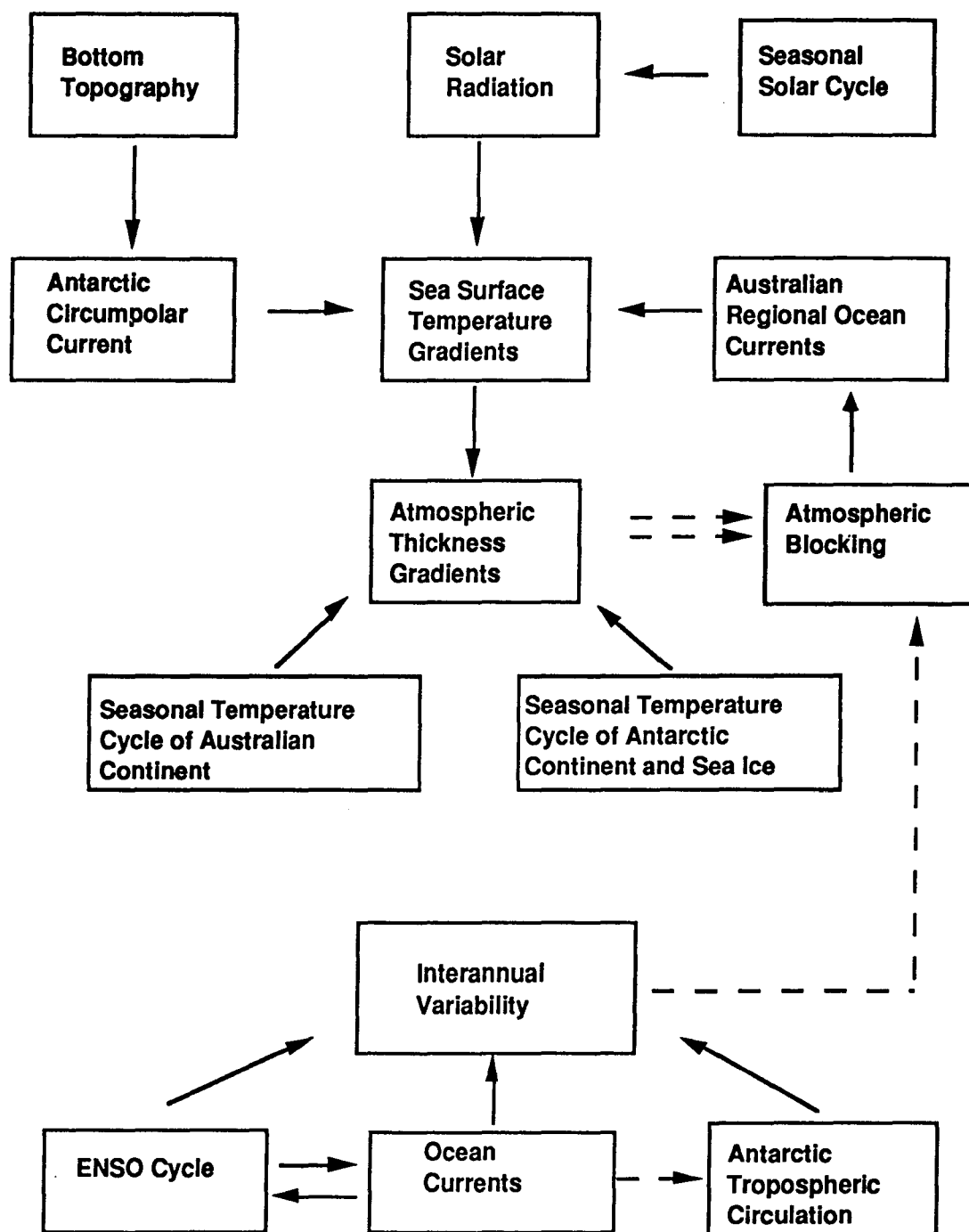
Fig. 5.30. A conceptual model of the interaction of physical influences, including feedbacks, on the seasonal and interannual cycle of atmospheric blocking.

5.11 Conclusion

In this chapter, the main features of the SST configuration in the Australasian region have been shown to be closely linked to the constraints imposed by the bottom topography of the Southern Ocean and the location of the continents. The strongest latitudinal temperature gradients are to be found to the south and southeast of Africa where the Agulhas Current (a western boundary current) interacts with a low latitude arm of the ACC. Other regions where the isotherms converge are found to the south of Western Australia and at high latitudes in the Antarctic Convergence Zone.

Previous studies have sought to establish a link between the region of maximum blocking frequency in the Southern Hemisphere and the observed gradient of sea surface temperature (SST) from the cold waters of the Indian Ocean sector of the Southern Ocean to the relatively warm surface waters located to the southeast of Australia. In this study, investigation of the distribution , intensity and seasonal cycles of SST gradients over the Southern Ocean suggests that the contribution of the west to east gradient in forcing the atmosphere is about an order of magnitude less than the effect of SST gradients in the meridional plane. North-south gradients undergo marked changes during winter because of the interaction of several major influences in the Australian region. These include the significant cooling of the continents of Australia and Antarctica and the configuration of the Antarctic Circumpolar Current (ACC). South of the Tasman Sea and New Zealand the ACC is forced to high latitudes (60 to 65°S) as it is diverted southeastwards by the Macquarie Rise and Campbell Plateau. Although SST gradients are gradually dissipated in the atmosphere with height, in regions where the ACC travels closer to the coast of East Antarctica low level atmospheric temperature gradients induced by the ACC are supported at higher levels by the strong temperature gradients generated by the elevated contours of the Antarctic continent. This gives rise to an enhanced westerly thermal wind at high latitudes (south of 50°S) which leads to a westerly wind maximum aloft. At the same time, the steady cooling of inland Australia acts to weaken the north to south temperature gradient between 30°S and 45°S leading to a minimum in the westerly winds in this latitude band. Further to the north strong gradients develop between northern Australia and central and southeastern Australia giving rise to an intense westerly thermal wind north of 30°S. Such a configuration of mean winds in the middle troposphere can be shown to generate a pattern of relative vorticity which displays significant positive values [about 0.14 planetary vorticity (f)] in the south and negative values [about 0.16 of the local planetary vorticity (f)] in the north. These mean values of relative vorticity suggest that blocking is a normal state for the Australasian region in winter.

Further to the east a region of slack north to south temperature gradients remains anchored near the Date Line at latitudes between 30°S and 45°S throughout the year. This region , referred to as the 'climatological split' by Trenberth and Mo (1985), is the area in which the highest frequency of blocking is observed in the Southern Hemisphere (van Loon, 1956; Wright, 1974; Hirst and Linacre, 1981; Trenberth and Mo, 1985). It appears likely that

a predisposition to blocking persists in this area in all seasons but enhancement takes place in winter as the gradient intensifies near Antarctica and further west the Australian continent comes into play.

An intense prolonged blocking event occurred in the Australasian region in the winter and spring of 1989. This event has been investigated in the context of interannual variabilty of blocking frequency. It is postulated that the active monsoon conditions over northern Australia associated with the La Niña of 1988-89 may have contributed to the colder than normal inland temperatures in the following winter thus enhancing the seasonal blocking cycle. The enhanced Antarctic polar vortex reported in 1989 is also presented as contributing to increased north -south atmospheric temperature gradients. Finally the configuration of SST anomalies in the autumn and early winter of 1989 is advanced as a significant precursor to the subsequent blocking event. In particular, the juxtaposition of the warm anomaly in the East Australian Current and the cold anomaly over eastern Australia contributed to the stronger than normal 500 hPa northerly wind component in the vicinity of the east coast, via the thermal wind.

Chapter 6

Blocking Signatures in an Atmospheric General Circulation Model Simulation

6.1 Introduction

The ability of numerical models to predict the onset, persistence and decay of anomalous patterns, including blocking, is a significant test of their usefulness for day to day forecasting. It can also be regarded as an indicator of the applicability of the models to studies of the climate system, providing insights into the relative contributions of the physical processes simulated in the model. Since the introduction of numerical prediction to weather forecasting, objective and subjective methods have been developed to evaluate the accuracy of the prognostic fields generated in the models. Typical of these objective methods are statistical 'skill scores' (Teweles and Wobus, 1954) and anomaly correlations (Simmons, 1986). A general improvement in skill over time has been demonstrated for numerical weather prediction as evidenced by statistics presented for the European Centre for Medium Range Forecasts (ECMWF) model by Simmons (1986).

Initially, numerical weather prediction and climate studies using General Circulation Models (GCM's) did not have very much in common. The short time-frames of the former and the need for critical climatological balances in the latter separated the two approaches. However, as Bengtsson (1992) has observed, climate simulations for relatively short periods (30-90 days) are essential components of the development process of modern global forecast models. He observes that "... a clear distinction can no longer be drawn between numerical atmospheric models for climate studies and weather forecasting..." (Bengtsson, 1992, p. 705)

Simmons (1986) has reported that the treatment of blocking in the ECMWF model did not present an extraordinary problem and any difficulties encountered were related to general deficiencies in the model itself. In support of this view, Bengtsson (1992) was able to show that improvements in the prediction and simulation of blocking were achieved in the ECMWF model between the winters (NH) of 1985-86 and 1987-88 following changes in the physical parameterization of radiation, convection and the reduction of vertical diffusion in the free atmosphere.

However, the scarcity and timliness of receipt of data remains a serious constraint on the ability of global models to improve performance in the Southern Hemisphere. Trenberth and Olson (1988) have drawn attention to significant differences in the Southern Hemisphere between analyses of the United States National Meteorological Centre (NMC) and ECMWF products and have identified serious errors, particularly over Antarctica. They conclude that the data assimilation schemes in these two models appear to

place too much weight on the 'first guess field' in preference to the observations.

In the Australasian region one of the first numerical experiments to investigate the association between atmospheric blocking and a positive SST anomaly centred in the southwest Pacific Ocean was conducted by Simpson and Downey (1975). Based on reported positive anomalies in the Tasman Sea region during the first few years of the 1970's and an apparent increase in the frequency of blocking activity in that period, they centred a warm anomaly (maximum value of 4°C) at 45°S, 180°E. The positive SST anomaly gradually decreased to zero at 25°S, 55°S, 150°E and 140°W. It is immediately apparent that this is a very large area over which to maintain a significant anomaly, an observation also made by the authors.

Simpson and Downey (1975) reported the results of two runs of a 9-level model adapted for the Southern Hemisphere and described by Anderson and Noar (1974). The second run was started 10 days after the first run. The most significant result occurred in the first run after 20 days when an intense thermal ridge developed at 500 hPa near 180°E and persisted for more than 10 days in association with a slow moving anticyclone at the surface. Prior to day 20 the model and control were closely matched in the Pacific sector as evidenced on the Hovmöller diagram in their Figure 4.

Noar (1983) has given a review of experimental simulations of atmospheric blocking followed by an examination of the success of numerical models in forecasting the onset and continuation of the phenomenon during a period of significant blocking in the Australian region during the month of June in 1982. He extended the statistical analysis of blocking forecasts by numerical methods to the Southern Hemisphere. An extensive numerical study of the June 1982 blocking event was also carried out by Mo *et al.* (1987) who concentrated on the conditions contributing to the maintenance of the blocking throughout a 15 day period from 8 to 22 June. By changing various forcing factors they were able to show by simulations in the GLA fourth-order GCM that the block was maintained by asymmetric heating resulting from land-sea thermal contrast in the Australia-New Zealand region. Mo *et al.* (1987) discounted the effect of SST anomalies as a possible cause and argued that these were the result of the atmospheric anomalies.

On the other hand, Kung *et al.* (1990) demonstrated that predictability of winter blocking in the Northern Hemisphere can be enhanced when a realistic SST pattern is prescribed. In their numerical simulations, the SST field was altered with observations during the model integration. Two major blocking events developed in the Pacific and Atlantic Oceans during a model run of one month, initialised by gridded analyses of the First GARP (Global Atmospheric Research Program) Global Experiment (FGGE) data set for 1 January 1979. Kung *et al.* (1990) identified blocking in their model runs by manual inspection of the resulting flow patterns and application of a blocking index which provides a measure of the relative intensity of the blocking dipole structure at 500 hPa with an adjustment for the degree of meridionality of the circulation.

This chapter reports the results of two experimental runs of a GCM forced by realistic SST anomalies. In the first run the SST anomaly has been taken from the situation of June 1989 and in the second, the anomaly has been altered by reverting to the model's SST climatology north of 25°S, thereby removing the anomalous tropical forcing. The experimental runs are compared with a 120 day control in which the model has been run in a 'perpetual July' mode with model climatology.

6.2 The Model

The model used in this study was the Melbourne University General Circulation Model (MU GCM), the main features of which have been discussed by Simmonds (1985). It is a global extension of the original version described by McAvaney et al. (1978), Simmonds (1981) and Simmonds and Lin (1983). Variables are represented in the model at 9 sigma levels in the vertical while the horizontal distribution of most variables is represented in terms of spherical harmonic series with rhomboidal truncation at wave number 21. The model climatology is discussed in detail by Simmonds et al. (1988). Further improvements were incorporated into the model employed in this study and have been summarised by Lynch (1993). In her Table 3.1 the characteristics of this version of the model (Version 7) are contrasted with the specifications in the earlier version 5 (Simmonds, 1985). Lynch (1993) points out that there are four major improvements in the later version of the model over version 5. The improvement in the convection scheme has been achieved by inclusion of dry convective adjustment while the soil moisture scheme has been modified by the adoption of a two-layer scheme. Boundary conditions have been revised in this version of the model by the use of more accurate or extensive data sets such as SST, degree of cloudiness and snow and ice cover. The fourth significant change is the introduction of the seasonal cycle in the radiation and prescribed fields.

The SST specification in version 7 of the model is of particular interest in this study as alterations to the SST field are used in the two experiments discussed below to force the model. Lynch (1993) has discussed in detail the significant effects a choice of SST field can have on modelled climates and has presented a comparison of global SST climatologies which have been employed in AGCM's in her Table 3.2. She reports that version 7 of the MU GCM incorporates a daily SST climatology derived from the Reynolds data set (1988) by assigning the monthly values to the 15th day of each month in the model and fitting a cubic spline to interpolate the daily values.

6.3 Experiment No. 1

In order to test the hypothesis that an SST anomaly could force a blocking event in the Australasian region, the SST anomaly field for June 1989 previously presented in Chapter 5 [see Fig. 5.24 (a)] was introduced into the model to provide the initial forcing. The model was then run in perpetual July mode for a total of 120 days. As a control, the model was run in perpetual July mode with its standard climatology (including SST) for a similar period. In the control simulation, SST are prescribed by the model July climatology while the surface continental temperatures result from the predictive scheme within the model.

Differences of geopotential height at 500 hPa between the model run with
the prescribed June 1989 SST anomaly and the control run are shown in Fig.
6.1 after averaging periods of 30 days, for the periods, day 1 to day 30, 31 to
60, 61 to 90, and 91 to 120. In the first 30 day period a strong (>10 dam)
negative anomaly appears south of Tasmania and extends a trough
northwards through the Tasman Sea while a positve anomaly (>6 dam)
develops east of New Zealand. The average anomaly field for the second 30
day period is characterised by large positive anomalies south-east of South
America (14 dam) and to the south of Western Australia (>9 dam). Of
particular interest is the appearance of a negative anomaly (~4 dam) over the
Australian continent. This negative anomaly intensifies during the
subsequent 30 day period (day 61-day 90) and major postive anomalies
emerge south of New Zealand (15 dam) and to the south-west of Western
Australia (~11 dam). During this third period an intense negative anomaly
(~25 dam) makes an appearance over the Ross Sea in Antarctica. This feature
weakens in the subsequent averaging period (day 91 - day 120) while
negative anomalies extend throughout the majority of the Southern Ocean.
The exception is found in the Australian region where positive anomalies
extend from the Antarctic coast south of Australia to the North Tasman Sea.

(a)
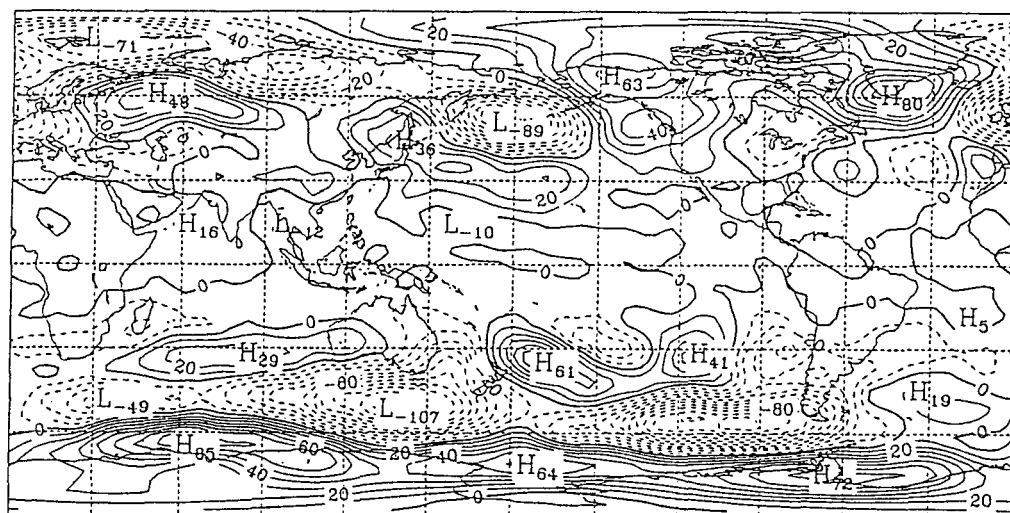
(b)
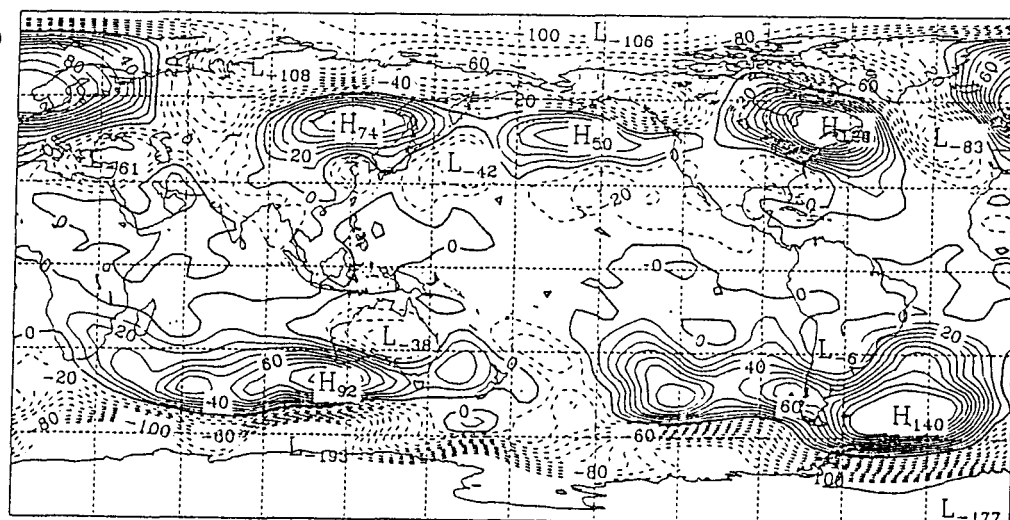
(c)
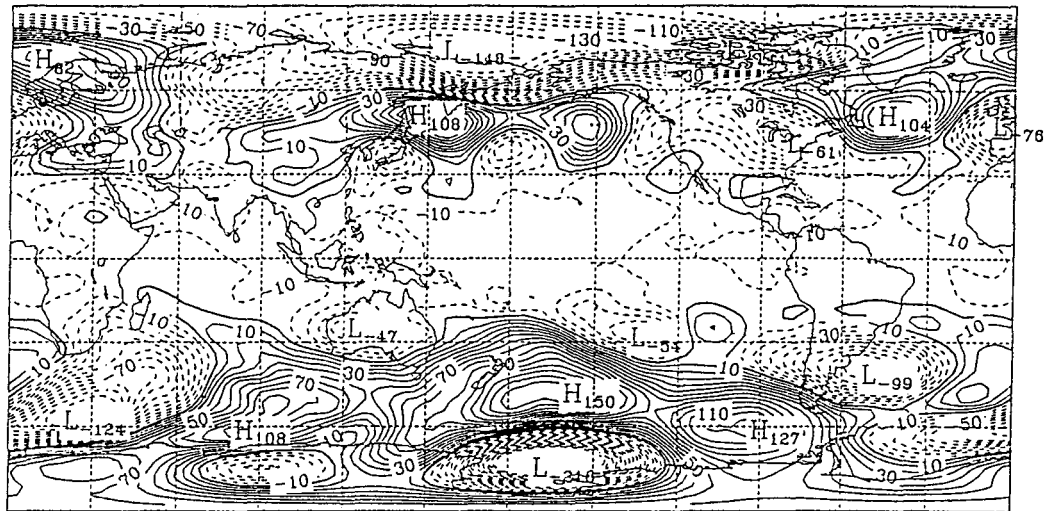
(d)
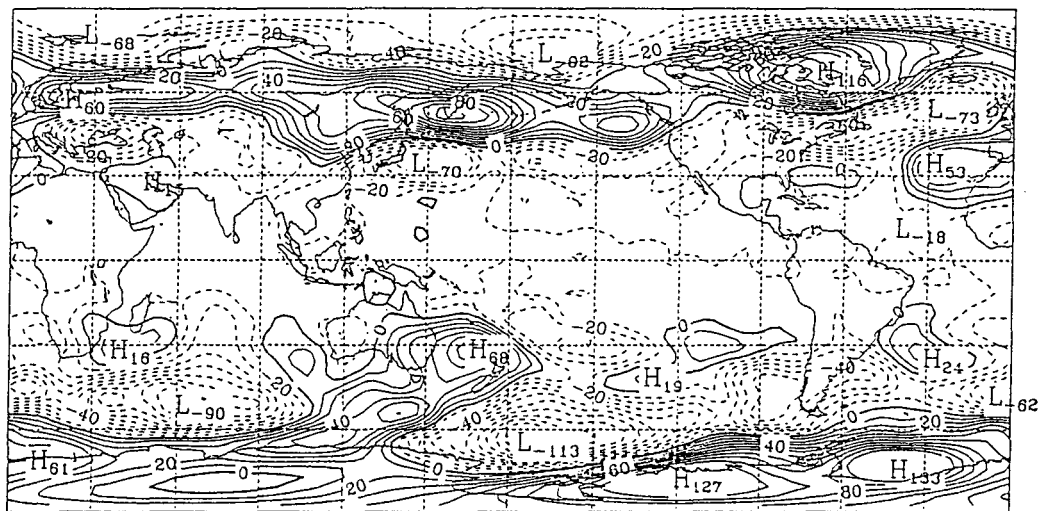
Fig. 6.1 Average anomaly of geopotential height (m)at the 500 hPa level between the model
run in Experiment 1 with the June 1989 SST anomaly and a control, for the periods
(a) day 1 to day 30, (b) day 31 to day 60, (c) day 61 to day 90, and (d) day 91 to 120.

A comparison between the 120 day averages of 500 hPa geopotential for the full model run in Experiment 1 and the control is shown in Fig. 6.2. It reveals areas of significant positive differences to the southwest of Australia, in the western and central Pacific Ocean and to the southeast of South America. Significant negative anomalies are apparent to the south of Africa and over northern Australia. Other negative anomalies are evident over the Ross Sea and South America.
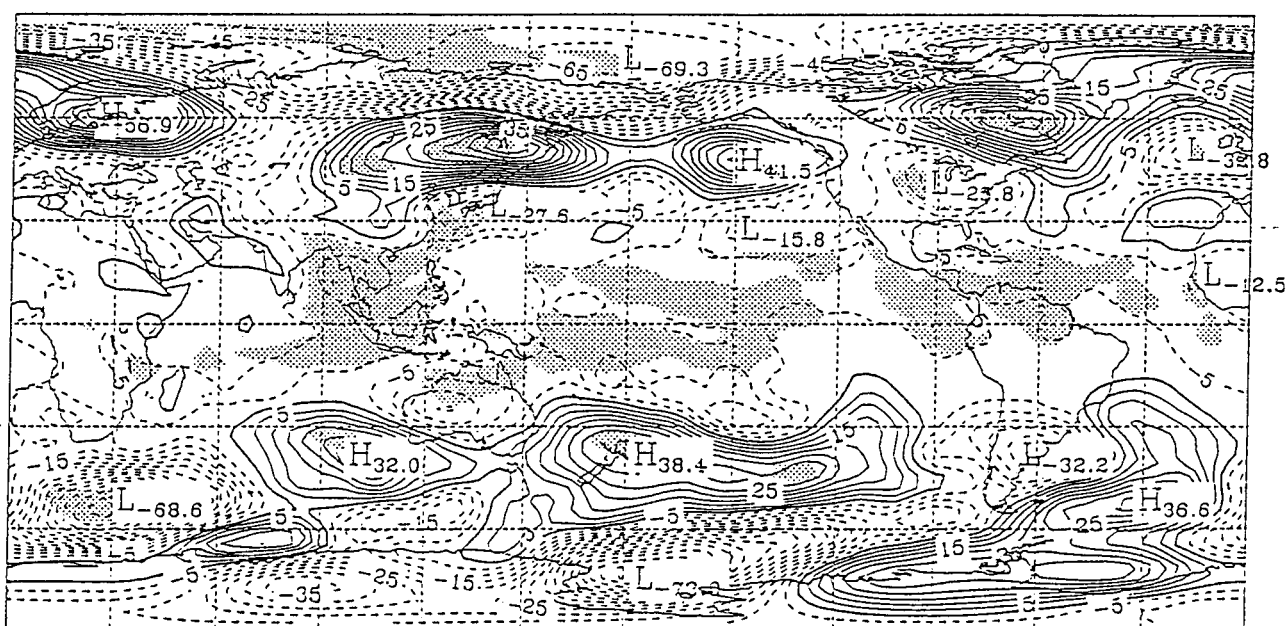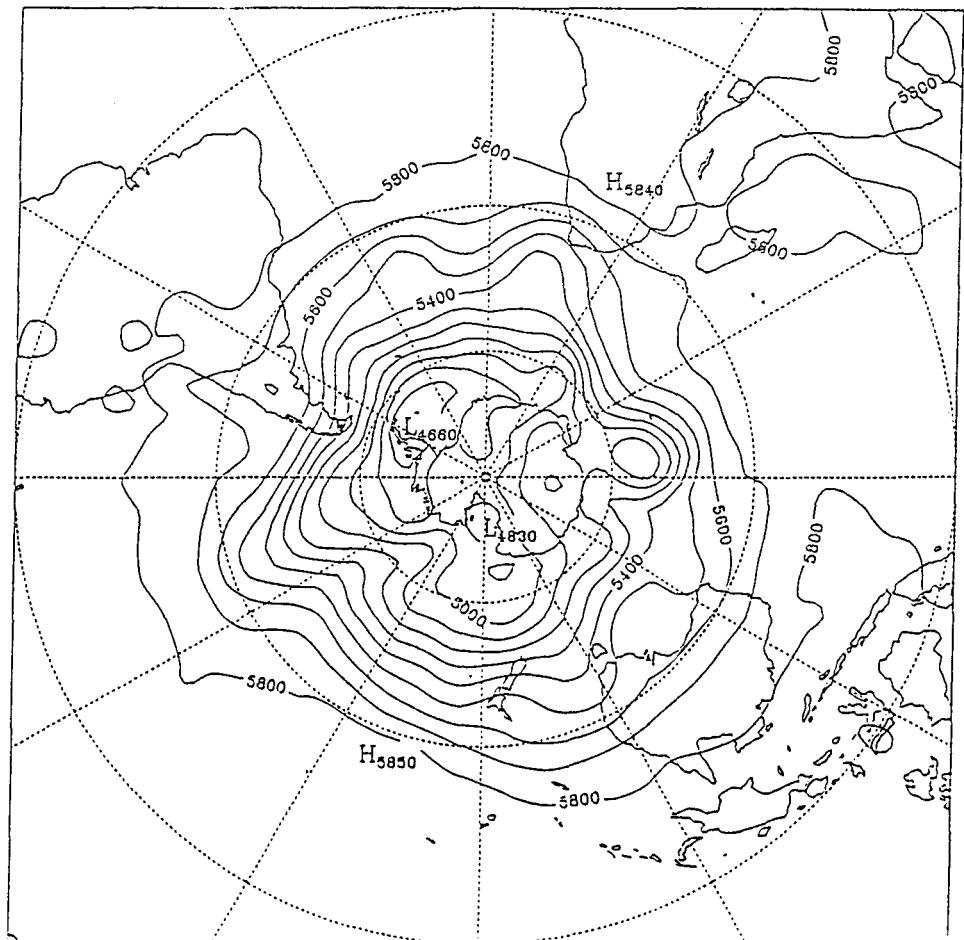

Fig. 6.2 Differences in geopotential height of the 500 hPa surface between a 120 day average of daily fields in Experiment 1 and a 120 day average for the control. Areas of stippling represent differences which are significant at the 95% confidence level. (Student's t-Test)
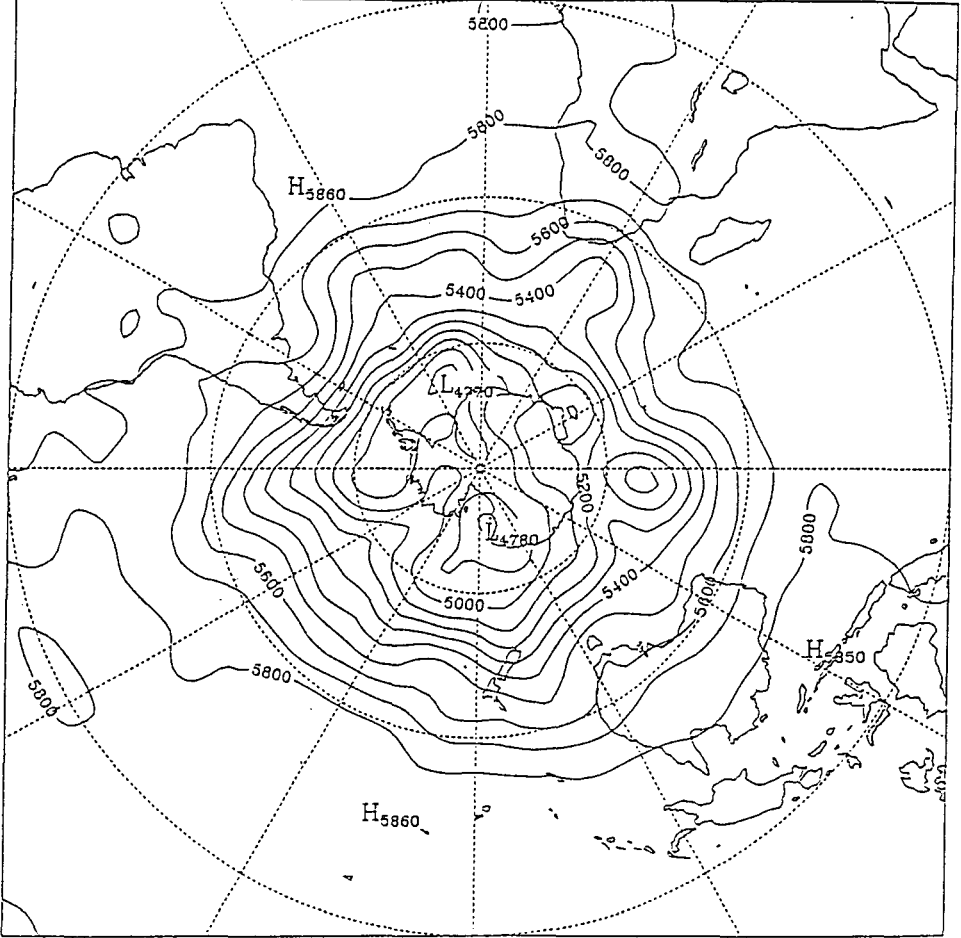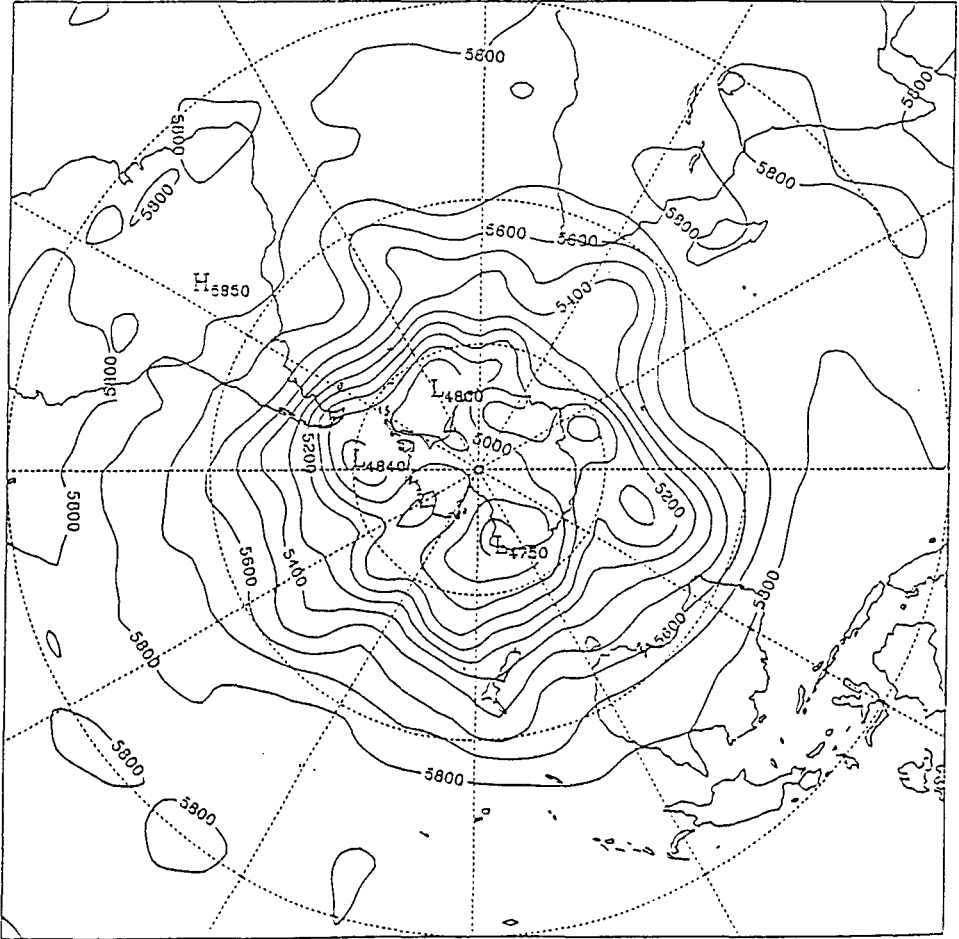
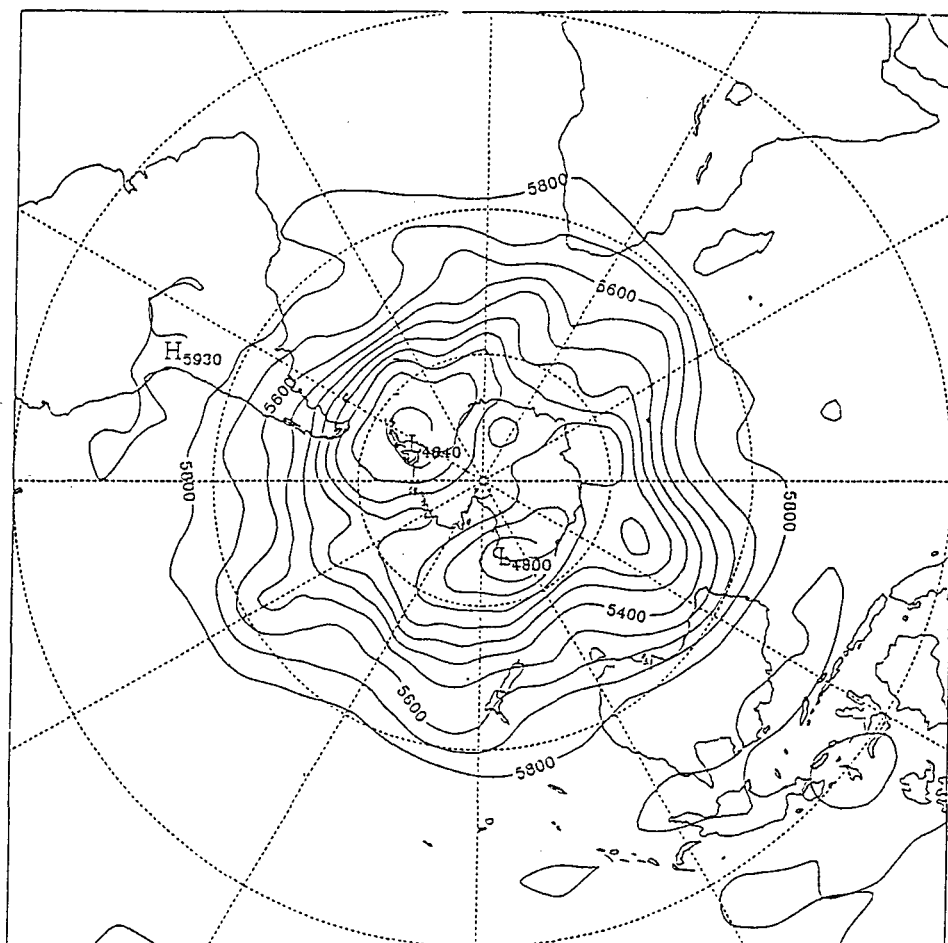The anomalous geopotential height field produced in the model in Experiment 1 relative to the control can be compared with the observed 500 hPa geopotential height anomaly between the mean for the period June, July, August and September, 1989 and a 20 year mean for that 4-month period calculated from ANMC analyses. In Fig. 6.3 large positive anomalies are evident to the southeast of South America and to the south and southeast of Australia, while marked negative anomalies appear over and to the north of Marie Byrd Land in West Antarctica. The magnitude of this negative anomaly of approximately 14 dam is almost a factor of two larger than the magnitude of other anomaly centres. It is of course advisable to treat anomalies in this data sparse region with caution. Russkaya and Byrd are the only stations in this sector which have contributed to the Antarctic reporting network in recent times (Smith and Stearns, 1993). There have been very few upper air stations in this region throughout the history of Antarctica and the oceanic region from the Antarctic coast to approximately 50°S is devoid of observing stations except for occasional drifting buoys which supply surface data only (Streten and Zillman, 1984). Nevertheless, the anomaly is remarkably intense and persistent over this four month period. Other regions of negative anomalies appear south of South Africa and over eastern Australia. The anomaly over Australia is consistent with cut-off lows moving over southern Australia in association with blocking patterns (Gaffney, 1990b).
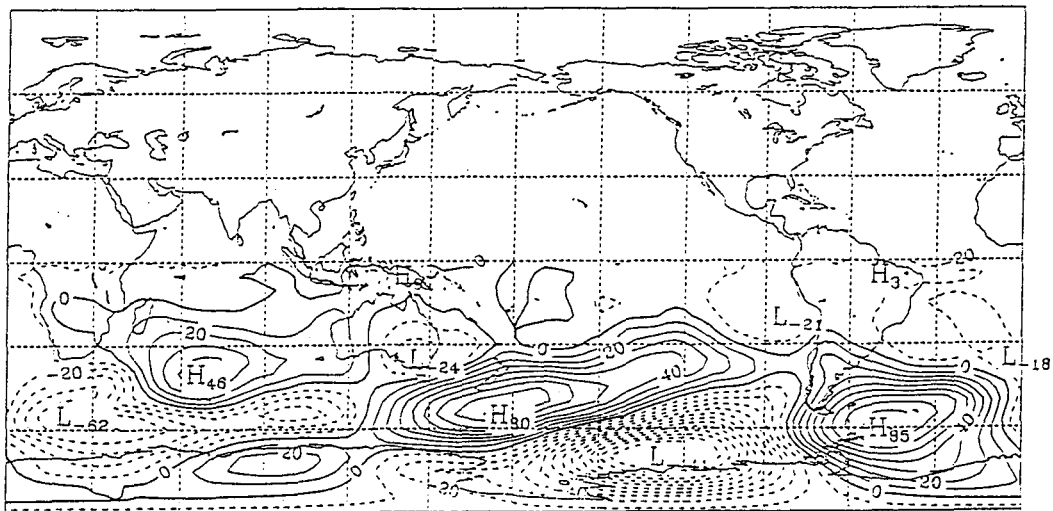
Fig. 6.3 Anomalies of geopotential height of the 500 hPa surface for the 4 month period June, July, August and September 1989 relative to a 20 year mean for that period (ANMC data).

Anomalies produced by the model averaged over 120 days display a broadly similar configuration over the Southern Hemisphere to the observed anomalies in Fig. 6.3 but are of approximately half the magnitude. It is immediately apparent that the positive anomaly to the southeast of Australia has developed at lower latitude in the model run, the maximum appearing approximately 10 latitude degrees further north than the observed 500 hPa geopotential anomaly in the 1989 event. There is good agreement over the Australian continent where the negative anomaly is of similar magnitude in each case but is centred further to the west in the model. The negative anomalies south of South Africa are of similar magnitude but the major negative anomaly over Antarctica is too far to the west in the model (near the Ross Sea) and about a factor of two lower in intensity than the observed anomaly. The anomalies produced by the model in the tropics are weak but universally negative.

6.4 Experiment No. 2

Shukla (1986) has demonstrated that the effects of tropical SST anomalies are likely to be more significant in creating heating anomalies throughout the atmosphere than those occurring at higher latitudes. In an effort to separate the influences of the high latitude SST from those observed in the tropics, the model was run in a second experiment with the prescribed SST field altered so that the anomaly, relative to the model SST climatology, was everywhere zero north of 25°S. The anomaly was unchanged south of 25°S from that discussed in Section 6.3.

(a) Average fields.

Differences of geopotential height at 500 hPa between the model run with the modified SST anomaly and the control run were calculated in a similar way to the procedure followed in Section 6.3. Fig. 6.4 gives the anomaly field for the 120 day average in Experiment No. 2. Comparison with Fig. 6.2 reveals broadly similar features in the Australian region. Over the Australian continent, the negative anomaly has intensified slightly and moved eastwards. Elsewhere, the positive anomaly to the southeast of South America has been replaced by negative values and there has been a marked strengthening of the positive anomaly in the southeastern Pacific Ocean. It is particularly interesting that small, but statistically significant negative anomalies, persist over the Tropics and become more extensive in the modified SST model run, that is to say, without the well-defined La Niña signal in Run 1. It should be noted that the positive height anomaly to the southeast of New Zealand, is not statistically significant at the 95% confidence level. Shukla (1986) has argued that it is more difficult to detect the influence of midlatitude SST anomalies on midlatitude flow because of the inherent instabilities present in the atmosphere at these latitudes. Nevertheless, the removal of the tropical component of the SST forcing does not alter the pattern of the anomalies in the Australasian sector. The areas which experience major change between runs 1 and 2 are in the south-eastern Pacific and the Atlantic sectors. Kalnay and Mo (1986) have reported that the persistence of stationary Rossby waves in the South American region is dependent on the existence of a strong South Pacific Convergence

Zone (SPCZ). The removal of the tropical SST anomaly may be important in this context.

Comparison with the observed 500 hPa geopotential height anomaly for June, July, August and September 1989 (Fig. 6.3) indicates that the location of major features in the 120 day average for Run 2 is similar in the Australian region although there is a northwards displacement of the positve anomaly near New Zealand as in Fig. 6.2. The most significant difference between the model and the observed fields is in the vicinity of South America where the negative anomalies centred to the east run counter to the observed positve anomaly over the Scotia Sea.
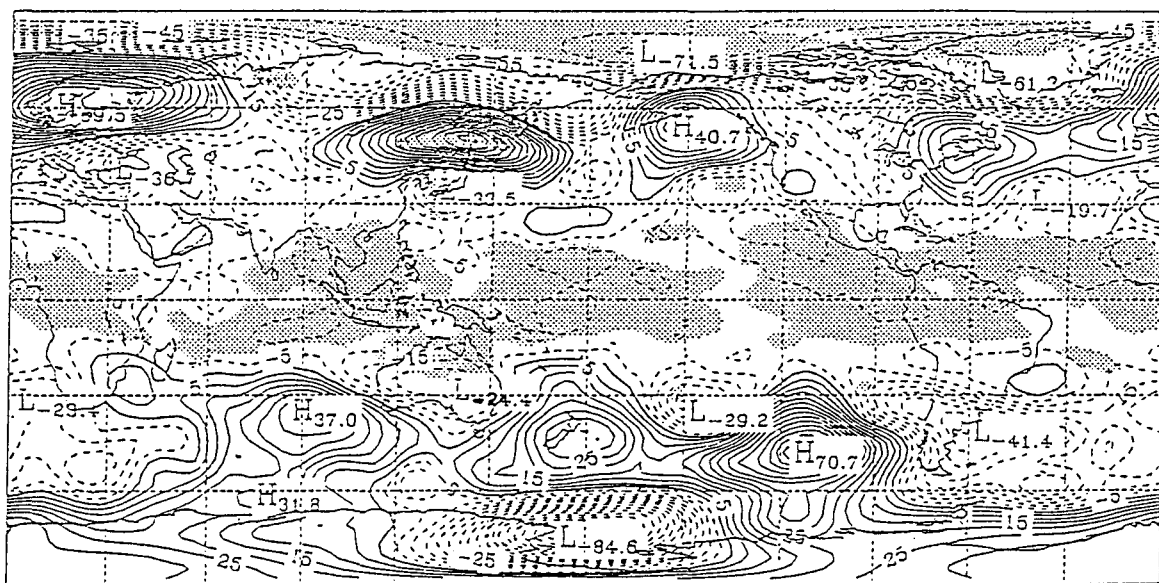
Fig. 6.4 Differences in geopotential height of the 500 hPa surface (metres) between a 120 day average from Experiment No. 2 and a 120 day average for the control. Areas of stippling represent differences which are significant at the 95% confidence level. (Student's t-Test)

(b) Daily Fields.

Although the average geopotential heights at 500 hPa in Run 2 display some of the characteristic anomaly patterns associated with blocking (Fig. 6.3), it is important to look for evidence of blocking or 'split flow' in the daily fields to evaluate the capability of the model to produce realistic atmospheric behaviour. In Fig. 6.5 geopotential height at 500 hPa is shown for the Southern Hemisphere for each day of a six day period from day 70 to day 75. The model fields show the evolution of a 'split' south of Western Australia early in the period (day 70 to day 74) and in the Pacific near 120°W from day 73.

In each case, full amplitude ridges develop in the model and extend across the coast of Antarctica. The evolution of the ridge south of Australia displays the characteristic splitting of the westerly flow into two branches but the dipole structure is not evident. Also, the event does not persist long enough to satisfy the definitions of blocking discussed in Chapter 3. By way of contrast, the system in the Pacific develops into a classical blocking pattern after the slowly moving ridge north of the Ross Sea on days 71 and 72 amplifies and extends across Marie Byrd Land on day 73.

(a)

(b)

(c)

(d)

(e)

(f)

Fig. 6.5 Daily 500 hPa geopotential fields (m) for Run No.2 of the MU GCM forced by a modified SST anomaly. The model days are in sequence from day 70 (a) to day 75 (f).

6.5 Discussion

The experiments carried out in this study have demonstrated that an AGCM can develop anomalies of 500 hPa geopotential height with a similar spatial pattern to that observed in a real blocking situation when a realistic SST anomaly is introduced. Moreover, the pattern of geopotential anomalies in the Australasian region was not substantially altered when the SST anomalies were removed north of 25°S. The magnitude of positive anomalies was largely underestimated by the model but the negative anomaly over the Australian continent was modelled faithfully in both runs.

As the surface temperature over land is determined within the model from the surface energy budget without energy storage (Simmonds *et al.*, 1988), the negative height anomalies at 500 hPa which developed over the continent in both model runs 1 and 2 point to effects of increased heating from the anomalously warm oceanic waters surrounding Australia. Warming the atmosphere from below encourages the formation of cyclonic circulations at the surface and anticyclonic activity aloft (Green, 1977). For negative 500 hPa geopotential heights to evolve over the continent, cooling and shrinkage of the atmospheric column would have to occur below the 500 hPa level. Troup (1974) demonstrated that the atmosphere over Australia in winter is characterised by outflow from the continent across the coastline to the ocean in the lowest levels up to at least the 3000 m (approximately 700 hPa) level. This low level outflow has to be balanced by a corresponding inflow at higher levels in order to maintain surface pressure values. In the absence of significant cooling of the surface this is most likely to be achieved by convergence across the coast of the continent towards the interior in the middle and upper levels of the troposphere.

6.6 Conclusion

The SST anomaly field for June 1989 developed from the Reynold's (1988) blended data set was used to force the MU GCM in a perpetual July model run. Averages of the differences between 500 hPa geopotential height in the model run forced by the SST anomaly and a control resulted in anomaly patterns in the Australasian region with marked similarities to the observed anomaly pattern during an extended blocking event in the winter of 1989.

Removal of the tropical portion of the SST anomaly resulted in a reduction in the amplitude of 500 hPa anomalies but the pattern of anomalies was preserved in the Australian region. However, a significant difference between the responses of the model was observed in the vicinity of South America indicating that tropical influences were critical in this region. A negative anomaly of geopotential height developed over Australia in both model runs. This anomaly was similar in magnitude to the anomaly in the observed geopotential field.

Daily 500 hPa fields demonstrated that individual instances of split flow or blocking occurred in the model runs .

Chapter 7

Conclusions

The prediction of the onset, maintenance and decay of blocking patterns, with their attendant anticyclones at abnormally high latitudes and cyclonic components at low latitudes, continues to be one of the most difficult problems for synoptic meteorology. This is despite the apparent steady improvement in the performance of numerical models. Difficulties in predicting blocking behaviour are experienced in both hemispheres, but the data-sparse Southern Hemisphere poses the biggest problem. Equally, if blocking remains an important question for day to day forecasting the difficulty of predicting interannual variability of blocking activity in a region presents a significant challenge for climatologists.

This study has employed traditional climatological and diagnostic techniques to examine a prolonged period of above-average blocking activity in the Australasian region in the winter and early spring of 1989. Several indicators have been employed to test the intensity, longevity and spatial extent of the blocks during this period and the events have been examined relative to blocking criteria which have been developed for the Southern Hemisphere. By these benchmarks the blocking events which occurred during this period qualify as good examples of the phenomenon in the Southern Hemisphere.

This analysis supports previous studies which indicate that wave number 3 is favoured in winter blocking situations in the region. It is noteworthy in this case that mean 500 hPa geopotential heights in the peak ridge in the Tasman Sea at 55 °S for the period, June, July, August and September, 1989, were a 20 year maximum. However, anomalies of geopotential height at 500 hPa and 300 hPa for the three months of the 1989 winter (June, July and August) were larger over the Antarctic Peninsula and Weddell Sea than for the region studied while positive MSLP anomalies southeast of South America and especially over the Weddell Sea region were only slightly below those in the southwest Pacific. This effectively includes one half of the hemisphere in the anomaly patterns during the period and demonstrates that double blocking patterns can be persistent. The hypothesis that blocking is a 'local' phenomenon in the Southern Hemisphere, even in the strict sense in which that term has been applied, may require further evaluation.

The implication of a broader mechanism operating in this situation, possibly extending over the Pacific Basin and environs, is further suggested by the persistence of the split jet stream structure over the South Pacific and Australia throughout the period May to September 1989 (see Section 4. 2). The phase and intensity of the Southern Oscillation has been shown to be correlated with circulation characteristics in the Australian region and in the vicinity of the Tasman Sea and New Zealand. The blocking episode discussed in Chapter 4 occurred as the La Niña episode of 1988-89 was drawing to an end. A possible mechanism suggested in this study to link this

phase of ENSO with blocking is associated with the increased cloudiness and rainfall over northern and central Australia during the late summer and autumn months preceding the winter of 1989. It has been demonstrated that temperatures over northern and central Australia remained below average during the autumn and winter of 1989 resulting in a cooling of the atmospheric column and the development of negative anomalies of 500 hPa geopotential height. This temperature anomaly pattern may have been a major contributing factor to the onset, intensity and persistence of the split jet stream structure in the Australasian region during the winter of 1989. The evidence presented in this study supports the hypothesis that the jet stream can split prior to the blocking episode being observed rather than occurring with, or as a consequence of a block forming.

The configuration of SST anomalies in the autumn and early winter of 1989 is advanced as a significant precursor to the subsequent blocking event. In particular, the juxtaposition of the warm anomaly in the East Australian Current and around northern and northwestern Australia and the cold anomaly over continental Australia contributed to the stronger than normal 500 hPa westerly and northerly wind components in the vicinity of the east coast, via the thermal wind. This configuration resulted in a pattern of negative relative vorticity generation over eastern Australia, north of 35°S. At high latitudes, the enhanced Antarctic polar vortex reported in 1989 is presented as contributing to increased north-south atmospheric temperature gradients. Intensification of the Polar Front Jet stream was ensured by the persistence of negative geopotential height anomalies over Marie Byrd Land in Antarctica and the eastern Pacific sector.

In Chapter 5 the main features of the SST configuration in the Australasian region have been shown to be closely linked to the constraints imposed by the bottom topography of the Southern Ocean and the location of the continents. The strongest meridional temperature gradients are to be found to the south and southeast of Africa where the Agulhas Retroflection interacts with a low latitude arm of the ACC. Other regions where the isotherms converge are found to the south of Western Australia and at high latitudes in the Antarctic Convergence Zone, particularly to the south of the Campbell Plateau.

Previous studies have sought to establish relationships between the region of maximum blocking frequency in the Southern Hemisphere and the observed west to east gradient of sea surface temperature (SST) from the cold waters of the Indian Ocean sector of the Southern Ocean to the relatively warm surface waters located to the southeast of Australia. In this study, investigation of the distribution, intensity and seasonal cycles of SST gradients over the Southern Ocean suggests that the contribution of the west to east gradient in forcing the atmosphere is considerably less than the effect of the meridional gradients. From the correlation between 1000-500 hPa thickness and SST over the Southern Ocean presented in Section 5.6 it is reasonable to assume that a significant depth of the atmosphere is affected by the temperature of the underlying ocean surface. Application of the thermal wind principle to obtain wind maxima in the upper air suggests that

the vorticity generated in the middle troposphere from the zonal gradient is about an order of magnitude less than the effect of SST gradients in the meridional plane.

North-south gradients undergo marked changes during winter in response to the interaction of several major influences in the Australian region. These include the significant cooling of the continents of Australia and Antarctica and the configuration of the Antarctic Circumpolar Current (ACC). South of the Tasman Sea and New Zealand the ACC is forced to high latitudes (60 to 65°S) as it is diverted southeastwards by the Macquarie Rise and Campbell Plateau. Although SST gradients are gradually dissipated in the atmosphere with height, in regions where the ACC travels closer to the coast of East Antarctica low level atmospheric temperature gradients induced by the ACC are supported at higher levels by the strong temperature gradients generated by the elevated contours of the Antarctic continent. This gives rise to an enhanced westerly thermal wind at high latitudes (south of 50°S) which leads to a westerly wind maximum aloft. At the same time, the steady cooling of inland Australia acts to weaken the north to south temperature gradient between 30°S and 45°S leading to a minimum in the westerly winds in this latitude band. Further to the north strong gradients develop between tropical northern Australia and central and southeastern Australia giving rise to an intense westerly thermal wind north of 30°S. Such a configuration of mean winds in the middle troposphere can be shown to generate a pattern of relative vorticity which displays significant positive values [about 0.14 planetary vorticity (f)] in the south and negative values [about 0.16 of the local planetary vorticity (f)] n the north. These mean values of relative vorticity suggest that blocking may be the more normal state for the Australasian region in winter than previously thought.

Further to the east a region of slack north to south temperature gradients remains anchored near the Date Line at latitudes between 30°S and 45°S throughout the year. This region has long been recognised as the area in which the highest frequency of blocking is observed in the Southern Hemisphere. It appears likely that a predisposition to blocking persists in this area in all seasons but enhancement takes place in winter as the temperature gradient intensifies near Antarctica and over northern Australia following the cooling of the continents.

The SST anomaly field for June 1989 was used to force the MU GCM in a perpetual July model run. Averages of the differences between 500 hPa geopotential height in the model run forced by the SST anomaly and a control resulted in anomaly patterns with marked similarities to the anomaly pattern obtained in the climatology of an extended blocking event in the winter of 1989. Removal of the tropical portion of the SST anomaly in the numerical experiment No. 2 (Section 6.4) altered the 500 hPa ridge to the southeast of South America and replaced it with a negative anomaly over that region. A positive geopotential appeared in the southeast Pacific but the pattern of anomalies was preserved in the Australian region. Of particular interest was the development of a negative anomaly of geopotential height

over Australia in both model runs. This anomaly was similar in magnitude to the negative anomaly in the observed geopotential field.

Isolation of daily 500 hPa geopotential fields demonstrated that individual instances of split flow or blocking developed in the model runs and persisted for several days. Hence anomaly patterns in the model runs appear to have formed as a result of realistic synoptic-scale systems developing in the numerical simulations.

The analysis carried out in this study suggests that the onset of a typical winter blocking event in the Australian region may take the following form. An instability develops in the pronounced baroclinic zone in the eastern Indian Ocean sector (see e.g. Fig. 5.7 (c)) and as the wave approaches Western Australia it amplifies as in the situation of 13, 14, 15 and 16 July 1989 (see MSLP analyses at Appendix A). Cold air is advected northeastwards over eastern Australia and warm subtropical air southeastwards over the Southern Ocean. The jet stream structure, already partially split by the seasonal cooling of central and eastern Australia steers the northern portion of the developing front northeastwards carrying a deep layer of cold air into relatively low latitudes. The resulting thermal trough over eastern Australia accelerates the local jet stream and enhances the curvature of the air flow in the upper atmosphere producing mass divergence which eventually induces the formation of a depression over the western Tasman Sea. Over the land the cold air assists in the maintenance of the surface high pressure ridge which is evident over eastern Australia during winter. The southern portion of the cold front tracks southeastwards following the climatological path of the winter depressions and strengthening the Polar Front Jet to the southeast of Australia, thereby injecting anticyclonic vorticity into the middle and upper levels of the troposphere over the southern Tasman Sea. The advection of a layer of cold air over eastern Australia strengthens the temperature gradients between the continent and surrounding ocean. Surface temperatures in the Australian region then acquire a quadrupole pattern with cold poles over and to the southwest of the Australian continent and relatively warm poles to the southeast and northwest of the continent.

The surface temperature distribution discussed above has been shown to be conducive to the maintenance of the split jet stream and blocking activity. Replenishment of the cold air reservoir over eastern Australia occurs as upstream fronts approach the block and are themselves sheared into a northern and southern section. Thus the blocking pattern is maintained by the replacement process as synoptic disturbances move into the region from the west.

It would seem reasonable to assume that the dissipation of the blocking pattern would be achieved by processes acting to break down the temperature distribution which has been established by seasonal factors, advection and interannual cycles. There is very little discussion of this phase of the blocking cycle in the literature. However, it has been established that the heating of the Australian continent in the early spring is accompanied by

a rapid increase in the ZI and a sharp decrease in the frequency of blocking activity in the Tasman Sea sector. The evidence presented in this study further suggests that the temperature contrast between the land and ocean can vary significantly from year to year. Perhaps the weakening of the land-sea thermal gradient by advection of warm air on the western flank and cold air to the east of anticyclones is an important component of the dissipation phase during winter as well. Other possibilities include the modification of the East Australia Current by changes to the curl of the wind stress generated in the northern Tasman Sea by the cyclonic portion of the block and changes to the wind driven oceanic circulation of the south Tasman Sea during prolonged periods of blocking.

Interannual variability can be introduced into this system by the phase of the ENSO cycle and the intensity of the circumpolar vortex, which itself may be a manifestation of a teleconnection with the Southern Oscillation. Mechanisms by which the phase of the Southern Oscillation could increase blocking activity in the Australian region appear to be particularly related to processes associated with and following periods of anti-ENSO or La Niña. It is generally agreed that strengthening of the trade winds during La Niña results in an amplification of the subtropical gyre in the Pacific Ocean which implies a strengthening of the western boundary current, the East Australia Current, conveying warm water from the 'Pacific Warm Pool' further south than normal. As well, an enhancement of the Indonesian Throughflow could be expected to occur with advection of warmer water to the northwest coast of Australia. The land-sea temperature contrast in the following autumn and winter would be amplified by elevated levels of soil moisture and cloudiness leading to lower than normal continental temperatures. By this reasoning, a lower than normal frequency of blocking could be expected once an ENSO phase was established. This hypothesis would not preclude blocking events early in an ENSO event, such as occurred in June 1982.

The problem of winter blocking in the Australasian region has been tackled from several angles in this investigation but many questions remain unanswered and further studies are required to make progress in these areas. In the first instance, it is important to undertake further case studies of blocking events in the Australian region and southwest Pacific. There is a need to compare and contrast the precursors to the events, the circulation anomalies accompanying blocking events in the region as well as the subsequent dissipation of the blocks. An important component of these studies should be an analysis of the extent to which the blocking occurrences have contributed to significant precipitation anomalies, particularly droughts, in the region.]

There is also a need to investigate the correlation between time series of blocking, most probably using a blocking index, and the phase of the Southern Oscillation as represented by the SOI to determine whether a long-term correlation can be established. A correlation of this nature would provide a crude means of predicting the liklihood of interannual variability in the frequency of blocking activity in the region in a manner similar to the

seasonal outlooks for precipitation currently issued by the Bureau of Meteorology.

Clearly, one of the most promising avenues of research is to be found in the numerical simulation of blocking events with various forcings. The availability of high quality data sets of SST and the promise of improved data coverage in the southern Pacific Ocean offer the possibility of realistic verification of model output. GCM's have already made substantial contributions to the study of the blocking phenomenon and as forecasting models become increasingly reliable the isolation of the critical factors involved in the development, persistence and eventual break-down of atmospheric blocking patterns could soon be realised.

Appendix A

Daily Weather Maps

at 0000 UTC

June, July, August and September 1989

References

Allan, R. J. 1988. El Niño Southern Oscillation influences in the Australasian region. *Progress in Physical Geography* , **12:** 313-348.

Allison, I., 1989. Antarctic Sea Ice in the Weather and Climate System. ASAC Conference and Workshop on Antarctic Weather and Climate, Adelaide, July,1989. *Extended Extracts* : 75-85.

Allison, I., R. E. Brandt and S. G. Warren, 1993. East Antarctic Sea Ice: Albedo, Thickness Distribution and Snow Cover. *JGR* , **98,** No. C7, 12,417-12,429.

Anderson, D. L. T. and P. F. Noar, 1974. The synoptic verisimilitude of a mid-latitude cyclone generated in a Southern Hemisphere General Circulation Model. *Monthly Weather Review,* **102,** 613-629.

Astapenko, P.D., 1964. Atmospheric Processes in the High Latitudes of the Southern Hemisphere. *Israel Program for Scientific Translations, 1964.* Oldbourne Press, 286pp.

Austin, J. F., 1980. The blocking of middle latitude westerly winds by planetary waves. *Q. J. R. Meteor. Soc.,* **106,** 327-350.

Baines, P. G., 1983. A survey of blocking mechanisms, with application to the Australian region.*Aust. Met. Mag..,* **31,** 27-36.

Baines, P. G., 1990. What's interesting and different about Australian meteorology? *Aust. Met. Mag..,* **38,** 123-141.

Bell, I. D., J. Wilson and N. Weston,1988. Satellite Cloud Imagery Interpretation Guide (Draft). Bureau of Meteorology Training School.

Bengtsson, L. O., 1992. Climate system modeling prospects. Ch. 23 in*Climate System Modeling* (ed. K. Trenberth), 705-724.

Bottomley, M., C.K. Folland, J Hsiung, R.E Newell and D.E. Parker, 1990. Global Ocean Surface Temperature Atlas. UKMO and MIT Department of Earth, Atmospheric & Planetary Sciences, 20 pp, 313 plates.

Bronowski, J., 1973. *The Ascent of Man.* British Broadcasting Corporation, 448 pp.

Budd, W. F., 1982. The role of Antarctica in southern hemisphere weather and climate. *Aust. Met. Mag.,* **30,** 265-272.

Budd, W. F., 1986. The Southern Hemisphere circulation of atmosphere, ocean and sea ice. *Second International Conference on Southern Hemisphere Meteorology* (Preprint Volume) American Meteorological Society, Boston, Mass.

Bureau of Meteorology, 1988. *Climatic Averages Australia.* AGPS 532 pp.

Bureau of Meteorology, National Climate Centre 1989a. *Climate Monitoring Bulletin ,*June 1989

Bureau of Meteorology, National Climate Centre 1989b. *Climate Monitoring Bulletin ,* July 1989

Bureau of Meteorology, National Climate Centre 1989c. *Climate Monitoring Bulletin ,* August 1989

Bureau of Meteorology, National Climate Centre 1989d. *Climate Monitoring Bulletin ,* September 1989

Bureau of Meteorology, Tasmania 1989a. *Monthly Climate Summary,* June1989

Bureau of Meteorology, Tasmania 1989b. *Monthly Climate Summary,*July 1989

Bureau of Meteorology, Tasmania 1989c. *Monthly Climate Summary,* August 1989

Bureau of Meteorology, Tasmania 1989d. *Monthly Climate Summary,* September 1989

Butler, E. C. V., J A Butt, E J Lindstrom, P C Tildesley, S Pickmere and W F Vincent, 1992. Oceanography of the Subtropical Convergence Zone around southern New Zealand. *New Zealand Journal of Marine and Freshwater Research,* **26,** 131-154.

Cane, M.A., 1992. Tropical Pacific ENSO models: ENSO as a mode of the coupled system. Ch. 18 in*Climate System Modeling* (ed. K. Trenberth), 583-614.

Carleton, A. M., 1989. Antarctic sea-ice relationships with indices of the atmospheric circulation of the Southern Hemisphere. *Clim. Dynam..,* **3,** 207-220.

Charney, J. G. and J. G. DeVore, 1979. Multiple flow equilibria in the atmosphere and blocking. *J. Atmos. Sci.,* **36,** 1205-1216.

Charney, J. G. J. Shukla and K. C. Mo, 1981. Comparison of a barotropic blocking theory with observation. *J. Atmos. Sci.,* **38,** 762-779.

Carleton, A. M., 1992. Synoptic interactions between Antarctica and lower latitudes.*Aust. Met. Mag..*, **40**, 129-147.

Coughlan, M. J. 1983. A comparative climatology of blocking action in the two hemispheres. *Aust. Met. Mag..*, **31**, 3-13.

Drosdowsky, W. 1988. Lag Relations Between the Southern Oscillation And The Troposphere Over Australia. BMRC Research Report No. 13. Bureau of Meteorology, 201pp.

Drosdowsky, W., 1993. Potential predictability of winter rainfall over southern and eastern Australia using Indian Ocean sea-surface temperature anomalies *Aust. Met. Mag..*, **42**,, 1-6

Egger, J., 1978. Dynamics of blocking highs. *J. Atmos. Sci.*, **35**, 1788-1801.

Enfield, D. B., 1989. El Niño, past and present. *Rev. Geophys.*, **27**, 159-187.

Frederiksen, J. S., 1983. The onset of blocking and cyclogenesis: linear theory. *Aust. Met. Mag..*, **31**, 15-26.

Frederiksen, J. S., 1989. The role of instability during the onset of blocking and cyclogenesis in Northern Hemisphere synoptic flows. *J. Atmos. Sci.*, **46** 1076-1092.

Gaffney, D. 1990a. Seasonal Climate Summary Southern Hemisphere (autumn 1989): a second peak in the Southern Oscillation Index. *Aust. Met. Mag.*, **38**: 73-79.

Gaffney, D. 1990b. Seasonal Climate Summary Southern Hemisphere (winter 1989): the Southern Oscillation Index falls to near average. *Aust. Met. Mag.*, **38**: 81-86.

Gentilli, J., 1971. Dynamics of the Australian Troposphere. Ch. 5 in *Climates of Australia and New Zealand* (Editor -in-Chief, H. E. Landsberg).*World Survey of Climatology* **13**, Elsevier, Amsterdam, p. 53-117.

Gibson, T. T., 1989. A Climatology of Midtropospheric Wind Maxima over the Coast of East Antarctica. ASAC Conference and Workshop on Antarctic Weather and Climate, Adelaide, July,1989. Extended Extracts : 48-51.

Gibson, T. T., 1992. An Observed Poleward Shift of the Southern Hemisphere Subtropical Wind Maximum - A greenhouse Symptom? *Int. J. Climatol.*, **12**, 637-640

Gibson, T. T., 1993. The Use of Large-Scale Circulation Indices in Monitoring Climatic Trends. Preprint Volume of Fourth International Conference on Southern Hemisphere Meteorology and Oceanography, Hobart. 195-196.

Gibson, T. T., 1993, personal communication.

Gibson, T. T., 1994, personal communication.

Gill, A. E., 1982. *Atmosphere - Ocean Dynamics.* Academic Press, London. 662pp. [Vol. **30**, International Geophysics Series (ed. W. L. Donn)]

Gloersen, P., W J Campbell, D J Cavalieri, J C Comiso, C L Parkinson and H J Zwally, 1992. *Arctic and Antarctic Sea Ice, 1978-1987: Satellite Passive-Microwave Observations and Analysis*: NASA SP-511, National Aeronautics and Space Administration, Washington, D.C., 290pp.

Gordon, A. L., 1967. Structure of Antarctic waters between 20°W and 170°W. *Antarctic Map folio Series.* Folio 6, American Geographical Society, New York, N. Y.

Gordon, A. L., E. Molinelli and T. Baker 1978 Large-scale relative dynamic topography of the Southern Ocean. *JGR* , **86,** 3023-3032.

Gordon, A. L., E. Molinelli and T. Baker 1982 *Southern Ocean Atlas.* Columbia University Press, New York, 34 pp. and 248 plates.

Green, J. S. A. 1977. The weather during July 1976: some dynamical considerations of the drought. *Weather,* **32,** 120-6.

Graham, N. E. and White, W. B., 1988. The El Niño Cycle: A Natural Oscillator of the Pacific Ocean-Atmosphere System. *Science,* **240,** 1293-1302.

Grant, A. M., 1952. A re-examination of the zonal wind-profile under conditions of constant vorticity. *J. Meteorol.,* **9,** 439-441.

Guymer, L. B., 1978. Operational application of satellite imagery to synoptic analysis in the Southern Hemisphere. Bureau of Meteorology,Technical Report, **29** : 87pp.

Heath, R. A., 1981. Oceanic fronts around southern New Zealand. *Deep Sea Research,* **28,** 547-560.

Heath, R. A., 1985. A review of the physical oceanography of the seas around New Zealand - 1982. *New Zealand Journal of Marine and Freshwater Research,* **19,** 79-124.

Hellerman, S. and M. Rosenstein, 1983. Normal monthly wind stress over the world ocean with error estimates. *J. Physical Oceanography* **13**, 1093-1104.

Hirst, A. C. and E. T. Linacre, 1981. Trends in the blocking of high-pressure systems in the Australian region. *Search* **12**, 409 - 11

Holbrook, N. J. and M. Tomczak, 1991. Anomalous temperature and salinity characteristics in the Western Tasman Sea during 1989 Tech. Report No. **23** Ocean Sciences Institute, University of Sydney 7 pp.

James, I. N., 1988. On the forcing of planetary-scale Rossby waves by Antarctica. *Q. J. R. Meteor. Soc.* **114,** 619-637.

Karelsky, S., 1954. Monthly and Seasonal Anticyclonicity and Cyclonicity in the Australian Region - 7 Years (1946-1952) Averages. Met. Study **3,** Bur. Met., Australia

Karelsky, S., 1956. Classification of the Surface Circulation in the Australasian Region. Met. Study **8,** Bur. Met., Australia

Karelsky, S., 1961. Monthly and Seasonal Anticyclonicity and Cyclonicity in the Australian Region - 15 Years (1946-1960) Averages. Met. Study **13,** Bur. Met., Australia

Karoly, D. J. 1983. Atmospheric teleconnections, forced planetary waves and blocking. *Aust. Met. Mag..,* **31,** 51-56.

Karoly, D. J. 1989. Southern hemisphere circulation features associated with El Niño-Southern Oscillation events. *Jnl Climate,* **2,** 1239-1252.

Knox, J. L. and J. E. Hay, 1985. Blocking signatures in the Northern Hemisphere: frequency distribution and interpretation. *Int. J. Climatol.,* **5,** 1-16.

Kung, E. C., C.C. Dacamara, W. E. Baker, J. Susskind and C. Park, 1990. Simulations of winter blocking episodes using observed sea surface temperatures. *Q. J. R. Meteor. Soc. ,* **116,** 1053-1070.

Lau, N.-C., 1992. Climate variability simulated in GCMs. Ch. 19 in*Climate System Modeling* (ed. K. Trenberth), 617-642.

Leighton, R. M. and R. Deslandes, 1991. Monthly anticyclonicity and cyclonicity in the Australasian region: averages for January, April, July and October. *Aust. Met. Mag..,* **39,** 149-154.

Leith, C. E., 1984. Global Climate Research. *The Global Climate* (ed. J.Houghton), Cambridge University Press. p.13-24.

Lejenäs, H., 1984. Characteristics of southern hemisphere blocking as determined from a time series of observational data. *Q. J. R. Meteor. Soc..*, **110**, 967-979.

Le Marshall, J. F., G. A. M. Kelly and D. J. Karoly, 1985. An atmospheric climatology of the southern hemisphere based on ten years of daily numerical analyses (1972-82), I, Overview. *Aust. Met. Mag.* **33**, 65-85.

Leslie, L. M., G. A. Mills, L. W. Logan, D. J. Gauntlett, G. A. Kelly, M. J. Manton, J. L. McGregor and J. M. Sardie, 1985. A high resolution primitive equations NWP model for operations and research. *Aust. Met. Mag..*, **33**, 11-35.

Levitus, S., 1982. *Climatological Atlas of the World Ocean.* NOAA professional paper 13. Rockville, Md., 173pp. and 17 microfiches.

Lindzen, R. S., 1986. Stationary planetary waves, blocking, and interannual variability. In *Anomalous atmospheric flows and blocking; Advances in Geophysics* **29** (Eds. R. Benzi, B Saltzman, A.C. Wiin-Nielsen) p 251 - 273.

Lough, J. M., 1992. Variations of sea-surface temperatures off North-Eastern Australia and associations with rainfall in Queensland: 1956-1987 *Int. J. Climatol.*, **12**, 765-782.

Lynch, A.H., 1993. The impact of sub-grid scale topographic parameterisations on a General Circulation Model. Unpublished PhD thesis, University of Melbourne.

Martin, D. W., 1968. Satellite studies of cyclonic developments over the Southern Ocean. *IAMRC Tech. Report* No. **9**. Bureau of Meteorology, 57 pp.

Mason, B. J., 1985. Progress in Cloud Physics and Dynamics. *Recent Advances in Metorology and Physical Oeanography.* The Royal Meteorological Society, p 1-14.

McAvaney, B. J., W. Bourke and K. Puri, 1978. A global spectral model for simulation of the general circulation. *J. Atmos. Sci.*, **35**, 1557-1583.

McBride, J. L. and N. Nicholls, 1983. Seasonal relationships between Australian rainfall and the Southern Oscillation. *Mon. Wea. Rev.*, **111**, 1998-2004.

Mills, G. A. and L. M. Leslie, 1985. The use of NWP model output in the prediction of significant weather events. *Aust. Met. Mag..*, **33**, 167-180.

Mo, K. C, J. Pfaendtner and E. Kalnay, 1987. A GCM study on the maintenance of the June 1982 blocking in the Southern Hemisphere. *J. Atmos. Sci.*, **44,** 1123-1142.

Namias, J., 1959. Recent Seasonal Interactions between North Pacific Waters and the Overlying Atmospheric Circulation *JGR* **64;** 631-646

Namias, J., 1963. Large-Scale Air-Sea Interactions over the North Pacific from Summer 1962 through the Subsequent Winter *Collected Works of J. Namias 1934 through 1974* (2 Vols.) Univ. of California, San Diego p. 441-456

Namias, J., 1965. Macroscopic Association between Mean Monthly Sea-Surface Temperature and the Overlying Winds *JGR* . **70;** 2307-2318

Namias, J., 1969. Seasonal interactions between the North Pacific Ocean and the atmosphere during the 1960's *Mon. Weather Rev.* **97**, 173-192.

Namias, J., 1970. Climatic anomaly over the United States during the 1960's *Science* **170,** 741-43

Namias, J., 1976. Negative ocean-air feedback systems over the North Pacific in the transition from warm to cold seasons *Mon. Weather Rev.* **104,** 1107-1121

Newell, R. E., and Zhong-Xiang Wu, 1992. The interrelationship between temperature changes in the free atmosphere and sea surface temperature changes. *JGR* **97**, No. D4: 3693-3709.

NMAC, 1989. Operations Bulletin No. 13 (15 September 1989), Bureau of Meteorology, Melbourne.

NOAA Climate Analysis Centre, 1989a. Climate Diagnostics Bulletin, June 1989

Noar, P. F., 1983. Numerical modelling of blocking, with reference to June 1982. *Aust. Met. Mag..*, **31,** 37-49.

Nowlin, W. D. Jr. and J. M. Klinck, 1986. The Physics of the Antarctic Circumpolar Current. *Reviews of Geophysics* **24**, 469-491.

Nunez, M., 1994. Personal communication.

Nydam, P. G. , Seasonal climate summary Southern Hemisphere (spring 1989): the 1988/89 positive phase of the Southern Oscillation draws to an end. *Aust. Met. Mag.* **38**, 293-298.

Olbers, D., V. Gorwetski, G. Seiß, and J. Schröter, 1992. *Hydrographic Atlas of the Southern Ocean*. Alfred Wegener Institute, Bremerhaven. 17pp. with 82 plates.

Pedder, M. A., 1981. Practical analysis of dynamical and kinematic structure: some applications and a case study. *Dynamical Meteorology - An Introductory Selection*. (Ed., B. W. Atkinson). Methuen & Co. Ltd. p 69-86.

Philander, S. G. 1990. *El Niño, La Niña and the Southern Oscillation*. Academic Press, San Diego. 293pp.

Physick, W. L., 1981. Winter Depression Tracks and Climatological Jet Streams in the Southern Hemisphere during the FGGE year. *Quart. J. R. Met. Soc.*, **107** (454): 883-898.

Pook, M. J., 1992. A note on the variability of the mid-tropospheric flow over the Southern Ocean in the Australian region. *Aust. Met. Mag.* **40,** 169-177.

Pook, M. J., 1993. Recent atmospheric blocking and SST gradients in the Southern Ocean, *Fourth International Conference on Southern Hemisphere Meteorology* (Preprint Volume) American Meteorological Society, Boston, Mass. 304-305.

Radok, U., 1971. The Australian region and the General Circulation of the Southern Hemisphere. Ch. 3 in *Climates of Australia and New Zealand* (Editor -in-Chief, H. E. Landsberg).*World Survey of Climatology* **13,** Elsevier, Amsterdam, p. 13-33.

Rex, D. F., 1950a. Blocking action in the middle troposphere and its effect upon regional climate, Part I: An aerological study of blocking action. *Tellus* **2,** 196-211.

Rex, D. F., 1950b. Blocking action in the middle troposphere and its effect upon regional climate, Part II: The climatology of blocking action. *Tellus* **2,** 275-301.

Reynolds, R. W. and L. Roberts, 1987. A global sea surface temperature climatology from in situ, satellite and ice data. *Tropical Ocean-Atmosphere Newsletter*, No. 37, 15-17, published by CIMAS, University of Miami.

Reynolds, R. W., 1988. A real-time Global Sea Surface Temperature Analysis. *Jnl Climate*, **1,** 75-86.

Rossby, C. G., 1947. On the distribution of angular velocity in gaseous envelopes under the influence of large-scale horizontal mixing processes. *Bulletin of the American Meteorological S,ociety*, **28,** No. 2, 53-68.

Russell, H. C., 1896. Moving anticyclones in the southern hemisphere. In *Three Essays on Australian Weather* [R. Abercromby (ed.)] Sydney.

Schwerdtfeger, W., 1970. The Climate of the Antarctic. In *World Survey of Climatology* (ed. S. Orvig) **14:** 253-331. Elsevier, Amsterdam.

Schwerdtfeger, W., 1984. Weather and Climate of the Antarctic. Elsevier 261 pp.

Shukla, J., 1986. SST anomalies and blocking. In *Anomalous atmospheric flows and blocking; Advances in Geophysics* **29** (Eds. R. Benzi, B Saltzman, A.C. Wiin-Nielsen) p 443 -452.

Simmonds, I., 1985. Analysis of the "Spinup" of a General Circulation Model. *J. Geophys. Res.,* **90** (D3), 5637-5660.

Simmonds, I., 1990. A modelling study of winter circulation and precipitation anomalies associated with Australian region ocean temperatures *Aust. Met. Mag.* **38,** 151-161.

Simmonds, I., and M. Dix, 1989. The use of mean atmospheric parameters in the claculation of modelled mean surface heat fluxes over the world's oceans. *J. Phys. Oceanogr.* **19,** 205-215.

Simmonds, I., and A. Rocha, 1991. The Association of Australian Winter Climate with Ocean Temperatures to the West. *Jnl Climate,* **4,** 1147-1161.

Simmons, A. J, 1986. Numerical prediction: some results from operational forecasting at ECMWF. *Advances in Geophysics* **29** (Ed.); 305-338.

Simpson, R. W. and W. K. Downey, 1975. The effect of a warm mid-latitude sea surface temperature anomaly on a numerical simulation of the general circulation of the southern hemisphere. *Quart. J. R. Met. Soc.* **101,** 847-867.

Slutz, R. J., S. J. Lubker, J. D. Hiscox, S. D. Woodruff, R. L. Jenne, D. J. Joseph, P.M. Steurer and J. D. Elms, 1985. COADS - *Comprehensive Ocean-Atmosphere Data Set* . Release 1, 262pp.

Smith, S. R. and C. R Stearns, 1993. Antarctic climate anomalies surrounding the minimum in the Southern Oscillation Index. In *Antarctic Meteorology and Climatology: Studies based on Automatic Weather Stations* (D. H. Bromwich and C. R. Stearns, eds.). Antarctic Research Series **61,** p149-174. American Geophysical Union, Washington D.C.

Streten, N. A, 1981. Southern Hemisphere sea surface temperature variability and apparent associations with Australian rainfall. *J. Geophys. Res.,* **86,** 485-497.

Streten, N. A, 1983. Extreme distributions of Australian annual rainfall in relation to sea surface temperature. *J. Climatol.*, **3**, 143-153.

Streten, N. A. and W. R. Kellas, 1973. Aspects of cloud pattern signatures of depressions in maturity and decay. *J. Applied Met.* **12**, 23-27.

Streten, N. A. and A. J. Troup, 1973. A synoptic climatology of satellite observed cloud vortices over the Southern Hemisphere. *Quart. J. R. Met. Soc.* **99**, 56-72.

Streten, N. A. and J. W. Zillman, 1984. Climate of the South Pacific Ocean. Ch. 3 in *World Survey of Climatology* (ed. Van Loon, H.) **15**: 263-429.

Taljaard, J. J., H. Van Loon, H. L. Crutcher and R. L. Jenne, 1969. Climate of the Upper Air: Southern Hemisphere, Vol. 1, Temperatures, Dew Points and Heights at Selected Pressure Levels. NAVAIR 50-IC-55, Chief Naval Operations, Washington, DC. 135pp.

Taljaard, J. J. 1972: Synoptic meteorology of the southern hemisphere. In Meteorology of the Southern Hemisphere. Met. Monogr., **13**, 139-213

Teweles, S and H. B. Wobus, 1954. Verification of prognostic charts. *Bulletin of the American Meteorological Society*, **35**, 455-463.

Treidl, R. A., E. C. Birch and P. Sajecki, 1981. Blocking action in the Northern Hemisphere: a climatological study. *Atmosphere-Ocean* **19**, 1-23.

Trenberth, K. E., 1979. Interannual Variability of the 500 mb Zonal Mean Flow in the Southern Hemisphere. *Mon. Wea. Rev.*, **107**: 1515-1524.

Trenberth, K. E. and K. C. Mo, 1985. Blocking in the Southern Hemisphere. *Mon. Weath. Rev.* **113**, 3 -21.

Trenberth, K. E. and J. G. Olson, 1988. An evaluation and intercomparison of global analyses from the National Meteorological Centre and the European Centre for Medium Range Weather Forecasts. *Bulletin of the American Meteorological Society*, **69**, No. 9, 1047-1057.

Trenberth, K. E. and G. S. Swanson, 1983. Blocking and persistent anomalies in the Southern Hemisphere.*First International Conference on Southern Hemisphere Meteorology* (Preprint Volume) American Meteorological Society, Boston, Mass. 73-76.

Trenberth, K. E., W. G. Large and J. G. Olson, 1990. The mean annual cycle in global ocean wind stress. *J. Phys. Oceanogr.* **20**,1742.

Troup, A. J., 1974. The mean flow at the boundary of the Australian continent. *Aust. Met. Mag.* **22**, 61-66.

Troup, A. J. and N. A. Streten, 1972. Satellite observed Southern Hemisphere cloud vortices in relation to conventional observations. *J. Applied Met.* **11,** 909-917.

Tyson, P. D., 1986. *Climatic change and variability in southern Africa.* Oxford University Press, Cape Town.

van Loon, H., 1956. Blocking action in the Southern Hemisphere. Part 1.*Notos* **5,** 171-5.

van Loon, H., 1967. The half-yearly oscillations in middle and high southern latitudes and the coreless winter. *J. Atmos . Sci.,* **24,** 472-486.

van Loon, H., 1972a: Temperature in the Southern Hemisphere. In Meteorology of the Southern Hemisphere. Met. Monogr., **13,** 25-58.

van Loon, H., 1972b: Wind in the Southern Hemisphere. In Meteorology of the Southern Hemisphere. Met. Monogr., **13,** 87-100

van Loon, H. and D. J. Shea, 1988. A Survey of the Atmospheric Elements at the Ocean's Surface South of 40°S. *Antarctic Ocean and Resources Variability* (ed. Sahrhage, D.) Springer-Verlag, Berlin, Heidelberg. p3-19.

van Loon, H., J. J. Taljaard, R. L.Jenne and H. L. Crutcher, 1971. Climate of the Upper Air: Southern Hemisphere, Vol. **2,** Zonal Geostrophic Winds. NAVAIR 50-IC-56, Chief Naval Operations, Washington, DC, 42pp.

Venter, R. J., 1957. Sources of Meteorological Data for the Antarctic. *Meteorology of the Antarctic* (ed. M.P. van Rooy), South African Weather Bureau, p.17-34.

Vincent, W F, C Howard-Williams, P Tildesley and E Butler, 1991. Distribution and biological properties of oceanic water masses around the South Island, New zealand. *New Zealand Journal of Marine and Freshwater Research,* **25,** 21-42.

Vowinckel, E., 1955. Southern Hemisphere weather map analysis: five year mean pressures. Part II. *Notos* **4,** 204-16.

Walker, G. T. and E.W. Bliss, 1932. World weather V. *Memoirs . R. Met. Soc.* **4,** 53-84.

Weldon, R., 1975. NWS Satellite Training Course Notes: **Part II** - The structure and evolution of winter storms. NOAA, 46 pp.

Wendler, G. and M. J. Pook, 1992. On the half-yearly pressure oscillation in eastern Antarctica. *Antarctic Journal of the US -1992 Review.* p. 284-285.

WMO, 1992. *The Global Climate System - Climate System Monitoring December 1988 - May 1991* (ed. D. Philips). 110 pp.

Woods, J. D.,1984. The upper ocean and air-sea interaction in global climate *The Global Climate* (ed. J.Houghton), Cambridge University Press. p.141-187

Worby, A. P. and I. Allison, 1991. Ocean-atmosphere energy exchange over thin, variable concentration Antarctic pack ice. *Ann. Glaciol.*, **15**, 184-190.

Wright, A. D. F. 1974: Blocking action in the Australian region. Tech. Rep. **10**, Bur. Met., Australia, 29pp.

Zillman, J. W., 1969. Interpretation of satellite data over the Southern Ocean using the technique of Martin (1968). *Proc. of the inter-regional seminar on interpretation of meteorological satellite data, Melbourne.* 43-47.

Zillman, J. W. and P. G. Price, 1972. On the thermal structure of mature Southern Ocean cyclones. *Aust. Met. Mag.* **20**, 34-48.

Zwally, H. J., J. C. Comiso, C. L. Parkinson, W. J. Campbell, F. D. Carsey and P. Gloersen, 1983. *Antarctic Sea Ice, 1973 -1976: Satellite Passive-Microwave Observations.* NASA SP-459, National Aeronautics and Space Administration, Washington, D.C., 206pp.

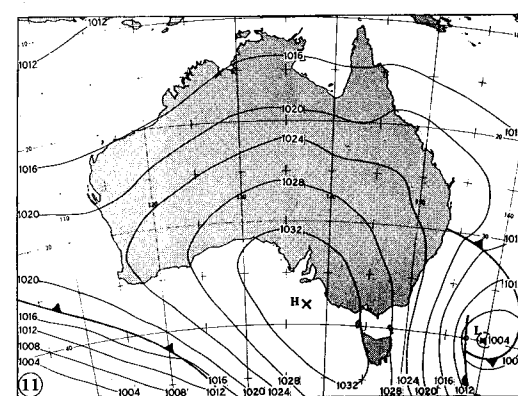# DAILY WEATHER MAPS

1000 K (00 GMT)

1 - 30 June 1989

Dates are ringed left-hand corner of each map.

LEGEND

Isobars are drawn at 4 hPa intervals
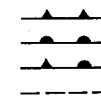
▲▲	Cold Front
●●	Warm Front
▲●▲	Occlusion
– – –	Trough
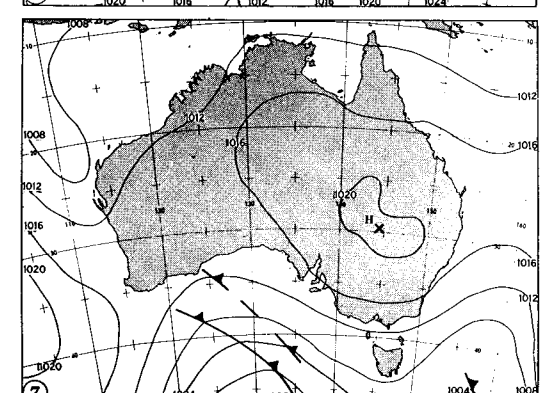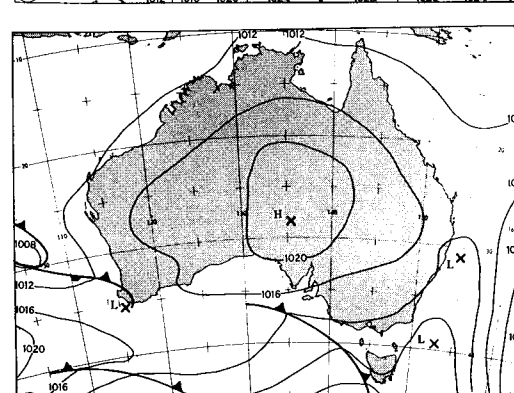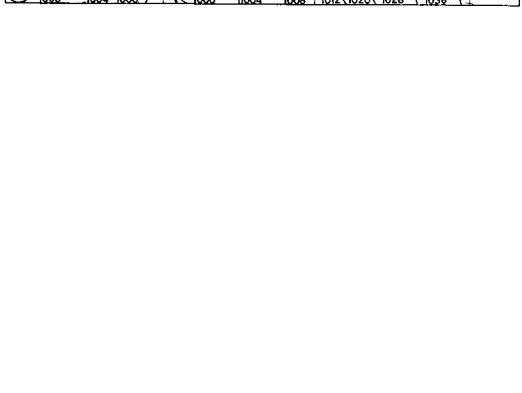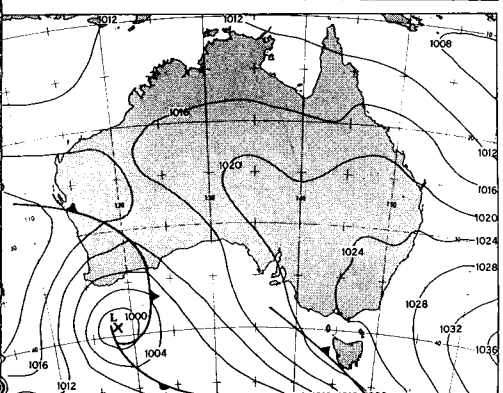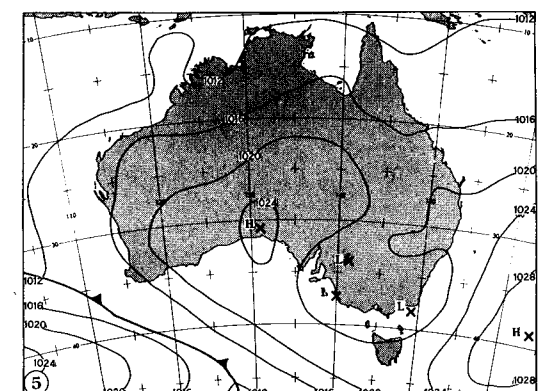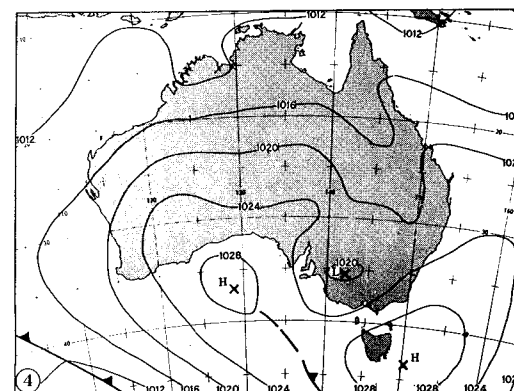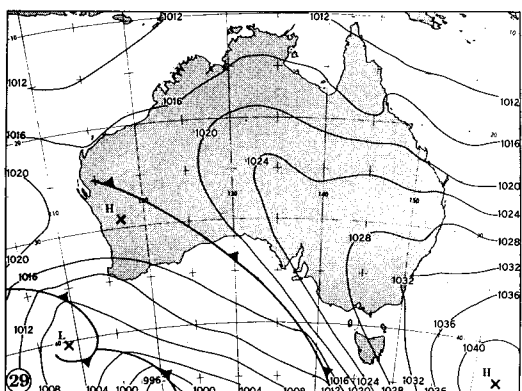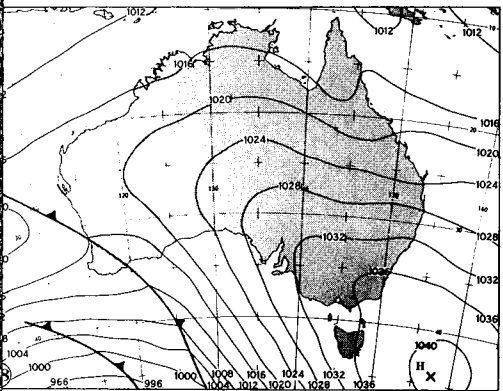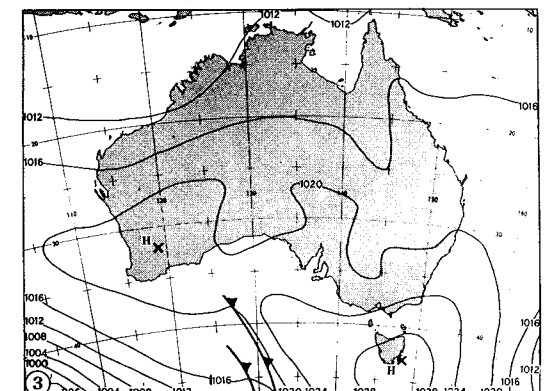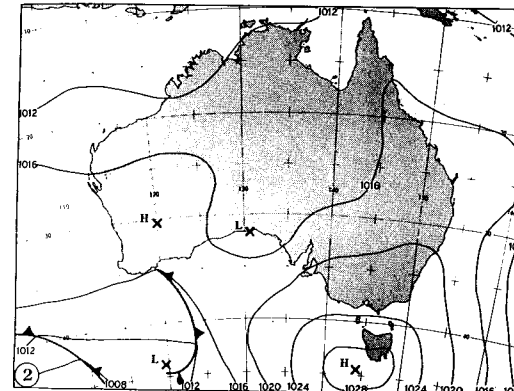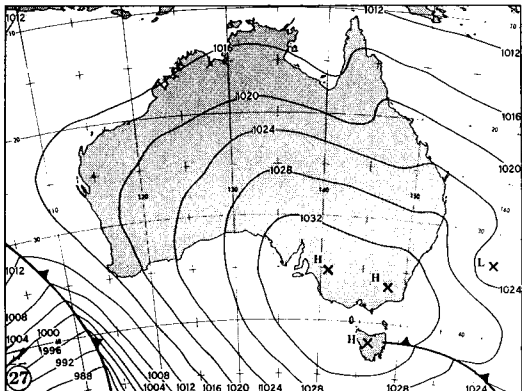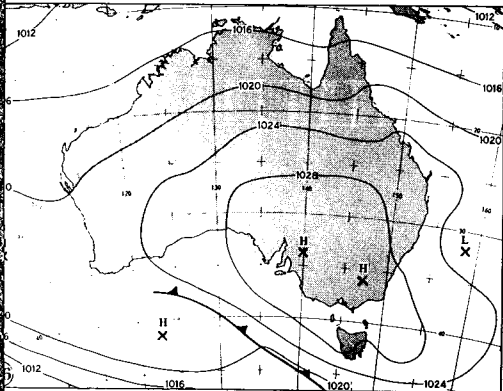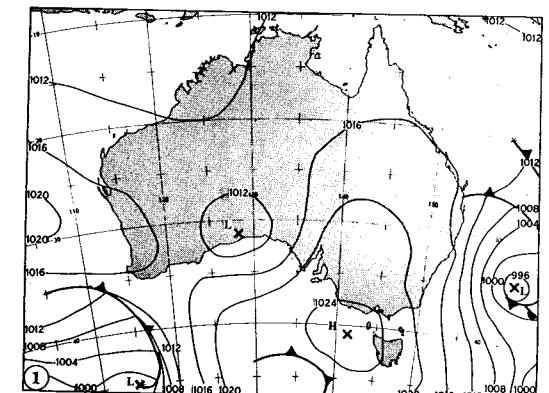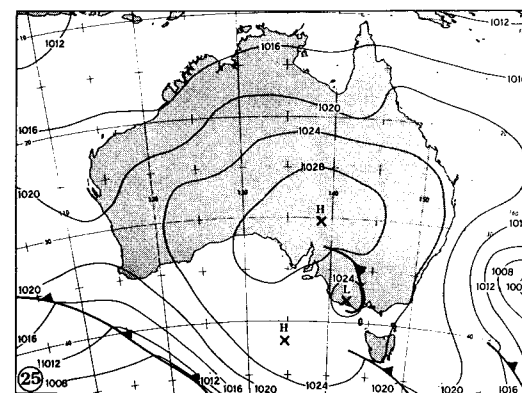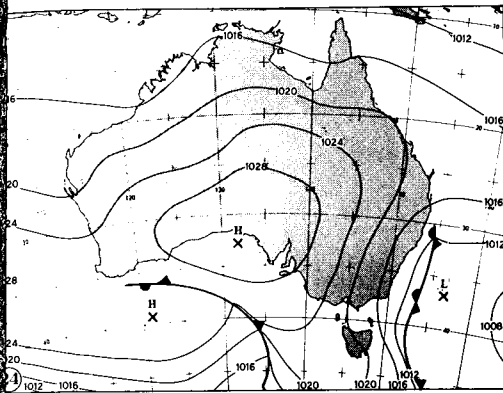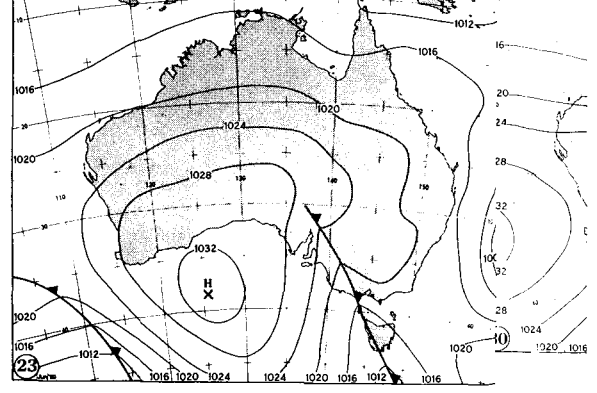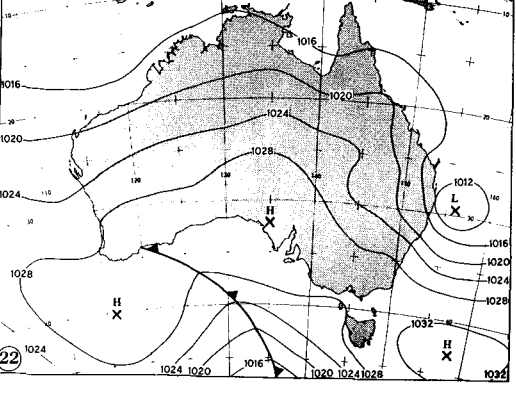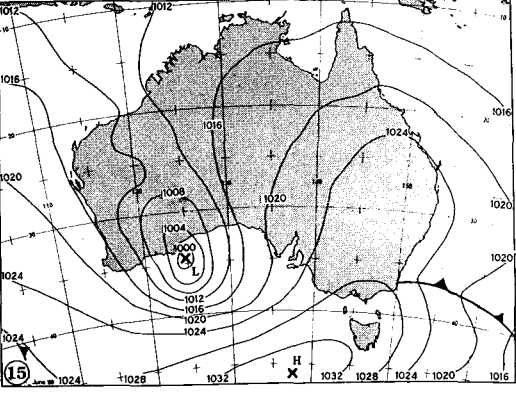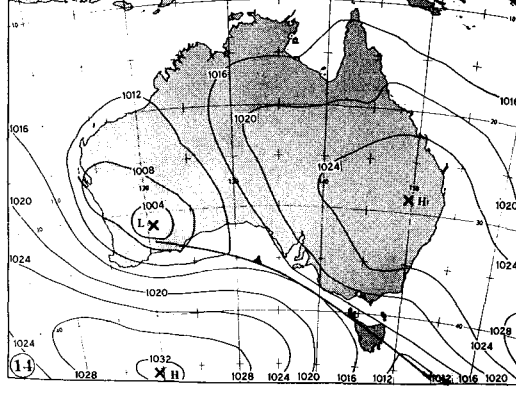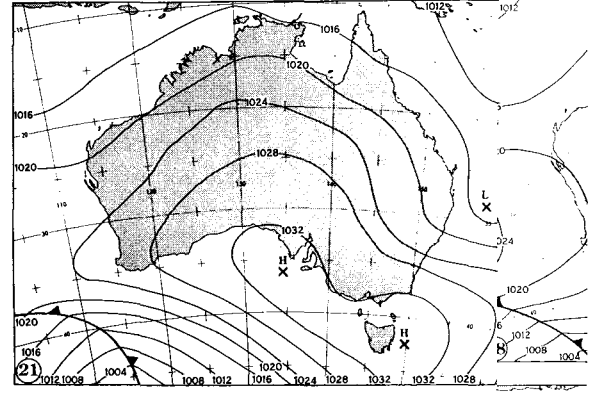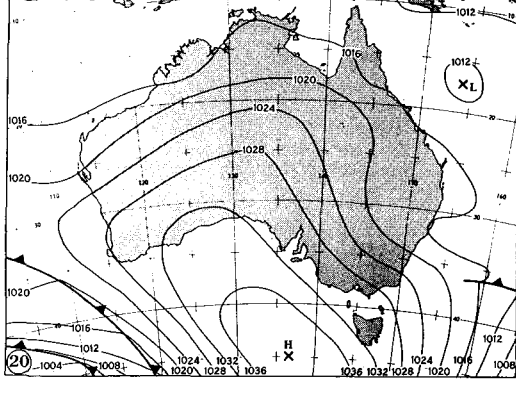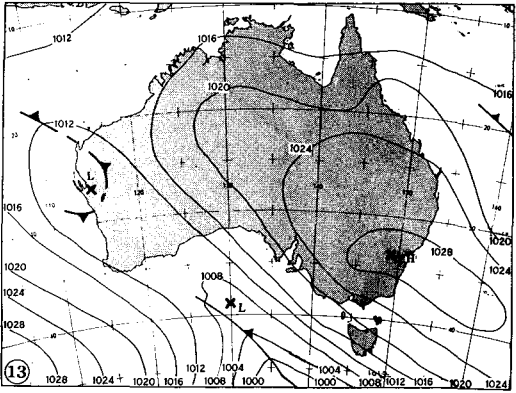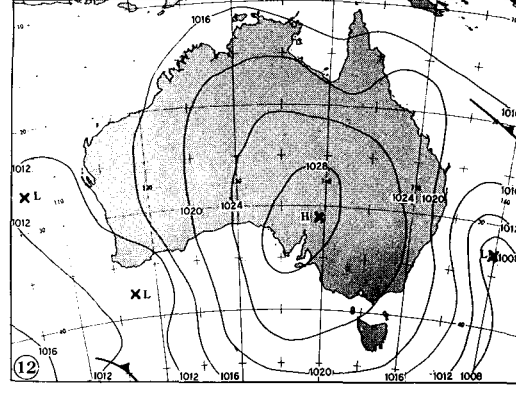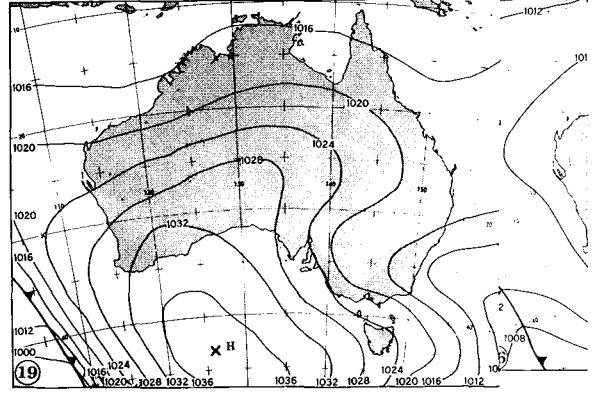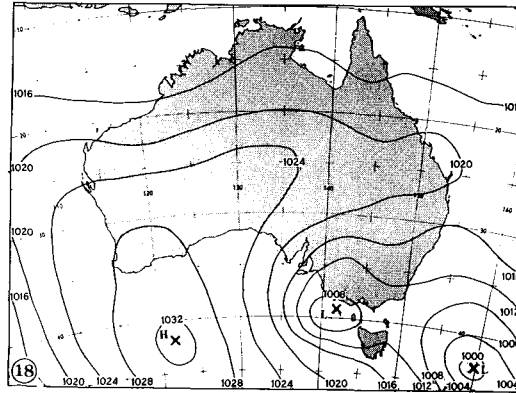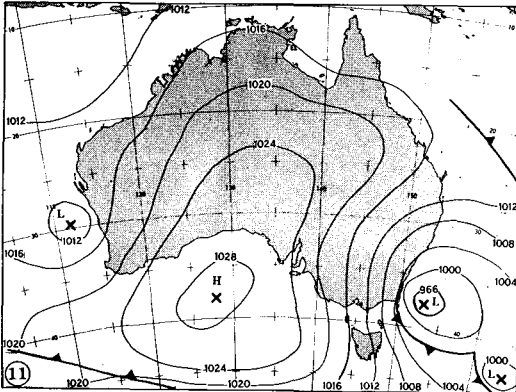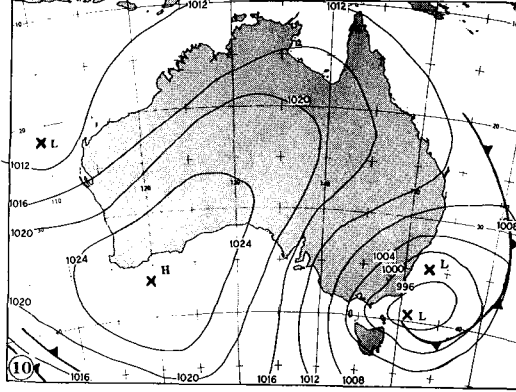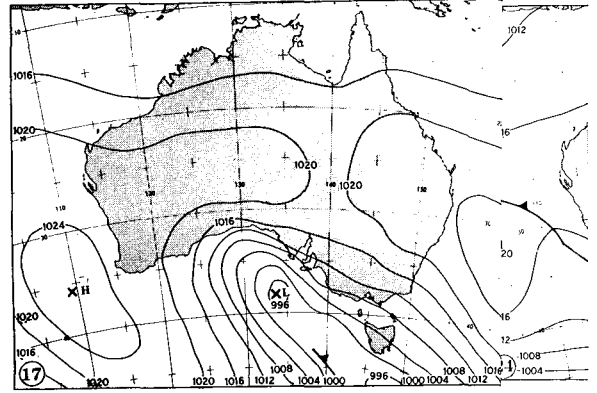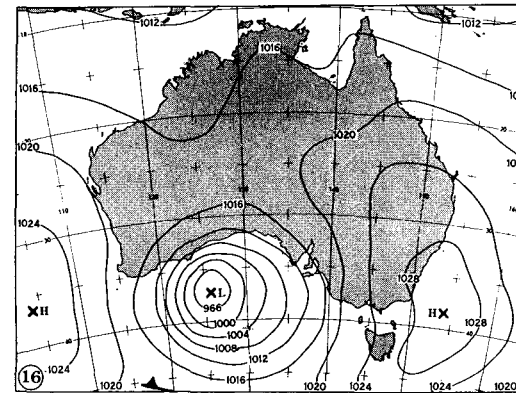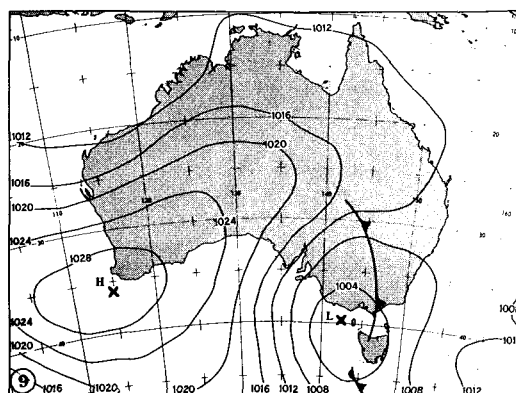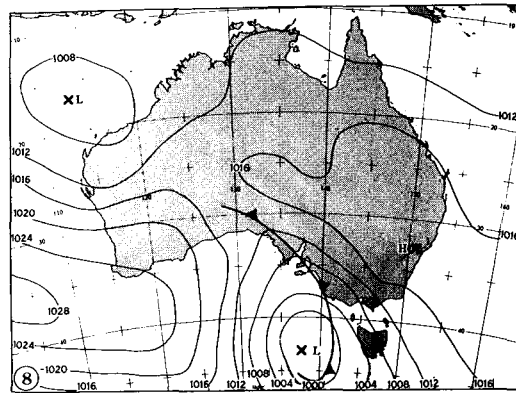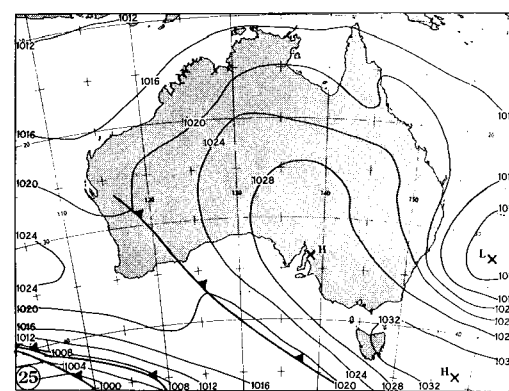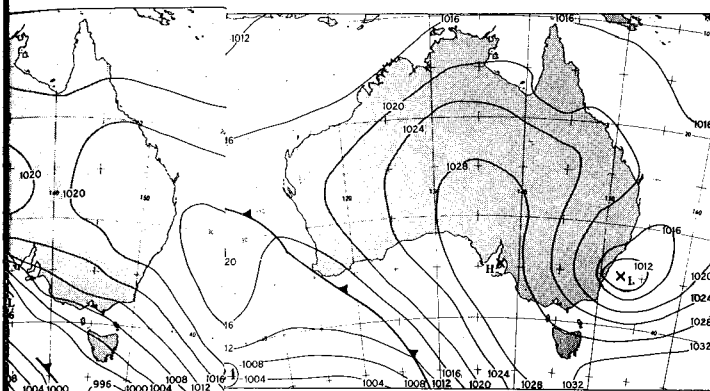
DAILY WEATHER MAPS

IOOO K (OO GMT)

1 - 31 July 1989.

Dates are ringed left-hand corner of each map.

LEGEND

Isobars are drawn at 4 hPa intervals

▲▲▲	Cold Front
●●●	Warm Front
▲●▲●	Occlusion
– – –	Trough
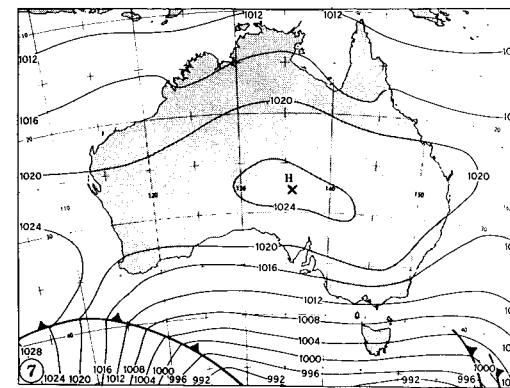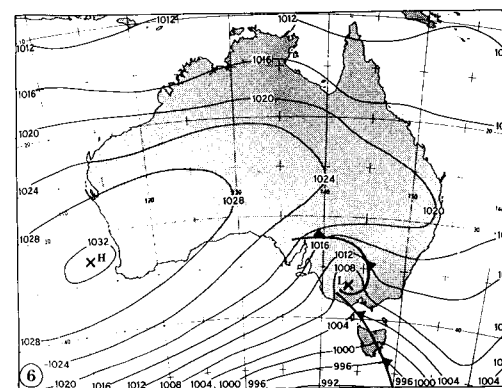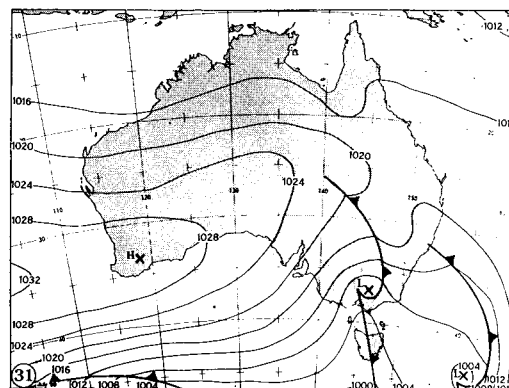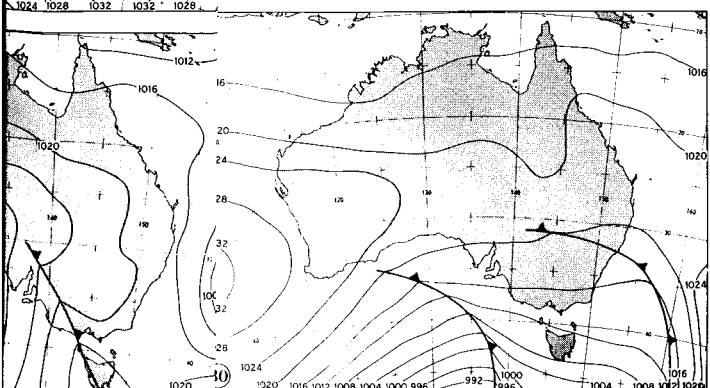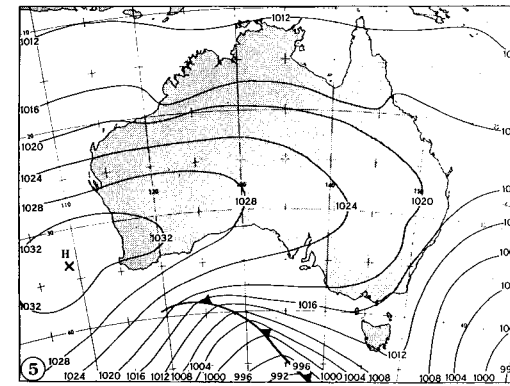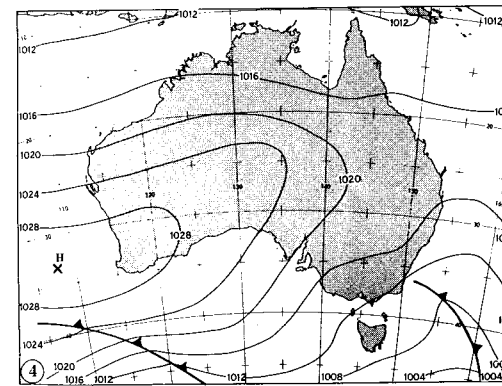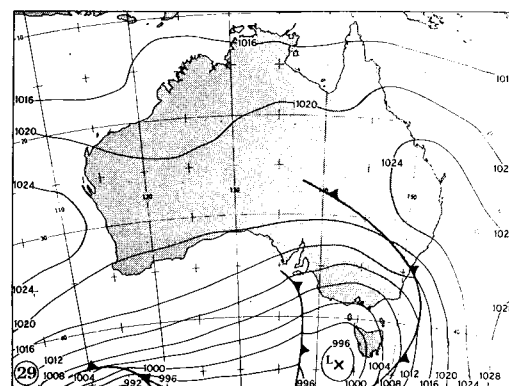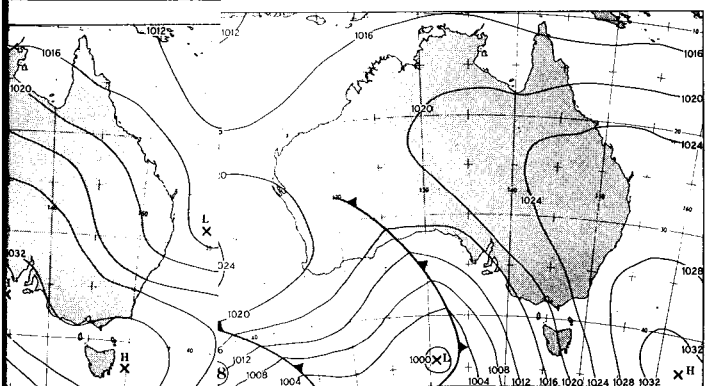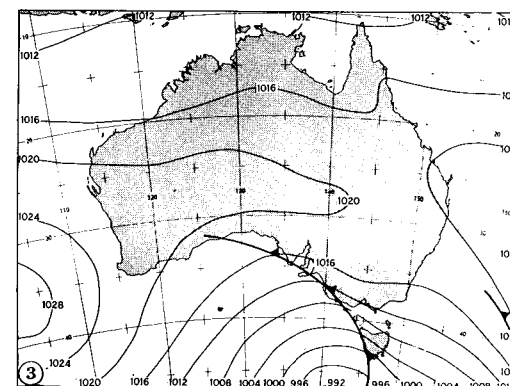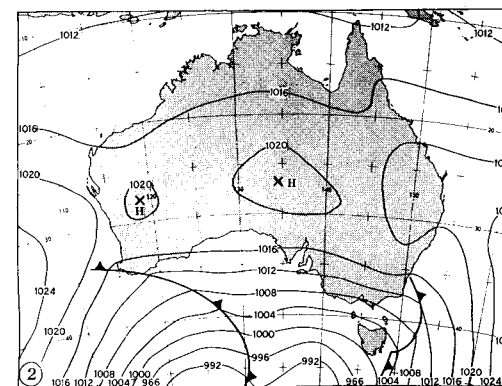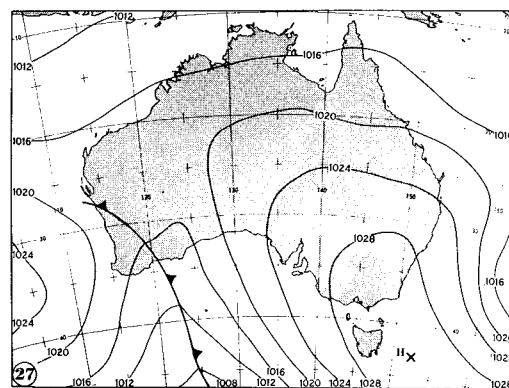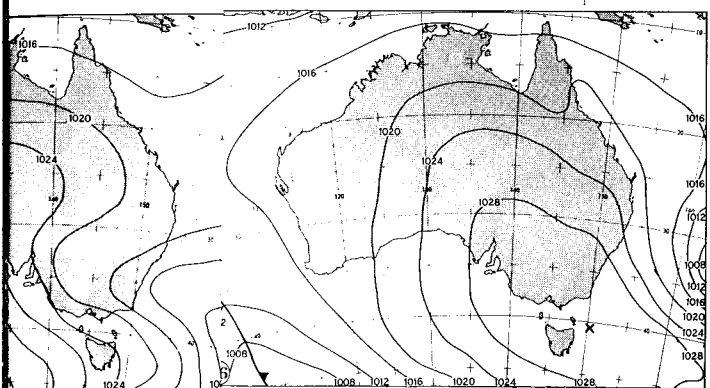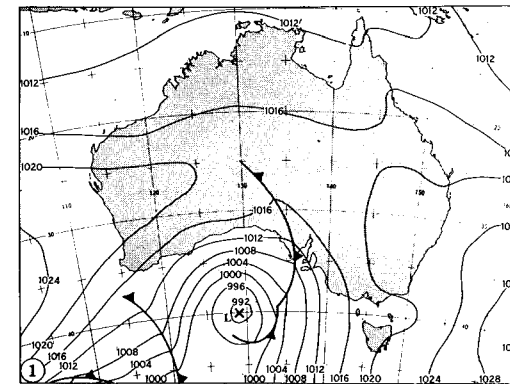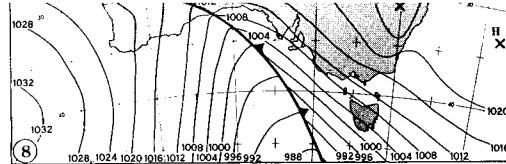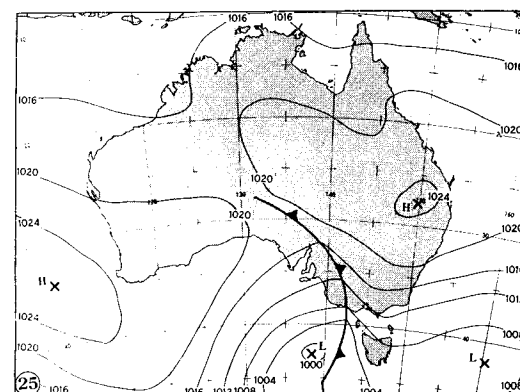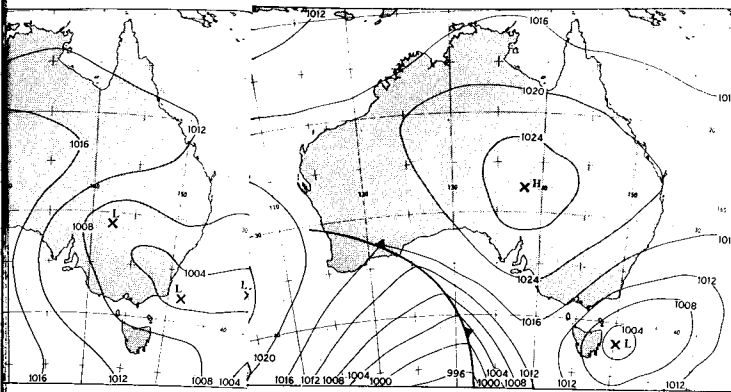
DAILY WEATHER MAPS

1000 K (00 GMT)

1 - 31 August 1989

Dates are ringed left-hand corner of each map.

LEGEND

Isobars are drawn at 4 hPa intervals

▲▲▲	Cold Front
● ●	Warm Front
▲●▲●	Occlusion
– – –	Trough
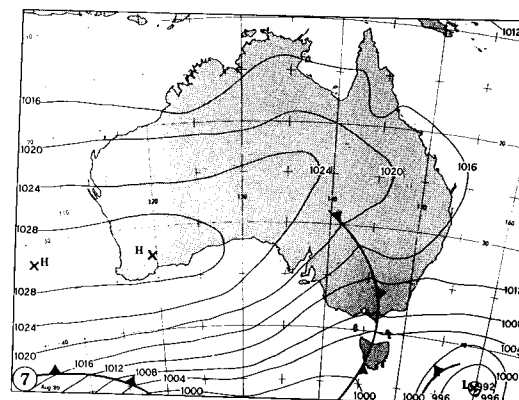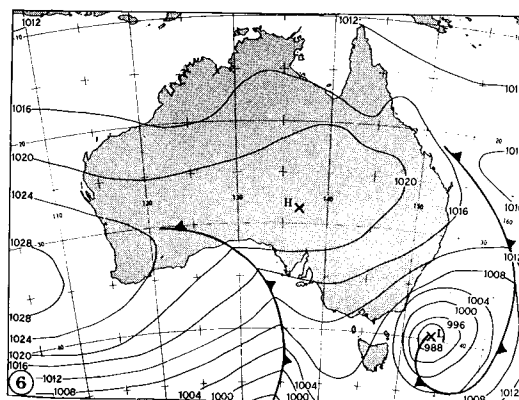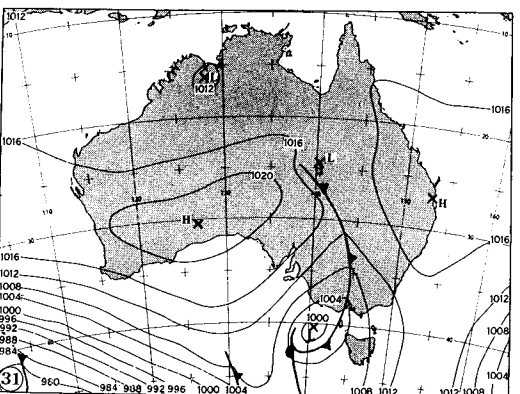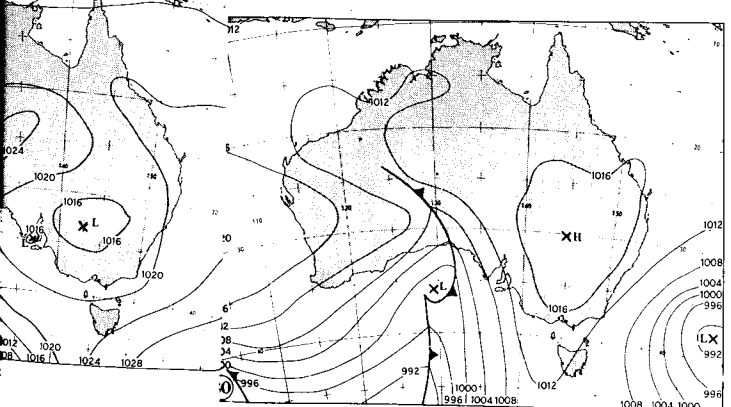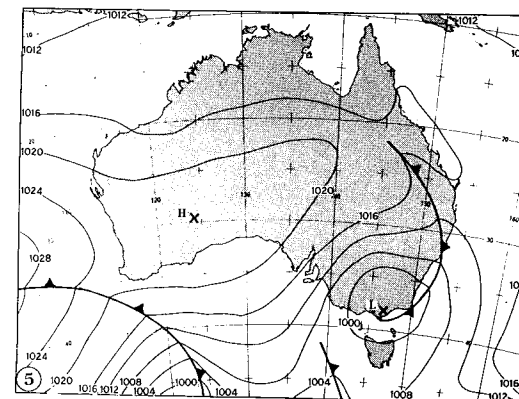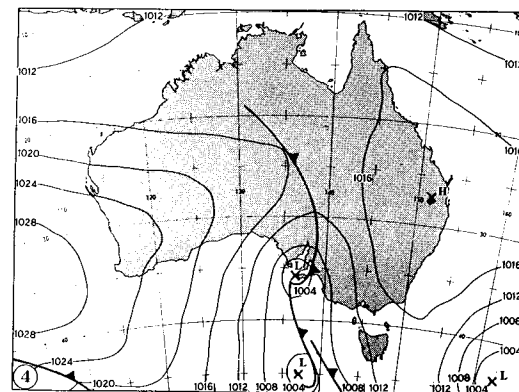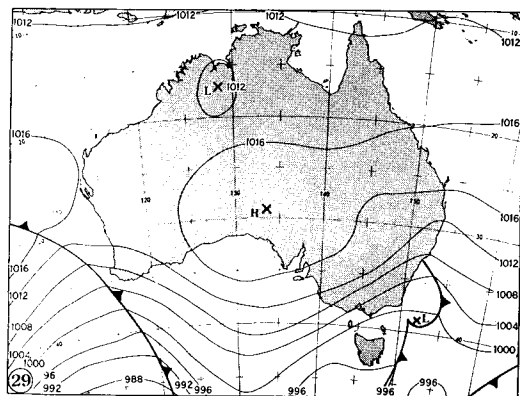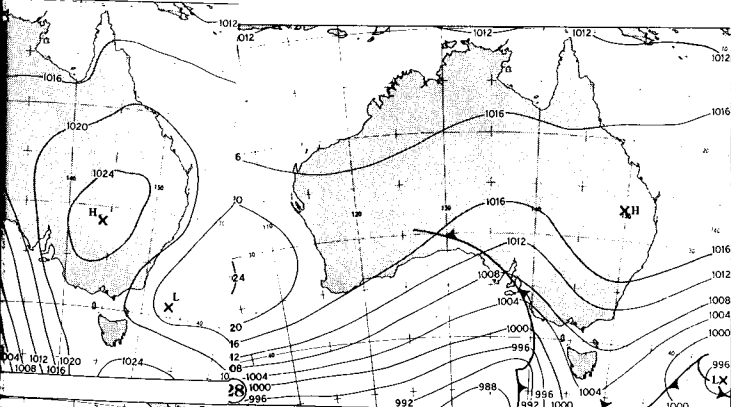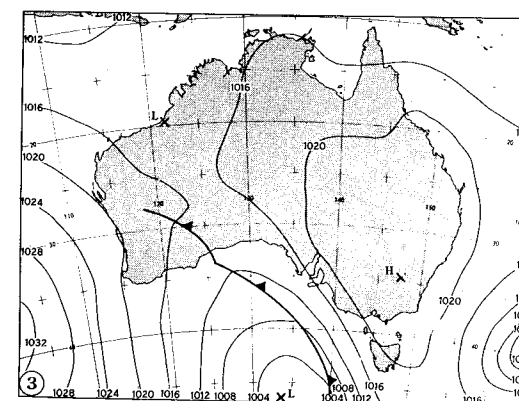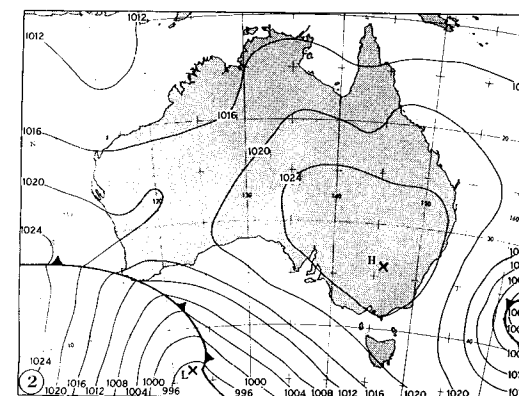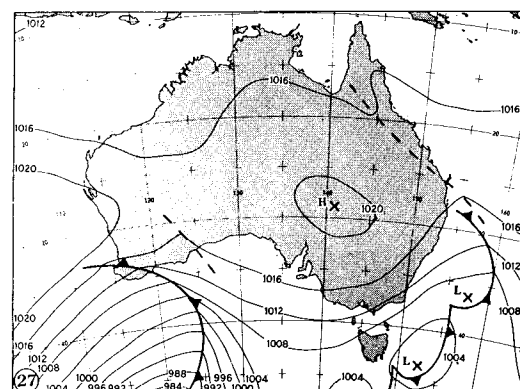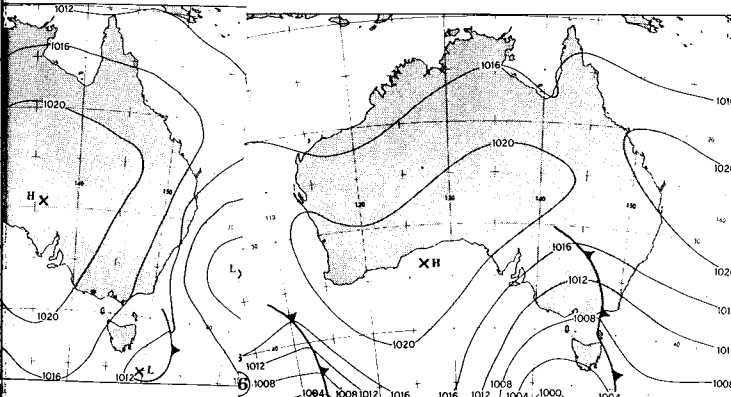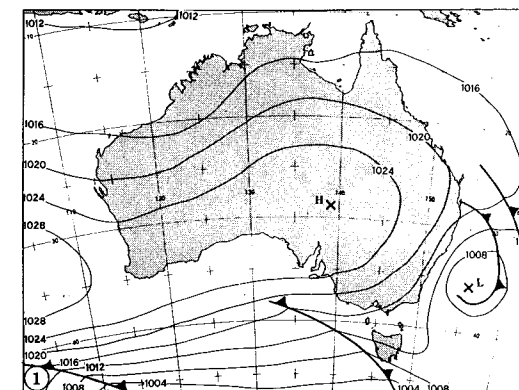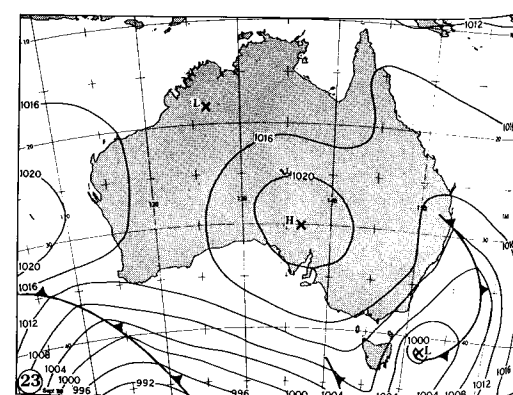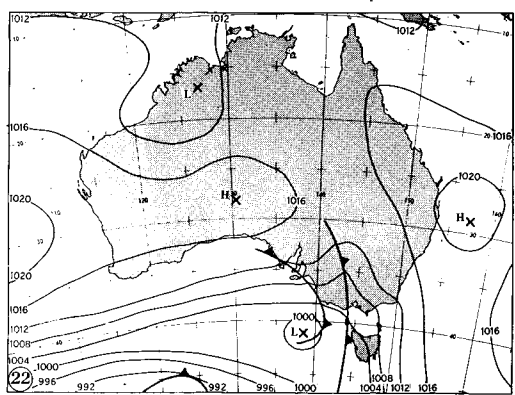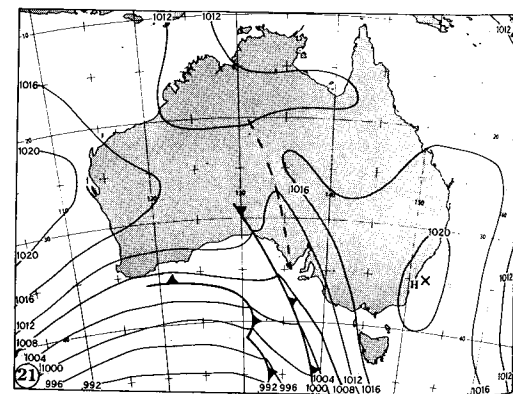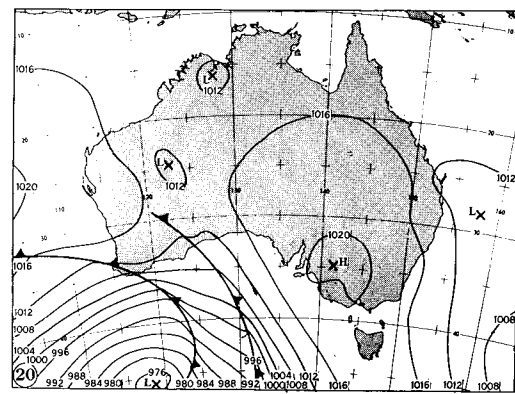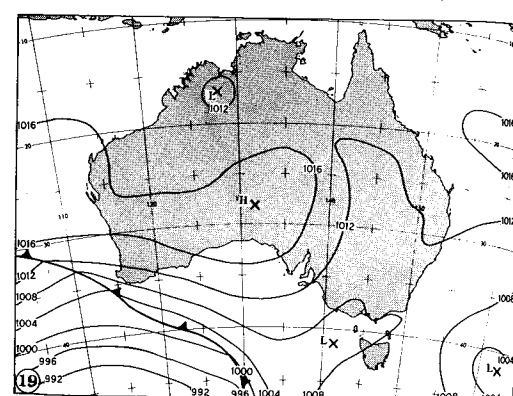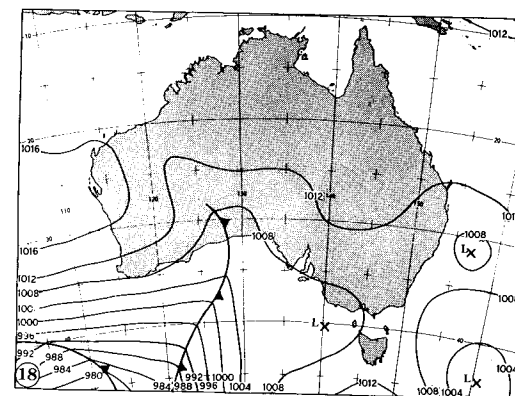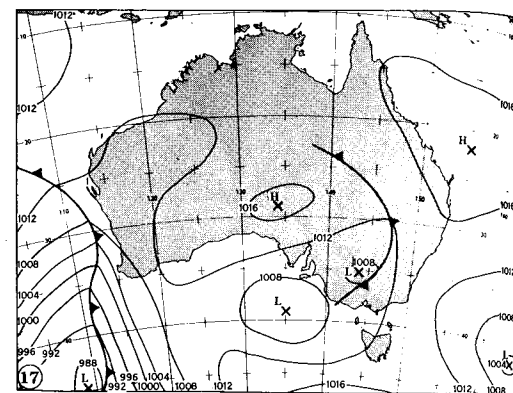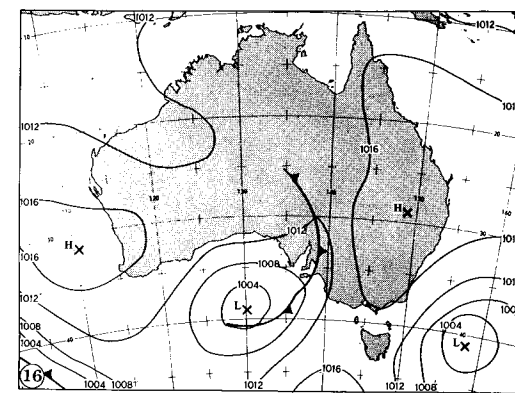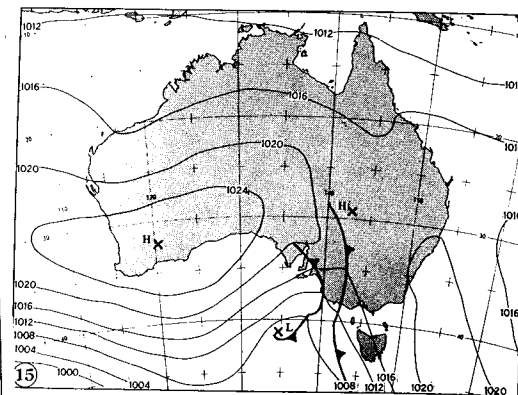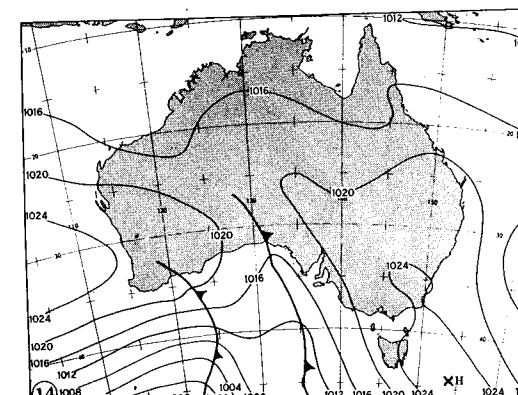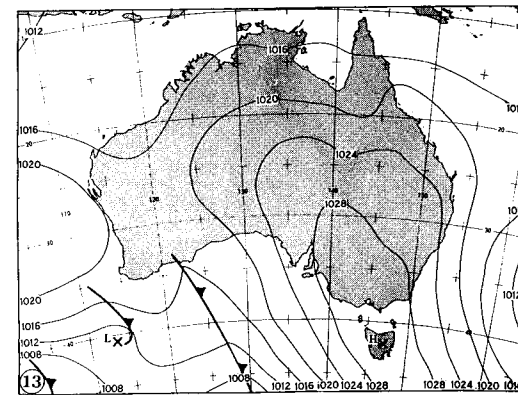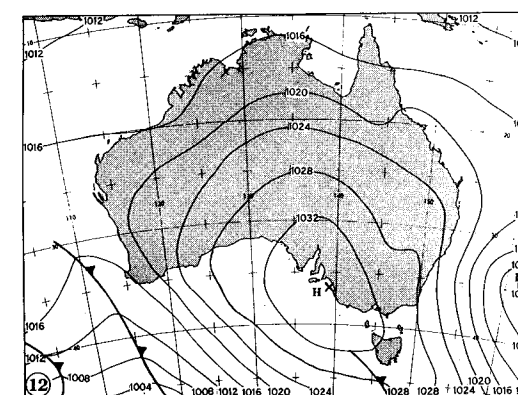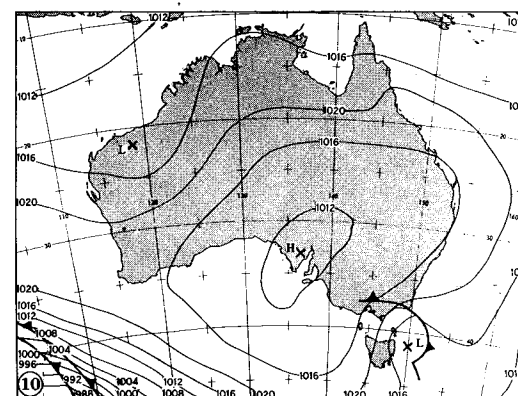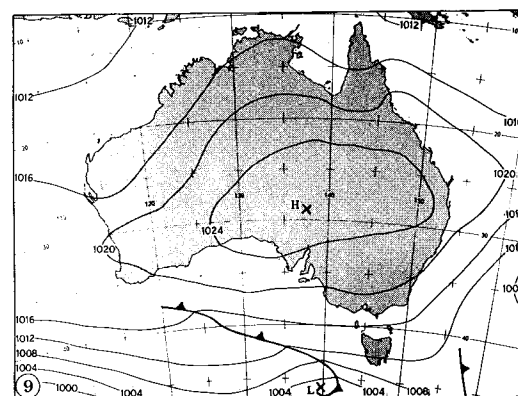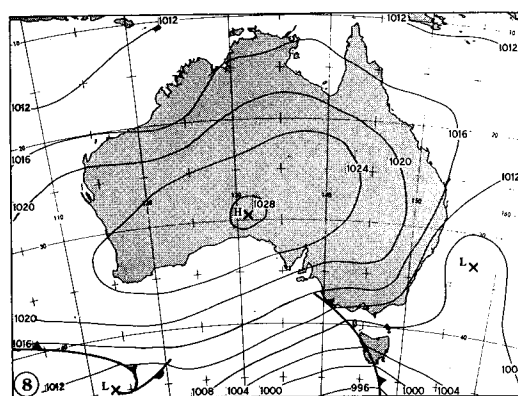
DAILY WEATHER MAPS

1000 K (00 GMT)

1 - 30 September 1989

Dates are ringed left-hand corner of each map.

LEGEND

Isobars are drawn at 4 hPa intervals

▲▲▲	Cold Front
●●●	Warm Front
▲●▲●	Occlusion
– – – –	Trough